The relationship between the algal toxin microcystin and the chemical, physical and biological parameters in Lake Winnipeg

by

Desiree Angela Lynn Stratton

A Thesis submitted to the Faculty of Graduate Studies of

The University of Manitoba

in partial fulfillment of the requirements of the degree of

MASTER OF SCIENCE

Department of Biological Sciences

University of Manitoba

Winnipeg, Manitoba

Copyright © 2022 Desiree Angela Lynn Stratton

ABSTRACT

Cyanobacterial algae blooms are of rising concern all over the world because of their increasing abundance and toxin release. Using an 18-year dataset (1999 to 2017), correlations between chemical, physical and biological parameters and the microcystin toxin in Lake Winnipeg were investigated. Multi-panel scatterplots with Pearson correlation coefficients found total boron in euphotic dataset and *Anabaena* biomass in the surface dataset had the strongest positive correlations. N variables such as total N, total Kjeldahl N, nitrate + nitrite and the N:P ratio may aid in controlling microcystin levels in Lake Winnipeg. Higher toxins correlated with higher N variables in the surface dataset (total N and total Kjaldahl N) and euphotic dataset (N:P ratio) and higher toxins and lower N variables correlated in the euphotic dataset (dissolved NO_3 + NO_2). Total suspended solids had a positive correlation with toxin levels in the surface dataset; Secchi disk depth and wind speed had negative correlations. Overall, I found that algal toxin concentrations in the epilimnion of Lake Winnipeg correlated best with several metrics of nitrogen availability, water clarity, *Anabaena* biomass and boron concentrations.

ACKNOWLEDGEMENTS

I would like to thank my advisor Dr. Gordon Goldsborough for his guidance and support through the thesis project. Your passion for aquatic sciences and energetic personality lead me to want to work with you as a graduate student and tackle a complicated Lake Winnipeg dataset. Thank you so much for meeting with me every week for the final year of writing to get my thesis done and for letting me be the lead in the fireworks show during your Wetland Ecology course. Thank you to my committee members Dr. Darren Gillis, Dr. C.J. Mundy and Elaine Page for their advice and knowledge during the writing of this thesis.

I would like to thank everyone in the Water Quality Management Section for all their knowledge on Lake Winnipeg and water quality in Manitoba as well as their support and encouragement through this process. For funding additional analysis of chemical and biological parameters at algal blooms sites on Lake Winnipeg. Thank you to Kelly-Anne Richmond and Nicole Armstrong for allowing me to take two months off work at the beginning of 2022 to finish my thesis. Thank you to Environment and Climate Change Canada for collecting additional algal samples on Lake Winnipeg.

Thank you to the Lake Winnipeg Research Consortium for allowing me to collect the data for this project and to all the ship and science crew members on the Namao for all their help in collecting the data for this project and for making my seven years on the Namao such a fun experience! Whether it was hanging out in Grand Rapids, going on workboat trips or making a bonfire on George Island, we always had a great time working on the Namao!

Thank you to my mom, dad, brother and husband Kyle for their love, encouragement and patience through this whole process! And finally, my pets Ozzy and Zale for keeping me company while working at home. I could not have done this without you all!

TABLE OF CONTENTS

ABSTRACT i
ACKNOWLEDGEMENTS ii
TABLE OF CONTENTS iv
LIST OF FIGURES vi
LIST OF TABLES xiii
LIST OF APPENDICES xv
1.0 LITERATURE REVIEW 1
1.1 Introduction to Algae 1
1.2 Introduction to Toxins 4
1.3 Environmental Factors Affecting Algal Growth and Toxin Release 8
1.3.1 Chemical Factors 8
1.3.2 Physical Factors 12
1.3.3 Biological Factors 15
1.4 Lake Winnipeg and its Watershed 16
1.5 History of Water Quality of Lake Winnipeg 18
1.6 Nutrient Concentrations and Loading 23
1.7 Conclusion 26
1.8 Objectives 27
1.9 Hypotheses 28
2.0 METHODS 34
2.1 Sampling Stations 34
2.2 Sampling Experience 37
2.3 Field Sampling 38
2.3.1 Field Equipment 38
2.3.2 Field Sampling Procedure on the MV *Namao* 40
2.4 Lab Analysis 43
2.5 Statistical Analysis 45
2.5.1 Datasets 45
2.5.2 Long-Term changes in Water Quality 1999-2017 47
2.5.3 Data Exploration 47

2.5.4 Multi-Panel Scatterplots 48
2.5.5 Linear Discriminant Analysis (LDA) 48
2.5.6 Linear Model 50
3.0 RESULTS 73
3.1 Long-Term changes in Water Quality 1999 to 2017 73
3.1.1 Phytoplankton Taxonomic Composition 73
3.1.2 Chemical, Physical and Biological Parameters 74
3.1.3 Toxins 76
3.2 Multi-panel Scatterplots of Correlations of Detectable Concentrations of Microcystin 77
3.2.1 Euphotic Dataset 77
3.2.2 Surface Dataset 78
3.2.3 Grouped analysis of Surface and Euphotic Datasets 79
3.3 Linear Discriminant Analysis (LDA) 80
3.3.1 Euphotic and Surface Datasets 80
3.4 Linear Model Selection and Hurdle Model 81
3.4.1 Euphotic Dataset 81
3.4.2 Surface Dataset 82
4.0 DISCUSSION 141
4.1 Objective 1. 141
4.1.1 Chemical parameters 141
4.1.2 Physical parameters 145
4.1.3 Biological Parameters 148
4.2 Objective 2. 151
4.3 Implications of Work 153
4.4 Evaluation of Hypotheses 154
4.5 Conclusion 156
5.0 REFERENCES 159
6.0 APPENDICES 173

LIST OF FIGURES

Figure 1. Lake Winnipeg Watershed. 30

Figure 2. Winter water quality sampling using a Bombardier on March 8, 2016..... 53

Figure 3. Winter water quality sampling using a helicopter on February 25, 2019. 54

Figure 4. Map of all W, auxiliary, nearshore and CAMP stations on Lake Winnipeg. 55

Figure 5. Picture of cyanobacteria algal bloom on Lake Winnipeg. 56

Figure 6. Picture of another cyanobacteria algal bloom on Lake Winnipeg..... 57

Figure 7. Map of Clean Beaches Program stations on Lake Winnipeg. 58

Figure 8. Picture of integrated tube sampler in use off the front deck of the MV *Namao*. 59

Figure 9. Picture of a DO sampler.. 60

Figure 10. Picture of a weighted sampler 61

Figure 11. MV *Namao* workboat and crew ready to head out to a nearshore station on Lake Winnipeg. 62

Figure 12. Desiree Stratton next to Environment and Climate Change Canada's Seabird Rosette on the top deck of the MV *Namao* on Lake Winnipeg. 63

Figure 13. Desiree Stratton filling sampling bottles from Environment and Climate Change Canada's Seabird Rosette off the top deck of the MV *Namao* on Lake Winnipeg. 64

Figure 14. The science and ship's crew sampling zooplankton and benthics on the stern of the MV *Namao* on Lake Winnipeg. 65

Figure 15. Cleaning off benthic sampling bags on the stern of the MV *Namao* on Lake Winnipeg. 66

Figure 16. Washing the aquatic invasive species Spiny Water Flea sample down the net to the bottom on the stern of the MV *Namao* on Lake Winnipeg 67
Figure 17. Proportion of total algal biomass in various taxonomic groups in samples from Lake Winnipeg between 1999 and 2017 in the north basin and south basin and narrows during the spring, summer, fall and winter. 84
Figure 18. Cyanobacteria genera biomass in Lake Winnipeg between 1999 and 2017 in the north basin and south basin and narrows during the spring, summer, fall and winter. 85
Figure 19. Cyanobacteria genera biomass in Lake Winnipeg between 1999 and 2017 in the north basin during the fall season..... 86
Figure 20. Cyanobacteria genera biomass in Lake Winnipeg between 1999 and 2017 in the north basin during the spring season. 87
Figure 21. Cyanobacteria genera biomass in Lake Winnipeg between 1999 and 2017 in the north basin during the winter season..... 88
Figure 22. Cyanobacteria genera biomass in Lake Winnipeg between 1999 and 2017 in the north basin during the summer season. 89
Figure 23. Cyanobacteria genera biomass in Lake Winnipeg between 1999 and 2017 in the south basin and narrows during the fall season. 90
Figure 24. Cyanobacteria genera biomass in Lake Winnipeg between 1999 and 2017 in the south basin and narrows during the spring season. 91
Figure 25. Cyanobacteria genera biomass in Lake Winnipeg between 1999 and 2017 in the south basin and narrows during the summer season. 92
Figure 26. Cyanobacteria genera biomass in Lake Winnipeg between 1999 and 2017 in

the south basin and narrows during the winter season. 93
Figure 27. Chlorophyll a concentration (µg/L) in Lake Winnipeg between 1999 and 2017 as an average of surface and euphotic W stations data per year in the north basin and south basin and narrows. 94
Figure 28. Total N concentration (mg/L) in Lake Winnipeg between 1999 and 2017 as an average of surface and euphotic W stations data per year in the north basin and south basin and narrows during the spring, summer, fall and winter seasons..... 95
Figure 29. Total N concentration (mg/L) in Lake Winnipeg with total N objective between 1999 and 2017 as an average of surface and euphotic W stations data per year in the north basin and south basin and narrows..... 96
Figure 30. Total P concentrations (mg/L) in Lake Winnipeg between 1999 and 2017 as an average of surface and euphotic W stations data per year in the north basin and south basin and narrows during the spring, summer, fall and winter seasons..... 97
Figure 31. Total P concentrations (mg/L) in Lake Winnipeg with total P objective between 1999 and 2017 as an average of surface and euphotic W stations data per year in the north basin and south basin and narrows 98
Figure 32. Turbidity levels (NTU) in Lake Winnipeg between 1999 and 2017 as an average of surface and euphotic W stations data per year in the north basin and south basin and narrows. 99
Figure 33. N:P molar ratio in Lake Winnipeg between 1999 and 2017 as an average of surface and euphotic W stations data per year in the north basin and south basin and narrows. 100
Figure 34. Microcystin concentrations (µg/L) in Lake Winnipeg between 2004 and 2017

as an average of surface and euphotic W and other stations data per year in the north basin and south basin and narrows. 101
Figure 35. Multi-panel scatterplot from the euphotic dataset of total boron, pheophytin *a*, pH and Cryptophyceae biomass against microcystin toxin with Pearson correlation coefficient and trend line. 102
Figure 36. Multi-panel scatterplot from the euphotic dataset of surface sample depth, total sample depth, hardness and total lithium against microcystin toxin with Pearson correlation coefficient and trend line. 103
Figure 37. Multi-panel scatterplot from the euphotic dataset of total magnesium, N:P ratio, total dissolved solids and air temperature against microcystin toxin with Pearson correlation coefficient and trend line. 104
Figure 38. Multi-panel scatterplot from the euphotic dataset of total thallium, total uranium and Dinophyceae biomass against microcystin toxin with Pearson correlation coefficient and trend line. 105
Figure 39. Multi-panel scatterplot from the euphotic dataset of alkalinity CO_3, total calcium, conductivity and DO against microcystin toxin with Pearson correlation coefficient and trend line. 106
Figure 40. Multi-panel scatterplot from the euphotic dataset of total potassium, total sodium and total sulphate against microcystin toxin with Pearson correlation coefficient and trend line. 107
Figure 41. Multi-panel scatterplot from the euphotic dataset of total antimony, total cadmium and acid-hydrolyzable P against microcystin toxin with Pearson correlation coefficient and trend line. 108

Figure 42. Multi-panel scatterplot from the euphotic dataset of total P, total dissolved P, total reactive P and total zirconium against microcystin toxin with Pearson correlation coefficient and trend line. 109
Figure 43. Multi-panel scatterplot from the euphotic dataset of total manganese, dissolved NO_3+NO_2 and wind speed against microcystin toxin with Pearson correlation coefficient and trend line. 110
Figure 44. Multi-panel scatterplot from the euphotic dataset of total Kjeldahl nitrogen, total carbon, total nitrogen and dissolved NO_3+NO_2 against microcystin toxin with Pearson correlation coefficient and trend line. 111
Figure 45. Multi-panel scatterplot from the surface dataset of *Anabaena* biomass, total Kjeldahl N, BOD and total suspended solids against microcystin toxin with Pearson correlation coefficient and trend line. 112
Figure 46. Multi-panel scatterplot from the surface dataset of Cyanophyceae biomass, Phytoplankton biomass, chlorophyll *a* and total N against microcystin toxin with Pearson correlation coefficient and trend line. 113
Figure 47. Multi-panel scatterplot from the surface dataset of Cryptophyceae biomass, Secchi disk depth and wind speed against microcystin toxin with Pearson correlation coefficient and trend line. 114
Figure 48. Multi-panel scatterplot from the surface dataset of pheophytin *a*, total carbon, dissolved NO_3 + NO_2 and N:P ratio against microcystin toxin with Pearson correlation coefficient and trend line. 115
Figure 49. Multi-panel scatterplot from the combined euphotic and surface dataset of pheophytin *a*, *Anabaena* biomass, N:P ratio and total Kjeldahl N against microcystin

toxin with Pearson correlation coefficient and trend line..... 116
Figure 50. Multi-panel scatterplot from the combined euphotic and surface dataset of dissolved NO_3+NO_2, wind speed, total C, pH and total N against microcystin toxin with Pearson correlation coefficient and trend line. 117
Figure 51. Linear discriminant analysis euphotic data observations. 118
Figure 52. Histogram for LD1 for the linear discriminant analysis euphotic data observations. 119
Figure 53. Histogram for LD2 for the linear discriminant analysis euphotic data observations. 120
Figure 54. Linear discriminant analysis surface data observations. 121
Figure 55. Histogram for LD1 for the linear discriminant analysis surface data observations. 122
Figure 56. Histogram for LD2 for the linear discriminant analysis surface data observations. 123
Figure 57. Euphotic dataset Q-Q plot of quantile residuals with log transformed microcystin concentrations and total boron and wind speed main effects in a Hurdle model Gaussian GLM with identity link..... 124
Figure 58. Euphotic dataset Q-Q plot of quantile residuals with microcystin presence/absence and Anabaena biomass and wind speed main effects in a Hurdle model Binomial GLM 125
Figure 59. Surface dataset Q-Q plot of quantile residuals with log transformed microcystin concentrations and the N:P ratio and wind speed main effects in a Hurdle model Gaussian GLM with identity link..... 126

Figure 60. Surface dataset Q-Q plot of quantile residuals with microcystin presence/absence and the N:P ratio and wind speed main effects in a Hurdle model Binomial GLM..... 127
Figure 61. Euphotic dataset predicted vs actual values plot with log transformed microcystin concentrations and total boron and wind speed main effects in a Hurdle model Gaussian GLM with identity link..... 128
Figure 62. Surface dataset predicted vs actual values plot with log transformed microcystin concentrations and the N:P ratio and wind speed main effects in a Hurdle model Gaussian GLM with identity link..... 129

LIST OF TABLES

Table 1. Cyanobacteria genera present in Lake Winnipeg that produce toxins and toxicity. 31

Table 2. Morphometric data of Lake Winnipeg. 33

Table 3. Selection of chemical, physical and biological parameters from Lake Winnipeg euphotic dataset. 68

Table 4. Model set of chemical, physical and biological parameters from Lake Winnipeg that could be predictors of the microcystin toxin from the euphotic dataset for the AIC analysis. 70

Table 5. Selection of chemical and physical parameters from Lake Winnipeg surface dataset. 71

Table 6. Model set of chemical and physical parameters from Lake Winnipeg that could be predictors of the microcystin toxin from the euphotic dataset for the AIC analysis ... 72

Table 7. Confusion matrix for the linear discriminant analysis test data for the euphotic dataset. 130

Table 8. Confusion matrix for the linear discriminant analysis test data for the surface dataset. 130

Table 9. Model selection table for the Gaussian GLM model sets from the euphotic dataset 131

Table 10. Model selection table for the binomial GLM model sets from the euphotic dataset 133

Table 11. Model selection table for the Gaussian GLM model sets from the surface dataset. 135

Table 12. Model selection table for the binomial GLM model sets from the surface dataset 137
Table 13. Model summary of the euphotic and surface datasets hurdle models 139
Table 14. K-fold cross-validation and McFadden’s Pseudo R-squared for the euphotic and surface Hurdle GLM. 140

LIST OF APPENDICES

Appendix 1. Table of vessels and workboats used for each spring, summer and fall research surveys on Lake Winnipeg from 1999 to 2017. 173

Appendix 2. Table of all the W, Auxiliary, Near Shore, CAMP, Clean Beaches Program and Non-Routine Stations on Lake Winnipeg from 1999 to 2017..... 174

Appendix 3. Table of all samples taken at all 14 W stations in the spring, summer and fall Lake Winnipeg science cruises from 1999 to 2017..... 181

Appendix 4. Table of the chemical, nutrient, metal and biological parameters taken at each station on Lake Winnipeg from April 2001 to March 2009. Cantest Laboratories (formerly Maxxam Analytics, now Bureau Veritas) analyzed any chemical, nutrient and metal parameters and ALS analyzed any biological parameters. 183

Appendix 5. Table of the chemical, nutrient, metal and biological parameters taken at each station on Lake Winnipeg from April 2009 to September 2017 and analyzed by ALS Laboratories. 186

Appendix 6. List of ALS and Cantest parameter methods, date ranges, if parameter is still analyzed presently, units, detection limit (DL), method source/ description or comment. 189

Appendix 7. R code for data exploration. 213

Appendix 8. Multi-panel Scatterplots of microcystin detected data. 214

Appendix 9. Linear Discriminant Analysis..... 219

Appendix 10. Linear Model – AIC Model Selection and Hurdle Model 221

Appendix 11. Ways to reduce the impacts of cyanobacteria algal blooms. 227

1.0 LITERATURE REVIEW

1.1 Introduction to Algae

The number of algal taxa that occur in the world has been estimated between one and ten million species where some of these groups contain species that produce a variety of toxins. Common types of freshwater algae are diatoms (Bacillariophytes), green algae (Chlorophytes), cyanobacteria (Cyanophytes), golden or golden-brown algae (Chrysophytes), cryptomonads (Cryptophytes), dinoflagellates (Dinophytes) and the euglenids (Euglenophytes) (Environment Canada & Manitoba Water Stewardship, 2011). The Division Cyanophyta are referred to as the cyanobacteria or blue-green algae and are the oldest oxygenic photoautotrophs on Earth (Lee, 2008; Paerl & Otten, 2013). There are said to have evolved over 2.8 billion years ago and are the living prokaryotic ancestors of eukaryotic algae (Evangelista et al., 2008).

Algae can occur worldwide in many different environments as well as can have a wide range of tolerances and forms. Algae can occur in marine, freshwater and terrestrial environments and in areas such as in polar, tropical and temperate regions (Lee, 2008). Marine algae can grow in sublittoral benthic environment from 200 m deep to shallow water levels; intertidal where they grow on exposed areas of the shore where the tidal cycles occur and supralittoral where they are exposed to waves and spray and are located at the high-tide level (Evangelista et al., 2008). Algae can occur in freshwater regions all around the world and live all year round (Lee, 2008). They can also occur on terrestrial environments such as on plants(epiphytic), animals (epizoic) or rocks (epilithic), on sand or mud (epipelic) and inside fungus (lichen) (Evangelista et al., 2008; Lee, 2008). Aquatic algae can tolerate many places around the world from salt

lakes to freshwater springs and can exhibit a wide range of tolerances to turbidity, temperature (<0 to extreme hot environments as high as 70 and 73°C), pH (<2 to >10), oxygen and carbon dioxide concentrations (Evangelista et al., 2008). Algae can form in aquatic environments as free-floating algae within the water column (phytoplankton), attached to surfaces (periphyton), previously attached to surfaces (metaphyton), or at the air-water interface (neuston) (Evangelista et al., 2008; Lee, 2008).

The cyanobacteria algae possess unique features from bacteria, plants and animals. The cyanobacteria are prokaryotic autotrophs that primarily contain the pigment chlorophyll *a* that is used for photosynthesis like all plants, has myxophycean starch as a storage product which is similar to glycogen in most animals, contains amino acids and amino sugars within their cell walls like some bacteria and have no flagella or chloroplasts unlike many eukaryotic algae (Graham et al., 2008b; Lee, 2008).

Cyanobacteria have biological and physical factors that allow them to thrive in freshwater lakes. Cyanobacteria have the ability to move between the poorly lit, cold, nutrient-rich hypolimnion and well-lit, warm, nutrient-poor epilimnion of stratified areas of the water column using their gas vacuoles for buoyancy (Cottingham et al., 2015). Negative buoyancy can be used to undergo luxury uptake of phosphorus (P) pools located within the sediments and in the hypolimnion of a stratified area that other phytoplankton species can not get to and move P and nitrogen (N) to the surface water and the rest of the lake system (Lee, 2008; Cottingham et al., 2015). With the temperatures around 25°C during the warmer months and stable water column due to no wind, there is more motility present using positive buoyancy from gas vesicles to

access higher light intensities in the epilimnion by the reduction of osmotically active solutes (Lee, 2008; Beaulieu et al., 2013).

Chemical factors such as a low (nitrogen to phosphorus) N:P ratio can allow cyanobacteria to thrive in eutrophic lakes. Some species of cyanobacteria are known as diazotrophs which allow them to fix inorganic N from the atmosphere into ammonia and can give them a competitive advantage when growing in N-limited waters (Lee, 2008). Cyanobacteria have a competitive advantage when the N:P ratio is low and the availability of N is limited for other phytoplankton growth due to their ability fix atmospheric N (Dolman et al., 2012). Non-N-fixing and N-fixing cyanobacteria species are found to dominate at low N:P mass ratios where *Microcystis* blooms in Meiliang Bay, China dominated when they coincided with lower N:P mass ratios (Liu et al., 2011). There was a large proportion of samples with detectable microcystin in Lake Winnipeg that had N:P molar ratios below 15:1 showing a similar relationship observed in Alberta lakes where detectable microcystin concentrations occurred at a N:P molar ratio of 5:1 (Kotak et al., 2000; Kotak, 2009). Also, on Lake Winnipeg in 2007, 64% of the whole water samples that had a detectable amount of microcystin had an N:P ratio that was less than 5:1 (Kotak, 2009). In freshwater lakes across Canada, there were higher microcystin concentrations when a mass N:P ratio of less than 23:1 occurred (Orihel et al., 2012; Scott et al., 2013).

Natural and anthropogenic factors can be important in driving cyanobacterial growth, dominance and toxin production in the water column. Enrichment of nutrients from sources such as runoff from urban areas, land fertilizers, manure from livestock, industrial and municipal wastewaters and atmospheric deposition has resulted in the

eutrophication in freshwater lakes (Environment Canada & Manitoba Water Stewardship, 2011). The N cycle has been altered by human activities such as fossil fuel combustion, combustion of biofuel, natural and agricultural soil emissions and agricultural waste by increasing the N to 140 Tg N/yr, around 9-fold increase from 1890 to 1990 (Galloway & Cowling, 2002; Beaulieu et al., 2013). The global P cycle has been altered due to agricultural crops, fertilizers, animal feeds as well as mining P to produce products such as plastics, paper, glass, rubber and flame retardants which are causing P to accumulate in soils and runoff into aquatic ecosystems (Bennett et al., 2001). P retention during the preindustrial era (before human scale global impact) has risen in freshwater systems from 1.2 Tg/yr to 3.1 Tg/yr (Bennett et al., 2001). The influx of nutrients such as P and N has increased the frequency of occurrence and size of algal blooms in the nearshore, beaches, and offshore which can cause a shift in phytoplankton dominance to cyanobacteria and can influence the production of toxins (Sivonen, 1990; Environment Canada & Manitoba Water Stewardship, 2011).

1.2 Introduction to Toxins

Toxins from different groups of algae can cause a variety of physiological effects on organisms, animals and humans. There are three main groups of toxins which are defined based on their human health effects such as the dermatoxins, lyngbyatoxin, aplysiatoxin and lipopolysaccharides; the hepatotoxins cylindrospermopsin, microcystin and nodularin and the neurotoxins anatoxin, β-methylamino-L-alanine (BMAA), neosaxitoxin and saxitoxin (Graham et al., 2008a). The cyanobacteria algae *Anabaena*, *Aphanocaspa*, *Microcystis* can produce many forms of toxins such as the dermatoxins, and the hepatotoxins microcystins, nodularians and cylindrospermopsin as well as the

neurotoixns anatoxin, saxitoxins and BMAA (Huisman et al., 2018). Dinoflagellate genera are able to produce saxitoxins, paralytic shellfish poisoning (PSP), diarrhetic shellfish poisoning, ciguatera shellfish poisoning and spirolide poisoning (Lee, 2008; Gopalakrishnakone et al., 2016). Some diatoms and red algae can produce a neurotoxic agent called domoic acid which causes amnesic shellfish poisoning (Lee, 2008; Gopalakrishnakone et al., 2016). The green algae *Caulerpa* can produce caulerpicin which can cause cold sensation and numbness to the extremities, difficult and rapid breathing, slight depression and loss of balance (Collins, 1978). The red algae can produce carrageenans, which are polysaccharides that can activate the Hagemann factor, toxicity to selective macrophages, immunosuppression and the induction of chronic and acute inflammatory responses (Collins, 1978). The golden algae species *Prymnesium parvum* and *Ochromonas* spp. have similarly shown ichthyotoxicity, hemolytic activity and antispasmodic effects except that these toxins are activated by different parameters (Collins, 1978) (Table 1).

Toxins are believed to be produced during the cyanobacteria's life cycle, which are then released into the surrounding aquatic environment from the cell. Laboratory studies of *Microcystis* suggest that toxin production may be related to the algal cell life cycle where the highest rate of production would be the early stationary and late logarithmic growth stage (Kotak et al., 1995; Vézie et al., 2002). A Finnish culture study on *Oscillatoria* strains confirmed that during the algal cell's growth, hepatotoxins are kept within cells and an increased leakage of toxins occurs around the end of the three-to-four-week period of growth (Sivonen, 1990). High temperatures and light intensities promoted the leakage of toxins from the cells and caused adverse effects on growth

(Sivonen, 1990). Cyanobacteria production of microcystin could be related to photoperiod where concentrations of microcystin were found to be highest during the daylight hours and decreased during the nighttime (Kotak & Zurawell, 2007). It is suggested that in the death phase, the cells decompose the toxins by the process of autolysis (Kaya & Watanabe, 1990). Cultures that were in the early stationary or late logarithmic growth phases had the highest concentrations of toxin of the Finnish *Microcystis* strains where higher growth occurred (Vézie et al., 2002). However, larger amounts of P and N concentrations occurred, but growth was poor with low combined concentrations of nutrients (Vézie et al., 2002).

It has been hypothesized that the functions of toxins, taste and odor compounds include primary roles in allelopathy, secondary metabolites, defense mechanisms and cellular processes. Studies have suggested that cyanobacteria produce toxins as a defense mechanism against herbivorous zooplankton grazing pressure which may control zooplankton composition and competitive relations (Kotak et al., 1996). Hepatotoxins can prevent invertebrate grazing within the environment by functioning as an anti-herbivore chemical where the increased grazing activity can cause an increase in toxin production (Lee, 2008). By an allelopathic interaction, cyanotoxins can also inhibit the growth of other species, for example, microcystin produced by *Microcystis* can inhibit the freshwater dinoflagellate *Peridinium gatunense* by abolishing carbonic anhydrase activity (Lee, 2008). It has been suggested that when conditions for algal growth are favorable, microcystin production is at its greatest (Long et al., 2001). Zooplankton have evolved mechanisms to reduce toxin susceptibility such as reduced filter feeding activity, rejection of toxin strains over non-toxic strains and increased toxin

resistance (Kotak et al., 1996). Grazing from zooplankton has been shown to influence the formation of cyanobacteria blooms, duration and decline (Rose et al., 2017). Where there were high concentrations of cyanobacteria, there was found to be higher concentrations of the microcystin toxin (Jones et al., 1998). When an algal bloom is in decline, toxin concentrations may still be present in the water at the same or higher amounts than what was present when the algal bloom was at its peak (Jones et al., 1998).

Worldwide, microcystins are generally the most commonly occurring cyanobacteria hepatotoxin (liver toxin). The microcystin toxin has a generalized structure comprised of a cyclic peptide with seven amino acids as well there are around 100 congeners of microcystin, the most common of which is microcystin-LR (Kotak & Zurawell, 2007). Depending on the microcystin dose present, impacts from exposure can vary. Furthermore, this can ultimately lead to death due to dysfunction, liver damage or hypovolemic shock (mammals) as well as acute exposure to the toxin can result in kidney and gastrointestinal damage (Kotak & Zurawell, 2007). When hepatotoxins are ingested by animals, they are transported to the liver which can cause bleeding and clinical symptoms can include diarrhea, vomiting, cold extremities, and weakness (Lee, 2008; Neilan et al., 2013). Also, human exposure with microcystin can occur by dermal contact through activities such as swimming, diving and bathing as well as accidental ingestion of a small quantity of water containing microcystins (Kotak & Zurawell, 2007). Aerosols created from watersports such as water skiing as well as inadequately treated water for showering can increase respiratory exposure to microcystin (Kotak & Zurawell, 2007). Chronic exposure may have a long-term

exposure potential through drinking water contamination (Kotak & Zurawell, 2007). A study in China reported a positive correlation between concentrations of microcystin in drinking water and colorectal cancer rates (Kotak & Zurawell, 2007).

1.3 Environmental Factors Affecting Algal Growth and Toxin Release

Some environmental (chemical, physical and biological) parameters have been linked to the cyanobacteria producing toxins. These parameters include chemical (chlorophyll *a*, total N, nitrate, nitrite, ammonia, total P, total dissolved P, orthophosphate and metals), physical (wind speed, light, temperature and Secchi disk depth) and biological (cyanobacteria genera and densities) parameters as well as the N:P ratio. In this section, I will describe the following parameters and how they link to algal growth and toxin release by algae.

1.3.1 Chemical Factors

The algal toxin microcystin has been known to have a strong positive correlation with chlorophyll *a*. Chlorophyll *a* is a pigment in cyanobacteria that absorbs light and provides energy for photosynthesis as well as can be a good indicator of the amount of cyanobacteria present in the water if there is a higher chlorophyll *a* concentration. For example, microcystin-LR demonstrated a strong positive correlation with chlorophyll *a* ($r=0.74$) in southwestern Manitoba in 1995 (Jones et al., 1998). Cellular microcystin-LR concentrations from 13 eutrophic and hypereutrophic central and northern Alberta lakes were positively correlated with chlorophyll *a* ($r=0.48$) (Kotak et al., 2000). Chlorophyll *a* concentrations from samples taken in the Midwestern United States were positively correlated with microcystin concentrations ($r_s=0.64$, $p<0.01$) (Graham et al., 2010). Microcystin showed to have a positive correlation with chlorophyll *a* ($r=0.18$, $p=0.015$) at

3 sites in the south basin of Lake Winnipeg in 2010 (Pip & Bowman, 2014). Furthermore, studies on Lake Erie have indicated that microcystin levels had a relationship with chlorophyll *a* concentrations (in 2013 r^2=0.70 and in 2014 r^2=0.57) as well as at low concentrations of chlorophyll *a* (14 µg/L), microcystin concentrations were low (1 µg/L in 2013 and 7 µg/L in 2014) (Stumpf et al., 2016). All of these lines of evidence suggest that there are variable positive correlations between microcystin and chlorophyll *a* concentrations in studies across Canada and the United States.

Studies across the world show cyanobacterial success and the existence of positive and negative correlations between microcystin and all forms of N concentrations. Under high N conditions, cyanobacteria will need to compete with other cells, where the production of an allelopathic compound could benefit cyanobacterial growth (Lee, 2008). Cyanobacteria have the ability to fix N from the atmosphere which can give them a competitive advantage against other phytoplankton when N is limiting (Dolman et al., 2012). A direct relationship between toxin production and concentrations of total N in strains of *Oscillatoria* isolated from Finnish freshwater lakes occurred, where toxin concentrations were higher (around 3 mg/g for strain CYA 128 and around 6 mg/g for strain 97) when high N concentrations (84 mg/L) were present (Sivonen, 1990). However, in Alberta, Coal, Driedmeat and Little Beaver Lake showed insignificant negative correlations with nitrate ($r=-0.34$, $p>0.12$) and ammonia ($r=-0.10$, $p>0.55$) (Kotak et al., 1995). Furthermore, there was a negative correlation between microcystin-LR and nitrate and nitrite ($r=-0.11$) in central and northern Alberta freshwater lakes (Kotak et al., 2000). Cultures using *Microcystis* spp. from France and Finland showed that increasing total N concentrations (0.84 to 8.4 mg/mL) increased microcystin

concentrations (Vézie et al., 2002). On Lake Winnipeg, at 53 sites in the north and south basin in 2007, there was a positive correlation ($r<0.25$) between microcystin and N, nitrate and ammonia forms (Kotak, 2009). In freshwater lakes across Canada, higher microcystin concentrations occurred with total N concentrations greater than 2600 µg/L ($r=0.39$, $p<0.01$) (Orihel et al., 2012; Scott et al., 2013). There was a positive correlation with nitrate-N concentration ($r=0.46$) in 2010 at nearshore areas on Lake Winnipeg south basin (Pip & Bowman, 2014). Microcystin concentrations in Bear and Muskegon lake in Ontario had a positive relationship with total N ($r^2=0.889$) (Xie et al., 2016). Therefore, studies across the world have shown positive and negative correlations and relationships between total N, nitrate and ammonia versus microcystin concentrations likely due to different dominant cyanobacteria species and nitrogen concentrations present.

P is important in cyanobacteria growth and studies correlating microcystin and P concentrations show positive correlations occurring between microcystin and all P forms. P is an essential nutrient for algal growth where it is a component of the adenosine triphosphate (ATP) molecule and can be used in the storage and transfer of energy. Microcystin production from cultured *Oscillatoria* strains from four Finnish freshwater lakes seemed to not be affected when total P concentrations were between 0.4 and 5.5 mg/L (Sivonen, 1990). In Coal, Driedmeat and Little Beaver lakes in Alberta, concentrations of total P ($r=0.57$) and total dissolved P ($r=0.49$) were positively correlated with microcystin-LR (Kotak et al., 1995). There was a positive correlation between microcystin-LR and total P concentrations ($r=0.46$) in a study on central and northern Alberta eutrophic and hypereutrophic freshwater lakes (Kotak et al., 2000).

There was a weak positive correlation ($r<0.25$) between total P and total dissolved P and microcystin concentrations on Lake Winnipeg in the north and south basin in 2007 (Kotak, 2009). In freshwater lakes across Canada, higher microcystin concentrations occurred with total P concentrations that are less than 219 µg/L ($r=0.36$, $p<0.01$) (Orihel et al., 2012; Scott et al., 2013). In the south basin nearshore area on Lake Winnipeg, there was a positive correlation with orthophosphate-P concentrations ($r=0.61$) and microcystin concentrations (Pip & Bowman, 2014). In Bear and Muskegon lake in Ontario, microcystin had a positive relationship with total P ($r^2=0.768$) (Xie et al., 2016). Overall studies have shown that total P, total dissolved P and orthophosphate-P concentrations are positively correlated with microcystin concentrations.

Macro and micronutrients aside from P and N are essential for algal cell growth and studies have shown that they may have an influence on toxin production whereas the metals aluminum, cadmium, calcium, chloride, chromium, manganese, potassium and tin showed no relationship. In lakes, biological surfaces such as algae have been shown to play a big role in heavy metal binding, therefore regulating the remaining dissolved metal concentrations (Lukač & Aegerter, 1993). *Microcystis aeruginosa* culture toxin production was shown to increase up to 138% ($p=0.02$ to 0.04) with the addition of iron concentrations of 0.1 to 2.5 µm and 30% ($P=0.0022$) with the addition of zinc concentrations of 0.01 and 0.25 µm (Lukač & Aegerter, 1993). Microcystin concentrations increased when cultures were iron starved (at 0.01 µM iron) and when cultures were given 0.1 µM or 1 µM of iron, there was no difference in microycstin concentrations despite differences in growth (Alexova et al., 2011). It was shown that in *Microcystis aeruginosa* cultures, copper (2.5 µm) and manganese (25 µm)

concentrations were added to a medium where tellurium was depleted, algal toxin production did not change (Lukač & Aegerter, 1993). Strains of *Microcystis aeruginosa* from Karelian Lakes in Russia showed that when zinc concentrations of 25 to 100 µg/L increased the intracellular concentrations of microcystin as well when concentrations of copper, nickel and zinc were increased to 45, 190 and 250 µg/L, no toxins were detected (Polyak et al., 2013). The metals aluminum, cadmium, chromium, nickel and tin did not affect toxin concentrations (Lukač & Aegerter, 1993). Looking at 13 lakes in central and northern Alberta showed that there was no relationship between microcystin and potassium, calcium, magnesium and chloride (Kotak et al., 2000). Therefore, studies have shown that iron and zinc were shown to increase microcystin concentrations as well as aluminum, cadmium, calcium, chloride, chromium, manganese, potassium and tin had no effect on microcystin.

1.3.2 Physical Factors

Low light intensities, shallow Secchi disk depths and high turbidity have shown to be associated with cyanobacterial growth as well as have a positive or a negative effect on toxin release. Light intensity from 15 µE/m^2/s to 100 µE/m^2/s at 15°C did not affect toxin production in *Microcystis viridis* culture (Song et al., 1998). Furthermore, at 25°C it was shown that light intensity was negatively correlated with toxin production where the high light intensity of 100 µE/m^2/s gave a lower toxin content (1.97 µg mg dry cells) compared to low light intensities where at low light intensity 15 µE/m^2s gave a high toxin content (3.13 µg/mg dry cells) (Song et al., 1998). Toxin production had been negatively affected by light intensity in a culture of *Microcystis aeruginosa* where low toxin content occurred at higher light intensities (100 µE/m^2/s) and lower light intensities (15 µE/m^2/s)

had higher toxin content detected (Song et al., 1998). It was shown in cultures of strain 97 of *Oscillatoria* strains that low light intensities (12 and 24 μE/m^2/s) had higher toxin production (6 to 8 mg/g), which may be due to light or the behavior of the different strains and species (Sivonen, 1990). In *Planktothrix agardhii* cultures, a positive relationship occurred where higher toxin concentrations occurred at low light intensities of 12 and 24 μmol photons/m^2/s rather than at higher light intensities of 50 and 95 μmol photons/m^2/s (Salvador et al., 2016). *Planktothrix agardhii* cultures in a 2005 study showed the opposite where total microcystin concentrations increased with higher light intensities of 60 μmol photons/m^2/s as well as toxin concentrations decreased with light intensities of greater than 100 μmol photons/m^2/s (Tonk et al., 2005). In *Microcystis aeruginosa* cultures, a small effect on toxicity occurred with light intensities of 20 and 30 μmol photons/m^2/s (Salvador et al., 2016). Overall studies have shown that different cyanobacteria species react to a variety of light intensities, which can increase microcystin concentrations.

Turbidity and Secchi disk depth are measures of clarity in the water and material such as sand, silt, clay, algae, organic and inorganic matter and other organisms can cause higher turbidity levels. A study on Buckeye Lake, Harsha Lake and Lake Erie in 2014 showed positive correlations between turbidity in situ measurements and microcystin concentrations ($p=0.62$, 0.73 and 0.80) (Francy et al., 2016). Turbidity was strongly correlated with extracellular $p=0.96$) and total cellular microcystin concentrations ($p=0.98$) in Lake Taihu in China in 2010 (Sakai et al., 2013). 13 lakes in northern and central Alberta, showed a weak positive correlation between turbidity levels and microcystin concentrations from 1990 to 1994 ($r=0.30$) (Kotak et al., 2000). In

two studies in Alberta on eutrophic and hypereutrophic freshwater lakes, it was found that cellular microcystin-LR was weakly correlated with the Secchi disk depth (r=-0.32 and r=-0.35) (Kotak et al., 1995, 2000). A study in 2014 on Buckeye Lake (r=-0.76), Harsha Lake (r=-0.69) and Lake Erie (r=-0.67) showed all negative correlations between microcystin concentrations and Secchi depth (ft) (Francy et al., 2016). Negative correlations, occur between microcystin concentrations and Secchi disk depth and weak and strong positive correlations between microcystin concentrations and turbidity levels.

Microcystin concentrations were higher in waterbodies when water temperatures were over 18°C and have shown positive or no relationships. Warmer water temperatures are optimal for cyanobacterial growth, therefore increased microcystin concentrations can occur with increased cyanobacteria biomass. *Microcystis aeruginosa* cells were more toxic when water temperature was at 20°C (25.4 mg/kg) and the toxicity in the cell was not reduced until temperatures were over 28°C (56-140 mg/kg) (van der Westhuizen & Eloff, 1985). However, it was shown that the cell toxicity occurs to be highest between 18°C and 25°C for *Microcystis aeruginosa* (Sivonen, 1990; Lukač & Aegerter, 1993). Higher production of toxins occurred at an optimum temperature of 25°C for one *Oscillatoria agardhii* strain and at temperatures of 15, 20 and 25°C for another strain as well as 30°C had low toxin production for both strains (Sivonen, 1990). In Coal, Driedmeat and Little Beaver lake in Alberta where temperature was not correlated with microcystin-LR (r=0.02) (Kotak et al., 1995). A study in 2014 on Harsha Lake (r=0.59) showed a positive correlation between microcystin concentrations and temperature where on Buckeye Lake (r=0.01) and Lake Erie (r=0.10) there was no/weak relationship (Francy et al., 2016). Water temperature showed to increase the

release of microcystin from *Planktothrix agaradhii* cultures ($P<0.001$) and showed that greater production of toxins are released at temperatures between 20 and 25°C (Walls et al., 2018). Therefore, studies have shown that higher microcystin concentrations occur with warmer water temperatures during summer months (18°C to 25°C).

1.3.3 Biological Factors

Studies looking at correlations between cyanobacteria densities and microcystin concentrations were found to be reported as either no, weak or strong relationships. When an algal bloom is in decline, toxin concentrations may still be present in the water at the same or higher amounts than what was present when the algal bloom was at its peak (Jones et al., 1998). In 1996, a Manitoba study sampling farm dugouts, Pelican Lake and municipal water supplies found that there was a weak correlation between total cyanobacteria density and microcystin-LR ($r=-0.23$) (Jones et al., 1998). In Brandenburg Germany there are high nutrient levels in particular high P and it was found that particulate microcystin concentrations had a strong relationship with *Planktothrix agardhii* biovolumes ($r^2=0.89$) (Dolman et al., 2012). Intracellular microcystin concentrations demonstrated a strong negative relationship ($p<0.001$) with cell volume as well as it was found that there were higher concentrations of microcystin in smaller cells compared to larger ones (Long et al., 2001). *Pseudoanabaena* biomass had a weak positive correlation ($r=0.55$) with microcystin concentrations in a study (Ruiz et al., 2013). The increase in growth rate of cell volumes of *Microcystis aeruginosa* gave a decrease in the size of cells (Long et al., 2001). As growth rate increased, there was a linear increase in microcystin represented as a cell dry weight ratio but was at its maximum once the algae reached the intermediate rate of growth (Long et al., 2001).

There was a weak positive correlation between *Anabaena* biomass and microcystin concentrations (r=0.40) on a study area of 30 eutrophic and hypereutrophic lakes in the lower and middle reaches of the Yangtze River in China (Wu et al., 2006). A study on 13 northern and central Alberta lakes from 1990 to 1994 showed no significant correlations between microcystin concentrations and *Anabaena flos-aquae* (r=-0.03) and *Aphanizomenon flos-aquae* (r=0.07) (Kotak et al., 2000). A study on Bear and Muskegon Lake in 2010 showed a weak positive relationship between *Aphanizomenon aphanisomenoides* and microcystin concentrations (r^2=0.312, p=<0.001) (Xie et al., 2016). There was no significant relationship between microcystin concentrations and phytoplankton species biomass or abundance in net or whole samples (Kotak, 2009). Correlations between microcystin and phytoplankton abundance show to either have a positive, negative or no relationship which may be due to the stage of the bloom whether it's the beginning or end of the cycle.

1.4 Lake Winnipeg and its Watershed

Created by the melting of the Laurentide glaciers 13,000 years ago, Lake Winnipeg is the tenth-largest freshwater lake by surface area in the world and is the largest lake in Manitoba (Environment Canada & Manitoba Water Stewardship, 2011). Lake Winnipeg lies on the boarder of Paleozoic and Archaean deposits where the western shores are composed of Paleozoic dolomites and limestones and the eastern shores are composed of granite (Bajkov, 1930). The south basin runs from the northern part of the Netley-Libau Marsh and the mouth of the Red River to the south portion of Black and Hecla Island while, the north basin runs from the northern part of Beren's island to the north shore (Environment Canada & Manitoba Water Stewardship, 2011).

The three main watersheds that flow into the lake are the Red, Winnipeg and Saskatchewan River as well as smaller rivers such as Berens, Bloodvein, Brokenhead, Dauphin, Manigotagan, and Poplar River flow into the lake with the Nelson River and Two-Mile Channel draining Lake Winnipeg eventually into Hudson's Bay (Crowe, 1972a). The mean depths in the north and south basin average at 13.3 and 9 m as well they are shallow compared to the Great Lakes where the average depths are above 19 m and have maximum depths over 64 m (Environment Canada & Manitoba Water Stewardship, 2011; Canada, 2017) (Table 2).

The Lake Winnipeg watershed is the second largest inter-jurisdictional watershed in Canada and is roughly 950,000 km^2 in area. The Lake Winnipeg watershed extends from the Canadian Rockies of Alberta through Saskatchewan and Manitoba to Lake Superior in Ontario as well as parts of North Dakota, South Dakota, Montana and Minnesota (Lake Winnipeg Stewardship Board, 2006) (Figure 1). The Lake Winnipeg watershed is composed of mainly the Saskatchewan, Red and Winnipeg River sub-watersheds. The Saskatchewan River makes up 40% of the Lake Winnipeg watershed, followed by the Red River sub-watershed at 31% and the Winnipeg River sub-watershed at 17% (Environment Canada & Manitoba Water Stewardship, 2011). The ratio of Lake Winnipeg's area (23,750 km^2) to the Lake Winnipeg watershed area (1,000,000 km^2) is 1:42 compared to the ratio of Lake Erie's area (25,700 km^2) and the Lake Erie watershed area (78,000 km^2) is 1:3 (Environment Canada & Manitoba Water Stewardship, 2011; Canada, 2017).

The Lake Winnipeg watershed is mainly composed of a portion of Canada and the United States human population and is influenced by human activities such as

farmland and hydroelectric development. There are roughly 6.7 to 6.9 million people from Canada and the United States are living within the Lake Winnipeg watershed, where the large majority of those people are located in a large cities such as Winnipeg, Calgary, Edmonton and Fargo (Environment and Climate Change Canada & Manitoba Agriculture and Resource Development, 2020). The watershed is dominated by agriculture land use which covers 500,000 km^2 of the area as well as 65% of the area is crop land (Environment and Climate Change Canada & Manitoba Agriculture and Resource Development, 2020). In 2006, 97 million tonnes of manure from cattle, pigs and sheep were produced in the Canadian portion of the Lake Winnipeg watershed (Environment Canada & Manitoba Water Stewardship, 2011). The increase of nutrients coincided with increased livestock production in the Red River Valley as well as an increase in the spring flooding frequency and intensity by transferring P from land to the lake (Schindler et al., 2012). Lake Winnipeg is also the largest hydroelectric reservoir in North America and third largest in the world (Environment Canada & Manitoba Water Stewardship, 2011).

1.5 History of Water Quality of Lake Winnipeg

Since the 1800s, the south and north basin of Lake Winnipeg has suffered from cyanobacteria algal blooms during the open water season that can degrade the structure of aquatic food webs, negatively affect recreation and tourism due to fouled beaches and nearshore areas and threatened drinking water in many communities.

There have been many studies on Lake Winnipeg dating back to the 1800s to 1960. The Red River Expedition by Captain G. L. Huyshe stated that there was green confervoid growth in the south basin of Lake Winnipeg (Huyshe, 1871). Summer bloom-

forming Cyanophytes and Chlorophytes from biochemical fossils were relatively constant during the 19th century, then increased 300-500% up until 1980 then have decreased since 1990 (Bunting et al., 2016). Throughout the 200-year record, *Anabanea* species microfossils were 10-fold more abundant than *Aphanizomenon* species, where an ecosystem state change occurred around 1990 and algal abundance has increased 3 to 5-fold during the 20th century (Bunting et al., 2016). A micrograph from a mid-summer algal sample in 1924 showed a population of a few cyanobacteria (*Anabaena*), some dinoflagellates (*Ceratium furcoides*) and mostly centric diatoms (*Aulacoseira* and *Stephanodiscus* species) (Kling et al., 2011). In the 1920s', Bajkov collected lake-wide over 500 chemical and biological samples as well as described *Aphanizomenon* and *Anabaena* blooms "as thick as carpets" in regions of the lake (Lake Winnipeg Research Consortium, 2008; Kling et al., 2011). A sediment core taken in the north basin in 1994 showed an increase in chlorophyll *a*, P and C since the late 1950s, this follows the Saskatchewan River hydro-electric development in the 1960s, the regulation of lake levels in 1976 and the increasing agricultural development within the Lake Winnipeg watershed (Kling et al., 2011).

Many studies arose on Lake Winnipeg in the 1960s looking at phytoplankton and limnological parameters. A study done in 1963 and 1964 showed diatoms such as *Asterionella*, *Fragilaria*, *Melosira*, *Synedra* and *Tabellaria* were the dominant phytoplankton found in 93% of the samples taken on Lake Winnipeg as well as the north basin had little thermal stratification (Rybicki, 1966). The effects of pollution in the south basin of Lake Winnipeg are confined to the southern portion of the basin (Crowe, 1972a). Another study from 1962 to 1969 from March to September in the south basin

showed concentrations of chloride, calcium and iron were higher in 1969 than in 1930 as well as maximum concentrations were reported in 1966 and 1967 (Crowe, 1972b). In 1969, Secchi disk maximum values such as 2-3.5 m occurred in the center of the north basin and lower values such as 0.1-0.2 m occurred in the Red River (Brunskill et al., 1979). Most of the light transmission data was correlated with concentrations of suspended sediments where high amounts of suspended sediments were around the Red River and southwestern part of the south basin and low amounts were found in the narrows and north basin (Brunskill et al., 1979). During times where there is prolonged hot and calm weather, surface algal bloom begin to appear as well as thermal stratification (Brunskill et al., 1979).

The CCGS *Namao* was built in 1975 in Riverton, Manitoba to serve vessels in distress as well as deploy and recover navigation buoys on Lake Winnipeg. In 1998 and 1999, the Department of Fisheries and Oceans (DFO) and the Lake Winnipeg Research Consortium (LWRC) made an agreement to use the Canadian Coast Guard Ship (CCGS) *Namao* for scientific research purposes on Lake Winnipeg and in August of 1999, a science survey of the whole lake was completed (Lake Winnipeg Research Consortium, 2005) (Appendix Table 1). The CCGS *Namao* was used for research in 1994 and 1996 by the Geological Survey of Canada to look at the geological history of Lake Winnipeg (Lake Winnipeg Research Consortium, 2005). In 2005, ownership of the CCGS *Namao* was transferred to the LWRC from DFO/CCG and the class of the ship was changed to (Motor Vessel) MV *Namao* (Lake Winnipeg Research Consortium, 2005).

On Lake Winnipeg, limnological studies continued from 1970 to 2000 where a few surveys occurred on the CCGS *Namao*. A study in 1974 showed the following phytoplankton phyla were present in the north basin of Lake Winnipeg: Chlorophyta (25.6%), Cyanophyta (33.5%), Chrysophyta (34%) and Pyrrophyta (6.9%) (Derksen & Hangasjarvi, 1979). The north basin has limited suspended sediments and nutrients than the south basin and the nutrients could be the limiting factor for the growth of phytoplankton (Derksen & Hangasjarvi, 1979). From 1969 to 1974, it was found that Lake Winnipeg was not characteristically a eutrophic lake but between an oligo- to mesotrophic lake despite the different flora and fauna in the north and south basin and the high rate of nutrient supply (Brunskill & Elliott, 1973). A hypothesis from the report states that algal growth in Lake Winnipeg (especially in the south basin) was limited by turbidity (light penetration) and not the excess amounts of nutrients present (Brunskill & Elliott, 1973). Since the 1969 lake-wide study, diatom bloom abundance and duration have been reduced and since 1999, bloom composition is presently about 90% cyanobacterial taxa during mid to late summer (Kling et al., 2011). There has been an increase in the frequency of surface algal blooms on Lake Winnipeg since the mid-1990s, as indicated by satellite remote sensing and production has increased, as indicated by the paleolimnological analysis of sediment cores from lake-wide surveys, over the last 50 years (Kling, 1998).

Lake Winnipeg monitoring was implemented during the 1997 flood to examine short-term and long-term environmental impacts, ensure that floodwater quality does not affect recreation and aquatic and wildlife habitats. Agencies involved in this study were the federal DFO and Environment and Climate Change Canada (ECCC), the

provincial Manitoba Agriculture and Resource Development (MARD) and state United States Geological Survey (USGS), Minnesota Pollution Control Agency (MPCA) and North Dakota Department of Health (NDDH) (Currie et al., 1998). Sources of potential contamination were release from municipal wastewater treatment plants, municipal flooding of sewage lagoons, private septic field and tanks flooded livestock holding areas, manure storage areas and feedlots as well as industrial distribution and manufacturing processes (Currie et al., 1998). During the peak of the 1997 flood, at the Red River at Selkirk site, discharge concentrations of total suspended sediment, P and N had reached peak rates of >50,000, 202 and 896 metric tonnes/day around the end of April as well a peak discharge of 4,587 m^3/s occurred on May 4, 1997 in Winnipeg, MB (Currie et al., 1998). Nutrients and sediment entered Lake Winnipeg from the Red River due to wet soil conditions, excessive snow accumulation and a blizzard that occurred during the snow melt period (Currie et al., 1998; Lake Winnipeg Research Consortium, 2008; Environment Canada & Manitoba Water Stewardship, 2011).

More studies and monitoring have occurred on Lake Winnipeg for the microcystin toxin from 2000 to present. Microcystin concentrations were mainly reported as non-detects (detection limit of <0.10 µg/L) but when microcystin was detected in whole water pelagic zone samples from 1999 to 2007 in Lake Winnipeg, they were lower than the water quality guideline of 20 µg/L (Environment Canada & Manitoba Water Stewardship, 2011). Microcystin values ranged from <0.10 to 2.31 µg/L on Lake Winnipeg in 2007 (Kotak, 2009). Since 1999, only a few microcystin samples in the north basin have gone over the water quality guideline (Environment Canada & Manitoba Water Stewardship, 2011). High microcystin concentrations from the nearshore or beach have been

sporadic during intense algal blooms but mainly all algal blooms were under the water quality guideline of 20 µg/L (Environment Canada & Manitoba Water Stewardship, 2011). Spring phytoplankton blooms have consisted mainly of centric diatom genera such as *Aulacoseira*, *Cyclostephanos* and *Stephanodiscus* as well as araphid genera such as *Asterionella*, *Diatoma*, *Fragilaria* and *Tabellaria* (Kling et al., 2011). During the summer, blooms in the south basin are dominated by non-N-fixing taxa such as *Microcystis* and *Planktothrix* while the north basin is dominated by N-fixing genera (*Anabaena* and *Aphanizomenon*) (Kling et al., 2011). By the fall time, centric diatoms begin to re-appear as well as cyanobacteria blooms from the summer can persist into the fall sometimes as late as November comprising mainly of *Aphanizomenon* species (Kling et al., 2011). Over 80% of the phytoplankton in Lake Winnipeg are the N-fixing cyanobacterial genera *Aphanizomenon* and *Anabaena*, the non-N-fixing genus *Microcystis* and diatoms where the cyanobacteria algae have the potential to release harmful toxins such as microcystin (Environment Canada & Manitoba Water Stewardship, 2011).

1.6 Nutrient Concentrations and Loading

P and N concentrations on Lake Winnipeg are higher in the south basin compared to the north basin. P had a decline in concentrations from the early 1970s to around 1991, then a rise in concentrations occurred during the flood of 1997 followed by stable concentrations after that (McCullough et al., 2012). Total P concentrations during the summer of 1969 averaged around 0.034 mg/L but due to numerous nutrient loading to the lake, concentrations of total P have since increased from 0.029 mg/L between 1971 to 1980 to 0.045 mg/L between 1996 to 2005 (McCullough et al., 2012; Benoy et

al., 2016). N concentrations had no clear pattern and large variability from year to year which can be due to denitrification and N fixation processes, wind-reduced suspension, N loading from Lake Winnipeg tributary rivers and internal loading (Government of Manitoba, 2019). From 1999 to 2016, P and N concentrations in the north basin have been hovering around the total P objective of 0.05 mg/L and total N objective of 0.75 mg/L (Government of Manitoba, 2019). In the south basin, concentrations are roughly 2 times higher than the objective for total P and just above the objective for total N (Government of Manitoba, 2019). Studies and data have shown that P and N concentrations are higher in the south basin compared to the north basin with large variability from year to year.

The Red River is the largest P-loading source in Lake Winnipeg with the Winnipeg, Saskatchewan and Dauphin River only accounting for 25%. On average from 1994 to 2016, the total P annual contribution was 7,368 tonnes per year (t/y) where the range of P annual loads into Lake Winnipeg were 3,093 to 10,932 tonnes of P (Environment and Climate Change Canada & Manitoba Agriculture and Resource Development, 2020). The Red River is the single largest contributor of P to Lake Winnipeg with the long-term average of 5,073 tonnes or 69% of the annual load of P per year where the Winnipeg, Saskatchewan, Dauphin and East side Rivers account for only 24% (Environment Canada & Manitoba Water Stewardship, 2011; Government of Manitoba, 2019). The Winnipeg, Saskatchewan and Dauphin River account for a long-term average of 1,051, 401 and 81 tonnes of P (Environment Canada & Manitoba Water Stewardship, 2011; Government of Manitoba, 2019). In the Red River, annual loads of total P have increased by 130% and concentrations have increased by 20% due to

higher flows (McCullough et al., 2012; Benoy et al., 2016). In Winnipeg, where the Red and Assiniboine Rivers meet, it was estimated that 68% of the total P comes from the Red River and 14% of the total P comes from the Assiniboine River, with the remaining total P coming from downstream the city of Winnipeg (Environment Canada & Manitoba Water Stewardship, 2011; Benoy et al., 2016). Since the mid-1990s, runoff from the Red River watershed has rose rapidly and the decadal mean discharge of P has been more than 50% higher than any earlier decade (McCullough et al., 2012). The Red River is a large contributor of P to Lake Winnipeg, especially the south basin.

N loading in Lake Winnipeg comes mainly from the Red and Winnipeg River as well as a large portion comes from N fixation and atmospheric deposition. From 1994 to 2016, a total N annual load of 91,263 t/y was transported into Lake Winnipeg as well as N annual loads ranged from 31,280 to 136,676 tonnes of N (Environment and Climate Change Canada & Manitoba Agriculture and Resource Development, 2020). The long-term average of approximately 31,500 t/y of total N were from the Red-Assiniboine River basin from 1994 to 2016 (Environment Canada & Manitoba Water Stewardship, 2011; Government of Manitoba, 2019). Upstream where the Red and Assiniboine Rivers meet in Winnipeg, it was estimated that 34% of the total N comes from the Red River and 22% of the total N comes from the Winnipeg River, with the remaining N coming from other smaller systems between Winnipeg and the outlet to Lake Winnipeg (Environment Canada & Manitoba Water Stewardship, 2011; Benoy et al., 2016). The Winnipeg River accounts for 22% of the total N loads into Lake Winnipeg, where the Saskatchewan, Dauphin and East side Rivers account for 12, 6 and 5% of total N loads (Environment and Climate Change Canada & Manitoba Agriculture and Resource

Development, 2020). The Winnipeg, Saskatchewan and Dauphin River account for a long-term average of 20,530, 10,730 and 5,412 tonnes of N (Environment Canada & Manitoba Water Stewardship, 2011; Government of Manitoba, 2019). N loading into Lake Winnipeg is also accounted for by atmospheric deposition (10%) and N fixation (10%) (Environment and Climate Change Canada & Manitoba Agriculture and Resource Development, 2020).

1.7 Conclusion

Cyanobacterial algae blooms are of rising concern all over the world because of their increasing abundance and toxin release. Studies have shown that many chemical, physical and biological parameters have an influence on the amount of cyanobacteria biomass and toxin production. Total N, nitrate and ammonia had positive correlations with microcystin and nitrate, nitrite and ammonia were found to have negative correlations with microcystin. Total P, total dissolved P and orthophosphate had positive correlations in the literature with microcystin suggesting that with an increase of P, an increase in microcystin will occur. High water temperatures (18 to 25°C) and lower light intensities are associated with elevated microcystin concentrations. Studies shown that there are positive, negative or no relationships between microcystin concentrations and phytoplankton biomass where *Anabaena*, *Apanizomenon* and *Microcystis* are the most common cyanobacteria in freshwater blooms. There have also been studies that have shown that cyanobacteria thrive in freshwater lakes with a lower N:P ratio.

There has been an increase in monitoring and studies on Lake Winnipeg from the 1990s to present looking at limnological parameters, sediment, aquatic invasive species, fish populations and algal blooms. The Lake Winnipeg watershed is the second

largest watershed in Canada with nutrient loading coming from four provinces and four states. Large amounts of P and N enter Lake Winnipeg from urban runoff, land fertilizers, atmospheric deposition, industrial and municipal wastewaters. Lake Winnipeg is considered hypereutrophic in the south basin and narrows and eutrophic in the north basin (Environment and Climate Change Canada & Manitoba Agriculture and Resource Development, 2020). More recently there has been consistent monitoring and studies done on Lake Winnipeg from provincial and federal agencies as well as academia. The south and north basin of Lake Winnipeg suffers from cyanobacteria algal blooms during the open water season that can degrade the structure of aquatic food webs, negatively affect recreation and tourism due to fouled beaches and nearshore areas and threaten many communities of their drinking water. With the large size of the Lake Winnipeg watershed compared to the shallowness of the lake as well as the land use intensity, this can cause increases in anthropogenically-derived elements that cause stress and push the lake's ecosystem beyond levels at which Lake Winnipeg can mediate and assimilate (Lake Winnipeg Stewardship Board, 2006; Environment Canada & Manitoba Water Stewardship, 2011).

1.8 Objectives

We currently do not know the main drivers of algal blooms that occur on Lake Winnipeg. Lake Winnipeg is shallow, with a mean depth of 13.3 and 9 m in the north and south basins and a volume of 284 km^3, and is polymictic (well mixed) (Environment and Climate Change Canada & Manitoba Agriculture and Resource Development, 2020). There are higher concentrations of the microcystin toxin in the nearshore as well as the offshore where there are very abundant amounts of algae present. Future studies

regarding if there is a transfer of microcystins from lower to higher trophic levels in the food web should be researched. More studies need to be done on Lake Winnipeg investigating the different kinds and concentrations of neurotoxins present. More research should be completed in isolating specific genes that could be responsible for the production of the microcystin toxin in cyanobacteria species. This study is important in determining the environmental parameters capable of causing cyanobacteria algae to produce the microcystin toxin, which can potentially be harmful to human health. High levels of algal toxins within the offshore and nearshore areas can produce potential health risks for adults and children. In the future, this study can help identify parameters associated with these harmful algal blooms as well as make beaches and nearshore areas safer for communities and people on Lake Winnipeg.

1. To determine which of many chemical, physical and biological parameters measured during routine monitoring on Lake Winnipeg over the past two decades are most closely associated with microcystin concentrations.

2. To examine the correlation, if any, between the N:P ratio in Lake Winnipeg and microcystin concentrations.

1.9 Hypotheses

1A. I hypothesize that as P and N are essential nutrients in algal production, there will be a positive correlation between P and microcystin concentrations. There will be a negative correlation between N and microcystin concentrations because many of the toxin-producers are also N-fixing cyanobacteria taxa, so they may not be affected negatively by a low N concentration.

1B. Increased turbidity is often associated with cyanobacterial success, so there will be a positive correlation between turbidity levels and microcystin concentrations.

1C. *Anabaena* and *Microcystis* are known to release the microcystin toxin, there will be a positive correlation between *Anabaena* and *Microcystis* and microcystin concentrations.

2A. I hypothesize that because most cyanobacterial taxa causing algal blooms can fix N and therefore can thrive at low levels of ambient N but cannot obtain P except from the surrounding environment, there will be a negative correlation between microcystin concentrations and N:P ratio.

Figure 1. Lake Winnipeg Watershed (Environment Canada & Manitoba Water Stewardship, 2011).

Table 1. Cyanobacteria genera present in Lake Winnipeg that produce toxins and toxicity (LD_{50} is the amount of toxin given at once, which causes 50% of the deaths of the group of test animals). (Lyngbyatoxin=LBT; Aplysiatoxin=APT; Lipopolysaccharides=LPS; Cylindrospermopsin=CYL; Microcystin=MC; Nodularin=NOD; Anatoxin=ANA; Neosaxitoxin=NEOS; Saxitoxin=SAX) (Edwards et al., 2008; Fristachi et al., 2008; Graham et al., 2008a, 2008b, 2010; Cheung et al., 2013; Jakubowska & Szeląg-Wasielewska, 2015).

	Dermatoxins			**Hepatotoxins**			**Neurotoxins**			
	LBT	**APT**	**LPS**	**CYL**	**MC**	**NOD**	**ANA**	**BMAA**	**NEOS**	**SAX**
Toxicity (LD_{50} based on mouse assays)	300 µg/kg	300 µg/kg	-	200-2100 µg/kg	25 to > 1000 µg/kg	50 µg/kg	20-250 µg/kg	-	-	10 µg/kg
Anabaena	-	-	X	X	X	-	X	X	X	X
Aphanizomenon	-	-	X	X	-	-	X	X	X	X
Aphanocapsa	-	-	X	-	X	X	-	-	-	-
Aphanothece	-	-	X	-	-	X	-	-	-	-
Chroococcus	-	-	X	-	-	-	-	-	-	-
Coelosphaerium	-	-	X	-	X	-	-	-	-	-
Gomphosphaeria	-	-	X	-	-	-	-	-	-	-
Limnothrix	-	-	X	-	X	-	-	-	-	-
Lyngbya	X	X	X	-	-	-	-	-	-	X
Merismopedia	-	-	X	-	X	X	-	-	-	-
Microcystis	-	-	X	-	X	-	X	X	-	-
Nostoc	-	-	X	-	X	-	-	X	-	-
Oscillatoria	X	X	X	-	X	-	X	X	-	X
Phormidium	-	-	X	-	X	-	-	-	-	X

Planktolyngbya	X	-	X	-	-	-	-	-	-	X
Planktothrix	X	X	X	-	X	-	X	X	-	X
Pseudanabaena	-	-	X	-	X	-	X	-	-	-
Snowella	-	-	X	-	X	-	-	-	-	-
Spirulina	-	-	X	-	-	-	-	-	-	-

Table 2. Morphometric data of Lake Winnipeg (Environment Canada & Manitoba Water Stewardship, 2011).

	South Basin	Narrows	North Basin	Total
Volume (%)	10	9	81	
Area (%)	11	15	74	23,750 km^2
Wide (km)	40	2.6	111	
Long (km)	-	-	-	436
Mean Depth (m)	9	-	13.3	
Maximum Depth (m)	-	60	-	
Water Level [1914-1976] (masl)	-	-	-	217.44
Water Level [1976-2007] (masl)	-	-	-	217.45
Average Euphotic Zone Depth (m)	0.5-0.6		0.9-2.1	

2.0 METHODS

2.1 Sampling Stations

The Water Quality Management Section (WQMS) under the Provincial Government has monitored Lake Winnipeg since 1999 to gain knowledge on the lake's chemical, physical and biological processes. Sampling on Lake Winnipeg during the open water season occurs on the CCGS/MV *Namao*, MV *Siggy Oliver* or various workboats and during the winter sampling via snowmobile, Bombardier and helicopter (Figure 2; Figure 3; Appendix Table 3). The routine long-term monitoring program samples Lake Winnipeg in the north and south basin four times a year (three times during the open water season and once during the winter) to assess long- and short-term changes in water quality. The MV *Namao* stops at many different stations such as W, auxiliary, nearshore and Coordinated Aquatic Monitoring Program (CAMP) stations (Appendix Table 4).

The WQMS Lake Winnipeg station network consists of 14 long-term W stations. The "W" in the name of long-term stations was added to distinguish the basic chemistry data sites (auxiliary) from the long-term monitoring data sites (W), where a more expanded suite of variables are analyzed. The stations W1 to W12 have been sampled since 1999 and stations W13 and W14 were added to the station network because of gaps in the geospatial distribution of sites, especially in the narrows region (Figure 4; Appendix Table 5). In 2006, W14 was initially sampled and W13 was initially sampled once in 2002 then consistently since 2006. The long-term W stations have been the most consistently sampled stations that provide information on Lake Winnipeg and not

only has a water quality suite of parameters, but also benthic invertebrate composition, and sediment chemistry and grain size.

The WQMS routinely sampled 51 auxiliary stations from 1999 to 2013 and in 2014, 27 auxiliary stations were removed to add nearshore stations to access the shoreline water quality and zebra mussel impacts. From 2014 to 2016, 19 of the 34 auxiliary stations the MV *Namao* visits were monitored by the WQMS and as of 2017, 24 of 34 auxiliary stations were monitored (Figure 4; Appendix Table 2).

There are 12 nearshore (NS) stations on Lake Winnipeg, seven in the south basin and narrows and five in the north basin. Nearshore stations 1NS and 2NS were added to the station network in 2012, 3NS to 13NS were added in 2014 and 10NS on George Island was only sampled in 2014 (Figure 4; Appendix Table 2). Nearshore stations in the south basin were chosen based off the ECCC nearshore sites created in 2008/2009 which would allow for pre- and post- zebra mussel colonization water chemistry comparisons. Nearshore stations in the north basin were chosen based on site access, geospatial distribution and general knowledge of the nearshore substrate and composition/nature of the shoreline.

Established in 2006, CAMP is a program run in conjunction with Manitoba Hydro and the Government of Manitoba to document the potential impact of hydroelectric generating systems from Manitoba Hydro (Manitoba & Manitoba, 2008). CAMP was designed to monitor the biological, chemical and physical aquatic components and gain an understanding of factors such as flooding and climate affect Manitoba's waterways over time that are housing hydroelectric operations (Manitoba & Manitoba, 2008). The need for a monitoring program to understand the effects of hydroelectric systems on the

aquatic environment was identified for the Washwatim generating system during the Section 35 Aboriginal Consultations (Manitoba & Manitoba, 2008). There are five CAMP stations near the two outlets of Lake Winnipeg: three nearshore stations, Warren Landing at the Nelson River (started sampling since the summer of 2012), Two-Mile Channel Inlet and Outlet (sampled since the spring of 2013) and two offshore stations, 22 and Big Mossy Point-10km SW of Two-Mile Channel (sampled since the spring of 2017) (Figure 4; Appendix Table 2).

Non-routine stations are areas on the lake that are not stopped at routinely and are sampled off the side of the MV *Namao*. Samples were taken at these areas in the north and south basin on Lake Winnipeg only if there was a large algal bloom present at that area of the lake (Figure 5; Figure 6).

The Clean Beaches Program was developed and has been operating since the early 1990s by MARD in conjunction with Manitoba Health. This program is run to make people using recreational waters in Manitoba aware of the current *E. coli* conditions and to reduce health risks (Manitoba Water Stewardship, 2011). The first beach to be sampled on Lake Winnipeg was Matlock beach on the west side because it was thought that the source of *E. coli* was from Winnipeg sewage and this beach was the closest on to the Red River outlet (Cassie McLean, Water Quality Specialist, personal communication, May 28, 2018). In the 1980s and 1990s, 10 beaches were sampled on Lake Winnipeg for *E. coli* and has since increased to 18 beaches (Environment Canada & Manitoba Water Stewardship, 2011). Only public beaches are monitored and were chosen on the east and west side of the lake based on historical bacteria data and recreational intensity (Cassie McLean, Water Quality Specialist, personal

communication, May 28, 2018). Most beaches on the east and west side of Lake Winnipeg have remained the same since the start of the program but there have been alterations to the beaches sampled over the years (Cassie McLean, Water Quality Specialist, personal communication, May 28, 2018) (Figure 7; Appendix Table 2). Beaches can be added to the Clean Beaches Program based on public demand, recommended by regional staff or the occurrence of recent events such as contamination spills (Cassie McLean, Water Quality Specialist, personal communication, May 28, 2018). Prior to 2003, beaches were sampled every two weeks but since 2004, beach sampling was increased to once a week at the Lake Winnipeg beaches (Environment Canada & Manitoba Water Stewardship, 2011). These sites are monitored weekly from June to the beginning of September for *E. coli* concentrations.

2.2 Sampling Experience

Sampling was done off the MV *Namao* for the WQMS, Wildlife and Fisheries Branch, ECCC, University of Manitoba as well as assisted with bacteria sampling with the Clean Beaches Program. I have been working on the MV *Namao* from the spring cruise 2012 to the fall cruise 2018 with additional training days in the spring cruise from 2019 to present. With the WQMS, sampling was done for water and sediment quality as well as benthic invertebrates. In addition to WQMS sampling, additional assistance was done for the Natural Resources and Northern Development departments Wildlife and Fisheries Branch fish trawls to assess forage fish species, zooplankton hauls for Spiny Waterflea and zebra mussel veligers as well as deploying and retrieving zebra mussel substrate samplers to determine their presence. ECCCs Seabird Rosette was ran to profile the offshore stations and collected water samples for many agencies and the

University of Manitoba. Samples were taken at the two lake outlets (Warren's Landing and Two-Mile Channel) for water and sediment quality on behalf of North/South Consultants. With the Clean Beaches Program, samples for *E. coli* on the east and west side of Lake Winnipeg were taken from 2012 to present.

2.3 Field Sampling

2.3.1 Field Equipment

An integrated tube sampler has been used since the early 2000s and is used to take a sample of the entire euphotic zone (1% light penetrance) at all 14 W stations during the spring, summer and fall surveys. The integrated tube sampler was added to take euphotic water samples to better characterize the long-term effects in the euphotic zone as well as the long-term results are more representative of change over time. Surface blooms forming during calm warm weather can alter the lake surface water chemistry. Euphotic zone sampling can eliminate any surface water effects that may not be representative of what is present in the euphotic zone during periods of calm warm weather in the summer months. This method involves using an 8 m long, 1 1/2" diameter tube with a one-way valve at the bottom end of the tube and a 15-liter Nalgene bottle into which the water is transferred (Figure 8). Once the integrated tube sampler is filled with water to the appropriate depth, it is pulled up onto the front deck of the MV *Namao*, then the open end of the sampler is put into the top of the Nalgene bottle and emptied. The integrated tube sampler and Nalgene bottle are rinsed out three times with lake water from that site prior to use.

DO is sampled within the euphotic zone with a DO sampler. The sampler is then lowered into the water at a constant rate until the desired depth (the euphotic zone) has been reached, then brought back up to the surface at the same rate (Figure 9).

The Seabird Rosette was used at the auxiliary stations to take a surface and bottom sample and at the W stations to take a bottom sample (Figure 12). The Seabird Rosette is lowered until the top caps of the canisters are just under the surface of the water. The canister top and bottom caps are released from the Seabird lab on the top deck of the MV *Namao* and the water sample is contained in the Seabird Rosette canisters.

Algal blooms at auxiliary stations were sampled off the side of the MV *Namao* using a weighted sampler. The weighted sampler consists of a 1L Nalgene bottle with a stainless-steel weight that is lowered into the water column just under the surface from 0-0.5m (Figure 10). Each surface test bottle was filled from the weighted sampler. The weighted sampler was rinsed out three times with lake water from that site prior to use.

Algal blooms at nearshore, CAMP nearshore and the Clean Beaches Program sites were sampled using the hand-dip method by lowering each bottle just under the surface of the water. The nearshore and nearshore CAMP stations are sampled off the side of the workboat. The Clean Beaches Program sites are sampled at about the height of the sampler's thigh using the hand-dip method from approximately elbow depth (0-0.5m) using a sweeping motion which is according to the sampling protocols by Health Canada's Guidelines for Canadian recreational Water Quality (Whitman & Nevers, 2003) (Figure 11).

The field parameters Secchi disk, wind speed and direction and water temperature are taken at all sites on Lake Winnipeg. A Secchi disk depth was used to determine clarity of the water column at all stations on Lake Winnipeg from 2005 to 2017. Wind speed and direction was at all sites using the MV *Namao* weather station or a Kestrel anamometer. Water temperature was taken at the offshore stations using the MV *Namao* and workboat depth sensor as well a digital thermometer was used at the Clean Beach Program sites.

2.3.2 Field Sampling Procedure on the MV *Namao*

Working on the MV *Namao* as the WQMS student was a lot of work and needed a lot of preperation and organization. Loading the MV *Namao* with field equipment, sample bottles and personal items are done a week prior to the first day of sampling for the spring, summer and fall cruise. On loading day, organization is need as to where certain equipment goes, whether its in the cargo hold under the front deck, on the front deck, at the stern (back of the ship) or in the Seabird lab (on the top deck). Furthermore, organization of where the different tests/coolers are going in the cargo hold and setting up my room in the accommedations area. The crew are always helping the scientists move equipment, pass equipment or coolers down to the cargo hold, helping set equipment up or just chatting and catching up on time off between cruises or over the summer.

On the days of sampling, most science crew wake up roughly one hour before the MV *Namao* is going to depart from dock or anchor to make sure sampling conditions are safe and begin setting up equipment and bottles. Sailing depends on the weather, if the wind speed is 20+ knots or there is a large fetch coming from the opposite side of

the lake then it is a blow day and is demed unsafe to sail and sample stations. On days when we do sail, when the MV *Namao* is close to a sampling station, the deck hands drop the anchor slowly so when the anchor hits the bottom sediment it minimally suspends sediment compared to free falling the anchor. When the anchor is being lowered, the Seabird Rosette (taking caps off sensors) is being set up and field comments/conditions are taken about the site. The Seabird Rosette is a water sampler and a multi parameter water quality reader with many sensors (DO, conductivity, temperature, turbidity, chlorophyll *a*, PAR) and is owned by ECCC (Figure 12; Figure 13).

The first thing that is done when the MV *Namao* stops at a station is the LWRC field coordinator takes log of weather information and coordinates from the station and the Seabird Rosette profile is completed. This information is entered into the Seabird computer program for that specific site at the Seabird lab. When the Seabird Rosette is set up, the winch is used to move the Rosette over the edge of the MV *Namao* and lowered down to just under the surface of the water. The Rosette stays just under the water surface for about 5-10 minutes until the parameter readings are stable. During this time, the cannisters are released to trap water in the cannisters for any agency or researchers who need surface water. The Rosette is then lowered slowly down the water column to about 1m above the station depth where the cannisters are released to trap water for bottom samples and the profile is stopped. If the Rosette is lowered any further than 1m above the bottom, there is a chance of hitting the bottom and stirring up the sediments. If this does happen, the Rosette is brought back up to the surface, the sediment is cleaned off and the bottom samples are to be taken again. The Rosette is

brought back onto the top deck of the MV *Namao*. If this is an auxiliary station, sampling is complete, the Rosette sensors are capped and the profiles are saved. If this was a W station then the DO sampler and integrated tube sampler would be used next on the front deck to get a euphotic surface sample.

After running the Seabird Rosette, the integrated tube sampler and DO sampler are used on the front deck. The integrated tube sampler is rinsed out three times before taking the station water sample. The tube sampler is then lowered to the euphotic zone (aquired from the Rosette) and emptied into a Nalgene bottle until there is enough water to fill the surface test package.

The last sample of the station is a sediment sample which is collected at the stern of the ship. Some cruises for Fisheries and Wildlife Branch, a Spiny Water Flea and Zebra Mussel veliger samples are taken in behalf. Deck hands lower the ponar dredge three times to get three sediment samples that are then pooled into one sample. After all samples are taken, the MV *Namao* starts to head to the next station, dock or anchor. While the MV *Namao* is enroute, sample bottles are filled with water and preserving some of bottles with acids, putting equipment away/getting it ready for the next station or washing out the sediment for benthic invertebrates (Figure 14; Figure 15; Figure 16).

Nearshore samples are taken from the workboat that is lowered off the side of the MV *Namao*. The wind speed and wave fetch is taken into account to make sure that the conditions are safe to not only drive the workboat but lower it into the water. If the waves are too large, then the station is cancelled and we move on to the next station. If the nearshore station is a go, then the MV *Namao* anchors as close to the station as

possible, then the deck hands lower the workboat into the water with the crane. At the nearshore stations, water samples and a water quality meter are used. After the nearshore transect is complete, the workboat heads back to the MV *Namao* where it is brought back onto the front deck and tied down.

Once all sampling is done for the day, lab paperwork is filled out, work stations are cleaned up and samples are taken to either the cargo hold fridge or put in coolers to take to the lab. If we are not docking at the Gimli pier, samples are placed in the fridges in the cargo hold to stay cool for the trip. If we are staying at Gull Harbour, Pine Dock or Victoria Beach, a WQMS employee or student meets us at the dock and picks up samples to take to the lab. If we are heading back to Gimli for the night, then all samples are packed into coolers with ice packs and driven to the lab.

After a cruise is complete, equipment stays on the ship in the cargo hold in between cruises and take it back to our warehouse after the open water sampling season is over. Any extra bottles are taken back to the office to be re-use for the next cruise. Personal items are taken home and a few rest days are taken off after the cruise and office tasks such as taking inventory of samples, typing out field notes, repairing equipment and calibrating water quality meters are completed.

2.4 Lab Analysis

Sample analysis of general chemistry, nutrients, metals, total microcystin concentration and phytoplankton species composition and biomass were done at several labs from 1999 to 2017 including Envirotest, Cantest and ALS laboratories. From the late 1990s to March 31, 2001, Envirotest (now ALS) analyzed any chemical, nutrient and metal parameters. From April 1, 2001 to March 31, 2009, Cantest (formerly

Maxxam Analytics, now Bureau Veritas) analyzed any chemical, nutrient and metal parameters and ALS analyzed any biological parameters. From April 1, 2009 to present, ALS analyzed both chemical, nutrient, metal and biological parameters (Appendix Table 4; Appendix Table 5). With the change in labs and parameter methods throughout time, this may cause results to be difficult to interpret.

In August of 2015, Dr. Gregory K. McCullough with the Centre for Earth, Observation and Science at the University of Manitoba did an analysis of inter-laboratory effects between Cantest and ALS on concentrations of P in rivers and lakes in Manitoba. Looking at 33 matched pairs, split-sample Lake Winnipeg and river dataset with total P concentrations lower than 0.2 mg P/l, Cantest reported total P and particulate P 12.5% and 37.4% higher than ALS and total dissolved P was not affected (McCullough, 2015). An indirect comparison using data from DFO showed that total P was 15% higher at Cantest than ALS (McCullough, 2015). Using other indirect data from the City of Winnipeg of more P-rich water (0.2-0.5 mg P/l) showed total P concentrations were around 30% higher at Cantest than ALS, where further studies need to be conducted with this range due to few samples were analyzed (McCullough, 2015). Total P Lake Winnipeg paired samples were on average 0.009 mg P/L higher at Cantest than ALS, TDP was not significantly different and TPP was 0.008 mg P/L higher at Cantest (McCullough, 2015). For four river paired samples, when total P was over 0.2 mg P/L, ALS reported higher or similar total P and particulate P but for lower total P values, Cantest reported higher values (McCullough, 2015). River paired observations, weren't significantly different between labs for total P and particulate P (McCullough, 2015). Total P averages for the Lake Winnipeg paired observations ranged between 0.03 and

0.32 mg P/L and averages in the paired river observations ranged between 0.01 and 0.69 mg P/L (McCullough, 2015). There were no paired samples from the April 1, 2001 to March 31, 2009 from ALS and Cantest. ALS and Cantest both used the same ammonium molybdate/potassium antimony tartate/ascorbic acid colorimetric method however, both labs used a different digestion method (McCullough, 2015). For the April 1, 2001 to March 31, 2009 data record, it is recommended that total P concentrations in Lake Winnipeg should be reduced by 12% and particulate P should be recalculated to the difference between total P corrected and total dissolved P (McCullough, 2015). The conversion of total P and total particulate P was not done in this study due to small sample size, differences between river and Lake Winnipeg paired samples and different procedures were done for the digestion step.

2.5 Statistical Analysis

2.5.1 Datasets

Chemical, physical and biological data were gathered from the Provincial Government of Manitoba's database. Data from 1999 to 2017 such as general chemistry, nutrients, metals and total microcystin were pulled from the Environmental Management System (EMS). Field data physical parameters and phytoplankton biomass and composition were added to each sample if there was data after the full dataset was pulled from EMS. Any parameter with multiple methods from 1999 to 2017 were combined into one column for each parameter. All metals sampled from July 2017 to October 2017 under the VMV codes 4761 to 4798, were converted from µg/L to mg/L to match the historical dataset units of mg/L. If total N was not calculated by Cantest or ALS, the parameters Nitrogen, Dissolved – NO_3 & NO_2 and Nitrogen, Total Kjeldahl

were added together to get a Nitrogen, Total value. Parameters such as (Nitrogen, Dissolved – NO_3 & NO_2; Phosphorus, Acid Hydrolyzable; Phosphorus, Total Dissolved and Phosphorus, Particulate) had instances where two results were attached to the sample from the lab re-running the analysis from a high to low range. The result that was analyzed under the low range detection limit was taken out of the dataset and the result that was analyzed under the high range detection limit was kept in the dataset. The parameter Oxygen, Biological Demand had five results that had a result of greater than (ex. G40, G50), which were taken out of the dataset due to the uncertainty of the result.

The full dataset was split into two datasets, euphotic and surface samples based on how it was sampled in the field. Within the euphotic dataset (samples taken within the area of the water column where light penetrates), there were 459 samples taken. Any parameter 10% or less of 459 (<46 samples) was taken out of the dataset and analysis. Within the surface dataset (samples taken within the first 0-0.5m of the water column), there were 196 samples taken. Any parameter with 10% or less of 196 (<20 samples) was taken out of the dataset and analysis.

There has been other individual parties and academia that have analyzed microcystin samples not included in this report from the north basin and south basin and narrows on Lake Winnipeg from 1999 to 2017 taken as whole water samples or with a

plankton net (Environment Canada & Manitoba Water Stewardship, 2011). I was present in sampling for microcystin concentrations from 2012 to 2018.

2.5.2 Long-Term changes in Water Quality 1999-2017

Long-term changes in water quality on Lake Winnipeg were examined using the following parameters, algae phylum, Cyanophyceae genera, chlorophyll *a*, microcystin, total N, total P, turbidity and N:P ratio. Data from all 14 W stations from 1999 to 2017 were split between the north basin and south basin and narrows. All four seasons (winter, spring, summer and fall) were averaged per year. The Cyanobacteria genera were averaged per year from the 14 W stations from 1999 to 2017 and were split between north basin and south basin and narrows and by the four seasons (winter, spring, summer and fall). The algae phylum and Cyanobacteria genera from the 14 W stations from 1999 to 2017 were split between the north basin and south basin and narrows and were averaged together for each phylum/genera found in Lake Winnipeg. For any values recorded as non-detects, half the detection limit was used in the changes in water quality analysis. Standard error bars were added to each average point on the figures. There are few averages that have no standard error bars on the figures, and this was due to there was only one sample was taken for that season and year. Any gap data on the figures was due to there was no data taken because the MV *Namao* was not running that cruise, or no winter sampling was completed for that year. Long-term changes in water quality figures were created in Microsoft Excel (2016).

2.5.3 Data Exploration

Data exploration was done using raw and log transformed euphotic and surface datasets using the eight-step protocol written by (Zuur et al., 2010). The eight-step

protocol looked at outliers, homogeneity, normality, zero values, collinearity, relationships between X and Y, interactions between the north basin, south basin and open water months and independence of observations (Zuur et al., 2010). I used the eight-step protocol to eliminate parameters and determine which parameters to use in the analysis. For any values recorded as non-detects, the full detection limit as the value was used. These graphs were created using R (R Core Team, 2021) with the packages lattice (Sarkar, 2008) and rcmdr (Fox et al., 2020).

2.5.4 Multi-Panel Scatterplots

Multi-panel scatterplots with Pearson correlation coefficients and trend lines plotted the response variable (microcystin) versus each covariate in the euphotic and surface data. This was done to show an explanatory correlation but ecological significance was not implied. I used log-transformed data of only detected microcystin concentrations. For any data that were non-detects, the full detection limit as the value was used. These graphs were created using R (R Core Team, 2021) with the package rcmdr (Fox et al., 2020) as well as using HighStatLib.R pre-written code from (Zuur et al., 2010).

2.5.5 Linear Discriminant Analysis (LDA)

A linear discriminant analysis is a technique used for dimension reduction and feature extraction (Ye et al., 2004). The goal is to remove the dependent and redundant features by transforming these features from a space with higher dimensions to a lower dimensional space (Tharwat et al., 2017). The continuous variables were chosen based on the following assumptions. The data were first tested for normality (bell shaped curve) and linearity (the relationship between the predictor variable and natural log of

these probabilities are linear) by creating histograms and scatterplots for each parameter. Parameters were log transformed based on whether the data was following a normal distribution. Independence of observations was tested with the remaining parameters by creating multi-panel scatterplots with the Pearson correlation coefficients where if two parameters were correlated above 0.4 or below -0.4, only one of those parameters was chosen for this analysis. Collinearity was tested by looking at the variance inflation factor (VIF) where all parameters were under a value of 2 indicating that between the predictor variables in the model, there was a moderate correlation but not enough to affect the analysis (Zuur et al., 2010).

Using microcystin concentration as the dependent variable, the euphotic dataset had 7 out of 98 independent parameters (*Anabaena* biomass, Cyanobacteria species richness, *Pseudoanabaena* biomass, total boron, DO, total P and wind speed) chosen for this analysis. The surface dataset had 4 out of 41 independent parameters (N:P ratio, pH, total P and wind speed) chosen for this analysis. Microcystin data were separated into three groups for this analysis: below-microcystin values were below 0.2 µg/L, middle-microcystin values were between 0.21 and 1.5 µg/L and above-microcystin values were above 1.51 µg/L. The value 0.2 µg/L was chosen due to this is the minimum detection limit given for analysis at ALS Environmental. The value 1.5 µg/L was chosen due to this is the maximum acceptable concentration of microcystin in drinking water. For any data that were non-detects, the full detection limit as the value was used. Predictor variables were considered significant in the linear discriminant analysis if $p<0.05$. The linear discriminant analysis was run using R (R Core Team,

2021) with the packages lattice (Sarkar, 2008), mda (Hastie et al., 2020), MASS (Ripley & Vanables, 2002) and rcmdr (Fox et al., 2020).

2.5.6 Linear Model

2.5.6.1 Model Selection - Akaike Information Criterion (AIC)

The Akaike Information Criterion (AIC) is a mathematical method used to evaluate different possible models (different combinations of independent variables) and determine the one that best fits the data (Bevans, 2021). The AIC is calculated from the models maximum likelihood estimate and the number of independent variables used to build the model (Bevans, 2021). The best fitting model is the one that uses the fewest possible independent variables and explains the greatest amount of variation (Bevans, 2021). I chose this approach to determine the best predictive model in the euphotic and surface dataset. The best-fit AIC model is the one that explains the highest amount of variation while using the lowest number of independent variables (Bevans, 2021). AIC uses the maximum likelihood estimate and number of independent variables in the model to determine the relative information value of the model (Bevans, 2021). The independent variables chosen were from the linear discriminant analysis assumptions for both the euphotic and surface datasets (Table 3; Table 5). There were 10 models chosen for the euphotic dataset and six models were chosen for the surface dataset. Each model had either one or two independent variables (Table 4; Table 6). The AIC analysis was run using R (R Core Team, 2021) with the packages AICcmodavg (Mazerolle, 2020) and rcmdr (Fox et al., 2020).

I omitted Cyanobacteria species richness and *Pseudoanabaena* biomass models from the euphotic data because I focused on which dominant Cyanobacteria are

present that can release the microcystin toxin in Lake Winnipeg. I omitted the DO concentrations from the euphotic dataset because cyanobacteria do not need DO for growth; they consume it during the decomposition stage. I omitted the pH model from the surface dataset because I know that Lake Winnipeg has a pH between 6.93 and 9.1 looking at the 1999 to 2017 data and Cyanobacteria flourish with basic pH values of 7.5 to 10.

2.5.6.2 Hurdle Model

Hurdle models can help in handling over dispersion (variability in the observed data) due to excess zero observations, positive correlations or heterogeneity between variables by having a truncated count component, which models positive counts, and a hurdle component, which models zero versus larger counts (Zeileis et al., 2008; Andika et al., 2021). Interpreting the zero model, a binomial linear model was used and the count data was interpreted using a Gaussian GLM with an identity link. Models from the AIC analysis from the euphotic and surface data runs that had the best fitting model (lowest AICc values) were chosen for the binomial and gaussian GLM analysis. The Hurdle model analysis was run using R (R Core Team, 2021) with the packages statmod (Smyth et al., 2021) and rcmdr (Fox et al., 2020).

A McFadden's pseudo R-squared is a value calculated for a goodness-of-fit measure and to see how strong the predictor model is (Bartlett, 2014). Its calculation is $R^2_{McF} = 1 - \ln L(M_{Full}) / \ln L(M_{Intercept})$ where ln is the natural logarithm, L is the estimated likelihood, M_{Full} is the value of the likelihood function for the model being estimated and $M_{Intercept}$ is the likelihood for a model with no predictors (UCLA: Statistical Consulting

Group, 2011; Bartlett, 2014). Values over 0.4 indicate that the model fits well (Statology, 2022).

Models were evaluated using the k-fold cross validation method that uses different subsets of the training data then calculates the average prediction error rate (Kassambara, 2018). This method splits the data into k-subsets or k-fold, reserves a subset of the model and trains it on all other subsets, uses the reserved subset to test the model and repeats this process until each k-subset has been used as a test set (Kassambara, 2018). The following output occurs from the k-fold cross validation; R-squared (R^2), root mean squared error (RSME) and mean absolute error (MAE). The R^2 value represents the squared correlation between predicted values and observed outcome values (Kassambara, 2018). The RSME value measures the average prediction error by calculating the average between the known observed outcome values and the predicted values from the model (Kassambara, 2018). The MAE value is the average absolute difference between the observed and predicted outcomes (Kassambara, 2018). A k value of 6 was used in the k-fold cross validation where the higher the R^2 value and the lower RMSE and MAE, the better the model (Kassambara, 2018). Model assumptions were verified by Q-Q plots of residuals for each best predicted model from the AIC. The following R packages tidyverse (Wickham & Girlich, 2022) and caret (Kuhn et al., 2022) were used for repeated k-fold cross-validation.

Figure 2. Winter water quality sampling using a Bombardier on March 8, 2016 (photo taken by Elise Watchorn).

Figure 3. Winter water quality sampling using a helicopter on February 25, 2019 (photo taken by Elise Watchorn).

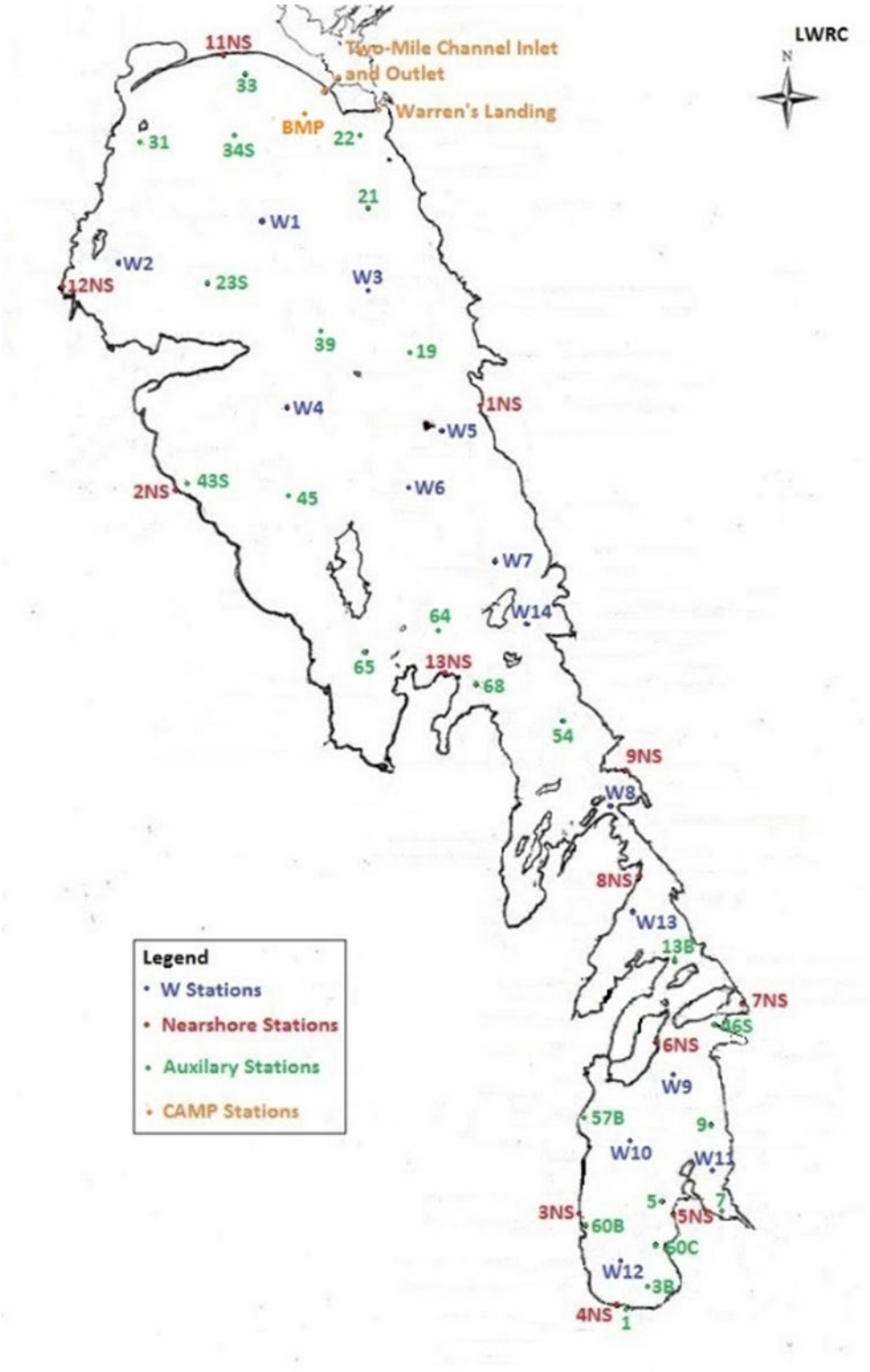

Figure 4. Map of all W, auxiliary, nearshore and CAMP stations on Lake Winnipeg.

Figure 5. Picture of cyanobacteria algal bloom on Lake Winnipeg (photo taken by Desiree Stratton).

Figure 6. Picture of another cyanobacteria algal bloom on Lake Winnipeg (photo taken by Desiree Stratton).

Figure 7. Map of Clean Beaches Program stations on Lake Winnipeg.

Figure 8. Picture of integrated tube sampler in use off the front deck of the MV *Namao*. The integrated tube sampler is used at all 14 W stations on Lake Winnipeg to get a euphotic sample. The euphotic depth is measured as the depth in the water column where 1% of light penetrates (photo taken by Marianne Geisler).

Figure 9. Picture of a DO sampler. The DO sampler is lowered down within the euphotic zone off the front deck of the MV *Namao* and used at all 14 W stations. The euphotic depth is measured as the depth in the water column where 1% of light penetrates (photo taken by Desiree Stratton).

Figure 10. Picture of a weighted sampler. The weighted sampler was used at one-off algal bloom sites sampled off the MV *Namao* on the front deck. The weighted sampler was lowered down from 0-0.5m below the surface and filled (photo taken by Desiree Stratton).

Figure 11. MV *Namao* workboat and crew ready to head out to a nearshore station on Lake Winnipeg (photo taken by Tracie Greenberg).

Figure 12. Desiree Stratton next to Environment and Climate Change Canada's Seabird Rosette on the top deck of the MV *Namao* on Lake Winnipeg. The Seabird Rosette can take water samples at any depth in the water column as well as in situ data such as temperature, conductivity, DO, turbidity, chlorophyll *a* and photosynthetically active radiation (PAR) (photo taken by Tracie Greenberg).

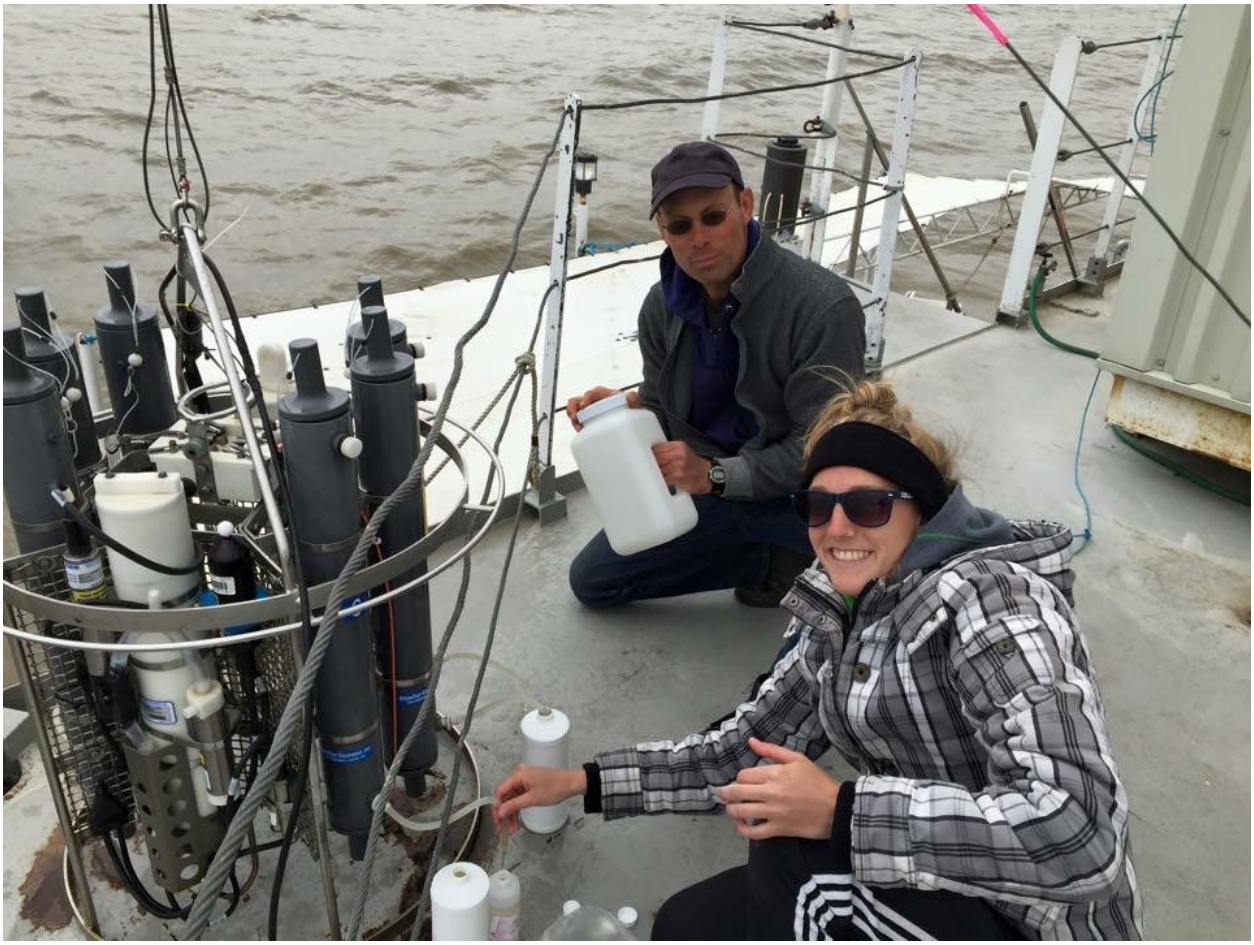

Figure 13. Desiree Stratton filling sampling bottles from Environment and Climate Change Canada's Seabird Rosette off the top deck of the MV *Namao* on Lake Winnipeg. The Seabird Rosette can take water samples at any depth in the water column as well as in situ data such as temperature, conductivity, DO, turbidity, chlorophyll *a* and photosynthetically active radiation (PAR) (photo taken by Tracie Greenberg).

Figure 14. The science and ship's crew sampling zooplankton and benthics on the stern of the MV *Namao* on Lake Winnipeg (photo taken by Tracie Greenberg).

Figure 15. Cleaning off benthic sampling bags on the stern of the MV *Namao* on Lake Winnipeg. The bags are cleaned off prior to shipping so that any sediment doesn't get on other sample bottles during shipping (photo taken by Tracie Greenberg).

Figure 16. Washing the aquatic invasive species Spiny Water Flea sample down the net to the bottom on the stern of the MV *Namao* on Lake Winnipeg (photo taken by Tracie Greenberg).

Table 3. Selection of chemical, physical and biological parameters from Lake Winnipeg euphotic dataset.

Factors	**Model Rationale**	**Source**
Anabaena (X_1)	*Anabaena* is known to produce the microcystin toxin, is a N-fixing cyanobacteria which can give them a competitive advantage when N is limiting and can use positive buoyancy from gas vacuoles to access higher levels of light from the surface. On Lake Winnipeg in July and August, large algal blooms can develop in the north and south basin with *Anabaena* and *Aphanizomenon* as the dominant species present.	(Kotak et al., 2000; Lee, 2008; Kling et al., 2011; Dolman et al., 2012; Beaulieu et al., 2013)
Boron (X_2)	Total boron is one of many micronutrients required for algal cell growth, helps with metabolic activities, membrane function, cell wall organization, heterocyst stabilization and may have a function in toxin production.	(Lukač & Aegerter, 1993; Srivastava et al., 2016)
Cyanobacteria species richness (X_3)	During an algal bloom event, there are many non-N-fixing and N-fixing Cyanobacteria species present depending on the amount of algal growth parameters present.	(Kling et al., 2011)
DO (X_4)	DO concentrations and distribution in the water column come from biological productivity, water and atmosphere exchanges and wind-induced mixing. Cyanobacteria produce oxygen as a bi-product of photosynthesis. Algal biomass decomposition can consume oxygen and create low oxygen areas in the water column.	(Graham et al., 2008; Environment Canada & Manitoba Water Stewardship, 2011)
Pseudoanabaena (X_5)	*Pseudoanabaena* is known to produce the microcystin toxin and is a non-N-fixing cyanobacteria. In Lake Winnipeg, *Pseudoanabaena* represented less than 0.1% of	(Graham et al., 2008)

	the total biomass from 1999 to 2007 between May to October.	
Total Phosphorus (X_6)	Total P can occur in waterbodies due to runoff of manure from livestock, land fertilizers, atmospheric deposition, urban areas and industrial and municipal wastewaters. Total P is a key component in algal growth and production as well as a key factor in controlling the production of microcystin.	(Kotak et al., 2000; Environment Canada & Manitoba Water Stewardship, 2011)
Wind Speed (X_7)	Depending on the wind speed, blooms can be accumulated at the surface or mix within the water column. Lower wind speed can create calm water conditions and allow for cyanobacteria to build up at the surface or push algal blooms into nearshore areas.	(Graham et al., 2008)

Table 4. Model set of chemical, physical and biological parameters from Lake Winnipeg that could be predictors of the microcystin toxin from the euphotic dataset for the AIC analysis. *Anabaena* biomass=X1, Total Boron=X2, Total Phosphorus=X6 and Wind Speed=X7. These models are linked to the selection of parameters from table 3. Models are in the form of logit[Prob(microcystin)]= $\beta_0 + \beta_z X_z$, where the notation in the table lists the intercept and response variables and relationships between one another.

Model Description	**Model Notation**
Anabaena ('Anabaena')	$\beta_0 + \beta_1 X_1$
Total Boron ('TB')	$\beta_0 + \beta_2 X_2$
Total Phosphorus ('TP')	$\beta_0 + \beta_6 X_6$
Wind Speed ('Wind Speed')	$\beta_0 + \beta_7 X_7$
Anabaena + TB	$\beta_0 + \beta_1 X_1 + \beta_2 X_2$
Anabaena + TP	$\beta_0 + \beta_1 X_1 + \beta_6 X_6$
Anabaena + Wind Speed	$\beta_0 + \beta_1 X_1 + \beta_7 X_7$
TB + TP	$\beta_0 + \beta_2 X_2 + \beta_6 X_6$
TB + Wind Speed	$\beta_0 + \beta_2 X_2 + \beta_7 X_7$
TP + Wind Speed	$\beta_0 + \beta_6 X_6 + \beta_7 X_7$
Intercept only	β_0

Table 5. Selection of chemical and physical parameters from Lake Winnipeg surface dataset.

Factors	**Model Rationale**	**Source**
N:P ratio (X_1)	Low N:P ratio and N deficiency in waterbodies allows cyanobacteria to thrive due to their capability to fix N from the atmosphere. A low N:P ratio can cue the cyanobacteria physiologically to produce microcystin and therefore increase the content of intracellular microcystin.	(Orihel et al., 2012; Scott et al., 2013)
pH (X_2)	Cyanobacteria that produce microcystin flourish with a basic pH between 7.5 and 10.	(de Maagd et al., 1999; West & Louda, 2011)
Total Phosphorus (X_3)	Total P can occur in waterbodies due to runoff of manure from livestock, land fertilizers, atmospheric deposition, urban areas and industrial and municipal wastewaters. Total P is a key component in algal growth and production as well as a key factor in controlling the production of microcystin.	(Kotak et al., 2000; Environment Canada & Manitoba Water Stewardship, 2011)
Wind Speed (X_4)	Depending on the wind speed, blooms can be accumulated at the surface or mixed within the water column. Lower wind speed can create calm water conditions and allow for cyanobacteria to build up at the surface or push algal blooms into nearshore areas.	(Graham et al., 2008)

Table 6. Model set of chemical and physical parameters from Lake Winnipeg that could be predictors of the microcystin toxin from the euphotic dataset for the AIC analysis. N:P ratio=X1, Total Phosphorus=X3 and Wind Speed=X4. These models are linked to the selection of parameters in previous table. Models are in the form of logit[Prob(microcystin)]= $\beta_0 + \beta_z X_z$, where the notation in the table lists the intercept and response variables and relationships between one another.

Model Description	**Model Notation**
N:P ratio ('N:P ratio')	$\beta_0 + \beta_1 X_1$
Total Phosphorus ('TP')	$\beta_0 + \beta_3 X_3$
Wind Speed ('Wind Speed')	$\beta_0 + \beta_4 X_4$
N:P ratio + TP	$\beta_0 + \beta_1 X_1 + \beta_3 X_3$
N:P ratio + Wind Speed	$\beta_0 + \beta_1 X_1 + \beta_4 X_4$
TP + Wind Speed	$\beta_0 + \beta_3 X_3 + \beta_4 X_4$
Intercept only	β_0

3.0 RESULTS

3.1 Long-Term changes in Water Quality 1999 to 2017

3.1.1 Phytoplankton Taxonomic Composition

Looking at all W stations averaged together, the two dominant algal groups, defined as those with the highest mean biomass between 1999 and 2017, were cyanobacteria (Cyanophyceae) in 2011 with a mean of 16,424 mg/m^3 and diatoms (Bacillariophyceae) in 2004 with a mean of 5,029 mg/m^3 (Figure 17). Cyanobacteria mainly dominated from 1999 to 2008 representing the highest mean biomass in six of the 10 years, whereas diatoms mainly dominated from 2009 to 2017 representing the highest mean biomass in six of the nine years (Figure 17). From 1999 to 2017, diatoms had the highest mean biomass in 10 of the 19 years and cyanobacteria had the highest mean biomass in nine of the 19 years (Figure 17). Cyanobacteria dominated in 2011, representing 83% of the total algae biomass in those years and diatoms dominated in 2012 representing 73% of total biomass (Figure 17).

The three dominant cyanobacterial genera from 1999 to 2017 were *Aphanizomenon* (74% of the total cyanobacteria), *Microcystis* (15%) and *Anabaena* (6%) (Figure 18). *Aphanizomenon* was the most abundant cyanobacterial taxon in 12 of the 19 years in the dataset whereas *Microcystis* was dominant in four years and *Anabaena* was dominant in three years (Figure 18). There was a shift in species composition over time. From 1999 to 2007, composition consisted mainly of *Microcystis* and *Aphanizomenon* then shifted to *Aphanizomenon*, *Anabaena* and *Aphanocapsa* from 2008 to 2017 (Figure 18). The highest amount of cyanobacterial biomass was attributable to the genera *Microcystis* in 2011 (90,525.6 mg/m^3) (Figure 18). In the north

basin during the summer and fall, *Aphanizomenon* dominated for 14 years between 1999 and 2017 (Figure 19, Figure 22). In the south basin and narrows, *Aphanizomenon* dominated for 12 years in the fall and nine years in the summer (Figure 19; Figure 22; Figure 23; Figure 25). There was no single genus that dominated in the spring and winter in the north basin from 1999 to 2017 (Figure 20; Figure 21). In the south basin and narrows, there was multiple genera such as *Anabaena*, *Aphanizomenon*, *Gomphosphaeria*, *Oscillatoria* and *Pseudoanabaena* occurring from 2008 to 2017 during the spring and *Aphanizomenon*, *Oscillatoria* and *Pseudoanabaena* during the winter (Figure 24; Figure 26).

3.1.2 Chemical, Physical and Biological Parameters

At all euphotic W stations averaged together, the highest measured chlorophyll *a* concentration was 79.1 µg/L in the north basin and 31.6 µg/L in the south basin and narrows, both in the fall of 2006 (Figure 27). In the south basin and narrows, chlorophyll *a* typically increased in the spring and summer and decreased in fall and winter (Figure 27). In the north basin, chlorophyll *a* was highest in the fall and generally higher than in the south basin and narrows (Figure 27).

Total N concentrations at the W stations in the north basin exceeded the Lake Winnipeg objective of 0.75 mg/L in 15 out of 68 surveys between 1999 and 2017 during the spring, summer, fall and winter (Figure 28). The south basin and narrows average concentrations exceeded the objective in 36 out of 73 surveys (Figure 28). The highest average concentrations in the north basin were in the summer of 2003 (1.43 mg/L) and in the south basin and narrows in the summer of 2010 (4.46 mg/L) (Figure 28). Total N was higher in the south basin and narrows than in the north basin (Figure 28, Figure

29). A downward trend in total N started in 2011, stabilizing after 2014 at around 0.5 mg/L in north basin and around 0.75 mg/L in the south basin and narrows (Figure 28, Figure 29). From 2009 to 2017, total N has been under the objective (Figure 29). Average annual total N in the north basin exceeded the objective four times and in the south basin and narrows exceeded the objective ten times (Figure 29). The highest average annual mean in the south basin and narrows was 1.15 mg/L in 2007 and 1.01 mg/L in 2003 (Figure 29).

Total P concentrations at the W stations varied around the Lake Winnipeg objective of 0.05 mg/L except for five of 73 surveys (Figure 30). In the north basin, average concentrations only went over the Lake Winnipeg objective in 17 of 70 surveys and was generally lower than in the south basin and narrows (Figure 30). Total P typically spiked in the fall and decreased in the winter and spring (Figure 30). Total P from 2005 to 2017 has average concentrations over the total P objective of 0.05 mg/L (Figure 30). Average annual mean total P in the south basin and narrows has been over the objective every year from 1999 to 2017 and has remained at a consistent average of around 0.08 mg/L from 2010 to 2017 (Figure 31). In the north basin, total P was over the objective six times (Figure 31). Total P was over the objective from 2007 to 2011 and from 2012 to 2017 has been under the objective (Figure 31). The highest average annual mean in the south basin and narrows was 0.11 mg/L in 2007 and 0.06 mg/L in 2005 in the north basin (Figure 31).

The highest turbidity levels in the north basin between 1999 and 2017 occurred in the fall of 2012 (15.2 NTU) whereas a peak in the south basin and narrows (42.2 NTU) occurred in the summer of 2000 (Figure 32). In the south basin and narrows,

three years had large standard errors in seasonal means: spring 2014 (12.6 NTU), summer 2000 (13.4 NTU), and fall 2003 (12.3 NTU) (Figure 32). Turbidity was generally higher in the south basin and narrows than in the north basin, with spikes in the summer and fall (Figure 32). In the north basin, spikes in the fall season were not as high as in the south basin and narrows (Figure 32).

The N:P molar ratio was almost always greater than the Redfield value of 16:1 indicating that Lake Winnipeg is primarily P-limited in the north basin and south basin and narrows (Figure 33). There was no apparent temporal trend with a molar ratio of about 40 in the north basin and 20 in the south basin and narrows (Figure 33). The highest ratio occurred in the north basin in 2003 (168) whereas, in the south basin and narrows, the highest value was in the summer of 2010 (93) (Figure 33). The W station and all stations on Lake Winnipeg average N:P molar ratio from 1999 to 2017 was 25:1 in the south basin and narrows and 37:1 in the north basin where an outlier of 14087 was removed from the south basin and narrows data and an outlier of 31870 was removed from the north basin data (Figure 33). Two probable average outliers in fall 2008 were omitted from the graphs and calculations, values of 4,570 (north basin) and 2,022 (south basin and narrows).

3.1.3 Toxins

The highest average microcystin concentration in the south basin and narrows, based on data from the euphotic and surface depths from all stations, between 2004 and 2017, was 1.46 µg/L in the summer of 2010 (Figure 34). The highest average concentration in the north basin was 9.90 µg/L in the summer of 2013 (Figure 34). The average exceeded the analytical detection limit (0.2 µg/L) only four times from 2004 to

2017 in the south basin and narrows and seven times in the north basin. No averages went over the Manitoba recreational water quality objective of 20 µg/L but two individual samples did so: one in the summer of 2013 (station 19 = 85 µg/L) and one in the summer of 2016 (Bloom 5 [along the east side of the north basin] = 43.7 µg/L). Values were relatively consistent over time from 2004 to 2017 except in the north basin, where there were spikes starting in 2013 (Figure 34).

There were 37 samples (8%) that had a detectable microcystin value and 422 (92%) that were a non-detect out of 459 samples collected in the euphotic zone between 1999 and 2017 (minimum=0.1 µg/L, maximum=4.9 µg/L, mean= 0.23 µg/L). Out of 196 samples taken between 1999 and 2017, there were 57 samples (29%) that contained detectable microcystin and 139 samples (71%) were non-detects (mean=1.10 µg/L; range 0.1 to 85 µg/L) in the surface zone. In total, 655 microcystin samples were taken either at the surface or in the euphotic zone between 1999 and 2017. Of these, 94 samples (14%) had detectible microcystin and 561 samples (86%) were non-detects.

In the summer and fall of 2016, 24 samples were analyzed for β-*N*-methylamino-L-alanine (BMAA), β-amino-N-methylalanine (BAMA), 2,4-diaminobutyric acid (DAB) and N-(2-aminoethyl) glycine (AEG). There were no detected amounts of any of these phytotoxic chemicals.

3.2 Multi-panel Scatterplots of Correlations of Detectable Concentrations of Microcystin

3.2.1 Euphotic Dataset

The euphotic dataset showed the strongest positive correlations were between microcystin and total boron (r=0.6), pheophytin *a* (r=0.6) and pH (r=0.6) (Figure 35).

Eleven parameters had a weak positive correlation (r>0.5) with microcystin concentration (Cryptophyceae biomass, surface sample depth, total sample depth, hardness, total lithium, total magnesium, N:P ratio, total dissolved solids, air temperature, total thallium, total uranium) (Figure 35; Figure 36; Figure 37; Figure 38) and nine parameters had a weak correlation with r>0.4 (Dinophyceae biomass, alkalinity CO_3, total calcium, conductivity, DO, total potassium, total sodium and total sulphate) (Figure 38; Figure 39; Figure 40). The N:P ratio was the only nutrient-based parameter with a relatively strong positive correlation with microcystin (r=0.5) (Figure 37).

Seven parameters (total antimony, total cadmium, acid-hydrolyzable P, total P, total dissolved P, total reactive P and total zirconium) had an r value of -0.5 and three parameters (total manganese, dissolved NO_3 + NO_2 and wind speed) that had an r value of -0.4 (Figure 41; Figure 42; Figure 43). Nitrate concentration had the strongest negative correlation (r=-0.6) of all 98 parameters in the euphotic dataset but there were only six samples (Figure 41). There were more fractions of N and P having weak negative correlations with microcystin than there were positive relationships. The euphotic dataset showed that, with increasing nitrate concentrations in the water column, there was a higher concentration of microcystin.

3.2.2 Surface Dataset

The surface dataset showed that the *Anabaena* biomass, total Kjeldahl N, BOD, and total suspended solids had positive correlations with microcystin concentration. *Anabaena* biomass had the strongest positive relationship (r=0.7) (Figure 45). Other weaker positive relationships were with total Kjeldahl N, BOD, and total suspended solids with an r value of 0.5 and Cyanophyceae biomass, phytoplankton biomass,

chlorophyll *a*, and total N with an r value of 0.4. Cryptophyceae biomass (r=-0.5) and Secchi disk depth have an r value of -0.5 and wind speed has an r value of -0.4 had a weak negative correlation with microcystin and the other 24 parameters had correlation coefficients between -0.3 and 0.3 (Figure 45; Figure 46; Figure 47).

3.2.3 Grouped analysis of Surface and Euphotic Datasets

Pheophytin *a* had the strongest positive correlation with microcystin concentration (r=0.6) in all lake data which had the same relationship in the euphotic data (r=0.6) but a weaker positive relationship in the surface data (r=0.2) (Figure 49). *Anabaena* biomass had a weak positive relationship (r=0.5) among all lake data where the surface data (r=0.7) had a strong positive relationship, and the euphotic data had a weak positive relationship (r=0.3) (Figure 45, Figure 49). The N:P ratio (r=0.5) and BOD (r=0.5) had similar weak positive relationship between the surface (N:P ratio (r=0.3); BOD (r=0.3)) and euphotic data (N:P ratio (r=0.5); BOD (r=0.3)) (Figure 49).

Dissolved NO_3 + NO_2 and wind speed had the strongest negative relationship with microcystin between all lake data. Both dissolved NO_3 + NO_2 and wind speed had weak negative relationship in the surface dataset (r=-0.2) and the euphotic dataset (r=-0.4) but among all lake data, there was a weak negative relationship (r=-0.4) (Figure 44, Figure 48, Figure 50). Dissolved NO_3 + NO_2 and wind speed had the strongest negative relationships where the other parameters had weak or no relationship with microcystin.

Total C, total Kjeldahl N and total N had weak positive relationships but among all lake data the positive relationships got stronger. Total C had a weak positive relationship in the surface dataset (r=0.2) and a weak negative relationship in the euphotic dataset (r=-0.09) but, among all lake data, total C had a weak positive

relationship (r=0.3) (Figure 44, Figure 48, Figure 50). Among all lake data, total Kjeldahl N had a weak positive relationship (r=0.5) but had no relationship in the euphotic data (r=-0.01) and a weak positive relationship in the surface data (r=0.3) (Figure 44, Figure 48, Figure 50). Total N had weak relationships in the surface dataset (r=0.3) and the euphotic dataset (r=-0.2) but, among all lake data, total N had a stronger positive relationship (r=0.4) (Figure 44, Figure 48, Figure 50).

3.3 Linear Discriminant Analysis (LDA)

3.3.1 Euphotic and Surface Datasets

In the euphotic and surface data, there was no significant separation of microcystin groups and the points scattered across both figures (Figure 51; Figure 54). The points on the figures consisted mainly of below detection limit values of 0.2 µg/L with the odd middle and above values. In the euphotic dataset, the below detection values were predicted correctly 94.6% of the time and in the surface dataset, predicted 96.7% of the time (Table 7; Table 8). There was one microcystin value that was predicted correctly in the middle group and the above group had zero predicted in the euphotic dataset (Table 7). There were zero microcystin values that were predicted correctly above 1.51 µg/L or in the middle between 0.21 and 1.5 µg/L in the surface dataset (Table 8). The prediction rate was very high due to over 90% of the samples being below 0.2 µg/L in both datasets. Histograms of the LD1 and LD2 for all three microcystin groups showed complete overlap of parameters, which provided no separation between the microcystin groups (Figure 52; Figure 53; Figure 54; Figure 55; Figure 56).

3.4 Linear Model Selection and Hurdle Model

3.4.1 Euphotic Dataset

In the euphotic dataset, the best GLM model with Gaussian distribution of positive microcystin values was between total boron and wind speed. The model carried 84% of the cumulative model weight and had the lowest AIC value (Table 9). The next best model was wind speed alone, which was just over 4 AIC units higher than the top model and carried an 11% of the cumulative model weight (Table 9). In the euphotic dataset, total boron was a statistically significant predictor variable in the Gaussian model (p=0.013), but wind speed was not significant (p=0.1314) (Table 13). Model validation was done using k-fold cross validation, where the R^2 was 0.94 showing that our model fit the data well and had high predictive power (Table 14). The Gaussian model showed a strong positive relationship where, as wind speed and total boron increased, microcystin increased.

The best GLM model with a binomial distribution of presence/absence of microcystin was between *Anabaena* biomass and wind speed (Table 10). The model carried 100% of the cumulative model weight and had the lowest AIC value (Table 10). There were no other models that carried any cumulative weight other than the top model. In the binomial model, *Anabaena* biomass (p=0.0001) and wind speed (p=0.0440) were both statistically significant predictor variables (Table 13). Model validation using k-fold cross validation showed the R^2 was 0.55 which indicates an adequate fit of our model to the data (Figure 61; Table 14). The McFadden's pseudo R-squared value showed that explanatory variables *Anabaena* biomass and wind speed explained 44% of the variation in microcystin concentrations (Table 14). The binomial

model showed a weak positive relationship where, as *Anabaena* biomass and wind speed increased, microcystin increased.

3.4.2 Surface Dataset

In the surface dataset, the best GLM model with Gaussian distribution of positive microcystin values was between the N:P Ratio and wind speed (Table 11). The model carried 97% of the cumulative model weight and had the lowest AIC value (Table 11). The total P and wind speed model only carried 2% of the cumulative model weight (Table 11). In the surface dataset Gaussian model, neither N:P ratio (p=0.269) nor wind speed (p=0.212) were statistically significant predictor variables for positive microcystin concentrations (Table 13). Model validation was done using k-fold cross validation, where the R^2 was 0.99 showing that our model had an excellent fit but points on the figure seemed more clustered (poor contrast in the predictor) (Figure 62; Table 14). The Gaussian model for the surface dataset showed a strong positive relationship where, as the N:P ratio and wind speed increased, microcystin increased.

The best GLM model with a binomial distribution of presence/absence of microcystin was between the N:P Ratio and wind speed (Table 12). The model carried 100% of the cumulative model weight and had the lowest AIC value (Table 12). There were no other models that carried any cumulative weight other than the top model. The binomial model had similar results to the Gaussian model where neither the N:P ratio (p=0.0642) nor wind speed (p=0.4583) were statistically significant predictor variables (Table 13). Model validation was done using k-fold cross validation, where the R^2 was 0.45 showing that our model had a good fit (Table 14). The McFadden's pseudo R-squared value showed that explanatory variables N:P ratio and wind speed explained

9% of the variation in microcystin concentrations (Table 14). The binomial model for the surface model showed a weak positive relationship where, as the N:P ratio and wind speed increased, microcystin increased.

Cross-validation R^2 values show a better fit to the model in the euphotic and surface Gaussian GLM than the euphotic and surface binomial GLM (Table 14). The null and residual deviances were both lower in the euphotic and surface Gaussian GLM than the euphotic and surface binomial GLM showing that the model was better able to predict the response variable values (Table 14). Model validation looking at the quantile residuals for all four models indicated the residuals are normally distributed in the regression analysis and that there was no heteroscedasticity (Figure 57; Figure 58; Figure 59; Figure 60; Figure 61; Figure 62).

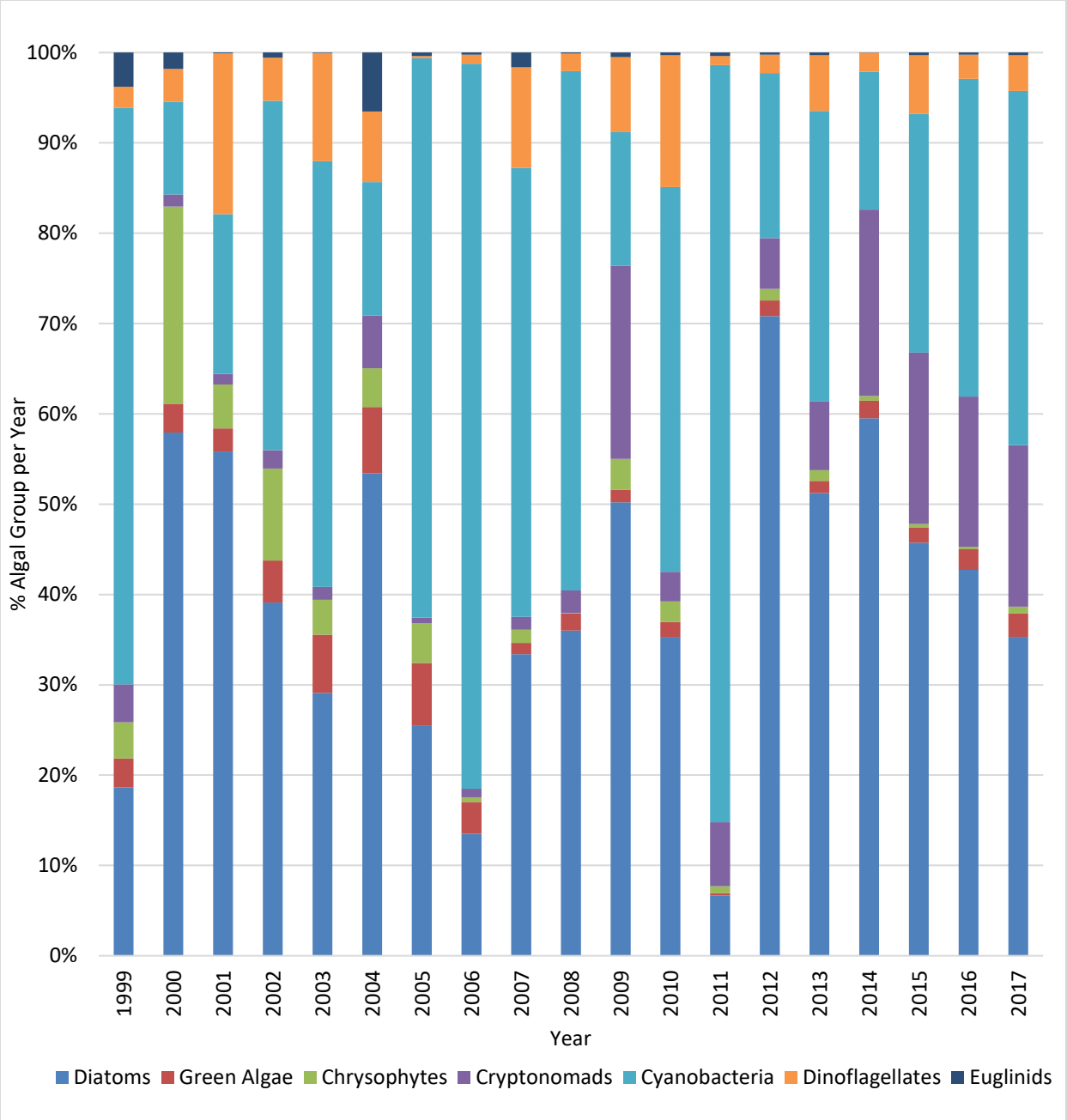

Figure 17. Proportion of total algal biomass in various taxonomic groups in samples from Lake Winnipeg between 1999 and 2017 as an average of surface and euphotic W stations data in the north basin and south basin and narrows during the spring, summer, fall and winter.

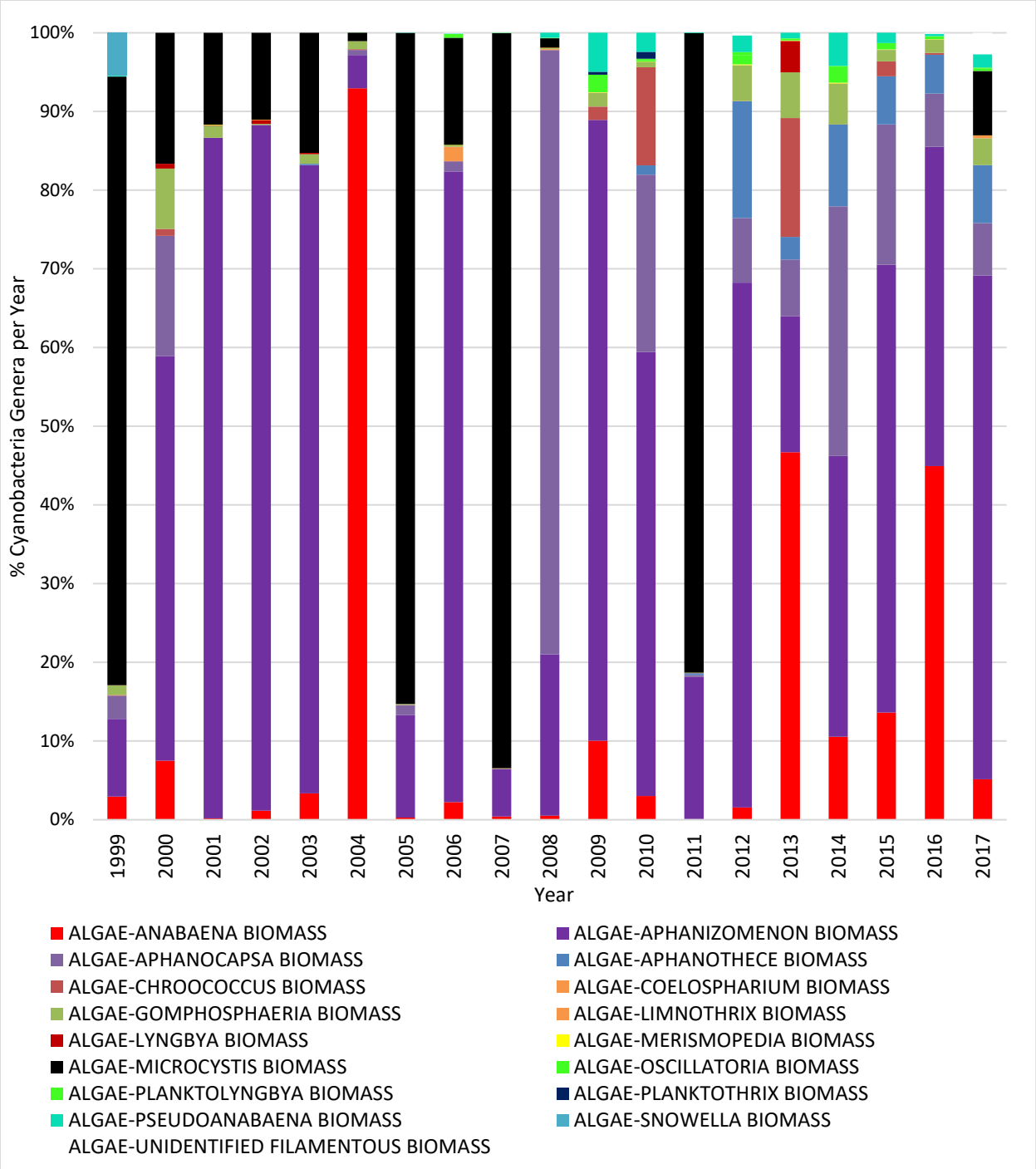

Figure 18. Cyanobacteria genera biomass in Lake Winnipeg between 1999 and 2017 as an average of surface and euphotic W stations data in the north basin and south basin and narrows during the spring, summer, fall and winter.

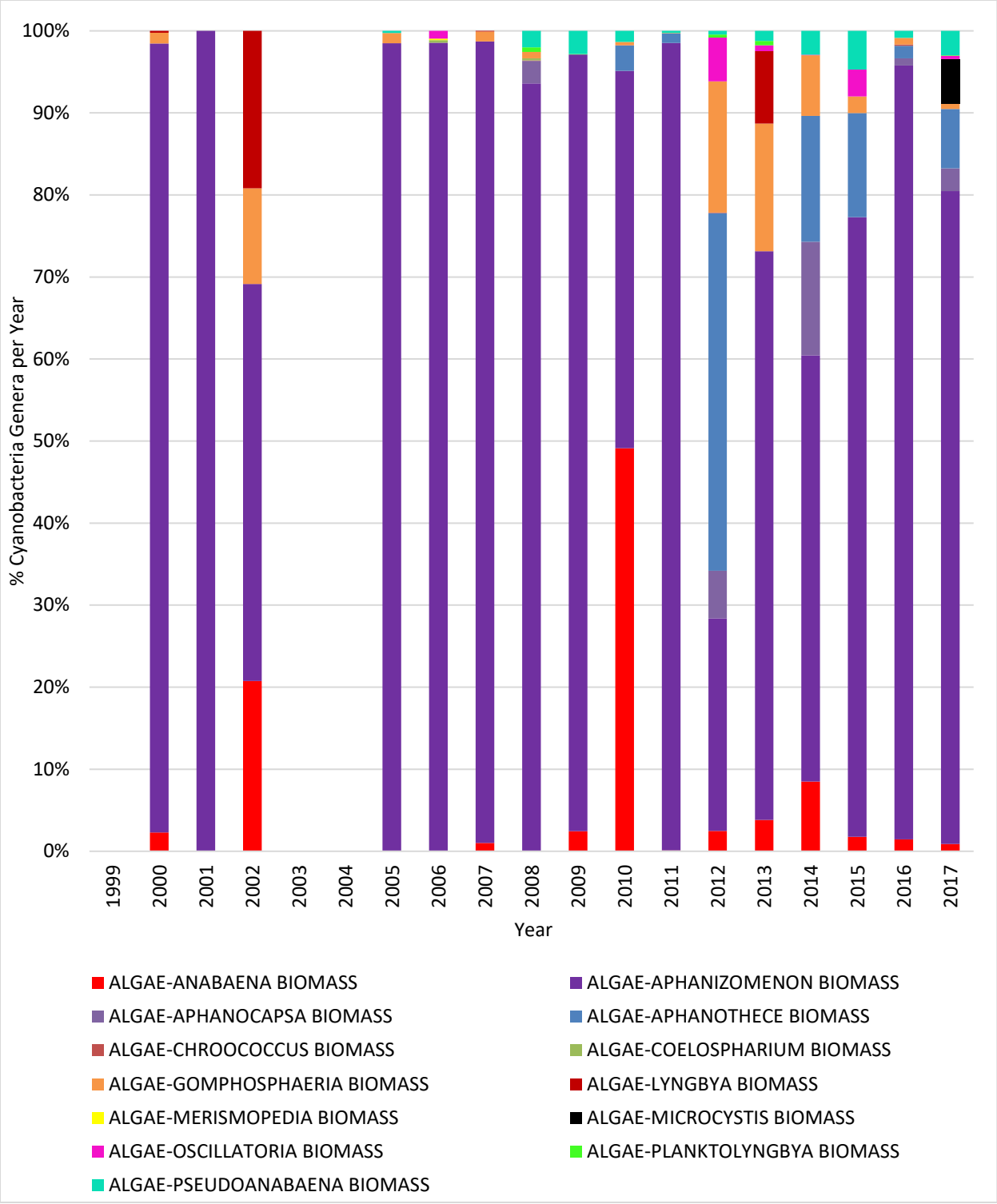

Figure 19. Cyanobacteria genera biomass in Lake Winnipeg between 1999 and 2017 as an average of surface and euphotic W stations data per year in the north basin during the fall season.

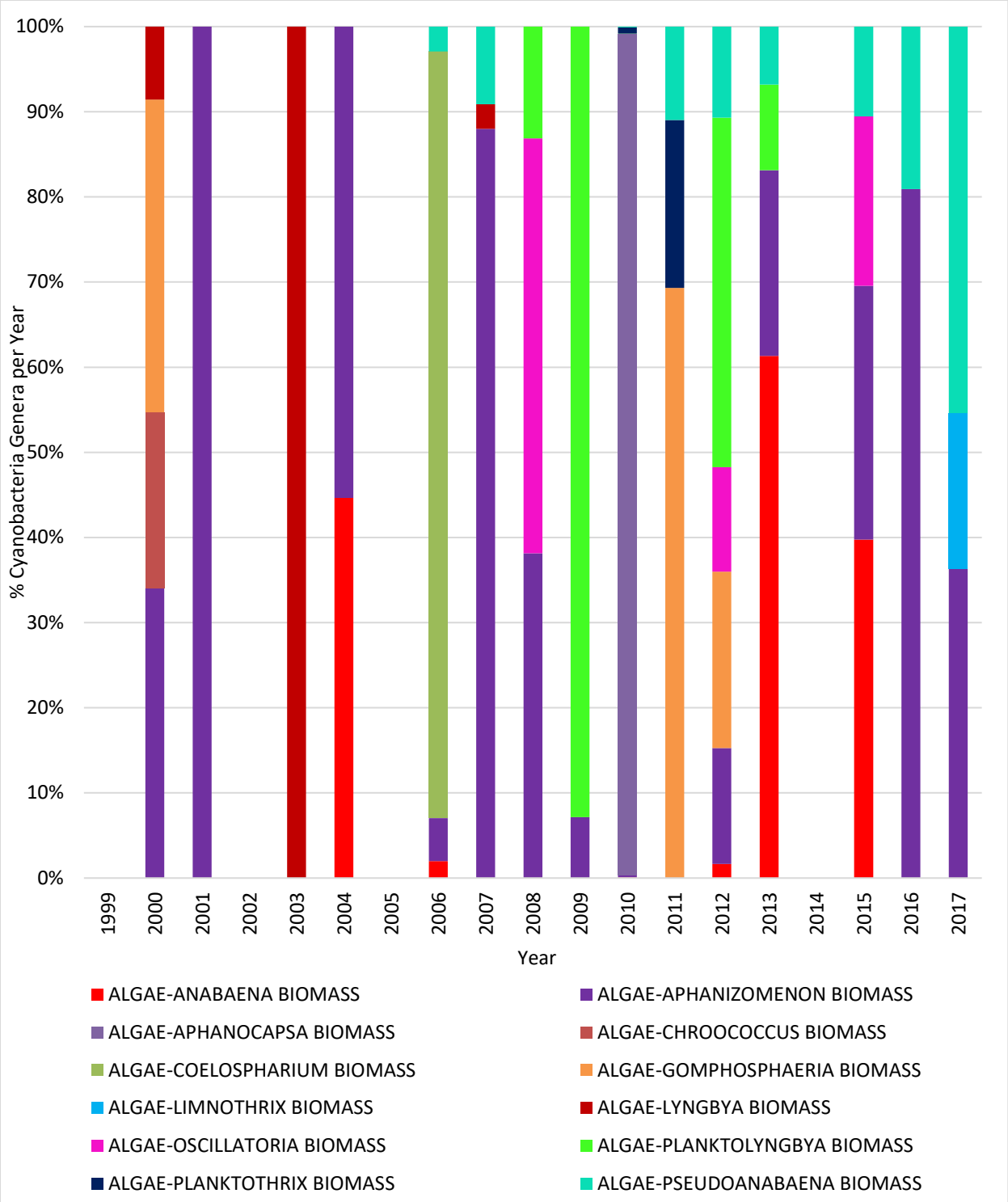

Figure 20. Cyanobacteria genera biomass in Lake Winnipeg between 1999 and 2017 as an average of surface and euphotic W stations data per year in the north basin during the spring season.

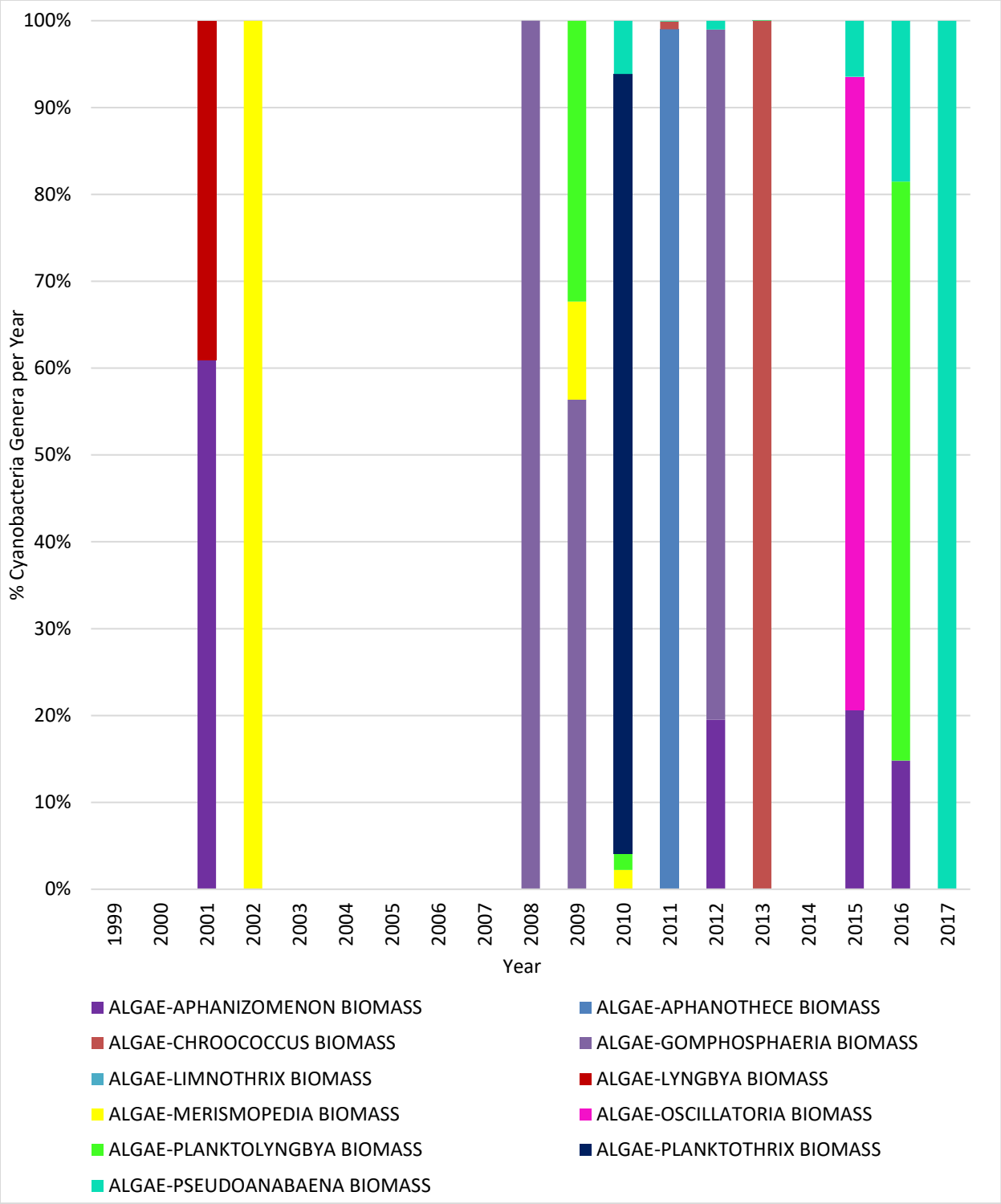

Figure 21. Cyanobacteria genera biomass in Lake Winnipeg between 1999 and 2017 as an average of surface and euphotic W stations data per year in the north basin during the winter season.

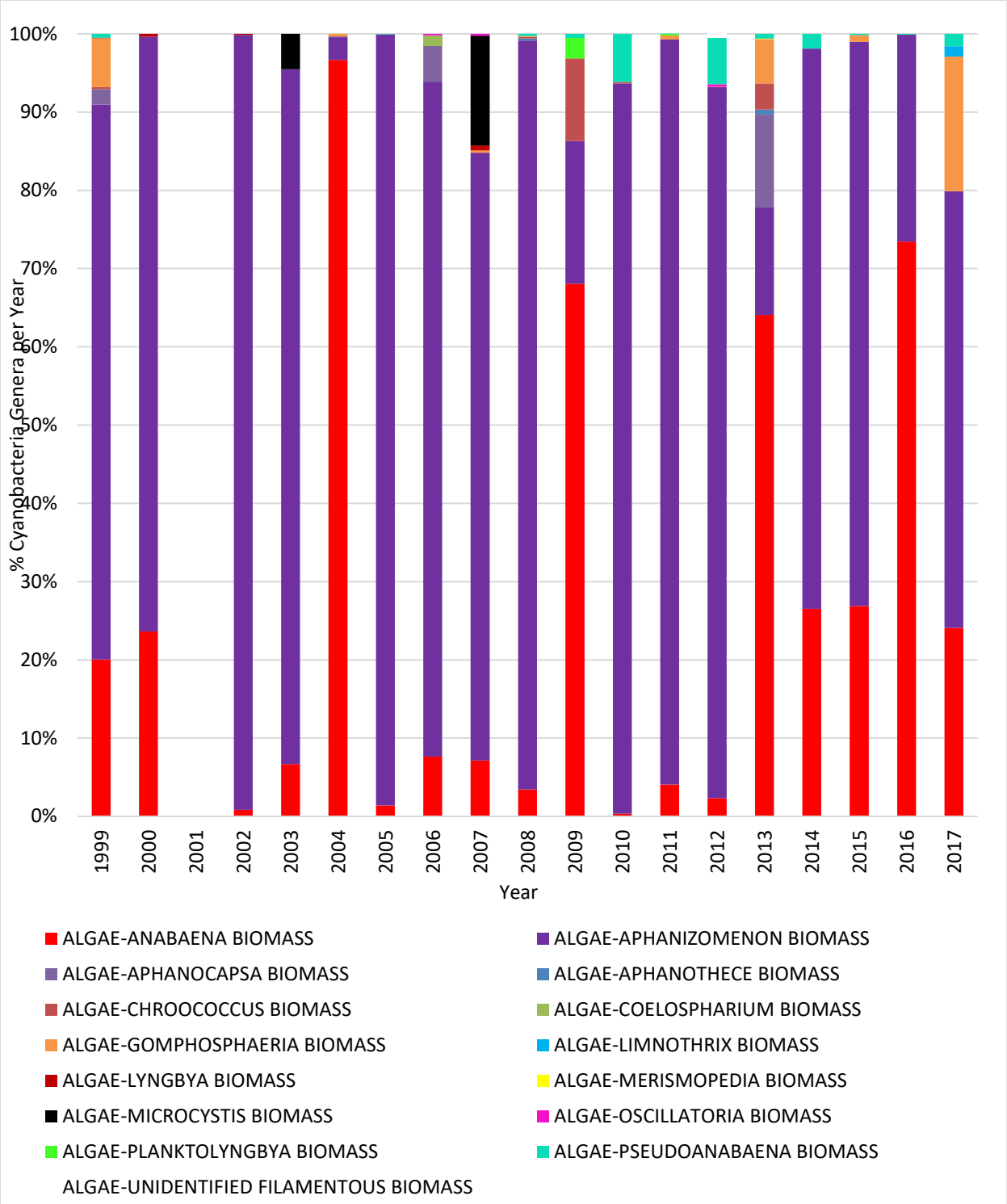

Figure 22. Cyanobacteria genera biomass in Lake Winnipeg between 1999 and 2017 as an average of surface and euphotic W stations data per year in the north basin during the summer season.

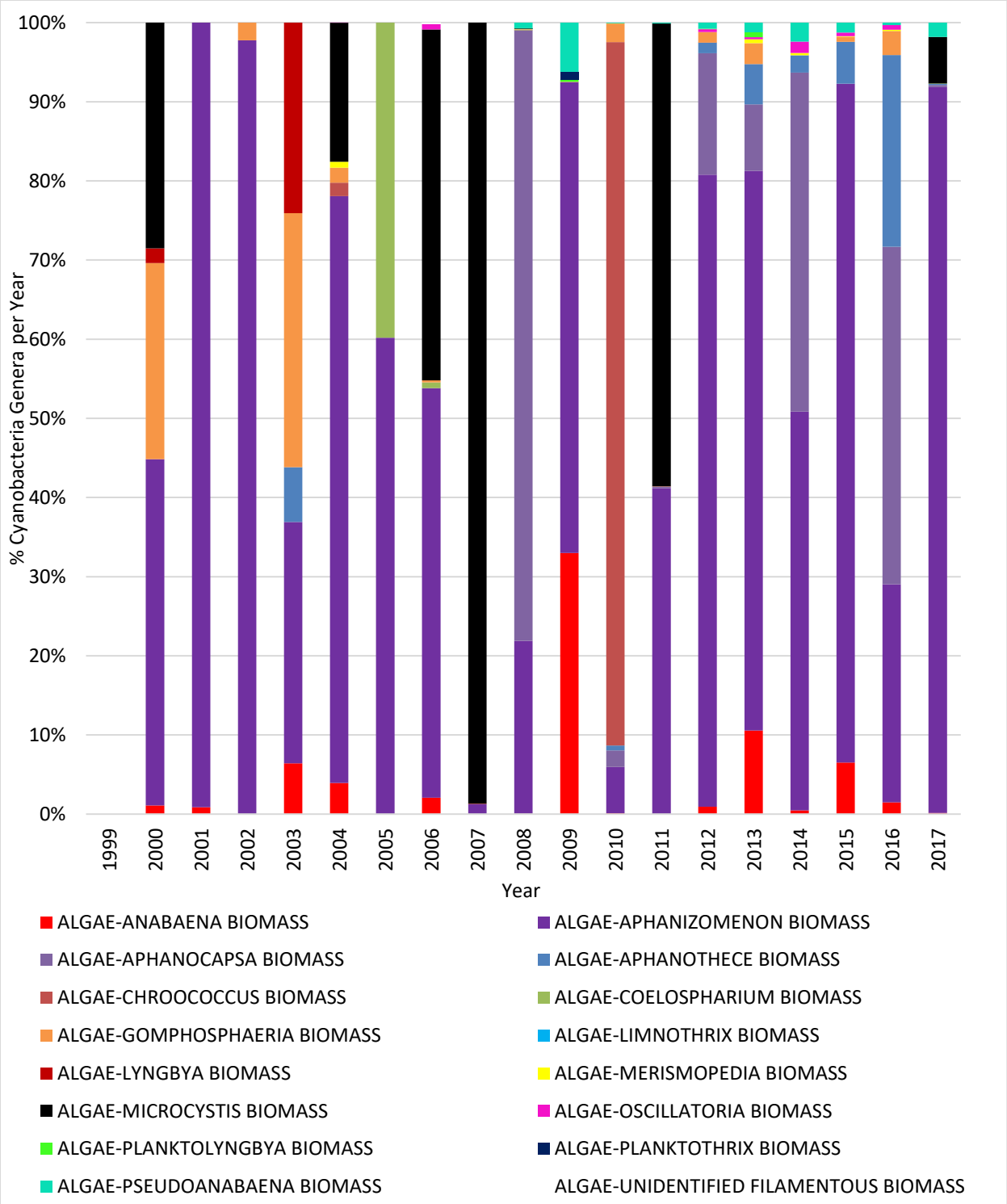

Figure 23. Cyanobacteria genera biomass in Lake Winnipeg between 1999 and 2017 as an average of surface and euphotic W stations data per year in the south basin and narrows during the fall season.

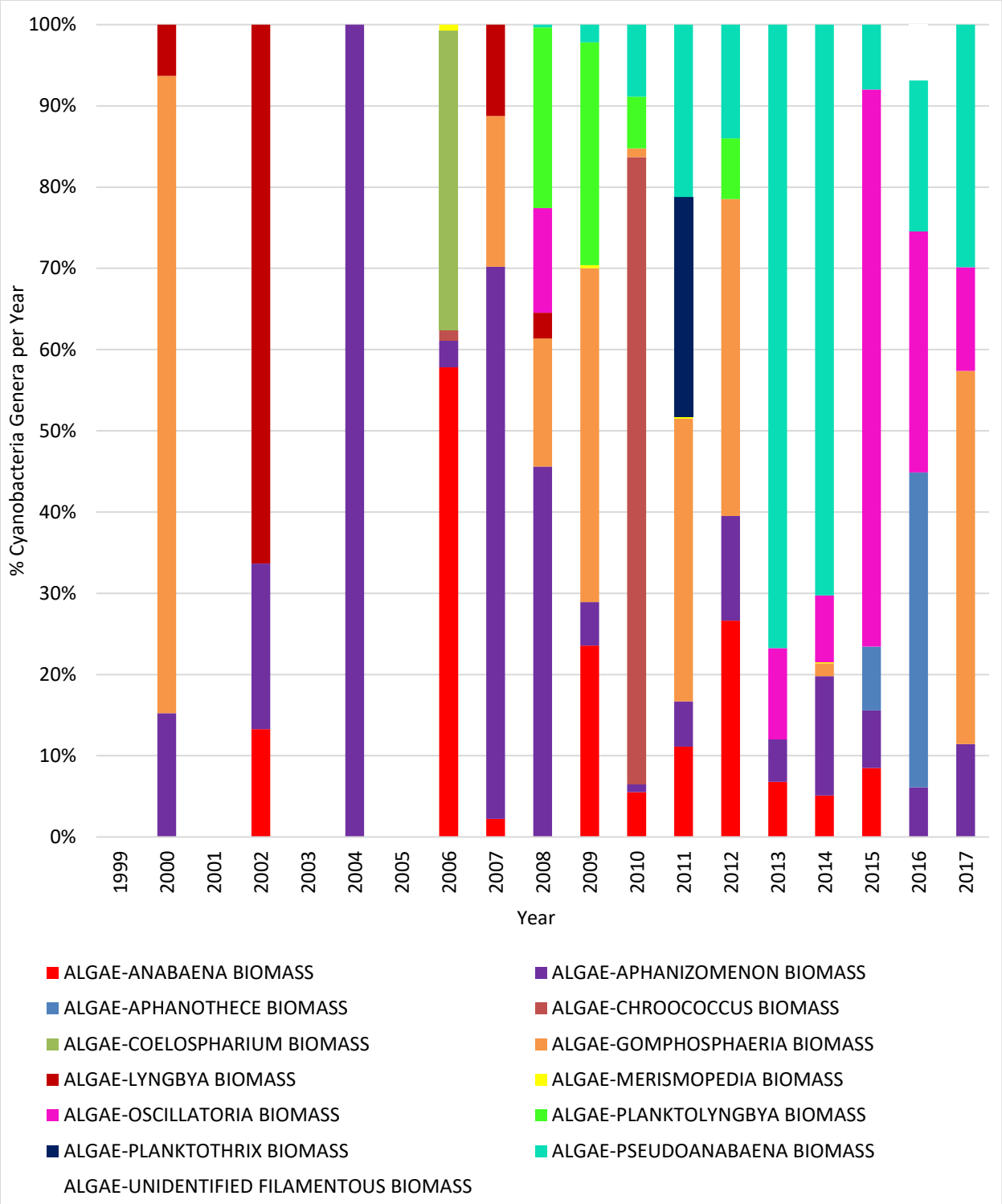

Figure 24. Cyanobacteria genera biomass in Lake Winnipeg between 1999 and 2017 as an average of surface and euphotic W stations data per year in the south basin and narrows during the spring season.

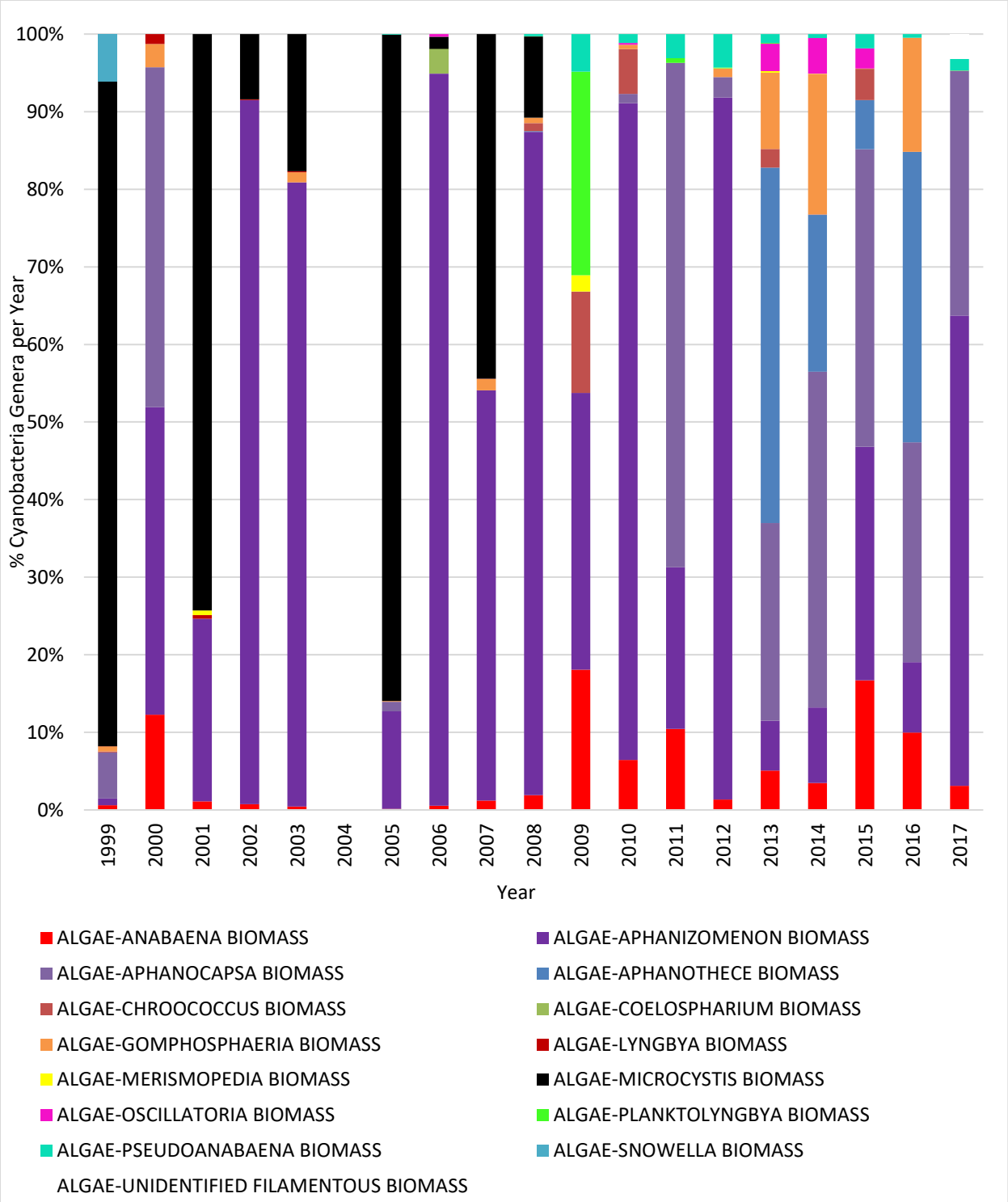

Figure 25. Cyanobacteria genera biomass in Lake Winnipeg between 1999 and 2017 as an average of surface and euphotic W stations data per year in the south basin and narrows during the summer season.

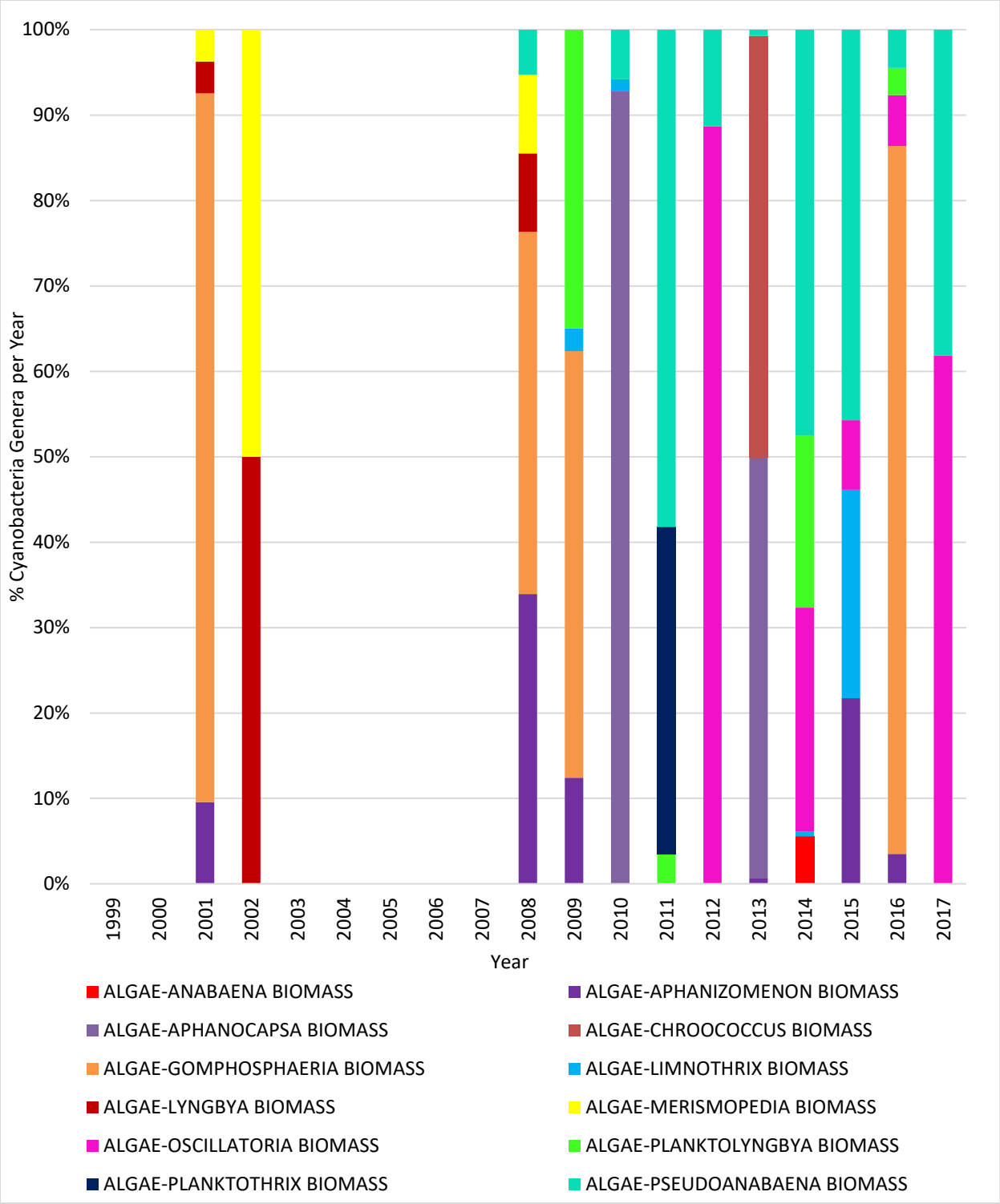

Figure 26. Cyanobacteria genera biomass in Lake Winnipeg between 1999 and 2017 as an average of surface and euphotic W stations data per year in the south basin and narrows during the winter season.

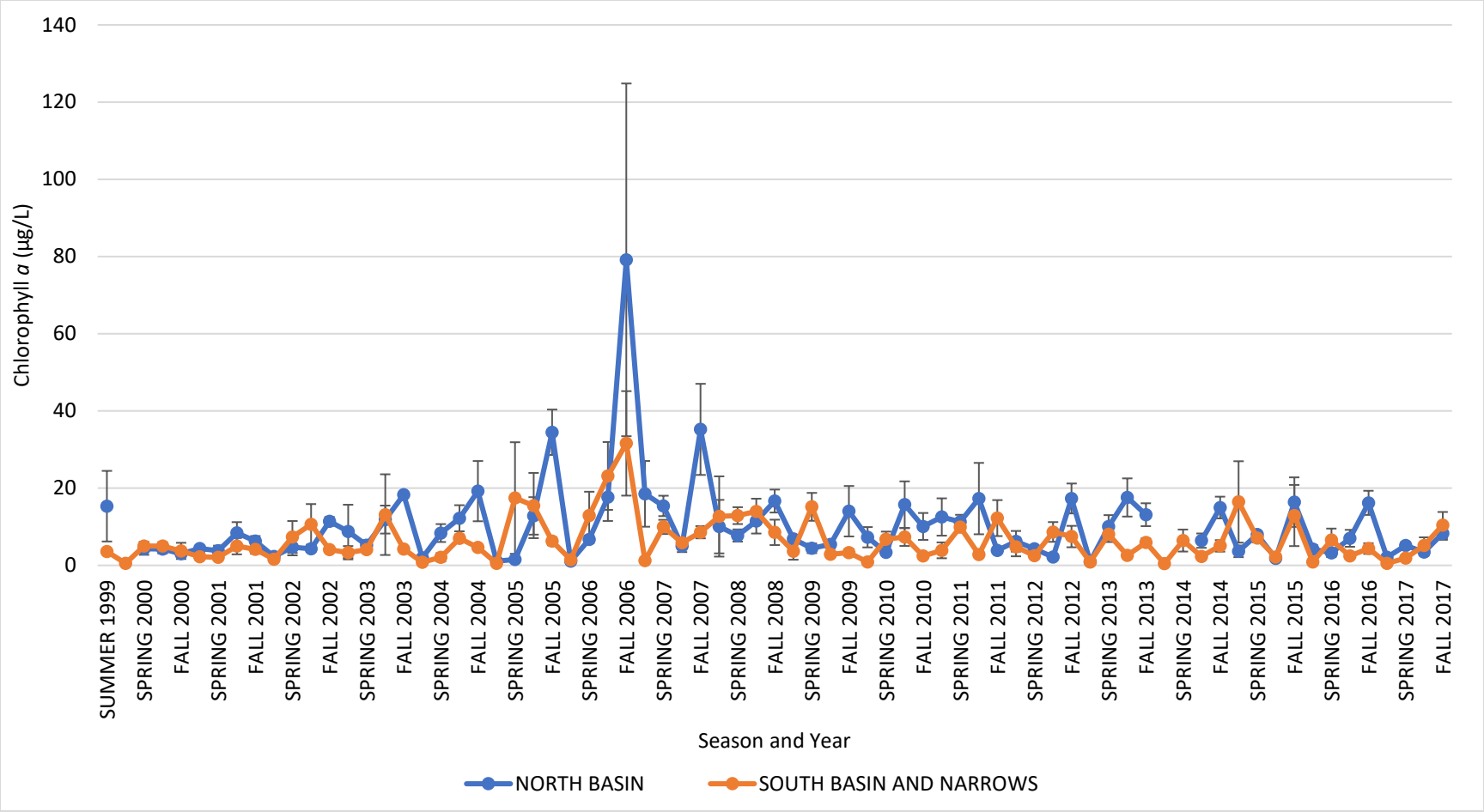

Figure 27. Chlorophyll *a* concentration (µg/L) in Lake Winnipeg between 1999 and 2017 as an average of surface and euphotic W stations data per year in the north basin and south basin and narrows during the spring, summer, fall and winter seasons (n=875, non-detects=62). Any non-detect values had $^{1/2}$ the detection limit used. Detection limit of 1 µg/L from 1999 to 2001, 0.1 µg/L from 2001 to 2003, 0.5 µg/L from 2003 to 2009 and 0.6 µg/L from 2009 to 2017.

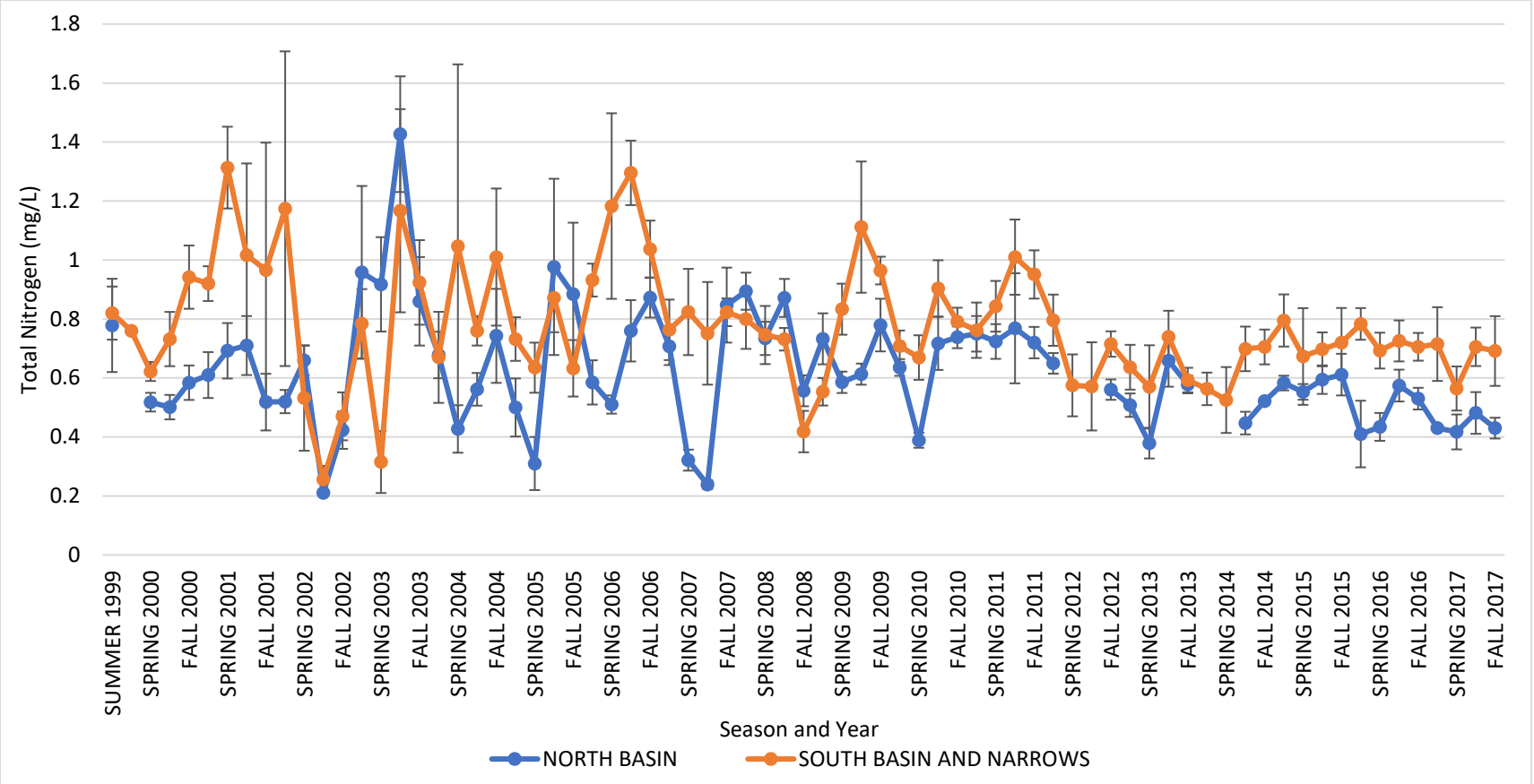

Figure 28. Total N concentration (mg/L) in Lake Winnipeg between 1999 and 2017 as an average of surface and euphotic W stations data per year in the north basin and south basin and narrows during the spring, summer, fall and winter seasons (n=866, non-detects=160). Any non-detect values had $^{1/2}$ the detection limit (0.2 mg/L) used. Detection limit of 0.2 µg/L from 2009 to 2017. Two samples from the south basin and narrows fall 2008 (566.2 mg/L) and summer 2010 (25.81 mg/L) and one sample from the north basin fall 2008 (1180.2 mg/L) were not included in the average calculations.

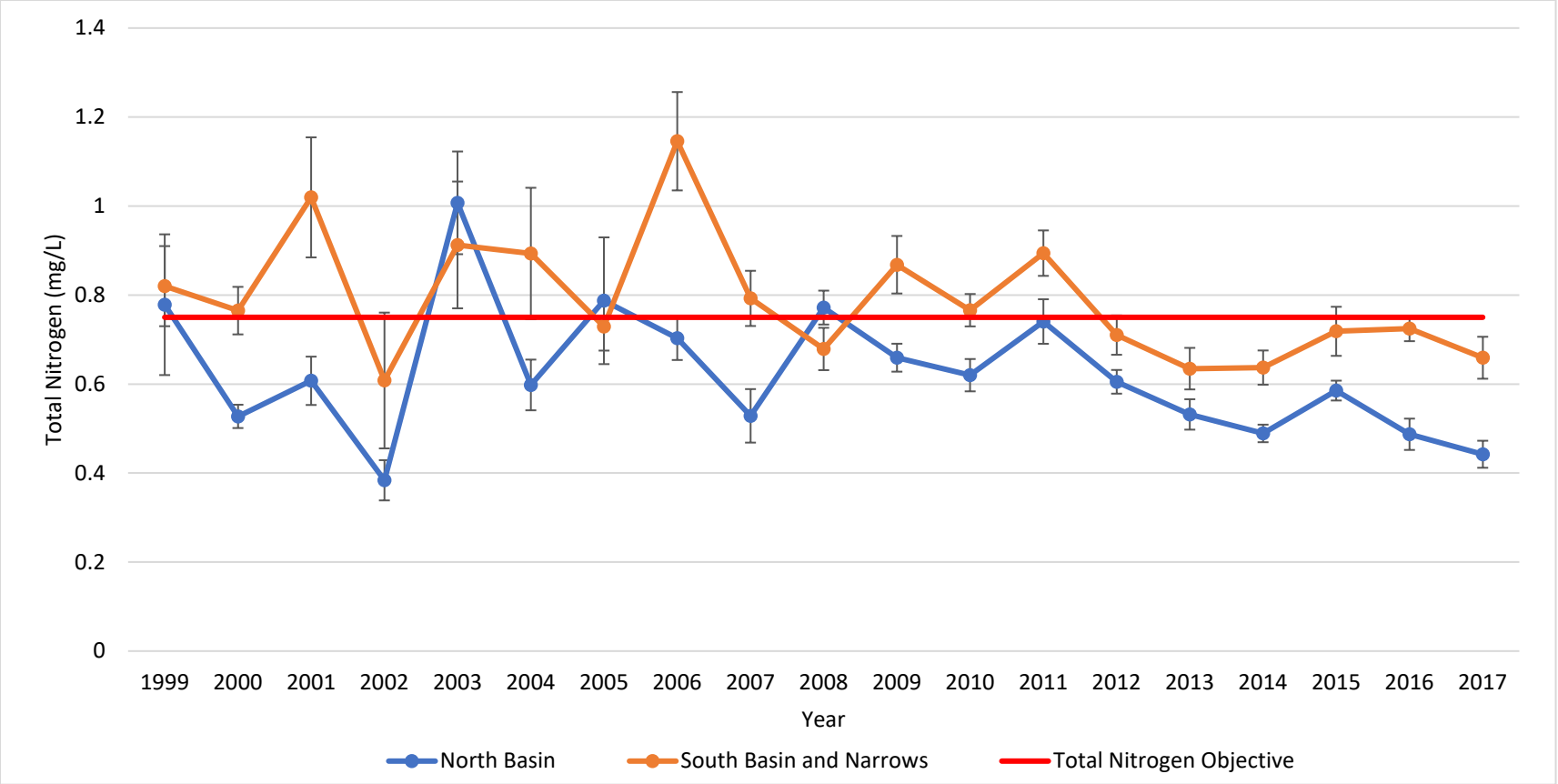

Figure 29. Total N concentration (mg/L) in Lake Winnipeg with total N objective between 1999 and 2017 as an average of surface and euphotic W stations data per year in the north basin and south basin and narrows (n=866, non-detects=160). Any non-detect values had $^{1/2}$ the detection limit (0.2 mg/L) used. Detection limit of 0.2 µg/L from 2009 to 2017. Two samples from the south basin and narrows fall 2008 (566.2 mg/L) and summer 2010 (25.81 mg/L) and one sample from the north basin fall 2008 (1180.2 mg/L) were not included in the average calculations.

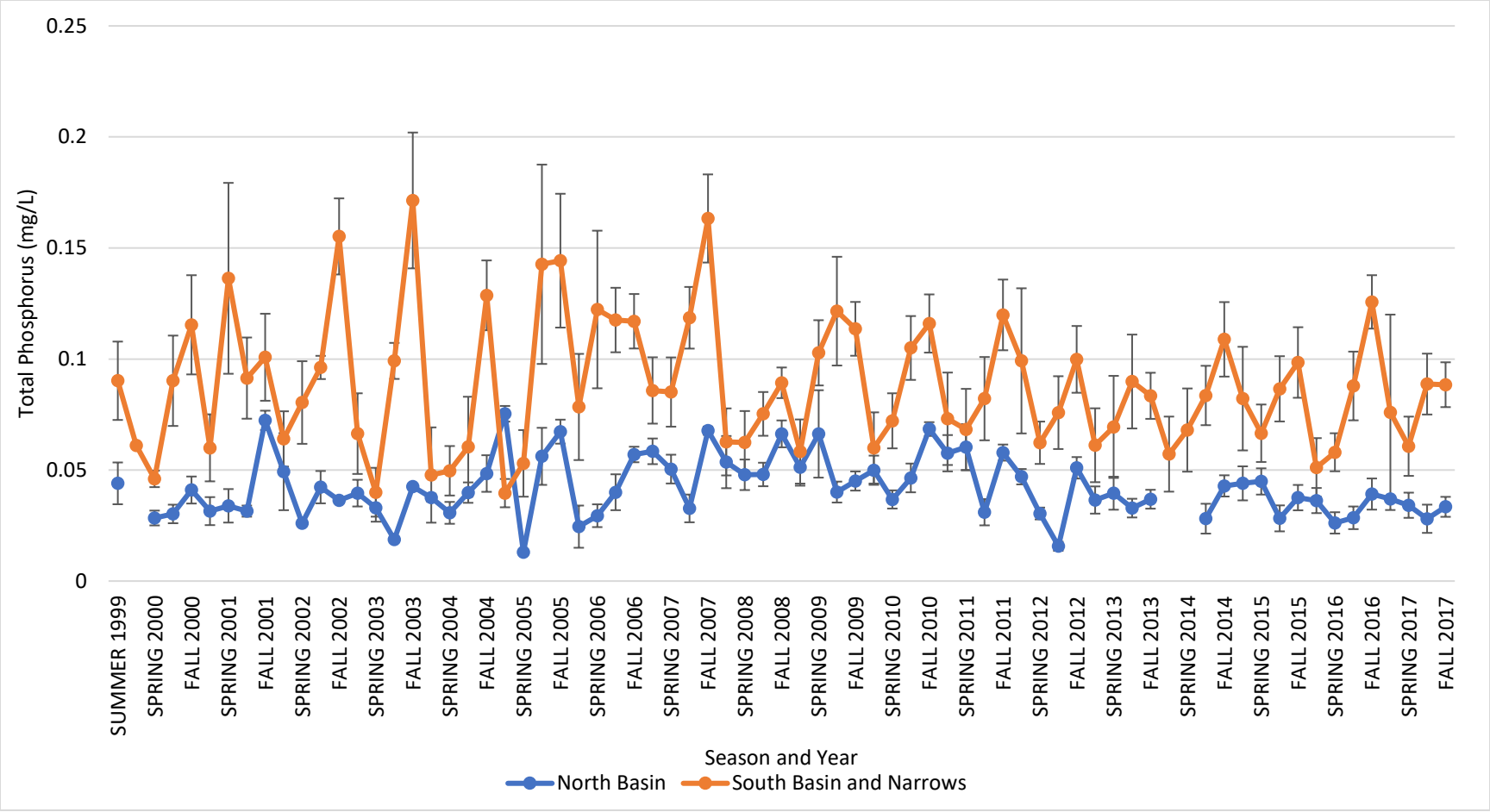

Figure 30. Total P concentrations (mg/L) in Lake Winnipeg between 1999 and 2017 as an average of surface and euphotic W stations data per year in the north basin and south basin and narrows during the spring, summer, fall and winter seasons (n=890, non-detects=1). Any non-detect values had $^{1/2}$ the detection limit used. Detection limit was 0.001 mg/L from 1999 to 2017 and 0.01 mg/L was the high range detection limit from 2011 to 2017.

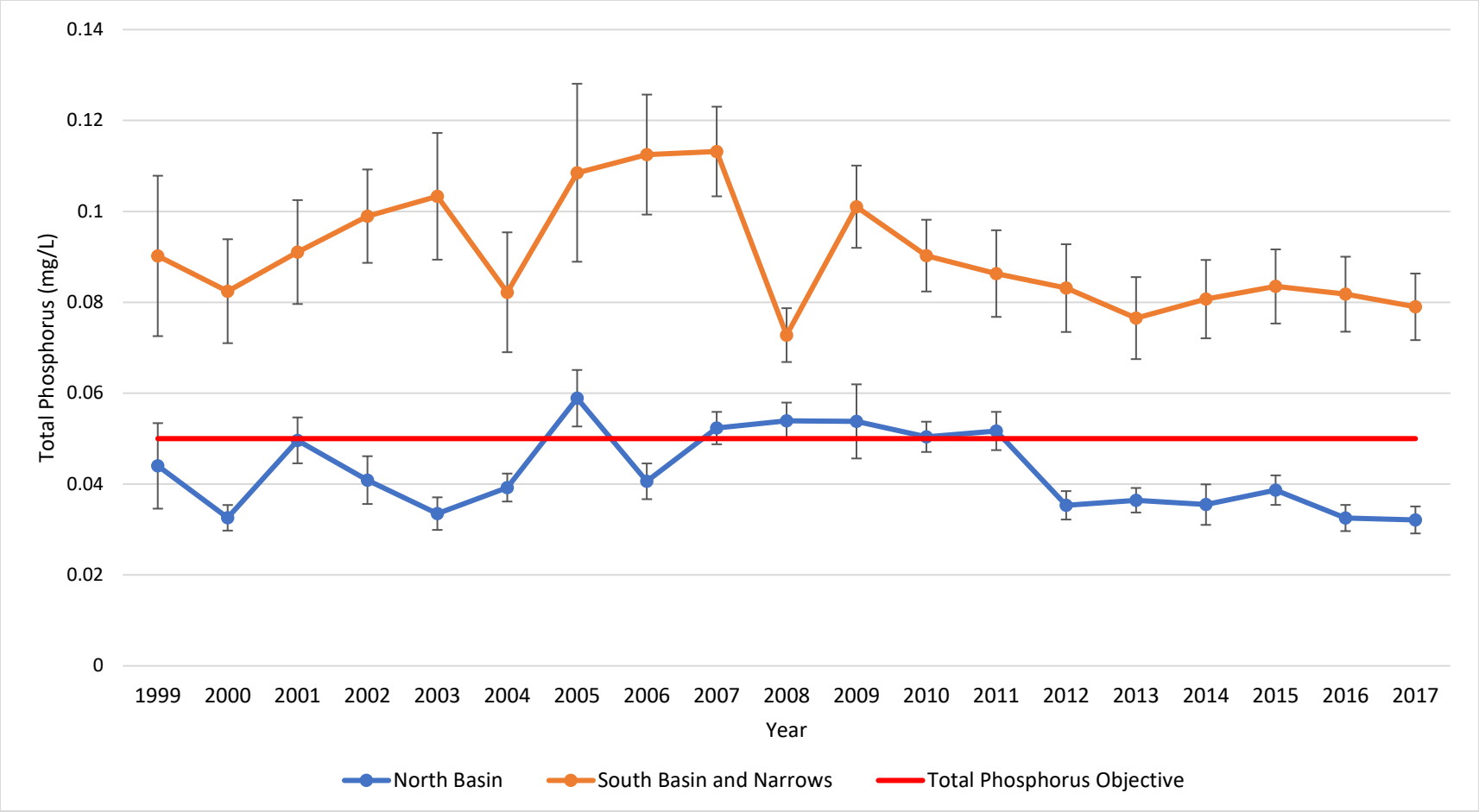

Figure 31. Total P concentrations (mg/L) in Lake Winnipeg with total P objective between 1999 and 2017 as an average of surface and euphotic W stations data per year in the north basin and south basin and narrows during the spring, summer, fall and winter seasons (n=890, non- detects=1). Any non-detect values had $^{1/2}$ the detection limit used. Detection limit was 0.001 mg/L from 1999 to 2017 and 0.01 mg/L was the high range detection limit from 2011 to 2017.

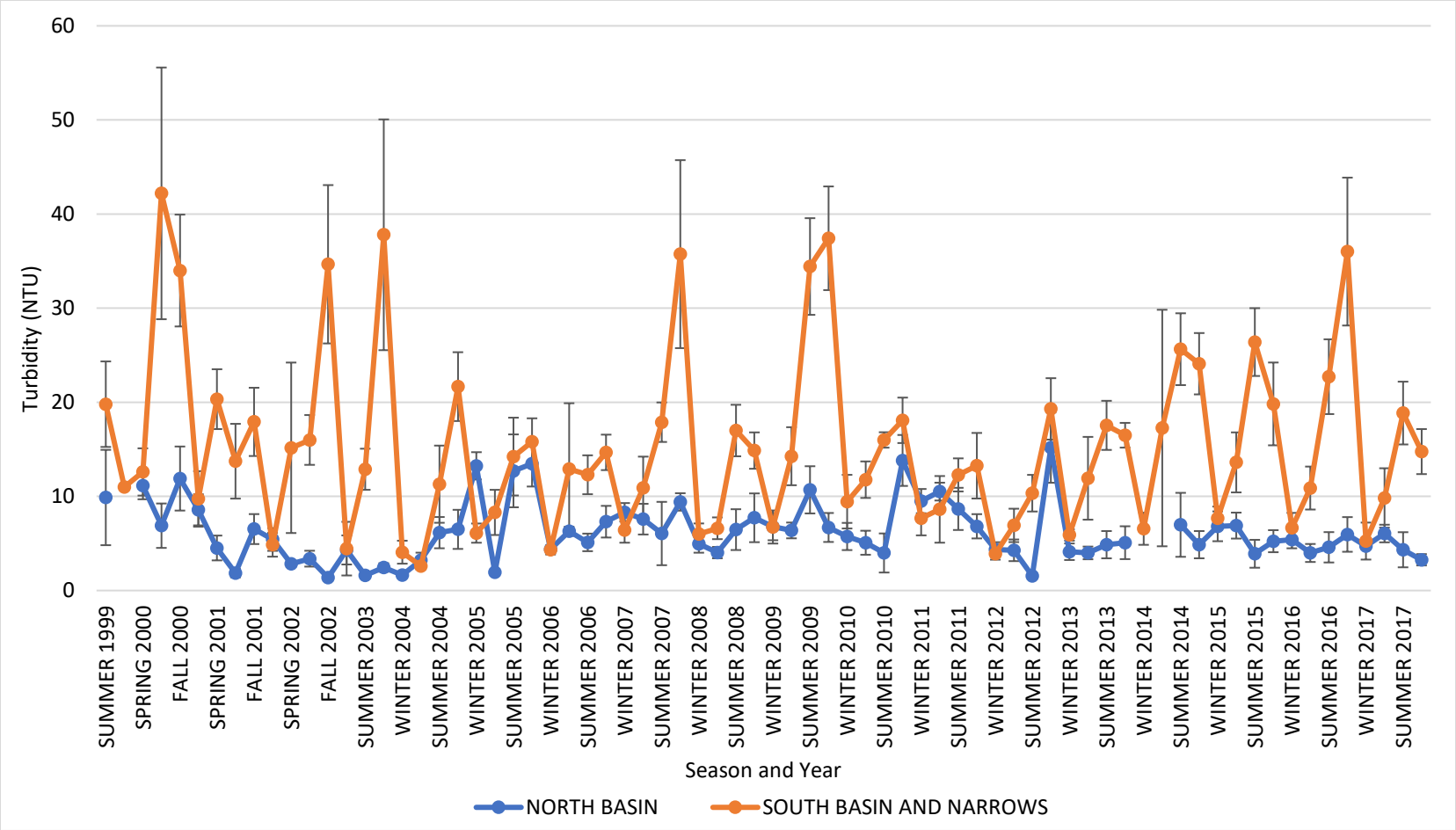

Figure 32. Turbidity levels (NTU) in Lake Winnipeg between 1999 and 2017 as an average of surface and euphotic W stations data per year in the north basin and south basin and narrows during the spring, summer, fall and winter seasons (n=857, non-detects=0). Detection limit was 0.01 NTU from 1999 to 2001 and 2009 to 2017 and 0.1 NTU was the high range detection limit from 2001 to 2009.

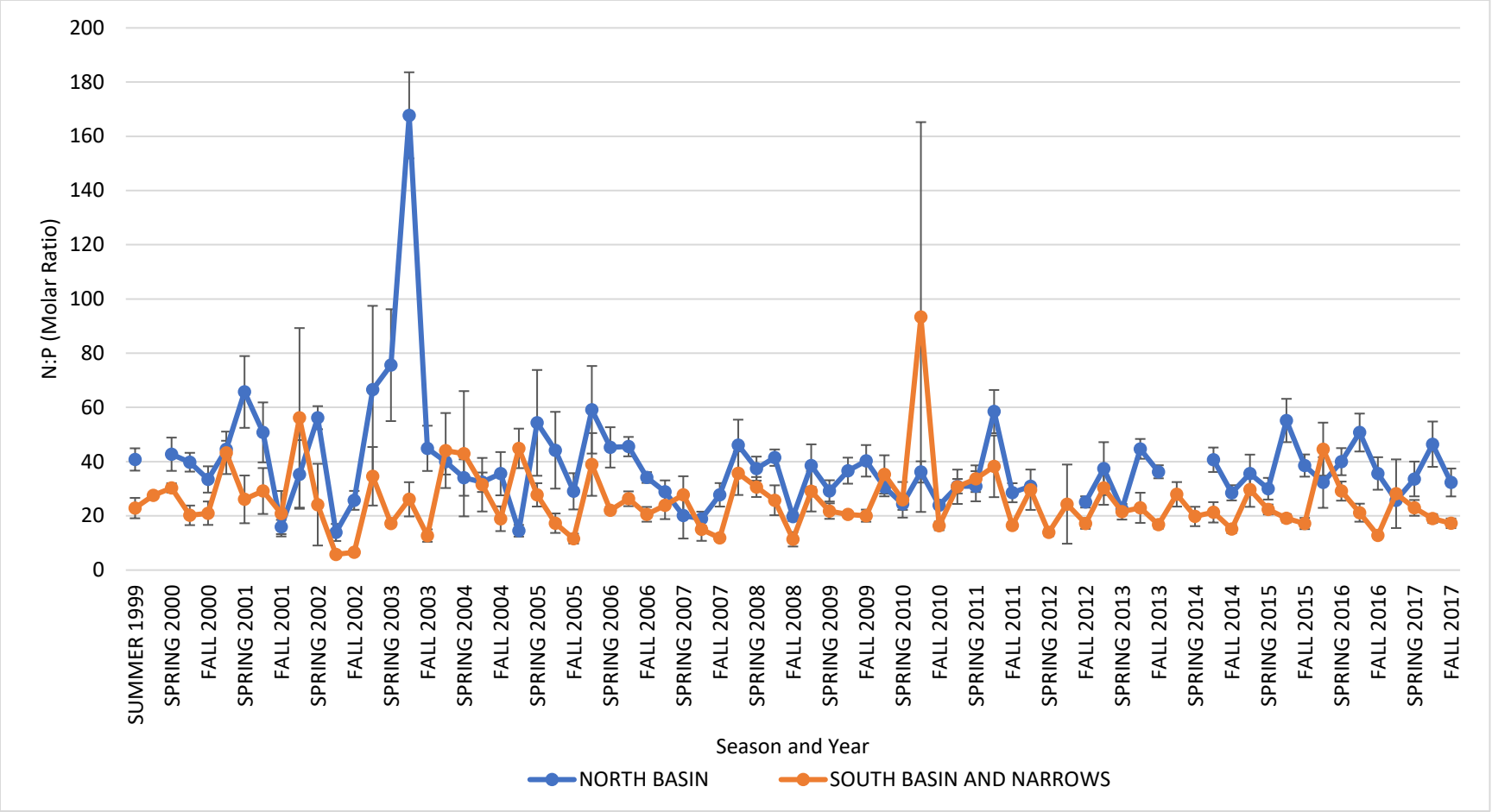

Figure 33. N:P molar ratio in Lake Winnipeg between 1999 and 2017 as an average of surface and euphotic W stations data per year in the north basin and south basin and narrows during the spring, summer, fall and winter. Two samples from the south basin and narrows fall 2008 (14087 molar ratio) and north basin fall 2008 (31870 molar ratio) were not included in the average calculations.

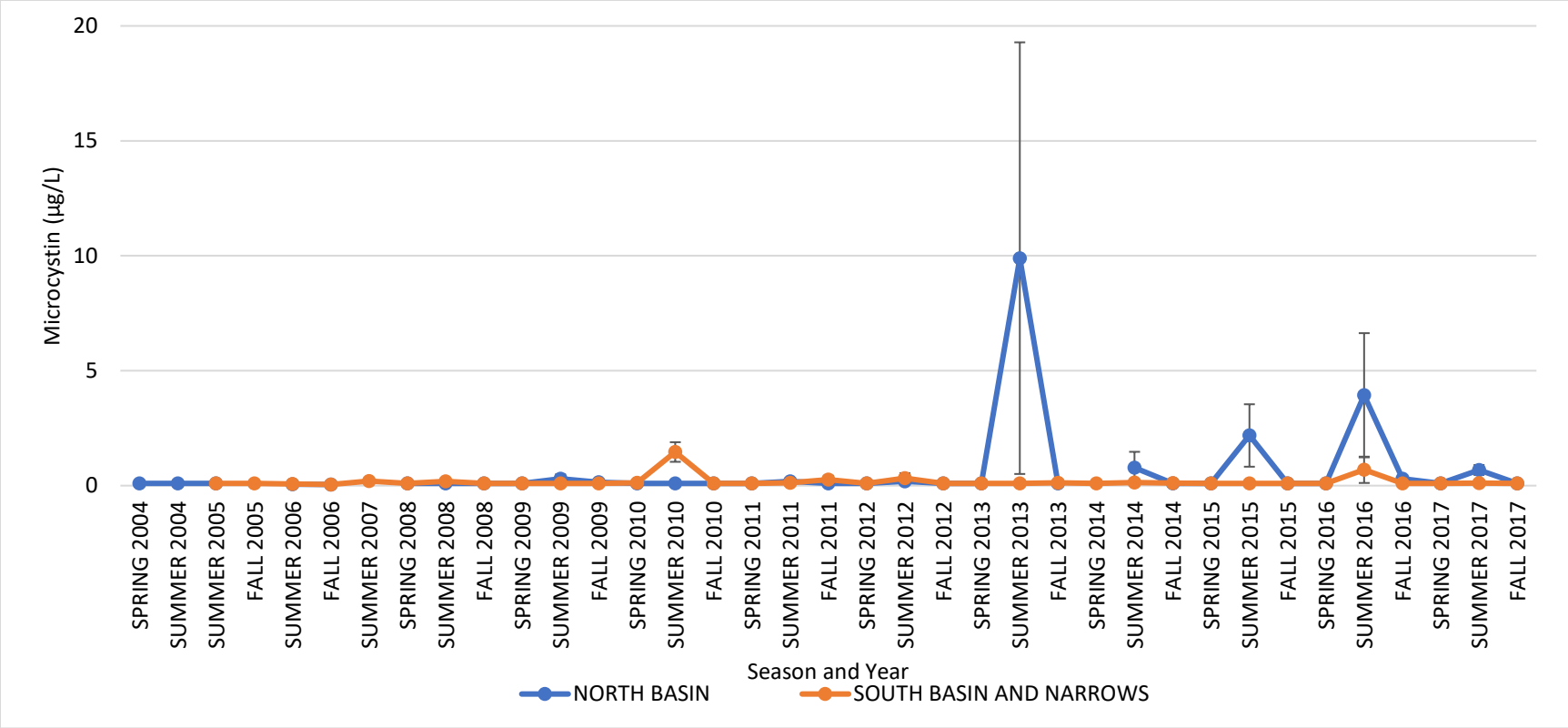

Figure 34. Microcystin concentrations (µg/L) in Lake Winnipeg between 2004 and 2017 as an average of surface and euphotic W and other stations data per year in the north basin and south basin and narrows during the spring, summer and fall seasons (n=655, non-detects=561). Any non-detect values had $^{1/2}$ the detection limit used. Detection limit of 0.2 µg/L from 2009 to 2017. Drinking water guideline = 1.5 µg/L and recreational guideline = 20 µg/L. Two samples one from summer of 2013 (station 19 = 85 µg/L) and one from the summer of 2016 (Bloom 5 [along the east side of the north basin] = 43.7 µg/L) were not included on the graph.

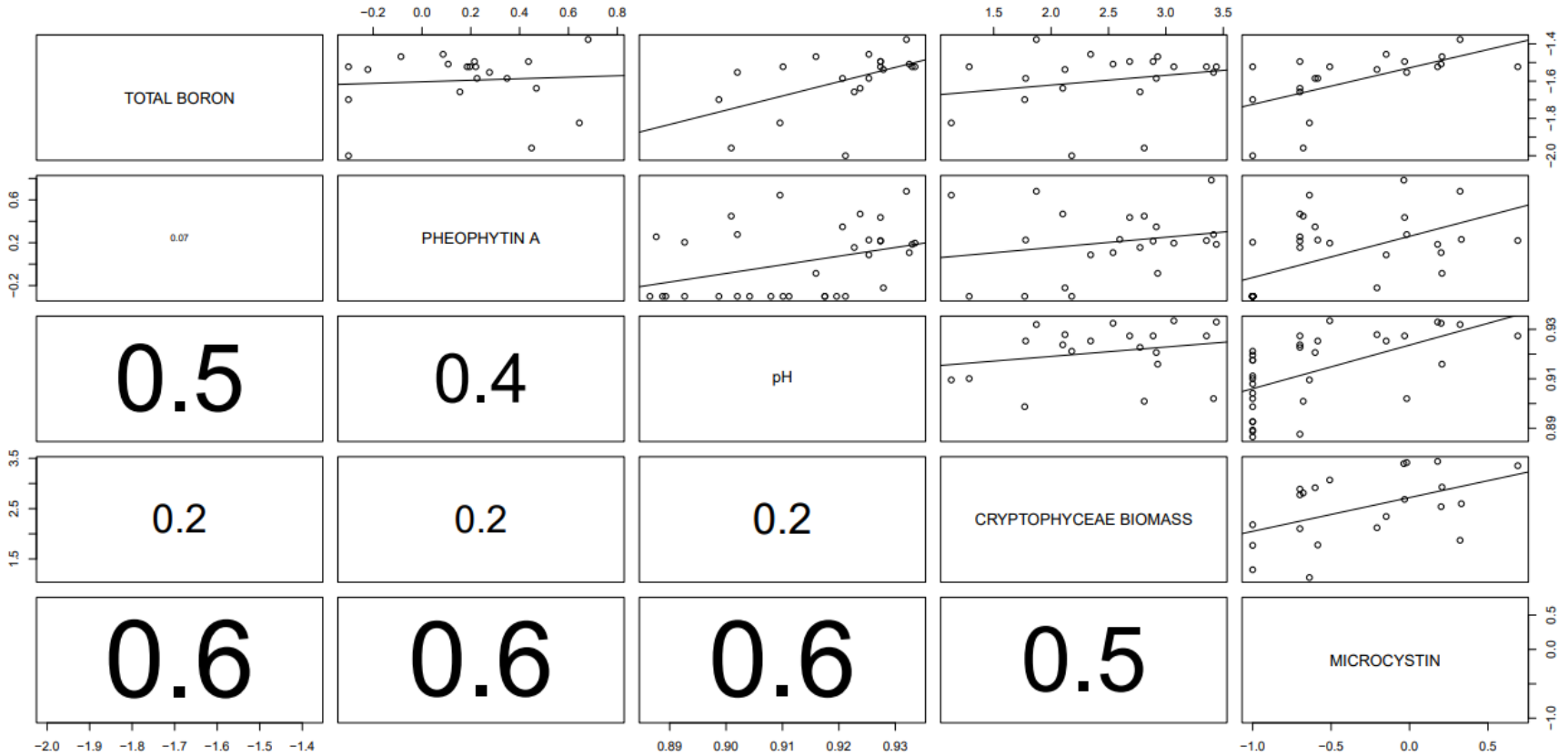

Figure 35. Multi-panel scatterplot from the euphotic dataset of total boron, pheophytin *a*, pH and Cryptophyceae biomass against microcystin toxin with Pearson correlation coefficient and trend line.

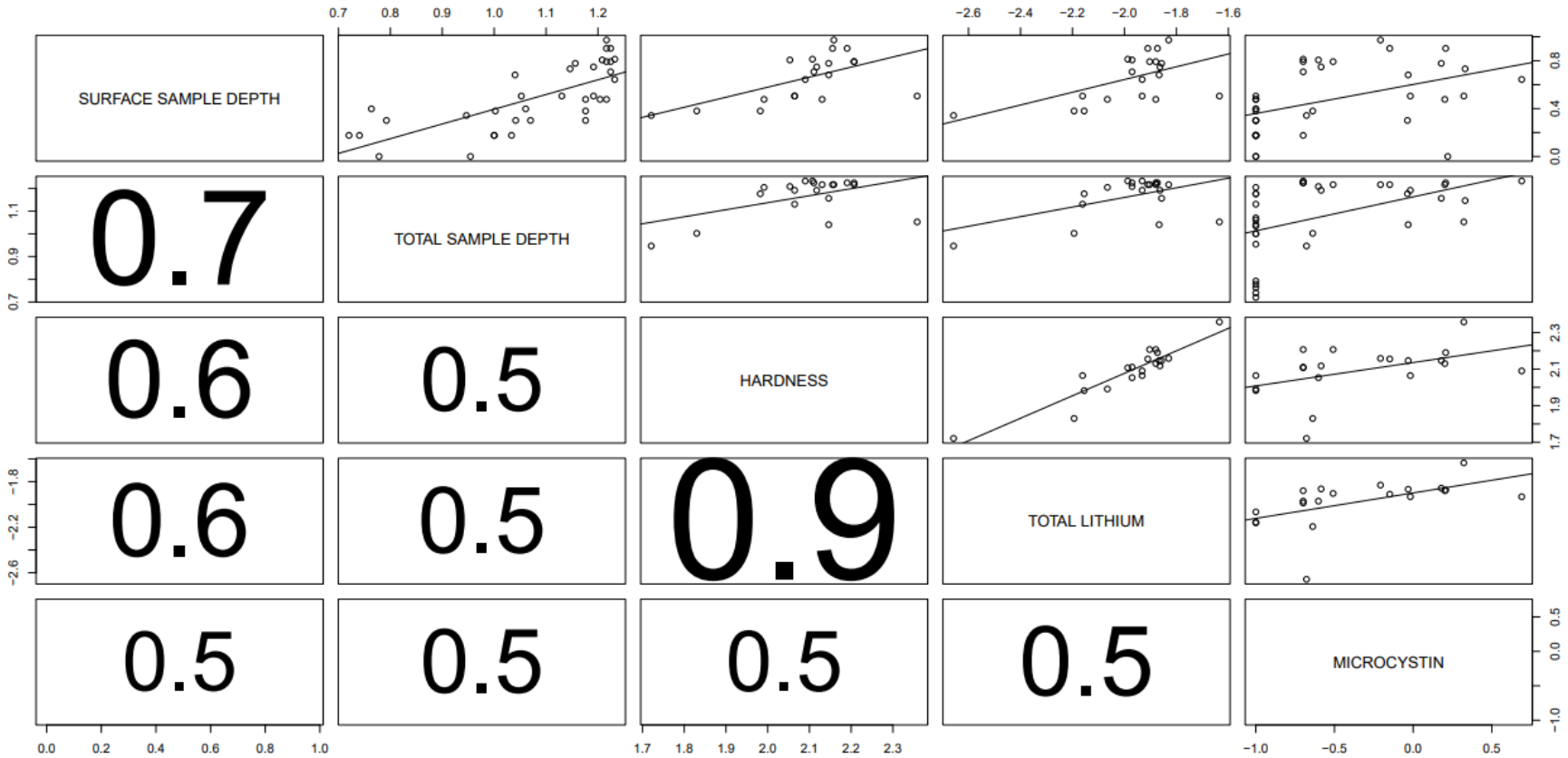

Figure 36. Multi-panel scatterplot from the euphotic dataset of surface sample depth, total sample depth, hardness and total lithium against microcystin toxin with Pearson correlation coefficient and trend line.

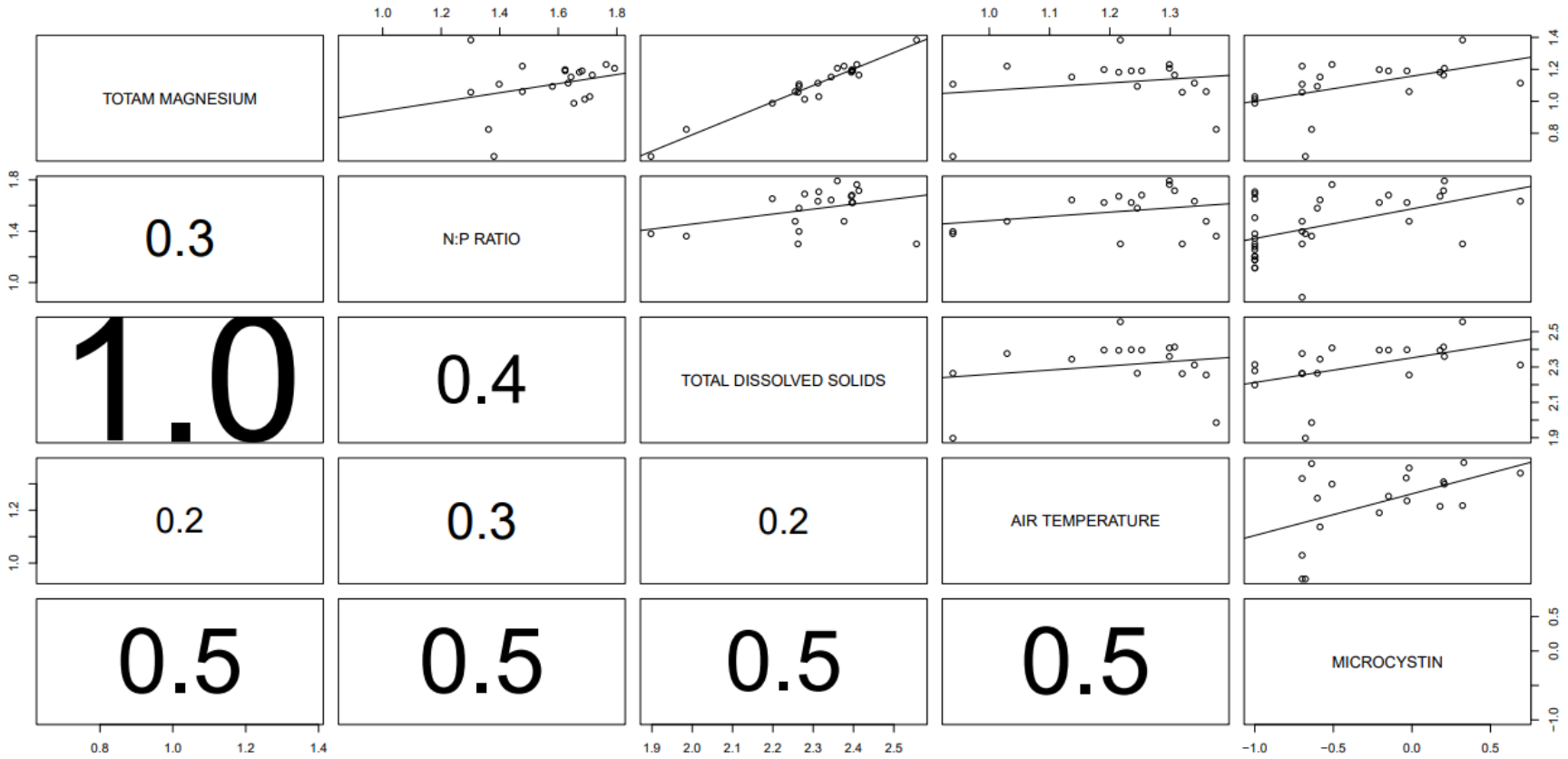

Figure 37. Multi-panel scatterplot from the euphotic dataset of total magnesium, N:P ratio, total dissolved solids and air temperature against microcystin toxin with Pearson correlation coefficient and trend line.

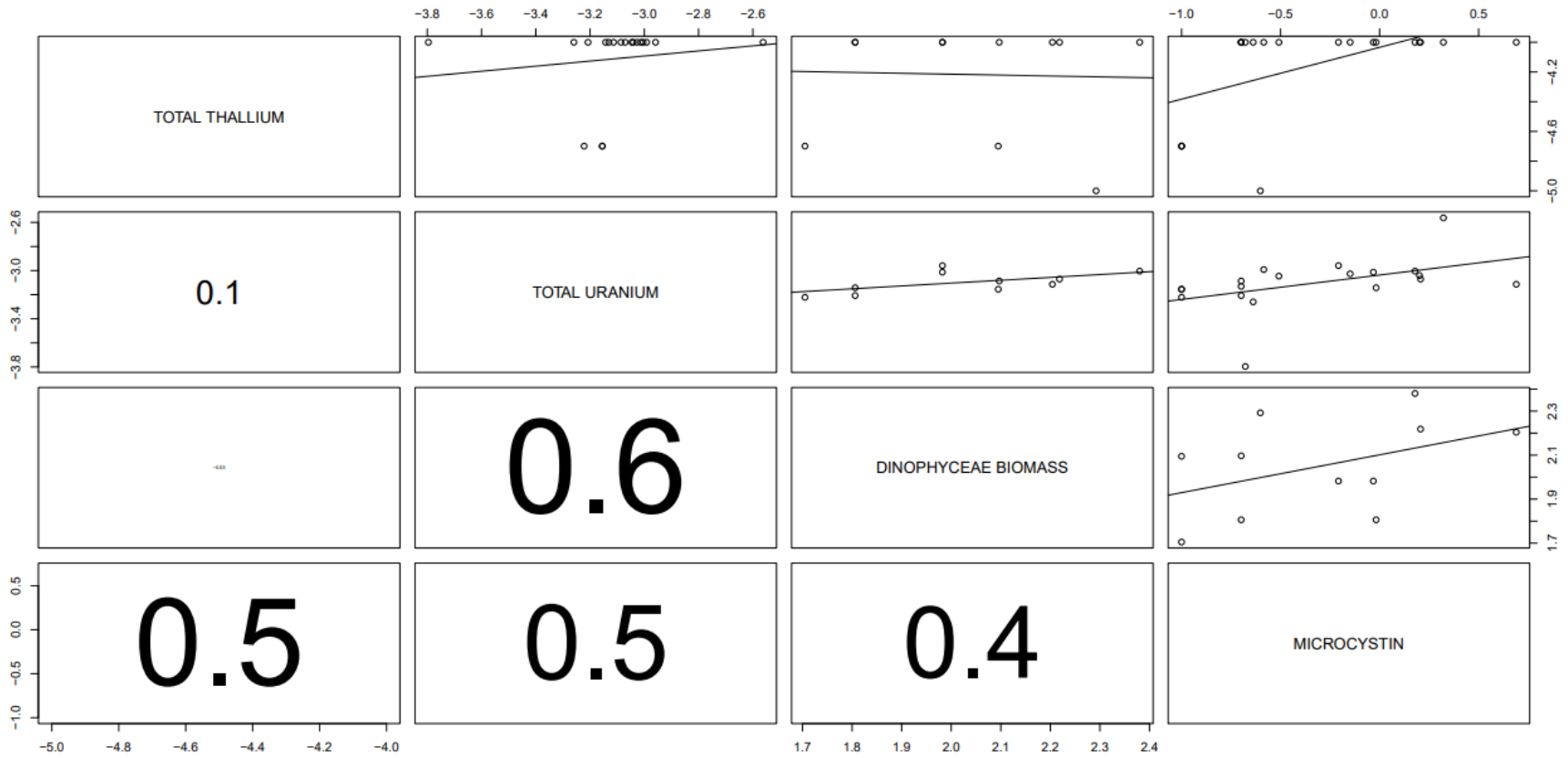

Figure 38. Multi-panel scatterplot from the euphotic dataset of total thallium, total uranium and Dinophyceae biomass against microcystin toxin with Pearson correlation coefficient and trend line.

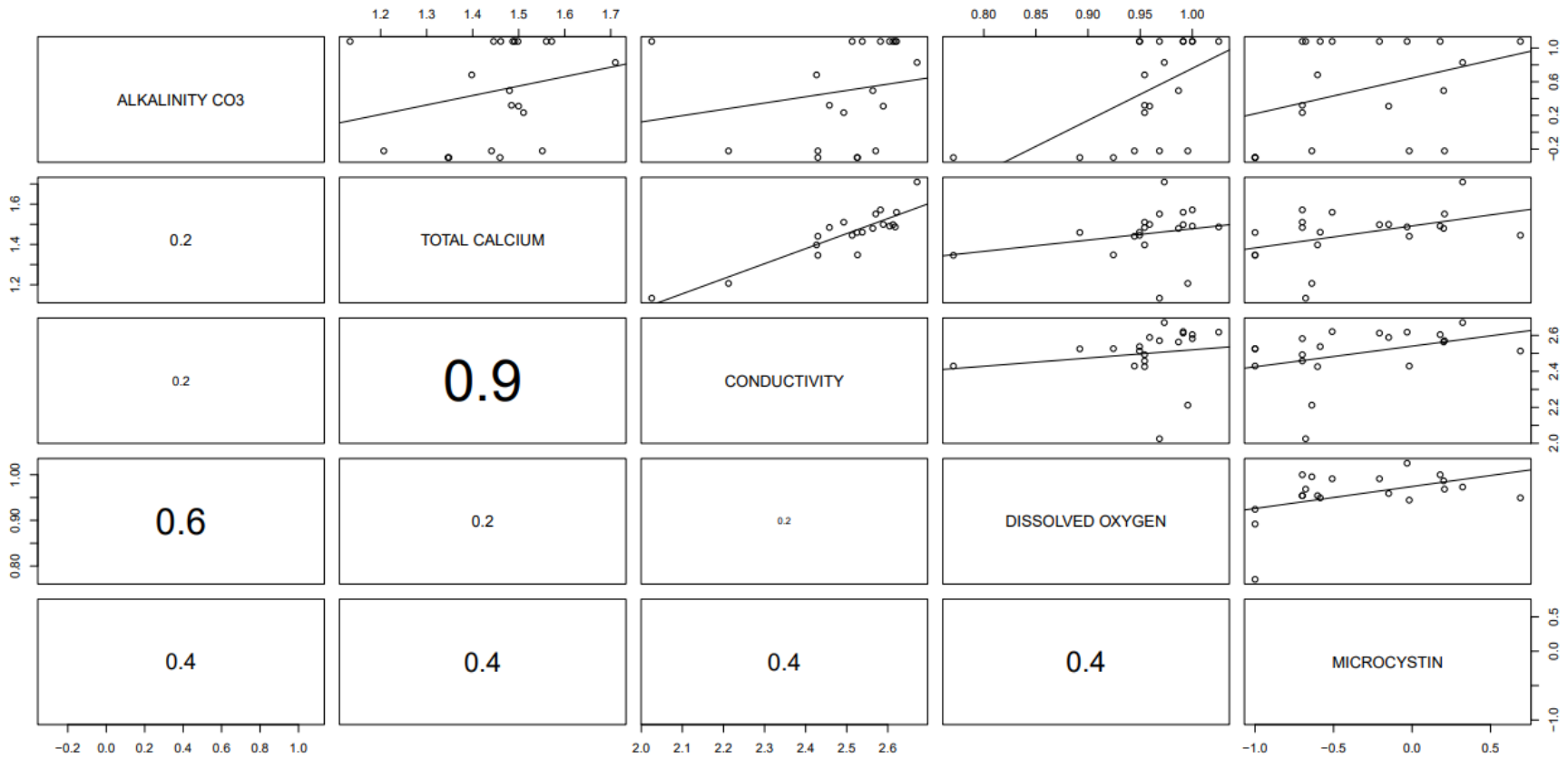

Figure 39. Multi-panel scatterplot from the euphotic dataset of alkalinity CO_3, total calcium, conductivity and DO against microcystin toxin with Pearson correlation coefficient and trend line.

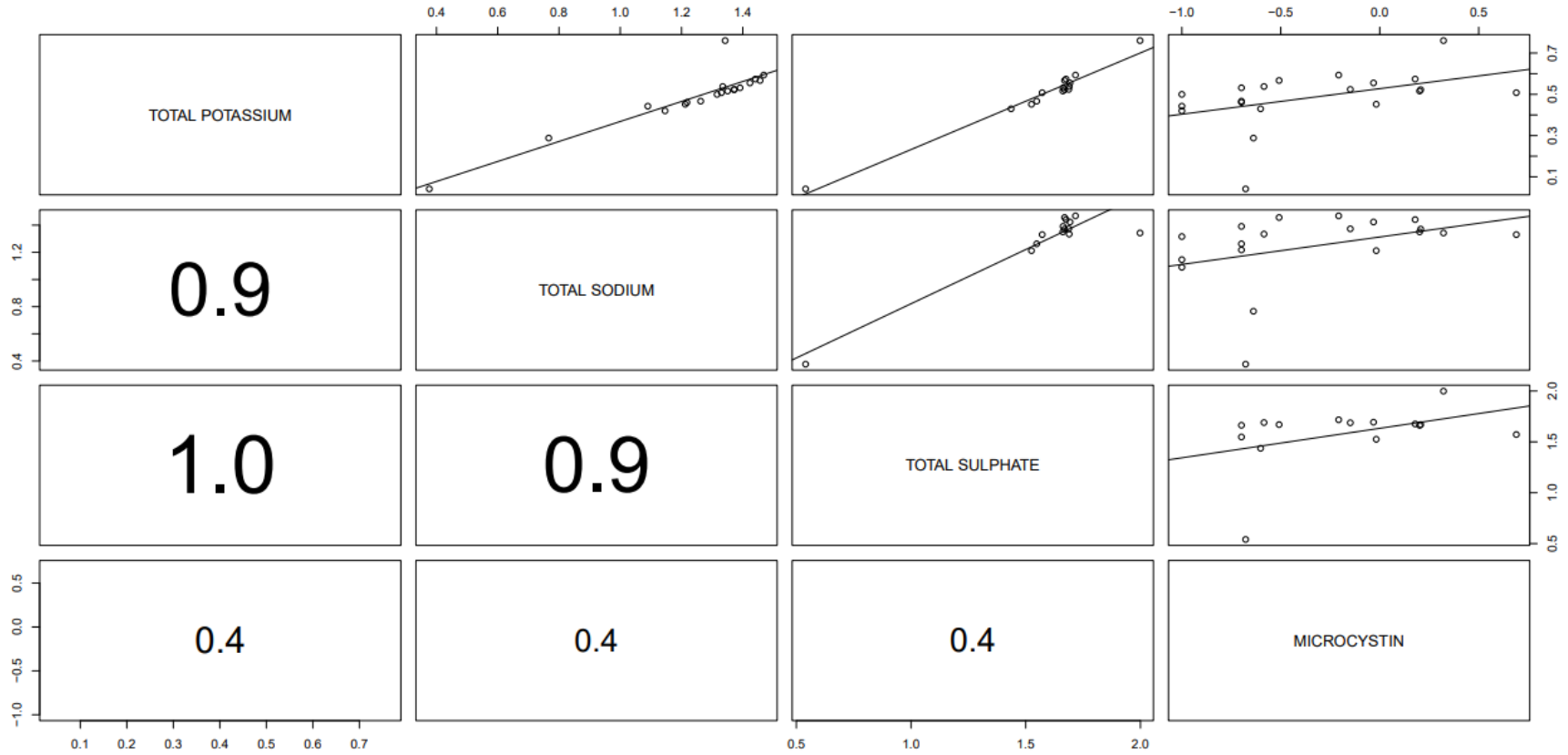

Figure 40. Multi-panel scatterplot from the euphotic dataset of total potassium, total sodium and total sulphate against microcystin toxin with Pearson correlation coefficient and trend line.

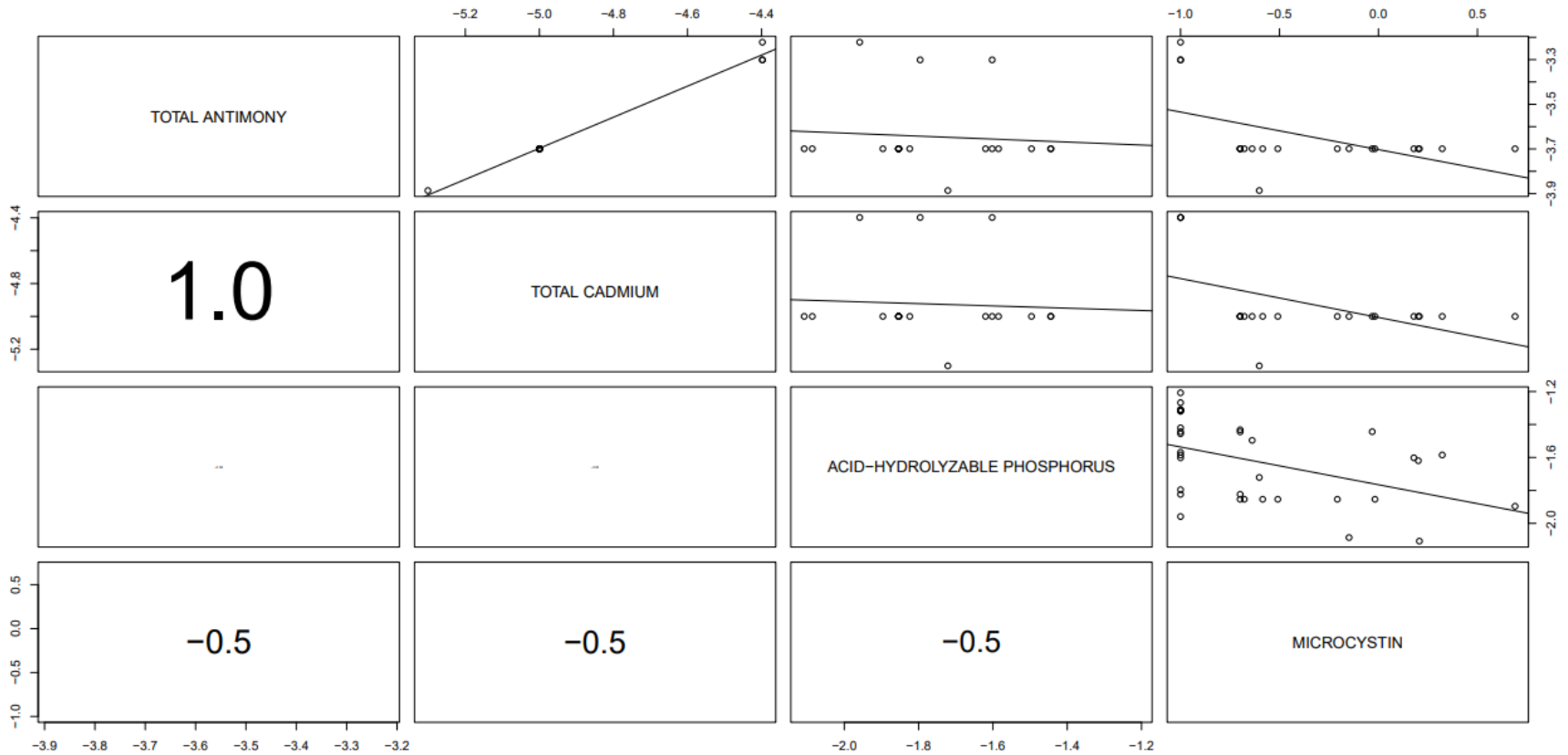

Figure 41. Multi-panel scatterplot from the euphotic dataset of total antimony, total cadmium and acid-hydrolyzable P against microcystin toxin with Pearson correlation coefficient and trend line.

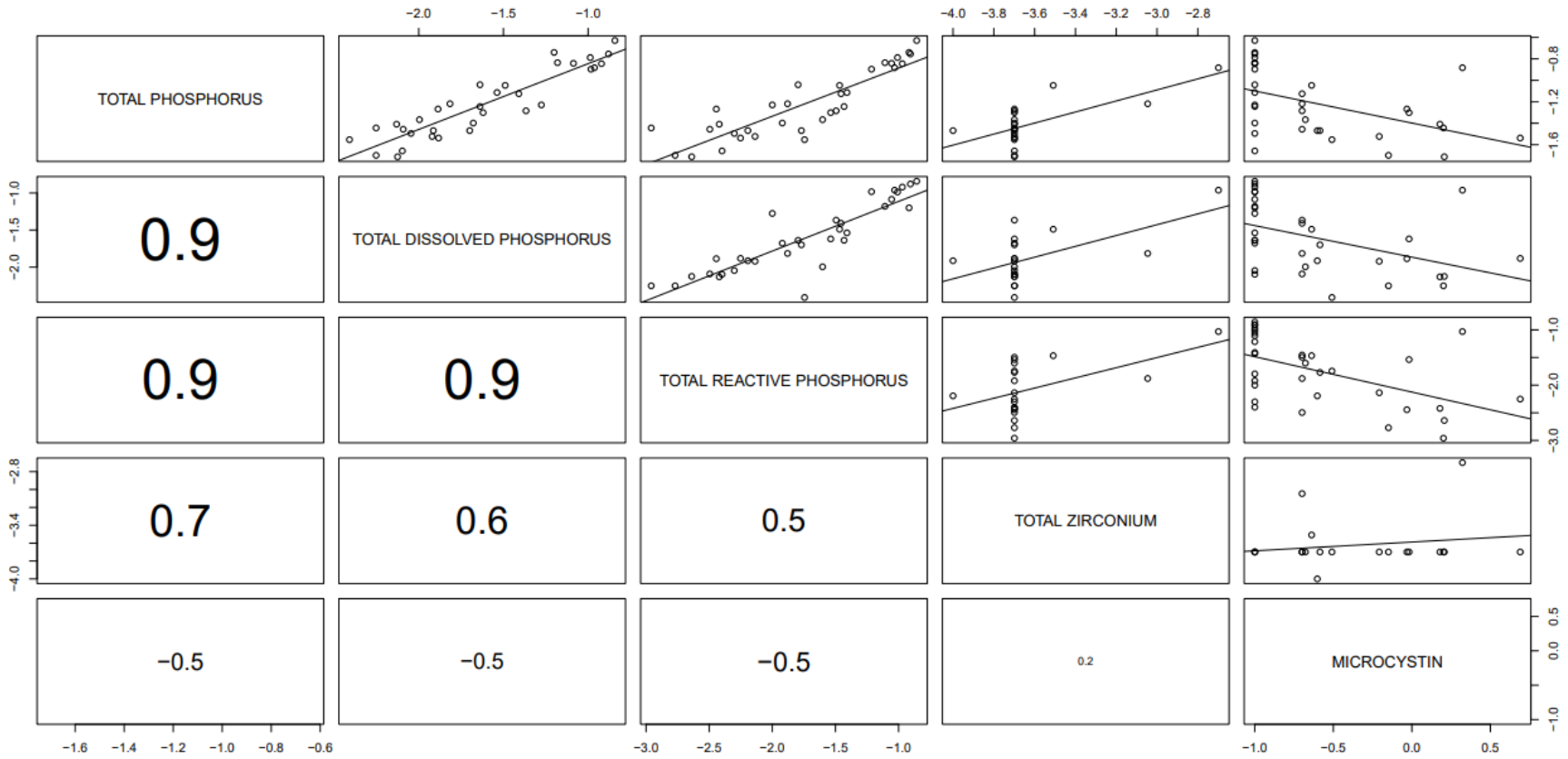

Figure 42. Multi-panel scatterplot from the euphotic dataset of total P, total dissolved P, total reactive P and total zirconium against microcystin toxin with Pearson correlation coefficient and trend line.

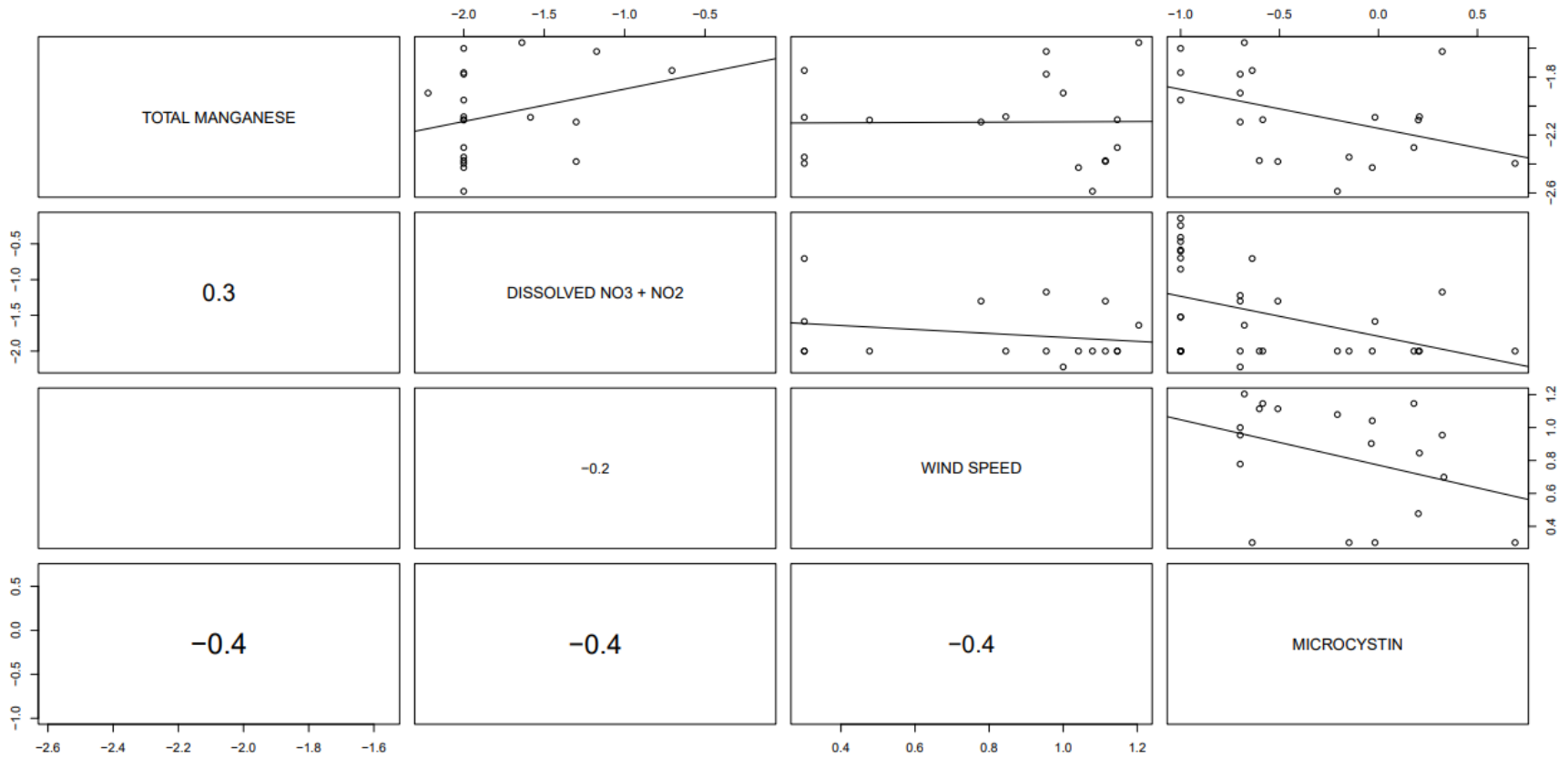

Figure 43. Multi-panel scatterplot from the euphotic dataset of total manganese, dissolved NO_3+NO_2 and wind speed against microcystin toxin with Pearson correlation coefficient and trend line.

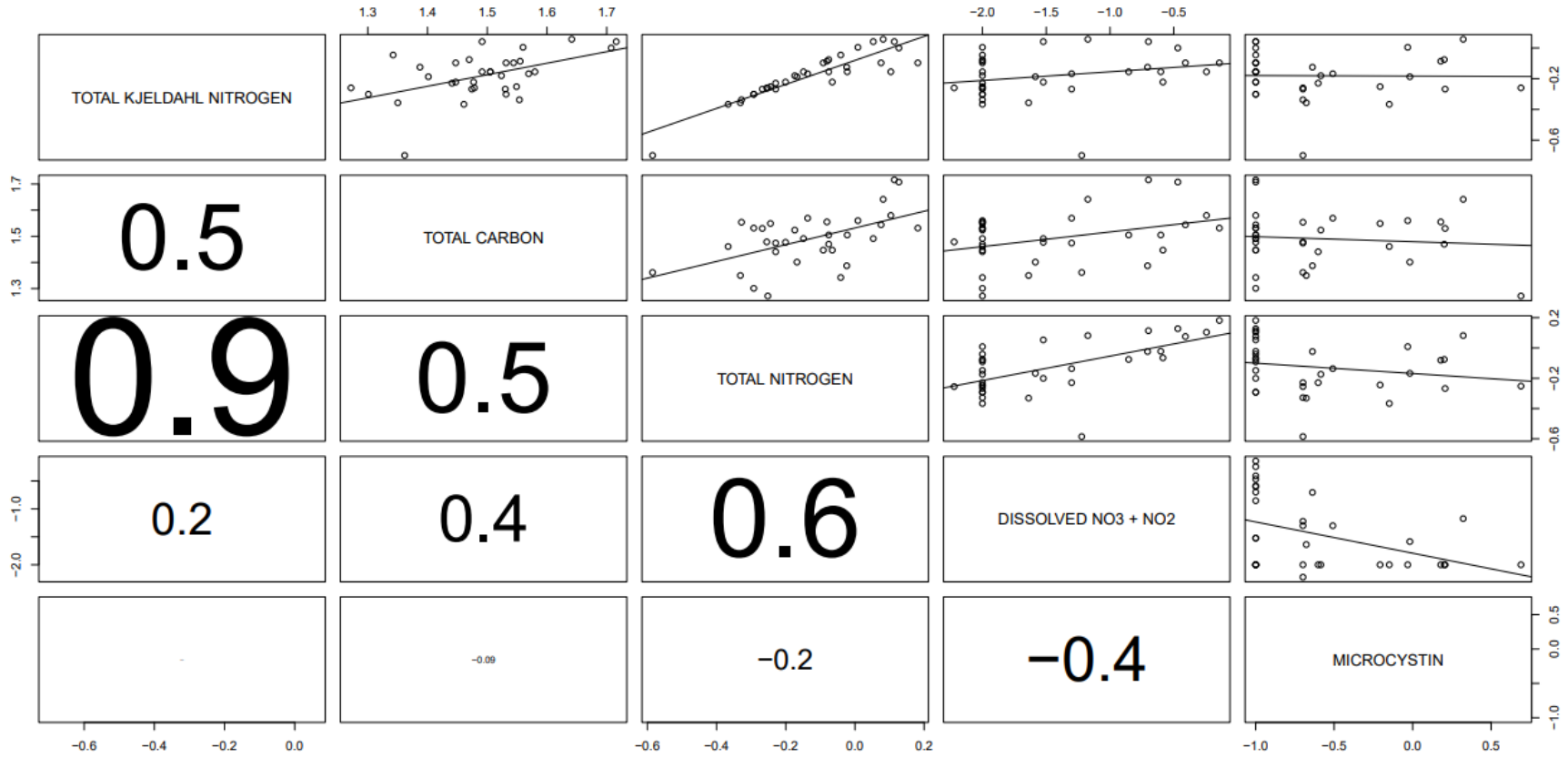

Figure 44. Multi-panel scatterplot from the euphotic dataset of total Kjeldahl nitrogen, total carbon, total nitrogen and dissolved NO_3+NO_2 against microcystin toxin with Pearson correlation coefficient and trend line.

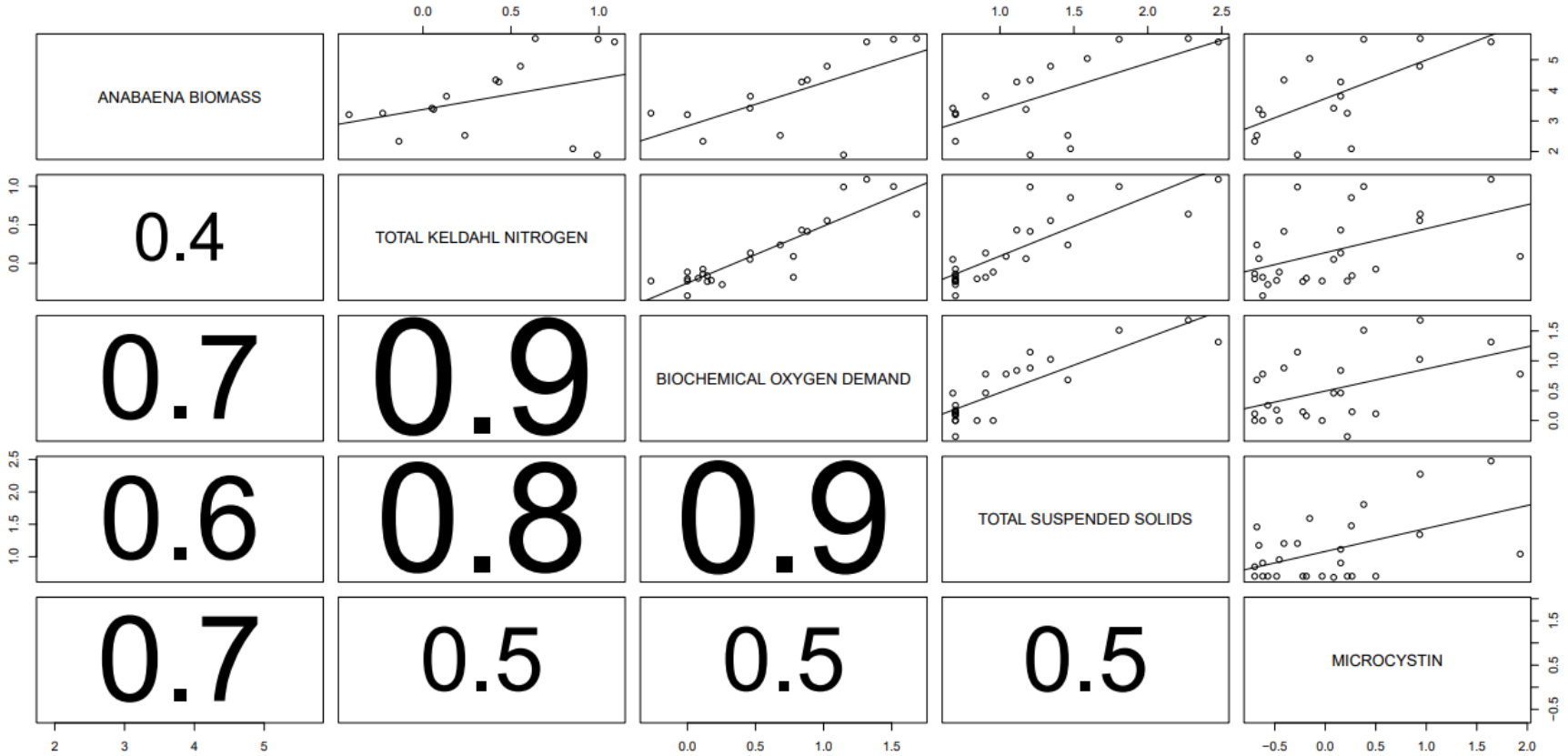

Figure 45. Multi-panel scatterplot from the surface dataset of *Anabaena* biomass, total Kjeldahl N, BOD and total suspended solids against microcystin toxin with Pearson correlation coefficient and trend line.

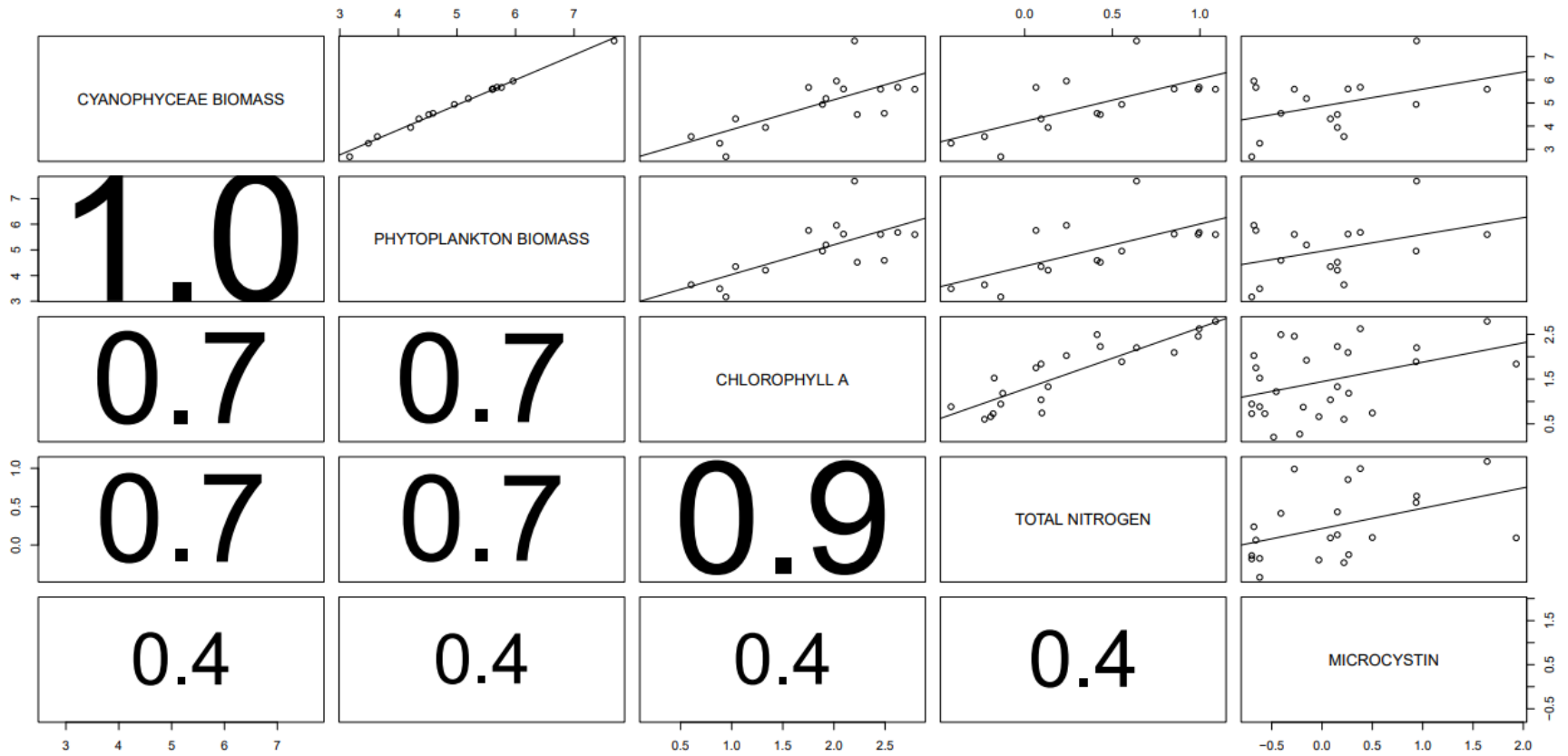

Figure 46. Multi-panel scatterplot from the surface dataset of Cyanophyceae biomass, Phytoplankton biomass, chlorophyll *a* and total N against microcystin toxin with Pearson correlation coefficient and trend line.

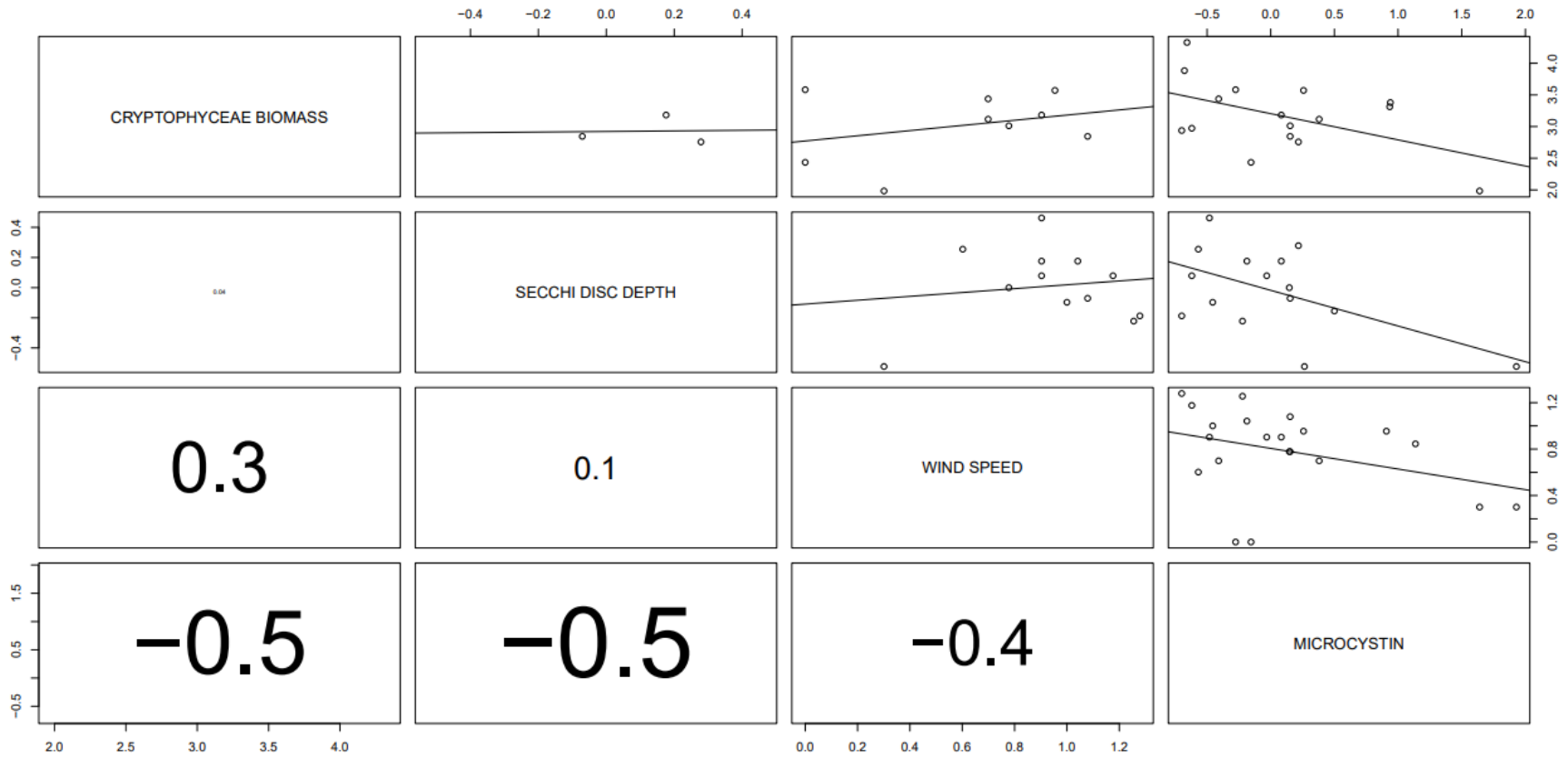

Figure 47. Multi-panel scatterplot from the surface dataset of Cryptophyceae biomass, Secchi disk depth and wind speed against microcystin toxin with Pearson correlation coefficient and trend line.

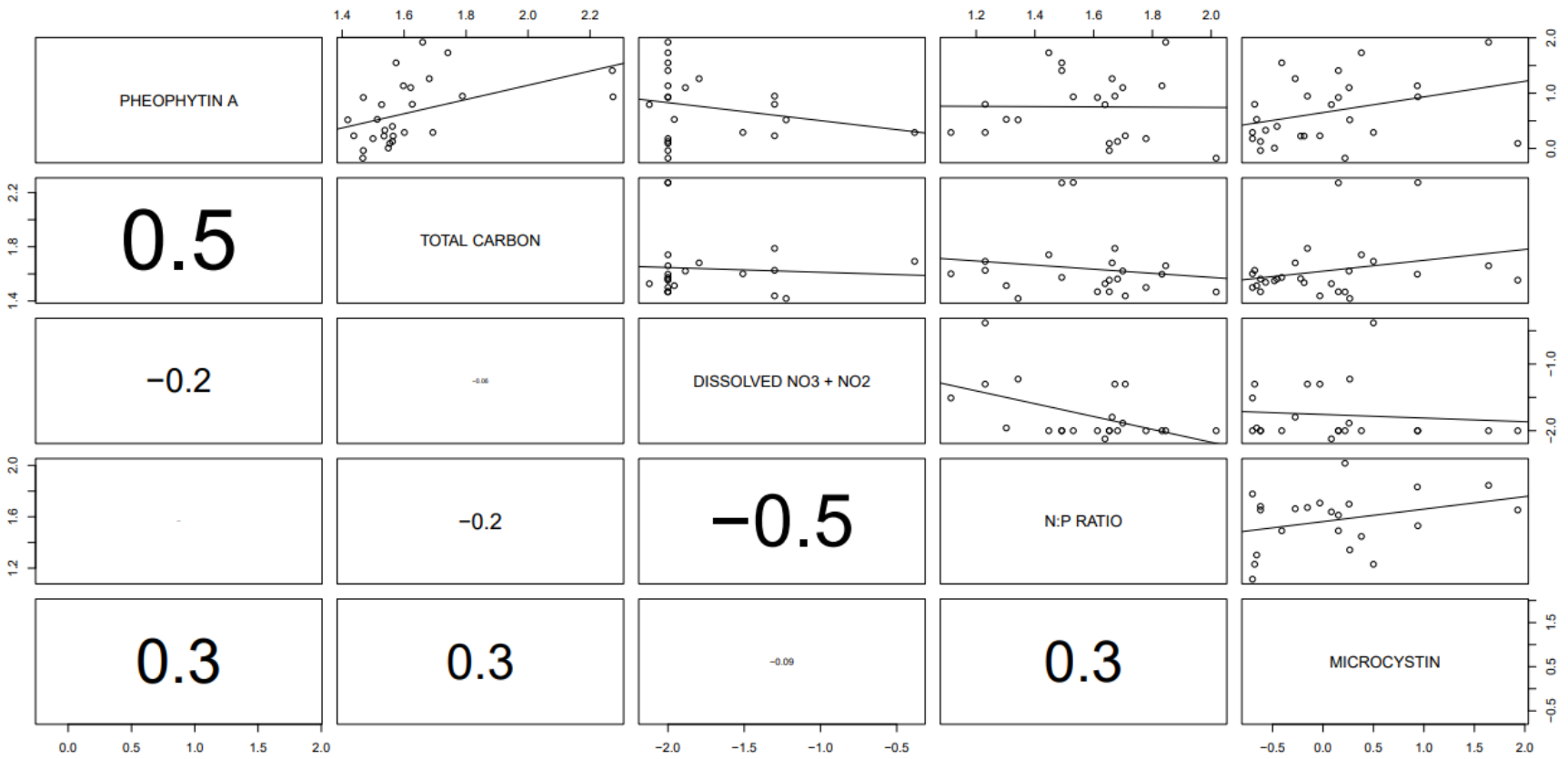

Figure 48. Multi-panel scatterplot from the surface dataset of pheophytin *a*, total carbon, dissolved NO_3 + NO_2 and N:P ratio against microcystin toxin with Pearson correlation coefficient and trend line.

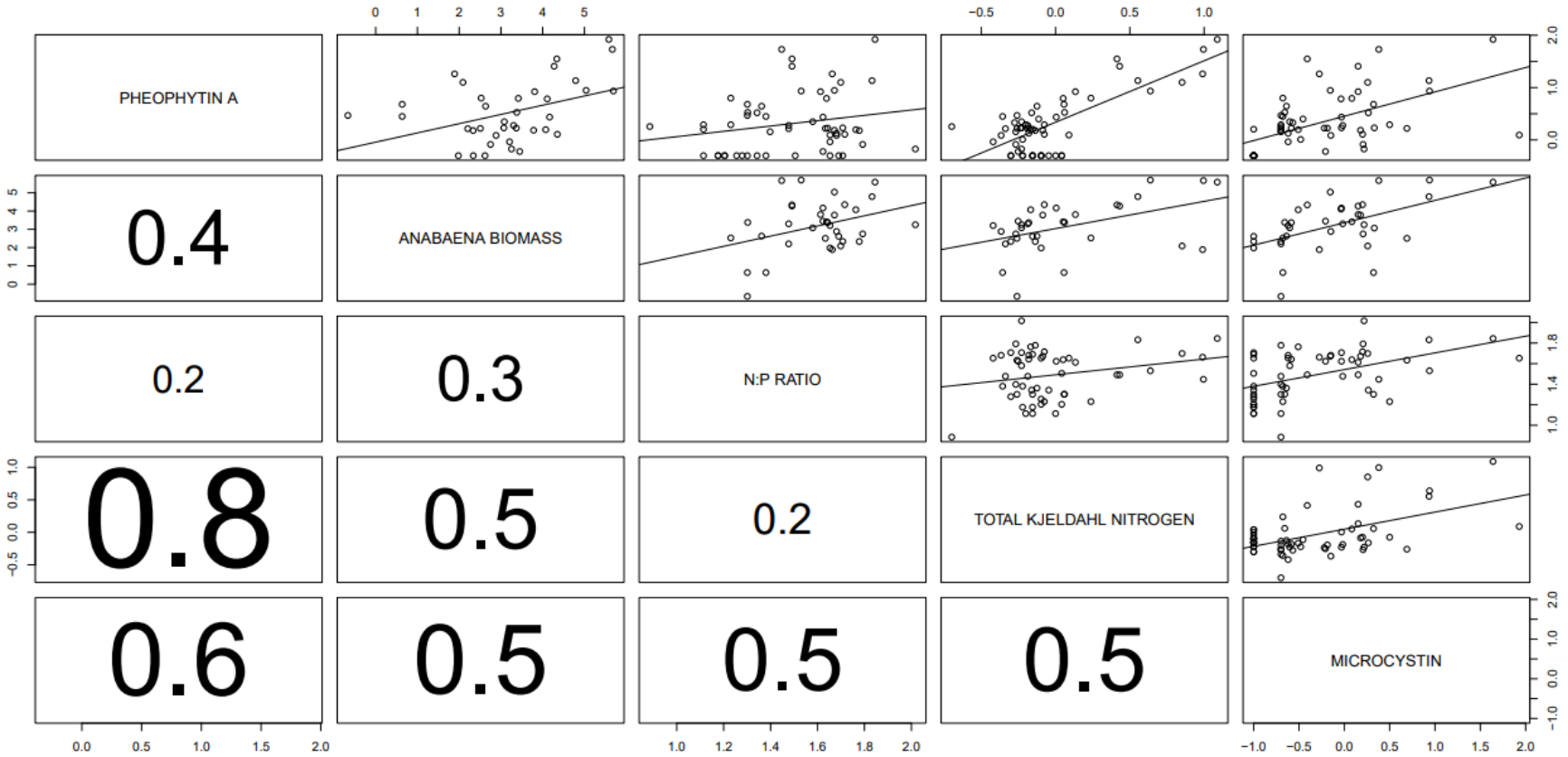

Figure 49. Multi-panel scatterplot from the combined euphotic and surface dataset of pheophytin *a*, *Anabaena* biomass, N:P ratio and total Kjeldahl N against microcystin toxin with Pearson correlation coefficient and trend line.

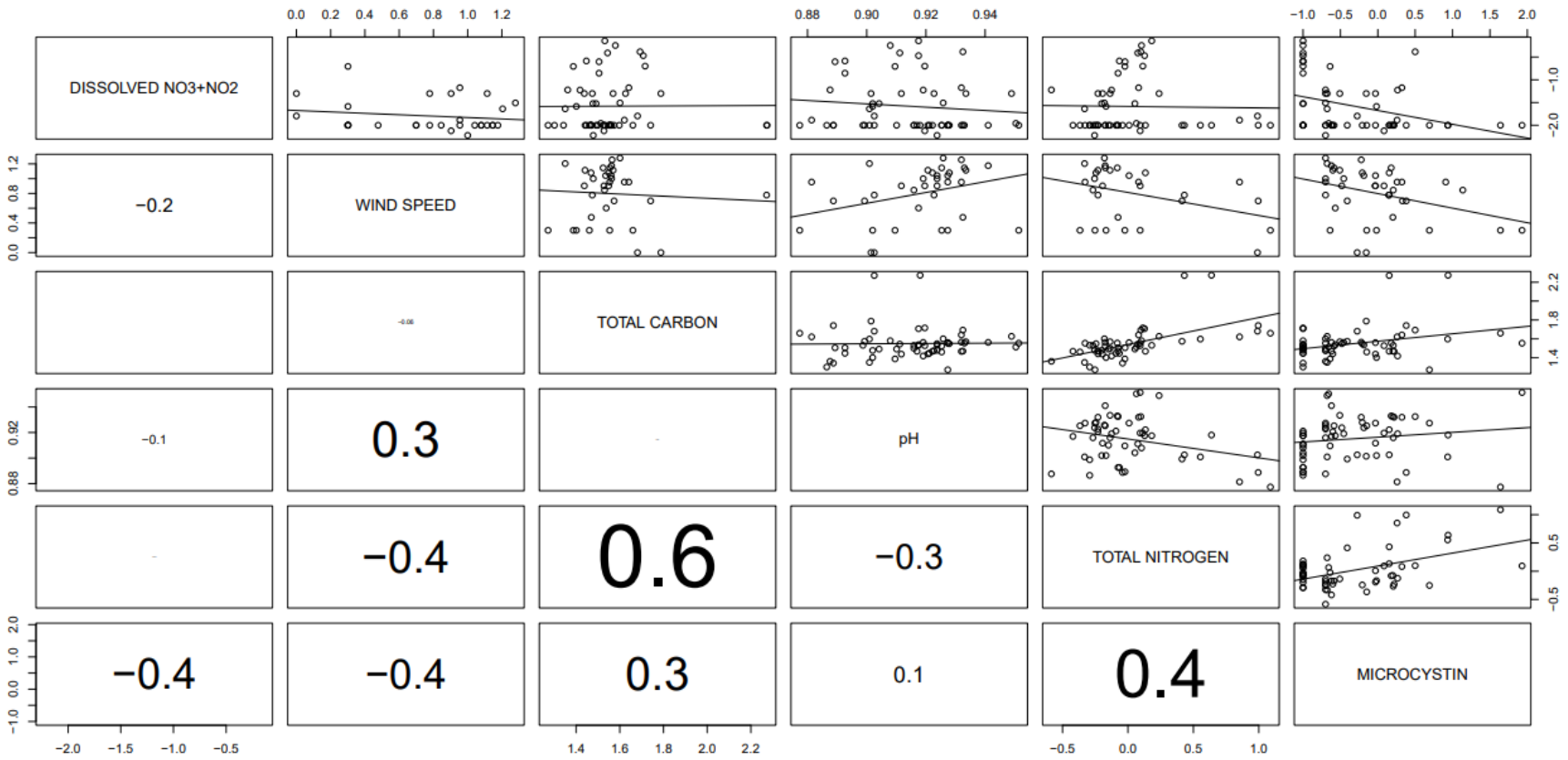

Figure 50. Multi-panel scatterplot from the combined euphotic and surface dataset of dissolved NO_3+NO_2, wind speed, total C, pH and total N against microcystin toxin with Pearson correlation coefficient and trend line.

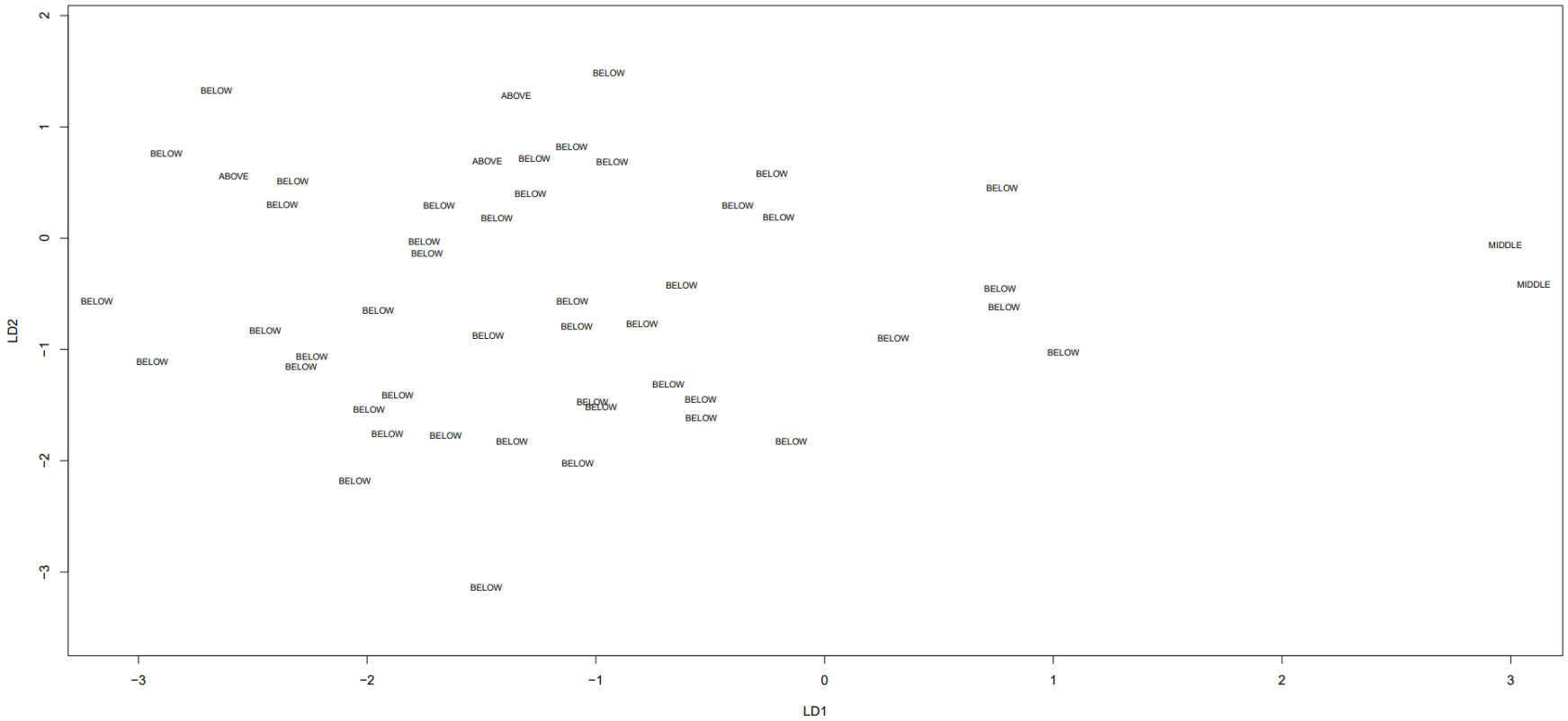

Figure 51. Linear discriminant analysis euphotic data observations.

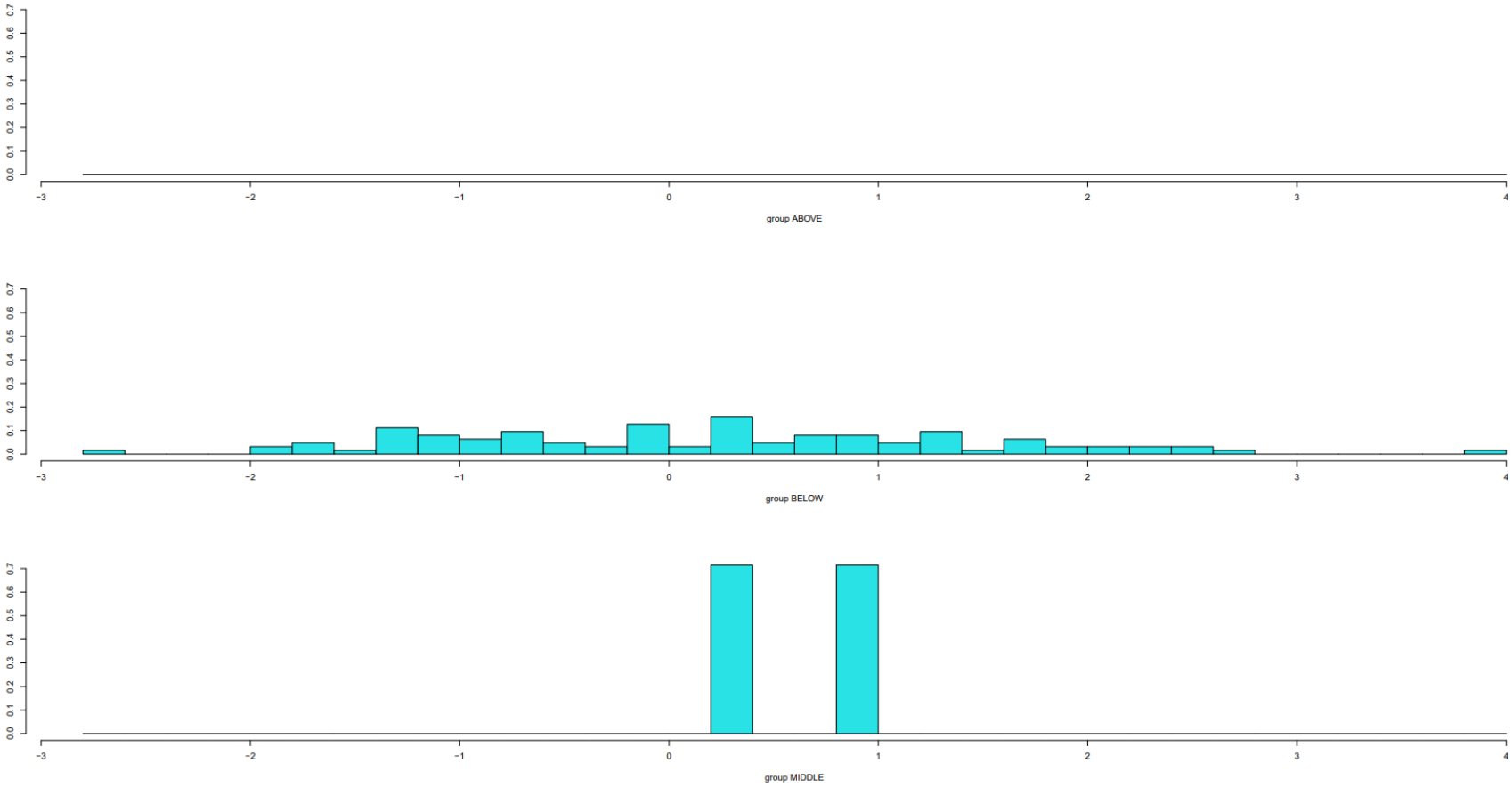

Figure 52. Histogram for LD1 for the linear discriminant analysis euphotic data observations.

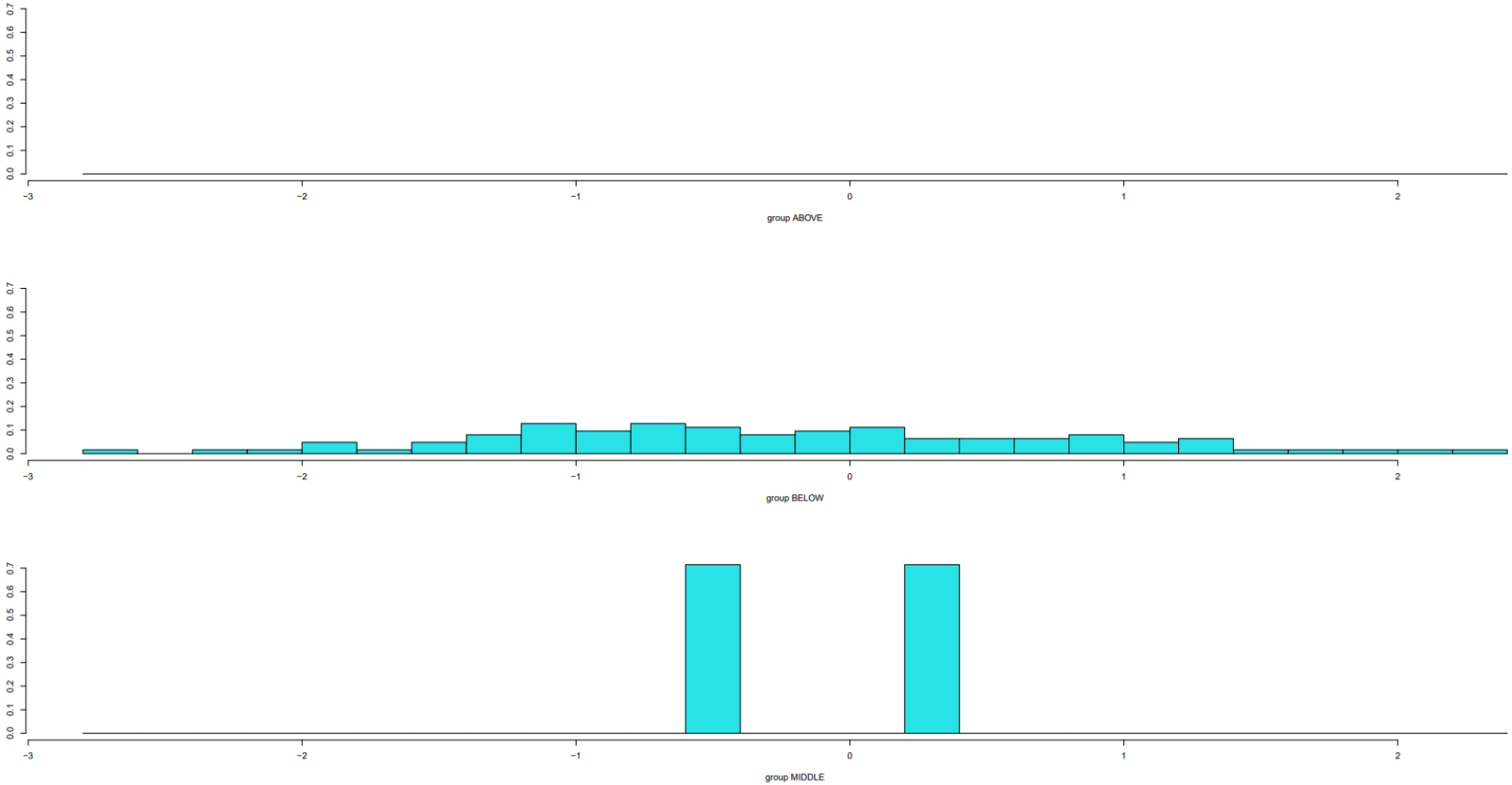

Figure 53. Histogram for LD2 for the linear discriminant analysis euphotic data observations.

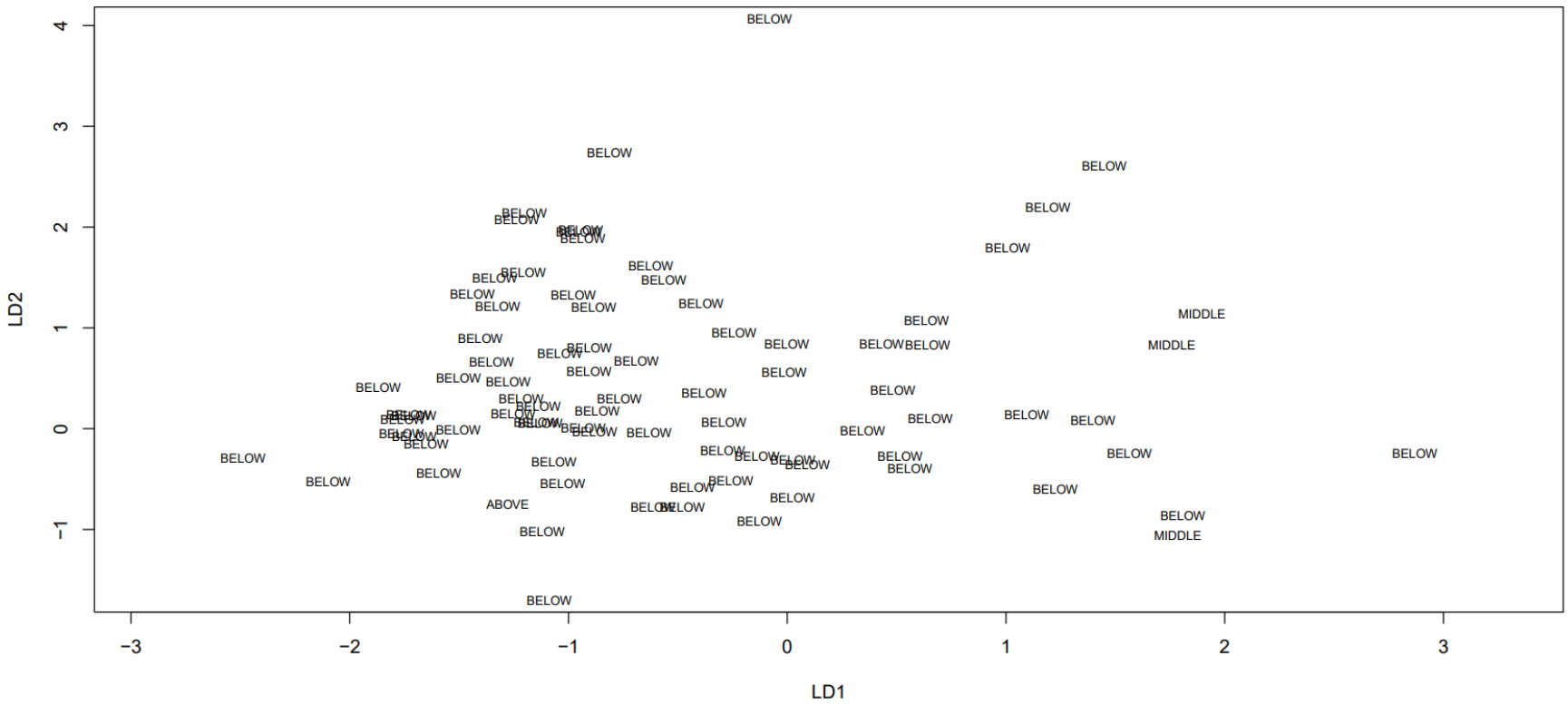

Figure 54. Linear discriminant analysis surface data observations.

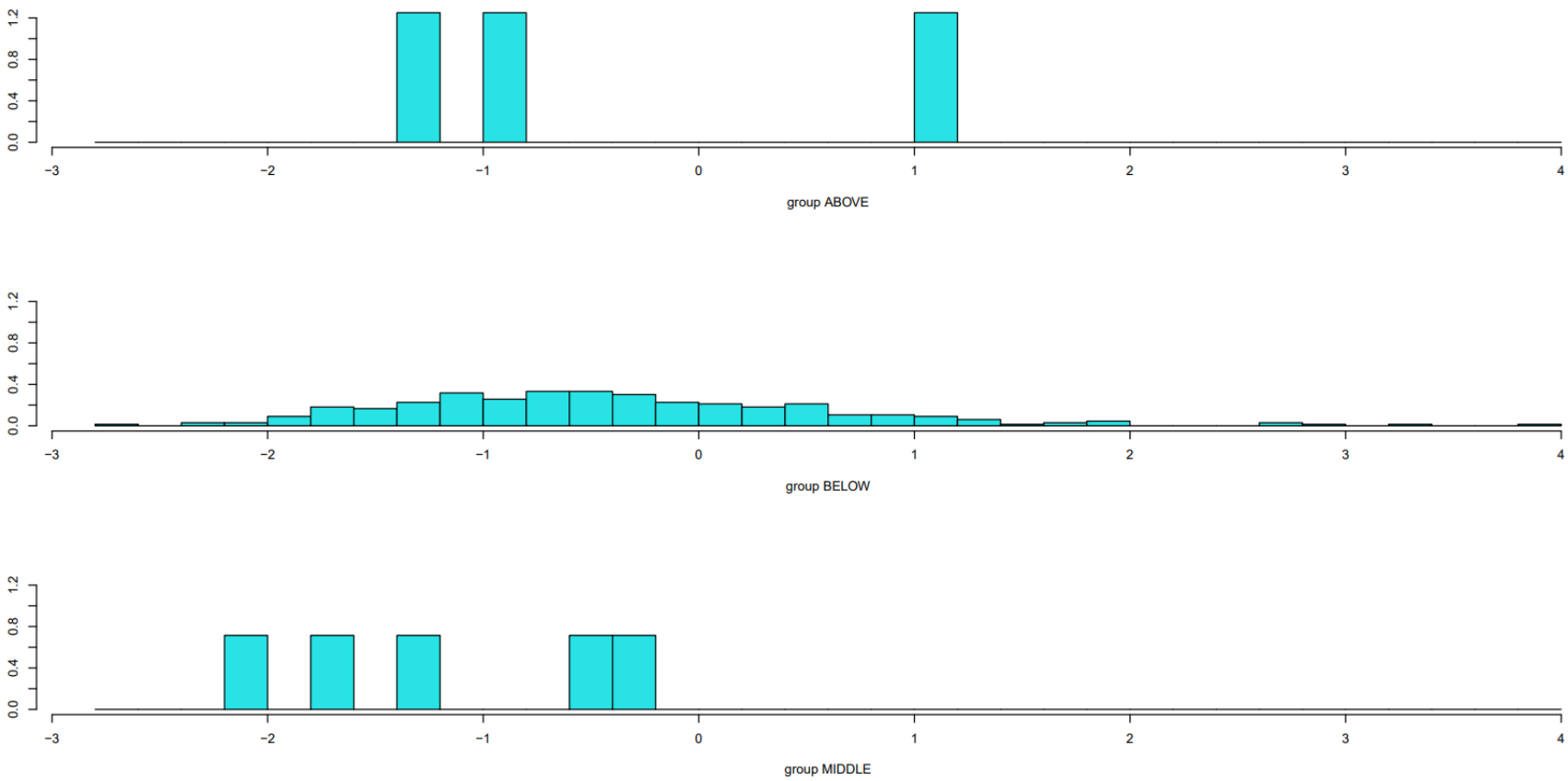

Figure 55. Histogram for LD1 for the linear discriminant analysis surface data observations.

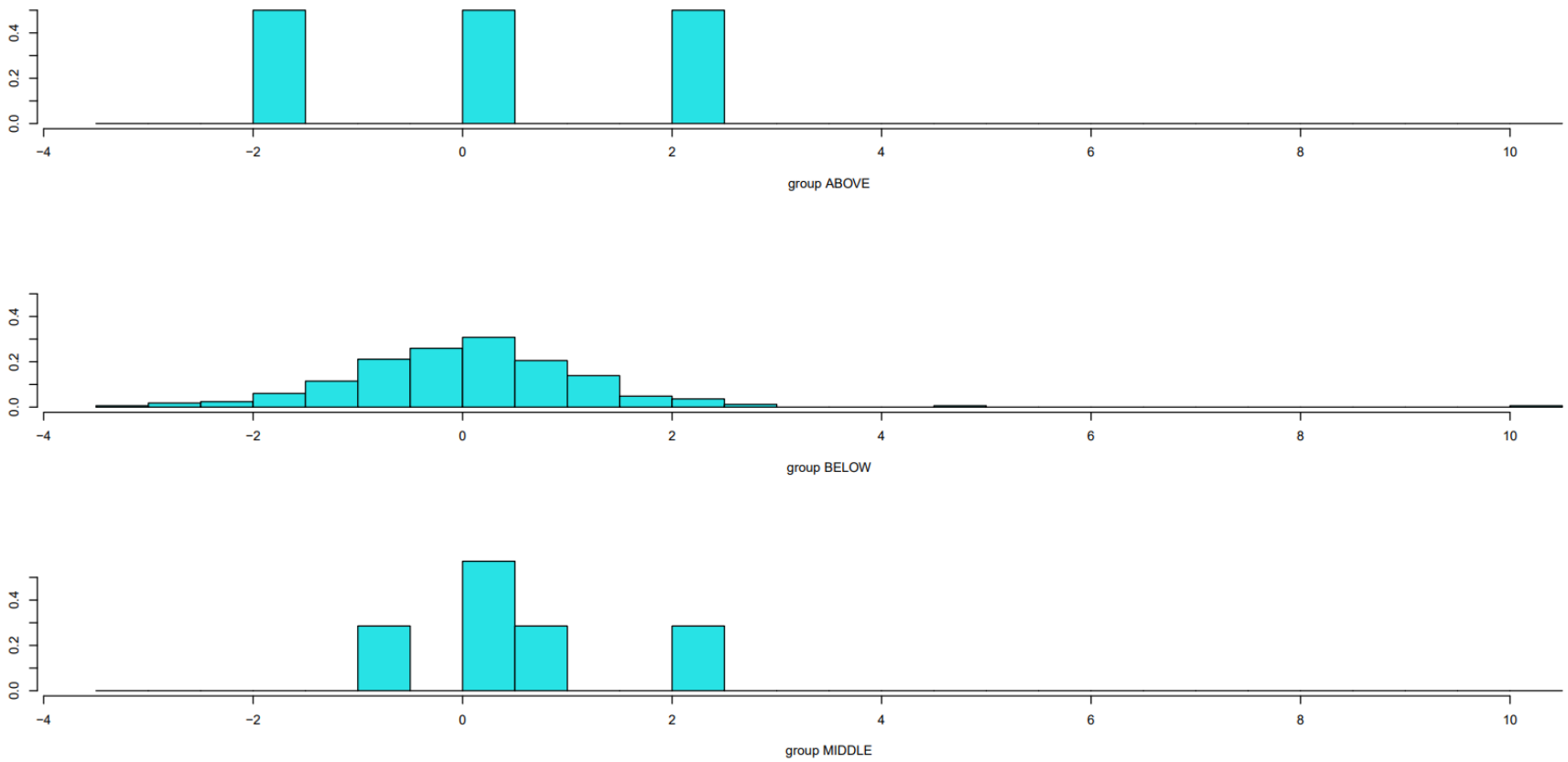

Figure 56. Histogram for LD2 for the linear discriminant analysis surface data observations.

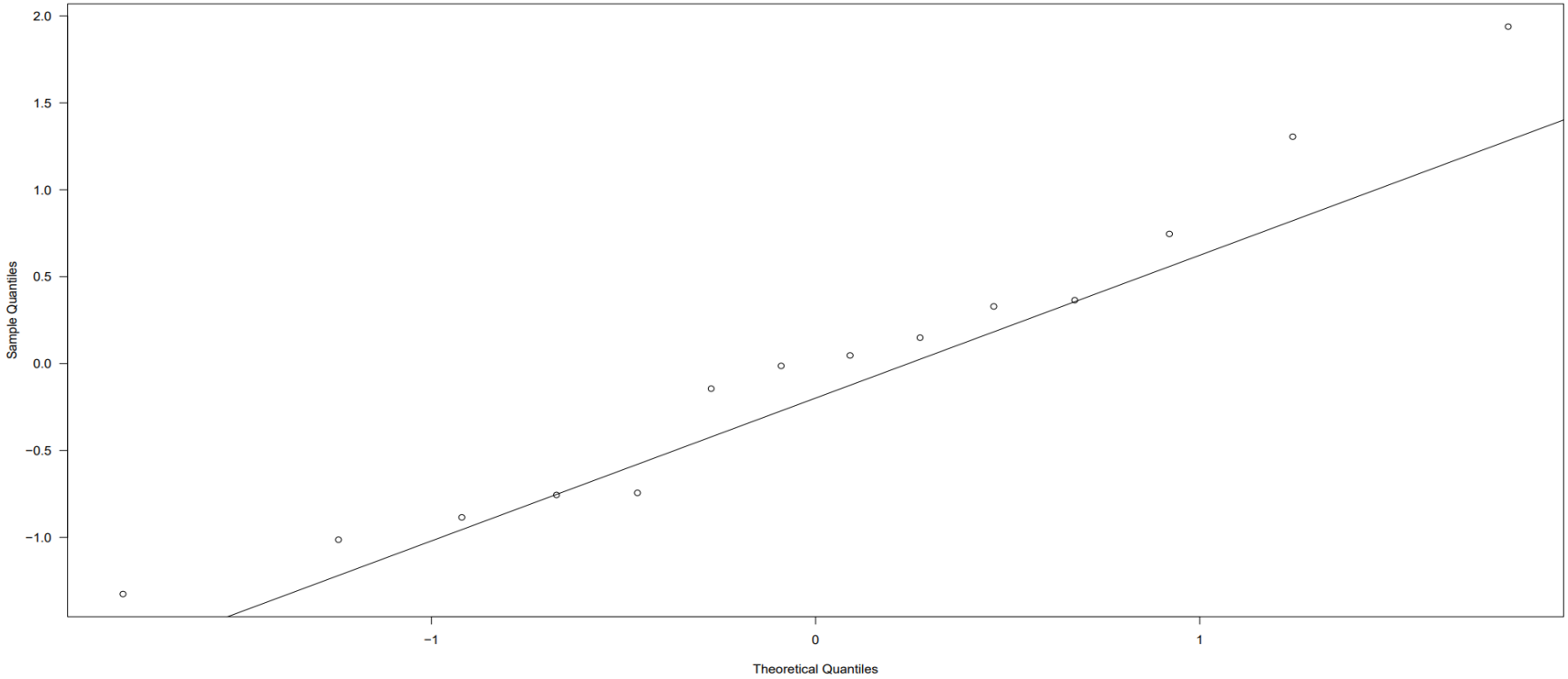

Figure 57. Euphotic dataset Q-Q plot of quantile residuals with log transformed microcystin concentrations and total boron and wind speed main effects in a Hurdle model Gaussian GLM with identity link. EUPH.gausBORW <- glm(logMICROCYSTIN ~ BORON + WINDSPEED, family = gaussian(link = "identity"), data = EUPHGLMP)

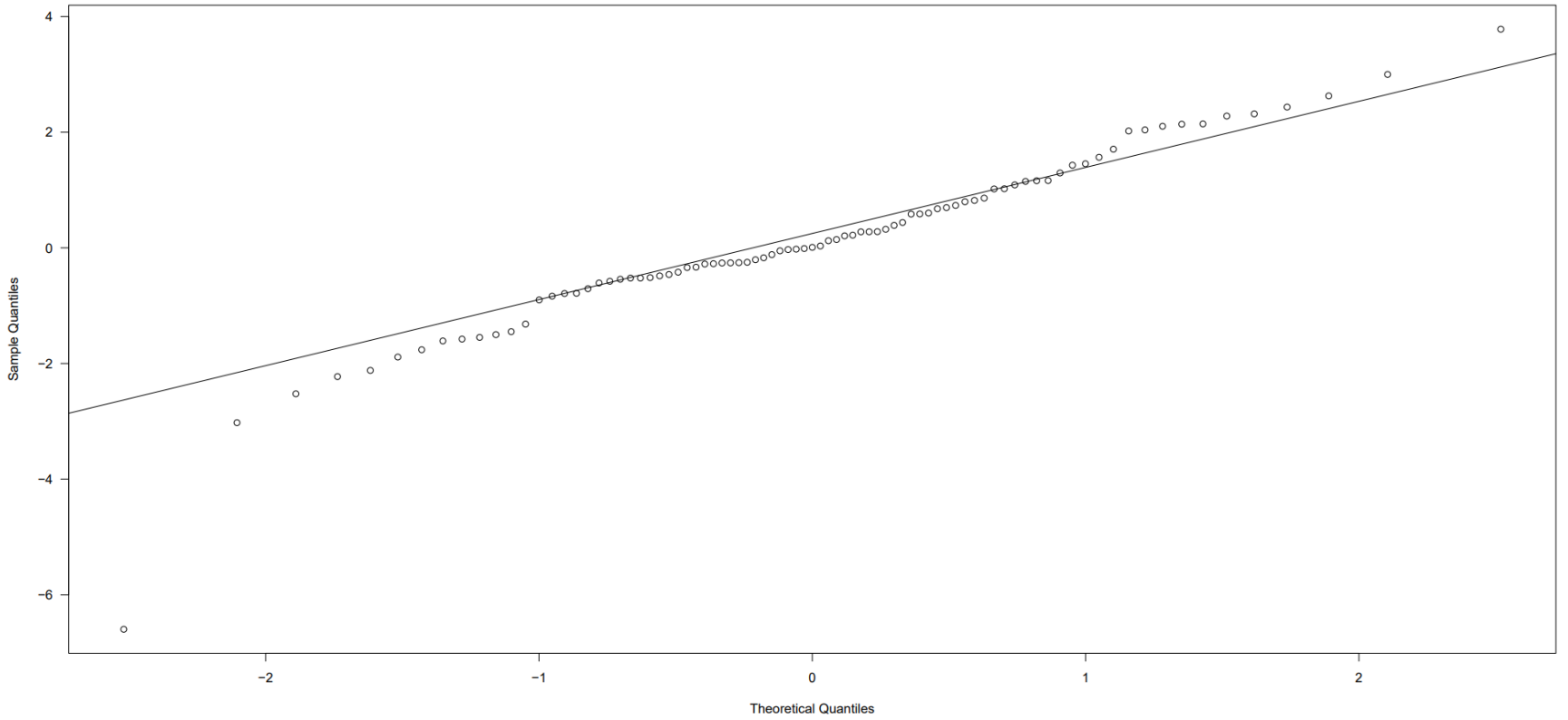

Figure 58. Euphotic dataset Q-Q plot of quantile residuals with microcystin presence/absence and *Anabaena* biomass and wind speed main effects in a Hurdle model Binomial GLM. EUPH.binAW <- glm(MICROCYSTIN_bin ~ ANABAENA + WINDSPEED, family = binomial, data = EUPHGLMP1)

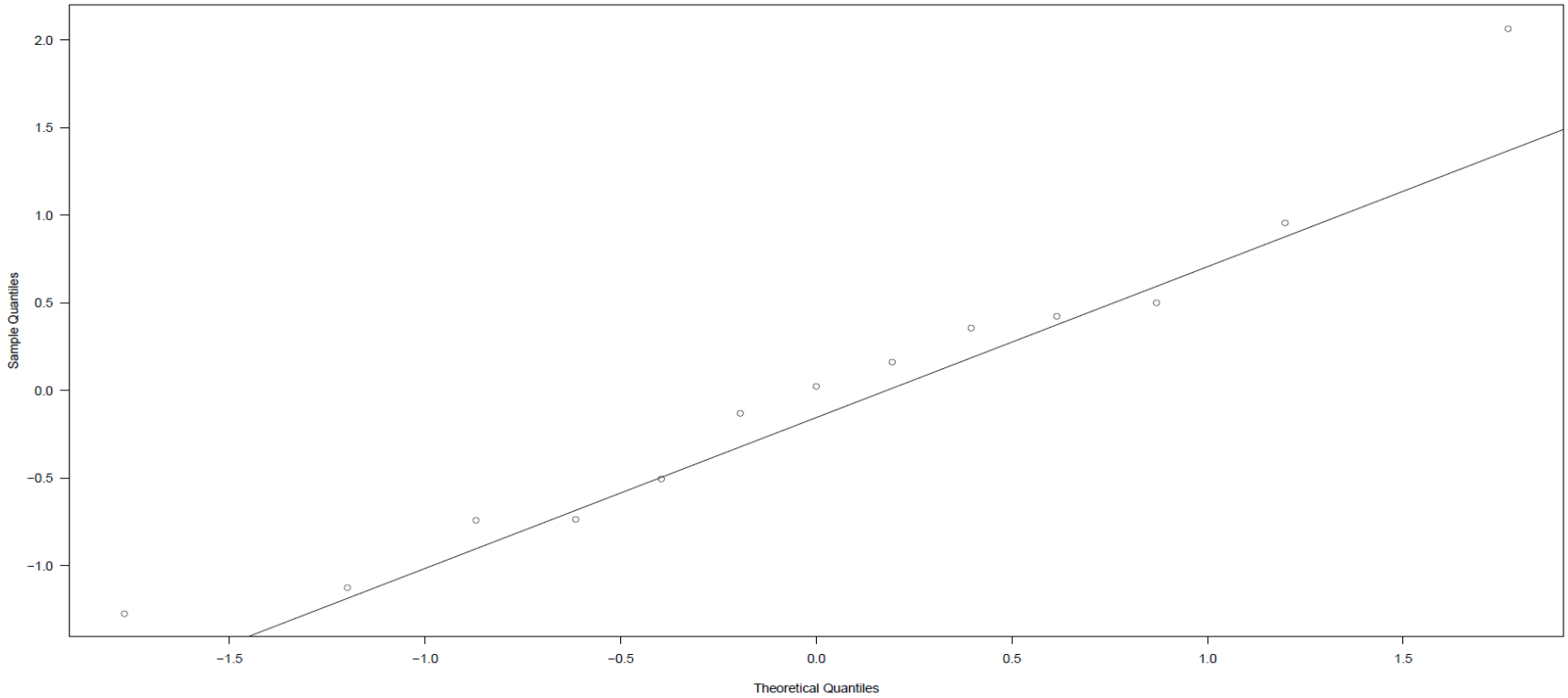

Figure 59. Surface dataset Q-Q plot of quantile residuals with log transformed microcystin concentrations and the N:P ratio and wind speed main effects in a Hurdle model Gaussian GLM with identity link. SUR.gausNPRW <- glm(logMICROCYSTIN ~ NPRATIO + WINDSPEED, family = gaussian(link = "identity"), data = SURGLMP)

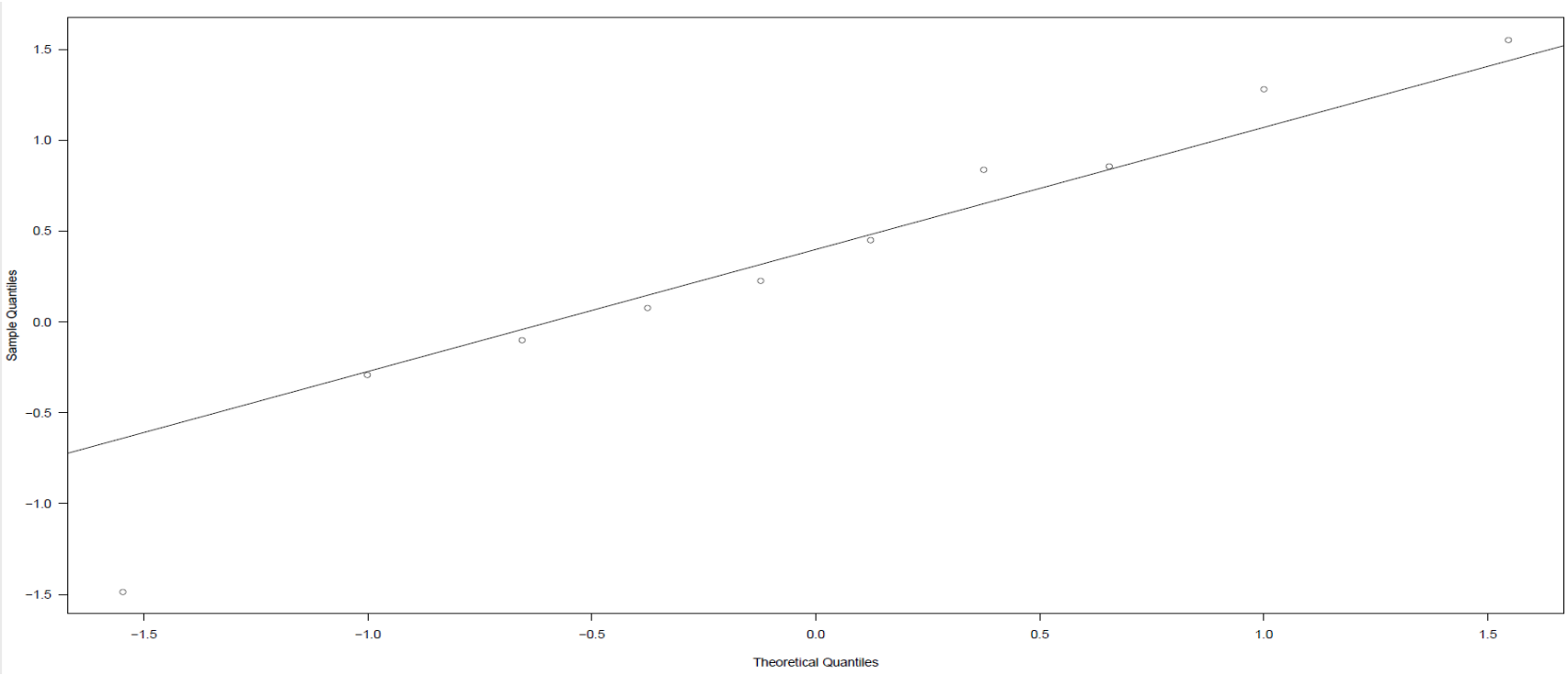

Figure 60. Surface dataset Q-Q plot of quantile residuals with microcystin presence/absence and the N:P ratio and wind speed main effects in a Hurdle model Binomial GLM. SUR.binNPRW <- glm(MICROCYSTIN_bin ~ NPRATIO + WINDSPEED, family = binomial, data = SURGLMP1)

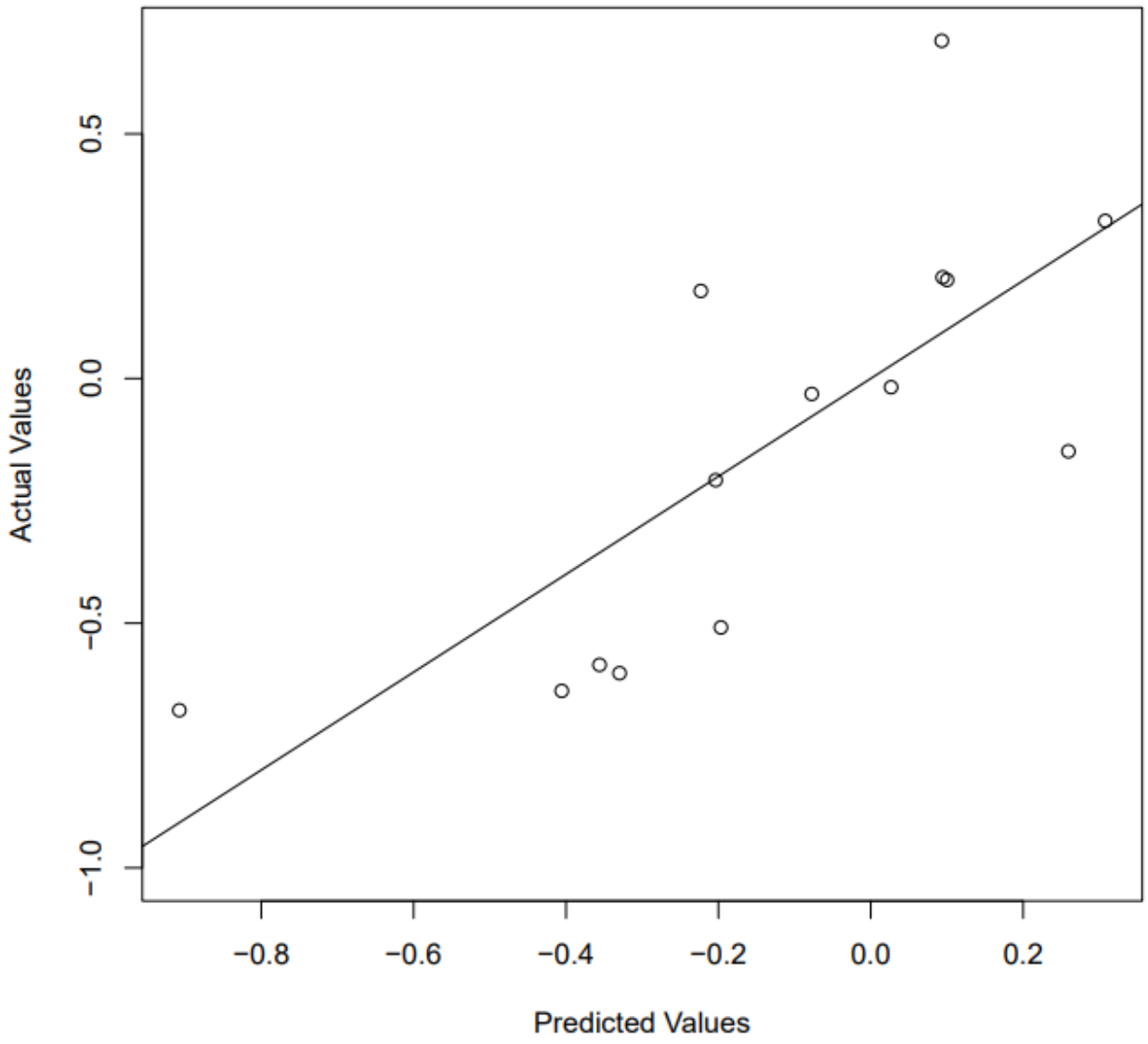

Figure 61. Euphotic dataset predicted vs actual values plot with log transformed microcystin concentrations and total boron and wind speed main effects in a Hurdle model Gaussian GLM with identity link.

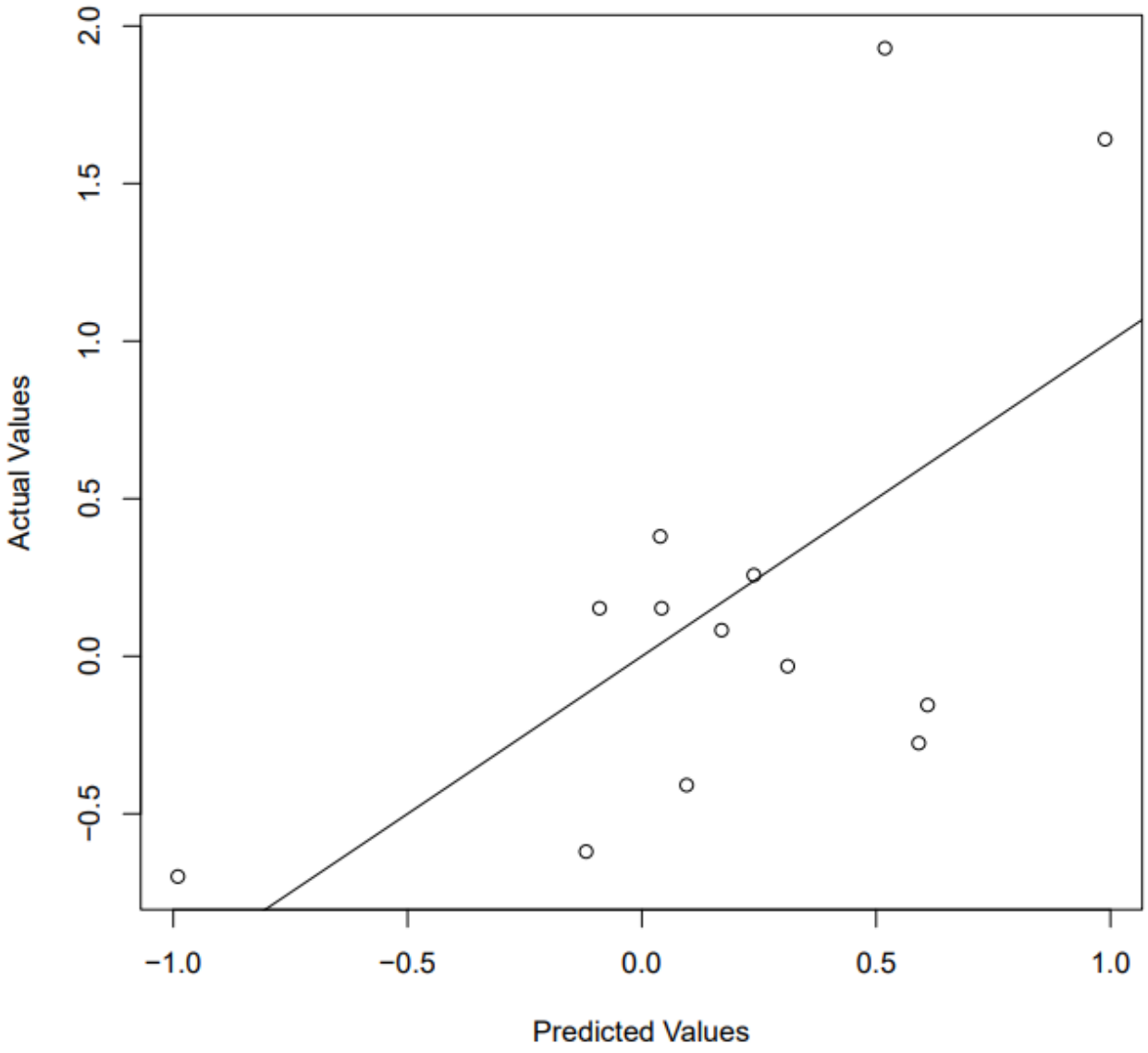

Figure 62. Surface dataset predicted vs actual values plot with log transformed microcystin concentrations and the N:P ratio and wind speed main effects in a Hurdle model Gaussian GLM with identity link.

Table 7. Confusion matrix for the linear discriminant analysis test data for the euphotic dataset.

	Actual			
Predicted	ABOVE	BELOW	MIDDLE	% Predicted Correctly
ABOVE	0	0	0	0
BELOW	1	87	4	94.6
MIDDLE	0	0	1	100

Table 8. Confusion matrix for the linear discriminant analysis test data for the surface dataset.

	Actual			
Predicted	ABOVE	BELOW	MIDDLE	% Predicted Correctly
ABOVE	0	0	0	0
BELOW	3	236	5	96.7
MIDDLE	0	5	0	0

Table 9. Model selection table for the Gaussian GLM model sets from the euphotic dataset where *Anabaena* biomass=X1; Total Boron=X2; Total P=X6; Wind Speed=X7. (K=the number of parameters in the model, where the default K was 2; AICc=the score of the model, where the better model fit has the smallest AIC; Delta_AICc=the difference in the AIC score between the model being compared and the best model; AICcWt=AICc weight, which was the proportion of the predictive power total amount provided by all model sets contained in the model being assessed; Cum.Wt=the sum of the AICc weights; LL=log-likelihood, where this was the value that describes how likely the model was based on the data) (Bevans, 2021).

Model Description	**Model Notation**	**K**	**AICc**	**Delta_AICc**	**AICcWt**	**Cum.Wt**	**LL**
Boron + Wind Speed	$\beta_0 + \beta_2X_2 + \beta_7X_7$	4	15.81	0	0.84	0.84	-1.68
Wind Speed	$\beta_0 + \beta_7X_7$	3	19.94	4.13	0.11	0.95	-5.97
Anabaena + Wind Speed	$\beta_0 + \beta_1X_1 + \beta_7X_7$	4	23.37	7.55	0.02	0.97	-5.87
Anabaena + Boron	$\beta_0 + \beta_1X_1 + \beta_2X_2$	4	23.93	8.12	0.01	0.98	-6.63
TP + Wind Speed	$\beta_0 + \beta_6X_6 + \beta_7X_7$	4	24.01	8.19	0.01	0.99	-5.78
Total Boron ('Boron')	$\beta_0 + \beta_2X_2$	3	26.62	10.81	0	1	-9.68

Boron + TP	$\beta_0 + \beta_2X_2 + \beta_6X_6$	4	28.34	12.52	0	1	-9.06
Anabaena + TP	$\beta_0 + \beta_1X_1 + \beta_6X_6$	4	42.15	26.33	0	1	-15.9
Anabaena ('Anabaena')	$\beta_0 + \beta_1X_1$	3	42.62	26.8	0	1	-17.71
Total Phosphorus ('TP')	$\beta_0 + \beta_6X_6$	3	66.33	50.51	0	1	-29.92
Intercept only	β_0	2	82.26	66.45	0	1	-39.02

Table 10. Model selection table for the binomial GLM model sets from the euphotic dataset where *Anabaena* biomass=X1; Total Boron=X2; Total P=X6; Wind Speed=X7. (K=the number of parameters in the model, where the default K was 2; AICc=the score of the model, where the better model fit has the smallest AIC; Delta_AICc=the difference in the AIC score between the model being compared and the best model; AICcWt=AICc weight, which was the proportion of the predictive power total amount provided by all model sets contained in the model being assessed; Cum.Wt=the sum of the AICc weights; LL=log-likelihood, where this was the value that describes how likely the model was based on the data) (Bevans, 2021).

Model Description	**Model Notation**	**K**	**AICc**	**Delta_AICc**	**AICcWt**	**Cum.Wt**	**LL**
Anabaena + Wind Speed	$\beta_0 + \beta_1X_1 + \beta_7X_7$	3	67.1	0	1	1	-30.48
Anabaena + Boron	$\beta_0 + \beta_1X_1 + \beta_2X_2$	3	95.57	28.47	0	1	-44.72
Anabaena + TP	$\beta_0 + \beta_1X_1 + \beta_6X_6$	3	107.79	40.7	0	1	-50.84
Anabaena ('Anabaena')	$\beta_0 + \beta_1X_1$	2	108.89	41.79	0	1	-52.42
TP + Wind Speed	$\beta_0 + \beta_6X_6 + \beta_7X_7$	3	118.73	51.63	0	1	-56.33
Boron + Wind Speed	$\beta_0 + \beta_2X_2 + \beta_7X_7$	3	122.25	55.15	0	1	-58.09

Wind Speed	$\beta_0 + \beta_7 X_7$	2	132.14	65.04	0	1	-64.05
Boron + TP	$\beta_0 + \beta_2 X_2 + \beta_6 X_6$	3	178.07	110.97	0	1	-86
Total Boron ('Boron')	$\beta_0 + \beta_2 X_2$	2	178.71	111.61	0	1	-87.34
Total Phosphorus ('TP')	$\beta_0 + \beta_6 X_6$	2	332.99	265.89	0	1	-164.48
Intercept only	β_0	1	354.16	287.06	0	1	-176.07

Table 11. Model selection table for the Gaussian GLM model sets from the surface dataset where N:P ratio=X1; Total P=X3; Wind Speed=X4. (K=the number of parameters in the model, where the default K was 2; AICc=the score of the model, where the better model fit has the smallest AIC; Delta_AICc=the difference in the AIC score between the model being compared and the best model; AICcWt=AICc weight, which was the proportion of the predictive power total amount provided by all model sets contained in the model being assessed; Cum.Wt=the sum of the AICc weights; LL=log-likelihood, where this was the value that describes how likely the model was based on the data) (Bevans, 2021).

Model Description	**Model Notation**	**K**	**AICc**	**Delta_AICc**	**AICcWt**	**Cum.Wt**	**LL**
N:P ratio + Wind Speed	$\beta_0 + \beta_1X_1 + \beta_4X_4$	4	36.54	0	0.97	0.97	-11.77
TP + Wind Speed	$\beta_0 + \beta_3X_3 + \beta_4X_4$	4	44.11	7.57	0.02	1	-16.51
Wind Speed ('Wind Speed')	$\beta_0 + \beta_4X_4$	3	48.1	11.56	0	1	-20.34
N:P ratio ('N:P ratio')	$\beta_0 + \beta_1X_1$	3	53.39	16.85	0	1	-23.03
N:P ratio + TP	$\beta_0 + \beta_1X_1 + \beta_3X_3$	4	54.3	17.76	0	1	-21.97

Total Phosphorus ('TP')	$\beta_0 + \beta_3 X_3$	3	60.03	23.49	0	1	-26.49
Intercept only	β_0	2	108.44	71.9	0	1	-52.11

Table 12. Model selection table for the binomial GLM model sets from the surface dataset where N:P ratio=X1; Total P=X3; Wind Speed=X4. (K=the number of parameters in the model, where the default K was 2; AICc=the score of the model, where the better model fit has the smallest AIC; Delta_AICc=the difference in the AIC score between the model being compared and the best model; AICcWt=AICc weight, which was the proportion of the predictive power total amount provided by all model sets contained in the model being assessed; Cum.Wt=the sum of the AICc weights; LL=log-likelihood, where this was the value that describes how likely the model was based on the data) (Bevans, 2021).

Model Description	**Model Notation**	**K**	**AICc**	**Delta_AICc**	**AICcWt**	**Cum.Wt**	**LL**
N:P ratio + Wind Speed	$\beta_0 + \beta_1X_1 + \beta_4X_4$	3	51.86	0	1	1	-22.59
N:P ratio ('N:P ratio')	$\beta_0 + \beta_1X_1$	2	83.51	31.65	0	1	-39.67
TP + Wind Speed	$\beta_0 + \beta_3X_3 + \beta_4X_4$	3	83.83	31.97	0	1	-38.74
N:P ratio + TP	$\beta_0 + \beta_1X_1 + \beta_3X_3$	3	85.68	33.82	0	1	-39.66
Wind Speed ('Wind Speed')	$\beta_0 + \beta_4X_4$	2	93.42	41.56	0	1	-44.63

Total Phosphorus ('TP')	$\beta_0 + \beta_3 X_3$	2	123.82	71.97	0	1	-59.85
Intercept only	β_0	1	238.35	186.49	0	1	-118.16

Table 13. Model summary of the euphotic and surface datasets hurdle models. Coefficient estimate=the average change in the response variable log odds associated with one unit increase for each predictor variable; standard error=the variability associated with the coefficient estimate; t value=ratio of the difference between the mean of the two sample sets and the variation in the sample sets; p-value=the probability associated with the t value (Statology, 2022).

	Estimate	Std. Error	t value	Pr(>|t|)
Euphotic Gaussian GLM				
(Intercept)	-0.8517	0.3820	-2.229	0.0476
BORON	33.2514	11.2336	2.96	0.013
WINDSPEED	-0.0264	0.0162	-1.63	0.1314
Euphotic Binomial GLM				
(Intercept)	-1.9165	0.7094	-2.702	0.0069
ANABAENA	0.0018	0.0005	3.82	0.0001
WINDSPEED	-0.1762	0.0875	-2.014	0.0440
Surface Gaussian GLM				
(Intercept)	-0.2201	0.8649	-0.254	0.8
NPRATIO	0.0188	0.0161	1.17	0.3
WINDSPEED	-0.0534	0.0400	-1.334	0.2
Surface Binomial GLM				
(Intercept)	-3.1012	1.3257	-2.339	0.0193
NPRATIO	0.0535	0.0289	1.851	0.0642
WINDSPEED	0.0607	0.0819	0.742	0.4583

Table 14. K-fold cross-validation and McFadden's Pseudo R-squared for the euphotic and surface Hurdle GLM. R-squared value=represents the squared correlation between predicted values and observed outcome values; Null deviance=how well the response variable was predicted in the model using the intercept only; residual deviance=how well the response variable can be predicted by the model in the model with our predictor variables.(Kassambara, 2018; Statology, 2022).

	R-squared	McFadden's Pseudo R-squared	Null Deviance	Residual Deviance
Euphotic Gaussian GLM - Boron + Wind Speed	0.94	0.77	2.36	1.04
Euphotic Binomial GLM - *Anabaena* Biomass + Wind Speed	0.55	0.44	109.44	60.97
Surface Gaussian GLM – N:P Ratio + Wind Speed	0.99	0.20	7.37	4.65
Surface Binomial GLM – N:P Ratio + Wind Speed	0.45	0.09	49.65	45.17

4.0 DISCUSSION

4.1 Objective 1: Which of many chemical, physical and biological parameters measured during routine monitoring on Lake Winnipeg over the past two decades are most closely associated with microcystin concentrations.

4.1.1 Chemical parameters

In the euphotic data, there were positive correlations between pheophytin *a* and microcystin concentrations but a negative correlation between chlorophyll *a* and microcystin in the surface dataset. Pheophytin *a* occurs at the end of an algal bloom and is a degradation product from the breakdown of the chlorophyll *a* pigment. This could mean that the detectable microcystin algal bloom samples that were taken on Lake Winnipeg were sampled towards the end of algal blooms thus the pheophytin *a* and microcystin relationship occurred. This finding is supported by a study, using cultured *Microcystis aeruginosa,* that found a positive relationship with microcystin and pheophytin *a* (r^2=0.529) (Aragão et al., 2020). In higher concentrations, chlorophyll *a* is a good indicator of the amount of cyanobacteria present in an area. Lake Winnipeg chlorophyll *a* concentration average trends were under 20 µg/L from 1999 to 2017 in both the north basin and south basin and narrows which was similar to concentrations on the Great Lakes from 2002 to 2011 (range of 0.19 µg/L to 33.55 µg/L) (Lesht et al., 2013). Positive correlations and relationships between chlorophyll *a* and microcystin were found in 1995 in southwestern Manitoba (r=0.74) (Jones et al., 1998), central and northern Alberta lakes (r=0.48) (Kotak et al., 2000) and on Lake Erie in 2013 (r^2=0.70) and in 2014 (r^2=0.57) (Stumpf et al., 2016). There was a negative correlation between chlorophyll *a* and microcystin concentrations in the Lake Winnipeg dataset but opposite

compared to other studies due to its longevity (18 years of data), which might obscure any short-term correlations found in other studies.

There were positive correlations between microcystin concentrations and total boron concentrations, as well as the combination of total boron and wind speed. In large quantities, total boron is one of many micronutrients required for algal growth but not as major as P and N. Boron has been found to be essential in higher plants but has no role in fungi or animals (Boyd, 1970; Bonilla et al., 1990). Plants can accumulate large amounts of a variety of nutrients without having any physiological requirement for them (Boyd, 1970). Boron has been found to play a protective role in the formation of the inner glycolipid layer of the heterocyst to prevent the diffusion of oxygen into the heterocyst (Garcia-Gonzalez et al., 1991; Abreu et al., 2014). Heterocystous cyanobacteria require boron for heterocyst envelope stability to prevent the access of nitrogenase-poisoning oxygen when cyanobacteria are grown under N-fixing conditions (Bolaños et al., 2004). Studies have shown boron plays a role in gene expression regulation and cell signaling events suggesting boron is involved with the regulation of heterocyst differentiation (Camacho-Cristóbal et al., 2008; Redondo-Nieto et al., 2012; Abreu et al., 2014). Additional studies have shown in non-heterocystous and heterocystous cyanobacteria that boron is not essential for cyanobacterial growth under low calcium conditions, where the addition of boron restored the uptake of nitrate, chlorophyll content and photosynthesis (Bonilla et al., 1995). Total boron has been shown to help with metabolic activities, membrane function, cell wall organization, heterocyst stabilization and growth functions (Jackson, 1964; Srivastava et al., 2016). When cyanobacteria are forced to fix N from the atmosphere, they have high calcium

and boron requirements and cyanobacteria that have high amounts of fixed N do not require calcium or boron (Jackson, 1964). A lab study on *Nostoc muscorum* showed that for N fixation to occur, the optimum boron concentration was 0.1 mg/L where Lake Winnipeg has an average of 0.0294 mg/L of boron (Eyster, 1952, 1958; Jackson, 1964; Environment and Climate Change Canada & Manitoba Agriculture and Resource Development, 2020). Cultures of the N-fixing *Nostoc muscorum* reported average boron concentrations of 25 µg/L, whereas the non-N fixing *Aphanizomenon flos-aquae* and *Microcystis aeruginosa* contained less than 5 µg/L (Boyd, 1970). Cultures of *Nostoc muscorum* that were grown with no boron added resulted in 39% reduction in cell count compared to cultures with boron added (Jackson, 1964). Boron could have an effect on the formation of the glycolipid layer in heterocysts therefore, this can effect N-fixation in N-fixing cyanobacteria and the potential release of the microcystin toxin.

Dissolved NO_3 + NO_2 had negative correlations between microcystin concentrations in the euphotic dataset where total Kjeldahl N and total N had a positive correlation in the surface dataset. N is a key nutrient component in algal growth and the cyanobacteria have a competitive advantage against other cyanobacteria due to their ability to fix N from the atmosphere when it is limiting in the water column. The negative correlation between dissolved NO_3 + NO_2 and microcystin was consistent with a study on three Ohio lakes (r=-0.35 to -0.64) (Francy et al., 2016). Total Kjeldahl N consists of the sum of organic N, ammonium and ammonia. A study on Lake Mendota, Wisconsin from 1995 to 2014, showed that total Kjeldahl N was positively correlated with Cyanophyta biovolume (r=0.568) which, can potentially aid in growth of large densities of cyanobacteria (Weirich et al., 2019). A study on 241 lakes in Missouri, Iowa,

northeastern Kansas and south Minnesota from 2000 to 2001 showed that there was a positive correlation between total N and microcystin (r=0.59) (Graham et al., 2004). This information suggests that in my study, higher total Kjeldahl N and total N as well as lower nitrate and dissolved NO_2 + NO_3 are correlated with the microcystin toxin in Lake Winnipeg, the basis for which is presently unclear.

Although P variables were not as significant as N variables, acid-hydrolyzable Ps, total P, total dissolved P and total reactive P had weak negative correlations with microcystin concentrations in the euphotic dataset and no correlations in the surface dataset which, could be due to luxury uptake of P during blooms. P is essential in the growth of cyanobacteria in Lake Winnipeg; it is in abundance from runoff of land fertilizers, manure from livestock, wastewaters and atmospheric deposition coming from across its watershed. Studies have shown that an increase in the biomass of primary producers such as chlorophyll *a* will cause an increase in log-linear function of total P suggesting that P can limit primary production (Filstrup et al., 2014). We would suspect that higher P would be associated with microcystin concentrations such as in the Lake Winnipeg study in 2007 where these P fractions had a weak positive correlations with microcystin concentrations ($r<0.25$) (Kotak, 2009). A study in central and northern Alberta (Kotak et al., 1995, 2000) as well as in three lakes in Ohio (Francy et al., 2016) showed that there was an increase in microcystin concentrations with the increase of P where in my study it shows to be opposite in the euphotic dataset. This could be likely due to the north basin and south basin and narrows both being P limited and there N:P ratios being over the Redfield ratio of 16:1. There was no correlations between microcystin concentrations and acid-hydrolyzable P, total P, total dissolved P and total

reactive P in the surface data suggesting that P is not associated with cyanobacteria releasing the microcystin toxin at the surface but are associated within the euphotic zone.

4.1.2 Physical parameters

There were no correlations found in the euphotic or surface datasets between turbidity levels and microcystin concentrations. Turbidity is a measure of water clarity and in high concentrations, there can be elevated particles in the water column such as sand, silt, clay and organic matter which can occur from high winds and mixing of the water column (Chaffin et al., 2018; Dzialowski et al., 2011; Ehmann et al., 2019). Turbid waters can be created by wind induced re-suspension from the bottom of the lake, sediment loading from tributaries, eroded banks or an abundance of phytoplankton in the water column (Chaffin et al., 2018; Dzialowski et al., 2011; Ehmann et al., 2019). High turbidity can reduce light conditions for the growth of cyanobacteria (Dzialowski et al., 2011). The reduction in clarity will decrease the transmission of photosynthetically active radiation (PAR) which can provide a niche for buoyant non-N and N fixing cyanobacteria such as *Anabaena*, *Aphanizomenon* and *Microcystis*, species which often co-exist together (Paerl, 2008). Several studies have shown that turbidity can reduce the dominance and/or biomass of the cyanobacteria however, other studies have shown that some species of cyanobacteria under low light conditions and/or shade tolerant are more buoyant and can increase production (Dzialowski et al., 2011). In a study on Alberta lakes from 1990 to 1994, it was found that turbidity had a weak positive correlation with *Microcystis aeruginosa* suggesting that certain parameters contribute to toxin production and others to algal growth (Kotak et al., 2000). A study from 1990 to

1994 on central and northern lakes in Alberta showed a weak positive correlation between turbidity levels and microcystin-LR concentrations (r=0.30) (Kotak et al., 2000). Turbidity was found to have a strong positive correlation between total cellular and extracellular microcystin (r=0.96 and r=0.98) on Lake Taihu in China in 2010 (Sakai et al., 2013). Given that all data from the north basin and south basin and narrows were combined together in my analysis, the turbidity levels over the 18 year data record may have obscured a short-term relationship with microcystin. Whereas, wind speed, Secchi disk depth and total suspended solids showed to have correlations with microcystin concentrations.

There were negative correlations with wind speed in the euphotic dataset, negative correlations with Secchi disk depth in the surface dataset and positive correlations with total suspended solids in the surface dataset. Lower wind speeds over a day or two can create water column stability (low total suspended solids and Secchi disk depth) which is favorable for the growth of cyanobacteria and could also give rise to the potential production of microcystin. A study on the Bay of Quinte on Lake Ontario showed that wind speeds under 36 km/hr or over 51 km/hr, temperatures over 14 °C and nutrient rich waters with TP over 26 µg/L were dominated with microcystin-LR (Taranu et al., 2019). In the Bay of Quinte, wind speeds under 37 km/hr combined with increased temperature, chlorophyll *a* and nutrients were associated with an increase in microcystin concentrations exceeding the drinking water guideline (Taranu et al., 2019). Wind speed thresholds will be different across lakes due to the varying lake shape and surface areas that can cause buildup of waves. A study from 2000 to 2001 in the midwestern United States and in central and northern Alberta from 1990 to 1994

showed that there was a weak negative correlation between Secchi disk depth and microcystin concentrations (r=-0.27 and -0.38) (Graham et al., 2004; Kotak et al., 2000). A study on Buckeye lake (r=-0.76), Harsha lake (r=-0.69) and Lake Erie (r=-0.67) from 2013 to 2014 showed that there was a negative correlation between Secchi disk depth and microcystin concentrations (Francy et al., 2016). My study suggests that lower Secchi disk readings is related to higher microcystin concentrations due to light is not being transmitted far because of large amounts of materials within the water column, which has been seen in numerous studies. In more productive water bodies with high amounts of suspended inorganic materials, large amounts of dissolved coloured materials or high concentrations of suspended photosynthetic organisms, the water will contain more materials that will reflect or absorb the light and not transmit it far (Dodds, 2002). If each basin was examined separately, there could be a relationship in the north or south basin and narrows. However, from the current analysis, it is concluded that turbidity is likely not a significant parameter in the release of the microcystin toxin but other water clarity parameters had correlations with microcystin.

In the euphotic dataset, there were positive correlations between pH and microcystin concentrations. The best pH for cyanobacterial growth is 7.5-10 (West & Louda, 2011) where in Lake Winnipeg, pH ranges from 6.93 to 9.1 (1999 to 2017 Lake Winnipeg data). Given optimal pH values in Lake Winnipeg, we could always expect a linear correlation. There was a similar positive correlation between pH and microcystin in Coal, Driedmeat and Little Beaver Lake in Alberta (r=0.58) (Kotak et al., 1995). Looking at a 14-day average of pH, there were positive correlations between microcystin and pH in Harasha Lake (r=0.73) and Lake Erie (r=0.77) in 2014 (Francy et

al., 2016). Inorganic C (CO_2) uptake during photosynthesis by phytoplankton can increase the pH, while pH can be decreased during the respiration process through the release of CO_2 (Hansen, 2002). Carbon dioxide exchange between the surface water and atmosphere can be dependent on the amount of vertical mixing within the water column from wind and wave action (Hansen, 2002). Lake Winnipeg is known to be well mixed throughout the open water season with few periods of vertical stabilization in the summer months (Environment and Climate Change Canada & Manitoba Agriculture and Resource Development, 2020). It has been shown that levels of pH increase due to the consumption of dissolved CO_2 during a cyanobacteria bloom (Francy et al., 2016). A study on diatoms suggested that when pH exceeded 9.2 in continuous cultures, *Phaeodactylum tricornutum* out competed *Dunaliella tertiolecta* (Goldman, Azov, et al., 1982; Goldman, Riley, et al., 1982). In the Mariager Fjord in Denmark showed the dinoflagellates *Prorocentrum* minimum and *Heterocapsa triquetra* blooms with pH over 9.2 and in the Santo Andre Lagoon in Portugal showed *Prorocentrum minimum* occurring at a 9.5 to 9.6 pH (Hansen, 2002). Although these studies are on marine phytoplankton, this suggests that there is a possibility that certain cyanobacteria species on Lake Winnipeg may flourish with a certain pH concentration present.

4.1.3 Biological Parameters

Looking at the W station dataset, it is clear that Lake Winnipeg has been dominated by diatoms and cyanobacteria for most of the period from 1999 to 2017. In general, their respective abundances have been reciprocal; when large cyanobacterial blooms were present on the lake, diatom abundance was low, and vice versa (Environment and Climate Change Canada & Manitoba Agriculture and Resource

Development, 2020). From 2008 to 2016 in the south basin, total P concentrations were increasing in the summer and fall months but lowest in the spring could be driven by resuspension processes and internal re-mobilization which is typical of euphotic and shallow lakes (Environment and Climate Change Canada & Manitoba Agriculture and Resource Development, 2020). However, in the north basin total P concentrations were highest in the fall (0.04 to 0.07 mg/L) and lowest in the summer (0.02 to 0.03 mg/L) (Environment and Climate Change Canada & Manitoba Agriculture and Resource Development, 2020). In the south basin, total N concentrations are highest in the summer months (>1.4 mg/L) and declined in the fall which, could be attributed to the transportation of N from the Red River into the south basin (Environment and Climate Change Canada & Manitoba Agriculture and Resource Development, 2020). N concentrations in the north basin were lowest in the spring, increased during the summer and stayed the same across the summer and fall which, could be because of large cyanobacteria blooms that have N-fixing species present (Environment and Climate Change Canada & Manitoba Agriculture and Resource Development, 2020). A study on Lake Winnipeg from 1994 to 2007 showed the composition of algal blooms in the mid to late summer has been 90% compromised of cyanobacteria taxa and an increase of algal blooms at the surface on Lake Winnipeg since the 1990s (Kling et al., 2011). A study taking core samples on Lake Winnipeg in 2006 showed that diatom and cyanobacteria concentrations were constant during the 19th century then diatoms increased two to 20-fold by 1980 and cyanobacteria increased 300 to 500% up until 1990 then declined around 50% in sediments (Bunting et al., 2016). A study on the San Roque Reservoir in Argentina showed that microcystin concentrations were positively

correlated with cyanobacteria composition ($r=0.51$, $p<0.05$) (Ruiz et al., 2013). Also, a study on 30 lakes along the Yangtze River in China showed that there was a weak positive correlation between cyanobacteria biomass and microcystin concentrations ($r=0.41$) (Wu et al., 2006). No literature has been found on any correlations or relationships between diatoms and microcystin concentrations. The cyanobacteria may outcompete the diatoms in the warm summer months due to the amount of nutrients (N and P) and mixed water column and the diatoms outcompete the cyanobacteria in the cool spring, fall and winter time due to cooler temperatures.

Weak negative correlation in the surface dataset occurred between Cryptophyceae biomass and microcystin concentrations. This could be due to the differences in north basin and south basin and narrows water quality as well as differences between seasons. There was no literature that suggests a correlation between Cryptophyceae biomass and microcystin concentrations. The Cryptophyceae are not known to release any toxins into the water column. Cryptomonads are facultatively heterotrophic algae and may be present when feeding on the decaying remains of cyanobacterial blooms. In my thesis, the Cryptophyceae appear to occur with cyanobacteria that produce the microcystin toxin in Lake Winnipeg.

In the surface dataset, the strongest positive correlation was between *Anabaena* biomass and microcystin concentrations, but no correlations were found with the other two major cyanobacterial taxa *Aphanizomenon* and *Microcystis*. All three genera are known to produce toxins and they are common in Lake Winnipeg. About 70% of the Lake Winnipeg phytoplankton present from 1999 to 2007 were the cyanobacteria *Aphanizomenon* (61.2%), *Anabaena* (5.3%) and *Microcystis* (5.2%), where all three

genera are capable of releasing harmful toxins (Environment Canada & Manitoba Water Stewardship, 2011). The north basin is dominated by the N-fixing genera *Aphanizomenon* and *Anabaena* and the south basin is dominated by non-N fixing *Microcystis* and *Planktothrix* (Kling et al., 2011). The following factors can give *Anabaena*, *Aphanizomenon* and *Microcystis* a competitive advantage over other species present in algal blooms. The cyanobacteria *Anabaena* and *Aphanizomenon* can fix N from the atmosphere when concentrations are low in the water. *Anabaena*, *Aphanizomenon* and *Microcystis* can use positive buoyancy from gas vacuoles to float to the water surface to access higher amounts of light. A study on 13 lakes in central and northern Alberta from 1990 to 1994 showed opposite of my study in that there was no correlation between *Anabaena flos-aquae* and microcystin (r=-0.03) but a correlation occurred between *Microcystis aeruginosa* and microcystin (r=0.52) (Kotak et al., 2000). My study shows that *Anabaena* biomass in large quantities is related to the production of the microcystin toxin in Lake Winnipeg. However, more specific research is required to examine why the correlation between microcystin and *Anabaena* biomass was observed.

4.2 Objective 2: Examine the correlation, if any, between the (nitrogen-to-phosphorus) N:P ratio in Lake Winnipeg and microcystin concentrations.

The N:P ratio had a weak positive correlation with microcystin concentrations in the euphotic and surface dataset as well as the combination of the N:P molar ratio and wind speed in the surface dataset. P and N are key components needed in algal growth and production. Some cyanobacteria have the ability to fix N from the atmosphere when concentrations are low in the water. The N:P ratio at lower ratios favors cyanobacteria

growth, some of which have the ability to produce harmful algal toxins. With the north and south basin being well-mixed areas with shallow average depth and large surface area, winds can build up and move cyanobacteria within the water column (Environment Canada & Manitoba Water Stewardship, 2011). I hypothesized that the N:P ratio should be inversely correlated with microcystin concentrations where microcystin should be produced when the phytoplankton assemblage is dominated by cyanobacteria. The north basin of Lake Winnipeg typically has lower average annual concentrations of N and P than the south basin and narrows. Looking at changes in water quality on Lake Winnipeg from 1999 to 2017, N:P ratios had an average of 37:1 in the north basin and 25:1 in the south basin and narrows, which were well above the Redfield ratio of 16:1. A low N:P ratio, therefore N deficiency, can benefit cyanobacteria, which can fix N from the atmosphere and use for growth. The N:P ratio could be a cue for the cyanobacteria to produce the microcystin toxin and increase their intracellular content of microcystin (Lee et al., 2000; Orihel et al., 2012). Cyanobacteria abundance and increased microcystins occurred with increasing trophic status in four northern Sardinia reservoirs (Mariani et al., 2015). Low N:P ratios could be a consequence instead of the cause of algal blooms (Xie et al., 2003; Orihel et al., 2012). Many species of planktonic cyanobacteria can luxury uptake P from the sediments and can dramatically decrease the water column N:P ratio (Xie et al., 2003; Orihel et al., 2012). P can be released from the sediments by dissolution and desorption of P bound in inorganic and precipitate materials, organic matter mineralized by microbial action and dissolved P diffusion from sediment pore waters (Hou et al., 2013). In an experiment in the Experimental Lakes Area Lake 227 showed that N-fixing cyanobacteria was not detected as N was in

excess of what cyanobacteria demanded and average values of N:P ratio were between 22-28 from 1969 to 2005 (Schindler et al., 2008). The Experimental Lakes Area study also showed that N-fixing cyanobacteria formed greater than 50% of the total phytoplankton biomass when N fertilization into the lake was ceased (Schindler et al., 2008). A few studies on Lake Winnipeg had shown that microcystin was detectable with N:P ratios under 15:1 and in 2007, 64% of whole water samples had detectable microcystin concentrations with N:P ratios below 5:1 (Kotak et al., 2000; Kotak, 2009). A study looking at microcystin across Canada showed that when N:P ratios were less than 23:1, there was higher microcystin concentrations (Scott et al., 2013). My results on Lake Winnipeg show that microcystin are correlated at a higher N:P ratio rather than a lower N:P ratio possibly due to higher N:P ratios and large cyanobacteria blooms in the north basin.

4.3 Implications of Work

A goal of this research was to contribute to a better understanding of the various chemical, physical and biological factors attaining to the cyanobacterial release of microcystin in Lake Winnipeg. Current water quality monitoring only samples total microcystin and phytoplankton biomass at the 14 W stations and total microcystin and cyanobacterial cell counts are sampled at areas on the lake where there is an algal bloom. Many of the measured parameters showed no correlation with toxin levels yet are costly to undertake. To deploy available analytical resources more efficiently, I suggest taking out the benthic invertebrates at the W stations and adding more stations and stops in the north basin and south basin and narrows to analyze for total microcystin concentration, phytoplankton biomass (measured via the proxy, chlorophyll

a concentration), and to assay nitrogenase enzyme concentrations as an indicator of nitrogen fixation rates. All sites on Lake Winnipeg would be sampled for the same parameters such as N and P variables, general chemistry, total microcystin, phytoplankton biomass and nitrogenase enzyme.

Consideration should be given to altering the deployment schedule of the research vessel MV *Namao* so that cruises bring the science crew to the north basin during peak algal bloom production time in July and August. The north basin usually has large cyanobacteria algal blooms forming in the offshore in the north basin during the summer.

Currently, analysis of the chemical, physical and biological datasets is based on the whole lake and where the sample was taken (euphotic or surface). A more in-depth analysis of the surface and euphotic data by breaking both datasets up based on basin as well as season (winter, spring, summer and fall). Both basins are considered to have different water quality present. Each season can pose differences in the chemical, physical and biological parameters present. By analyzing data on individual basins separately, it may be possible to detect an environmental correlation with microcystin concentration that I did not see when data for all basins were combined.

4.4 Evaluation of Hypotheses

Hypothesis 1A (I hypothesize that as P and N are essential nutrients in algal production, there will be a positive correlation between P and microcystin concentrations and a negative correlation between N and microcystin concentrations) was not supported in that there was a negative correlation between total P and microcystin concentration, and a positive correlation between total N and microcystin. I

found that with higher total N concentrations and lower total P concentrations, there was higher microcystin concentrations. This may be related to the common bloom-forming cyanobacteria taxa present in Lake Winnipeg having the ability to fix N from the atmosphere. Although total P is an essential nutrient in algal production but N-fixing cyanobacteria may not need high concentrations of P to produce large blooms.

Hypothesis 1B (Increased turbidity is often associated with cyanobacterial success, so there will be a positive correlation between turbidity and microcystin concentrations) was not supported in that there was no significant correlation between turbidity levels and microcystin concentrations. However, I did find that variables related to water clarity – such as total suspended solids, Secchi disk depth and wind speed (which relates to water column stability)– had correlations with microcystin concentrations. A lower Secchi disk depth indicates a low water clarity and with the north and south basin having shallow depths, there is an abundance of total suspended solids present, which can be resuspended in the water column due to higher wind speeds. The suspension of sediments can aid in affecting light levels in the water column where common bloom-forming cyanobacteria thrive.

Hypothesis 1C (As *Anabaena* and *Microcystis* are known to release the microcystin toxin, there will be a positive correlation between *Anabaena* and *Microcystis* with microcystin concentrations) was supported in that *Anabaena* biomass in the surface dataset had a positive correlation with microcystin concentration. However, the hypothesis was not supported for *Microcystis* biomass and microcystin, suggesting that the level of toxin production is dependent on the taxonomic composition of the prevailing blooms at a particular time. In theory, *Anabaena* and *Microcystis* both have

the ability to produce the microcystin toxin. The south basin is dominated by *Microcystis* and the north basin is dominated by *Anabaena*. *Anabaena* have the ability to fix N from the atmosphere and *Microcystis* do not. This may give *Anabaena* the competitive advantage over *Microcystis* genera when concentrations of N are low in the water column.

Hypothesis 2A (I hypothesize that because N-fixers are mainly causing phytoplankton blooms, there will be a negative correlation between microcystin concentrations and N:P ratio) was not supported in that there were positive correlations between the N:P ratio and microcystin concentrations in the surface and euphotic datasets. A higher N:P ratio – meaning an increasing magnitude of phosphorus deficiency, possibly because cyanobacterial N requirements were met by N fixation – correlated with higher microcystin concentrations. Differences between seasons and the north basin and south basin and narrows could be the cause of this inverse relationship. Changes in water quality on Lake Winnipeg in the north basin (37:1) and south basin and narrows (25:1) show N:P ratios above the Redfield ratio of 16:1 meaning that N is not limiting in Lake Winnipeg.

4.5 Conclusion

Overall, I found that algal toxin concentrations in the epilimnion of Lake Winnipeg correlated best with several metrics of nitrogen availability, water clarity, Anabaena biomass and boron concentrations.

The concentration of N variables such as total N, total Kjeldahl N, nitrate + nitrite and the N:P ratio may aid in controlling microcystin levels in Lake Winnipeg. Higher toxins correlated with higher N variables in the surface dataset and euphotic dataset

and higher toxins and lower N variables correlated in the euphotic dataset. Common bloom-forming cyanobacteria taxa have a competitive ability to fix N from the atmosphere when nutrients are limiting in the water column. The north basin of Lake Winnipeg can have large cyanobacteria algal blooms that could be dominated by the N-fixing genus *Anabaena*. There may be a link between microcystin concentrations in conjunction with N concentrations and *Anabaena* biomass.

In terms of water clarity parameters, total suspended solids had a positive correlation with toxin levels in the surface dataset; Secchi disk depth and wind speed had negative correlations. These variables can be factors in the resuspension of sediment within the water column and the algal cell abundance in the epilimnion that together can affect levels of light needed for algal photosynthesis. In the south basin, turbidity was higher and Secchi disk depths was lower than corresponding values in the north basin where there can be large cyanobacteria algal blooms. The north and south basin are well-mixed areas due to the shallow depths as well as large surface areas where winds can build up and move cyanobacteria within the water column. When photosynthetically active radiation is reduced by high turbidity in the water column, common cyanobacterial bloom-forming taxa such as *Anabaena* may be better adapted to low light than other algal taxa. This can be a factor promoting large cyanobacteria algal blooms that potentially yield microcystin toxin.

The microcystin toxin is detected more at the end of an algal bloom due to its release upon the decomposition of dying algal cells. An indication of this possibility in Lake Winnipeg is that levels of pheophytin *a*, a degradation product of the chlorophyll *a* pigment used in photosynthesis, tend to increase as algal blooms break down.

Frequently, I found positive correlations between total boron and microcystin concentrations. When cyanobacteria are grown under N-fixing conditions, boron has been found to play a protective role in the formation of the inner glycolipid layer for the stability of the heterocyst envelope to prevent the diffusion of nitrogenase-poisoning oxygen (Garcia-Gonzalez et al., 1991; Bolaños et al., 2004; Abreu et al., 2014). Additional studies have shown in non-heterocystous and heterocystous cyanobacteria that boron is not essential for cyanobacterial growth under low calcium conditions, where the addition of boron restored the uptake of nitrate, chlorophyll content and photosynthesis (Bonilla et al., 1995). *Anabaena* biomass was found to have a correlation with microcystin concentrations and does have the ability to fix N from the atmosphere. This could give them a competitive advantage when N concentrations are low although, N:P ratios in the south basin and narrows and the north basin show that Lake Winnipeg is N abundant. Total calcium and total boron concentrations averaged 28.1 and 29.7 µg/L in the south basin and narrows and 29.3 and 29.1 µg/L in the north basin (Environment and Climate Change Canada & Manitoba Agriculture and Resource Development, 2020). Total boron present in the water column at certain concentrations could aid in the formation of heterocysts therefore, can allow for N-fixation to occur in N-fixing cyanobacteria which could release the microcystin toxin.

5.0 REFERENCES

Abreu, I., Orús, I., Bolaños, L., & Bonilla, I. (2014). The interaction of boron with glycolipids is required to increase tolerance to stresses in *Anabaena* PCC 7120. *Phytochemistry*, *106*, 55–60. https://doi.org/10.1016/j.phytochem.2014.07.017

Ahn, C. Y., Park, M. H., Joung, S. H., Kim, H. S., Jang, K. Y., & Oh, H. M. (2003). Growth inhibition of cyanobacteria by ultrasonic radiation: Laboratory and enclosure studies. *Environmental Science and Technology*, *37*(13), 3031–3037. https://doi.org/10.1021/es034048z

Alexova, R., Fujii, M., Birch, D., Cheng, J., Waite, T. D., Ferrari, B. C., & Neilan, B. A. (2011). Iron uptake and toxin synthesis in the bloom-forming *Microcystis aeruginosa* under iron limitation. *Environmental Microbiology*, *13*(4), 1064–1077. https://doi.org/10.1111/j.1462-2920.2010.02412.x

Andika, A., Abdullah, S., & Nurrohmah, S. (2021). Hurdle Negative Binomial Regression Model. *ICSA - International Conference on Statistics and Analytics 2019*, *1*, 57–68. https://doi.org/10.29244/icsa.2019.pp57-68

Aragão, M. C., Reis, K. C. dos, Souza, A. C., Rocha, M. A. M., & Neto, J. C. (2020). Modeling total microcystin production by *Microcystis aeruginosa* using multiple regression. *Journal of Water Supply: Research and Technology - AQUA*, *69*(5), 415–426. https://doi.org/10.2166/aqua.2020.128

Babin, J., Prepas, E. E., & Zhang, Y. (1992). Application of Lime and Alum to Stormwater Retention Lakes to Improve Water Quality. *Water Pollution Research Journal of Canada*, *27*(2), 365–381.

Bajkov, A. (1930). Biological Conditions of Manitoban Lakes. *Contributions to Canadian Biology and Fisheries*, *5*(12), 383–421.

Barrington, D. J., & Ghadouani, A. (2008). Application of hydrogen peroxide for the removal of toxic cyanobacteria and other phytoplankton from wastewater. *Environmental Science and Technology*, *42*(23), 8916–8921. https://doi.org/10.1021/es801717y

Barrington, D. J., Ghadouani, A., & Ivey, G. N. (2011). Environmental factors and the application of hydrogen peroxide for the removal of toxic cyanobacteria from waste stabilization ponds. *Journal of Environmental Engineering*, *137*(10), 952–960. https://doi.org/10.1061/(ASCE)EE.1943-7870.0000401

Bartlett, J. (2014, February). *R squared in logistic regression*. https://thestatsgeek.com/2014/02/08/r-squared-in-logistic-regression/#

Batt, R. D., Carpenter, S. R., Cole, J. J., Pace, M. L., Johnson, R. A., Kurtzweil, J. T., & Wilkinson, G. M. (2015). Altered energy flow in the food web of an experimentally darkened lake. *Ecosphere*, *6*(3), 1–23. https://doi.org/10.1890/ES14-00241.1

Beaulieu, M., Pick, F., & Gregory-Eaves, I. (2013). Nutrients and water temperature are significant predictors of cyanobacterial biomass in a 1147 lakes data set. *Limnology and Oceanography*, *58*(5), 1736–1746. https://doi.org/10.4319/lo.2013.58.5.1736

Bennett, E. M., Carpenter, S. R., & Caraco, N. F. (2001). Human Impact on Erodable Phosphorus and Eutrophication: A Global Perspective. *BioScience*, *51*(3), 227–234. https://doi.org/10.1641/0006-3568(2001)051[0227:HIOEPA]2.0.CO;2

Benoy, G. A., Jenkinson, R. W., Robertson, D. M., & Saad, D. A. (2016). Nutrient delivery to Lake Winnipeg from the Red—Assiniboine River Basin – A binational application of the SPARROW model. *Canadian Water Resources Journal*, *41*(3), 429–447. https://doi.org/10.1080/07011784.2016.1178601

Bevans, R. (2021). *Akaike Information Criterion | When & How to Use It*. https://www.scribbr.com/statistics/akaike-information-criterion/

Bolaños, L., Lukaszewski, K., Bonilla, I., & Blevins, D. (2004). Why boron? *Plant Physiology and Biochemistry*, *42*(11), 907–912. https://doi.org/10.1016/j.plaphy.2004.11.002

Bonilla, I., Bolaños, L., & Mateo, P. (1995). Interaction of boron and calcium in the cyanobacteria *Anabaena* and *Synechococcus*. *Physiologia Plantarium*, *94*, 31–36.

Bonilla, I., Garcia-González, M., & Mateo, P. (1990). Boron Requirement in Cyanobacteria: Its Possible Role in the Early Evolution of Photosynthetic Organisms. *Physiology*, *94*(4), 1554–1560.

Boyd, C. E. (1970). Boron Accumulation by Native Algae. *The American Midland Naturalist*, *84*(2), 565–567.

Brunskill, G. J., Campbell, P., & Elliott, S. E. M. (1979). Temperature, Oxygen, Conductance and Dissolved Major Elements in Lake Winnipeg. *Fisheries and Marine Service Manuscript Report 1526*, 134.

Brunskill, G. J., & Elliott, S. E. M. (1973). Rates of Supply of Nitrogen and Phosphorus to Lake Winnipeg, Manitoba, in relation to the Diversion of Missouri River water into the Red and Assiniboine Rivers. *Verhandlungen Der Internationalen Vereinigung Für Theoretische Und Angewandte Limnologie*, *18*(3), 1755–1759.

Bunting, L., Leavitt, P. R., Simpson, G. L., Wissel, B., Laird, K. R., Cumming, B. F., St. Amand, A., & Engstrom, D. R. (2016). Increased variability and sudden ecosystem state change in Lake Winnipeg, Canada, caused by 20th century agriculture. *Limnology and Oceanography*, *61*(6), 2090–2107. https://doi.org/10.1002/lno.10355

Camacho-Cristóbal, J. J., Herrera-Rodríguez, M. B., Beato, V. M., Rexach, J., Navarro-Gochicoa, M. T., Maldonado, J. M., & González-Fontes, A. (2008). The expression of several cell wall-related genes in *Arabidopsis* roots is down-regulated under boron deficiency. *Environmental and Experimental Botany*, *63*(1–3), 351–358. https://doi.org/10.1016/j.envexpbot.2007.12.004

Canada, G. of. (2017). *Great Lakes Maps*. https://www.canada.ca/en/environment-climate-change/services/great-lakes-protection/maps.html

Chaffin, J. D., Kane, D. D., Stanislawczyk, K., & Parker, E. M. (2018). Accuracy of data buoys for measurement of cyanobacteria, chlorophyll, and turbidity in a large lake (Lake Erie, North America): implications for estimation of cyanobacterial bloom parameters from water quality sonde measurements. *Environmental Science and Pollution Research*, *25*(25), 25175–25189. https://doi.org/10.1007/s11356-018-2612-z

Chen, J.-J., & Yeh, H.-H. (2005). The mechanisms of potassium permanganate on algae removal. *Water Research*, *39*(18), 4420–4428. https://doi.org/10.1016/j.watres.2005.08.032

Cheung, M. Y., Liang, S., & Lee, J. (2013). Toxin-producing Cyanobacteria in Freshwater: A Review of the Problems, Impact on Drinking Water Safety, and Efforts for Protecting Public Health. *Journal of Microbiology*, *51*(1), 1–10. https://doi.org/10.1007/s12275-013-2549-3

Collins, M. (1978). Algal Toxins. *Microbiological Reviews*, *42*(4), 725–746. http://www.pubmedcentral.nih.gov/articlerender.fcgi?artid=281454&tool=pmcentrez&rendertype=abstract

Cottingham, K. L., Ewing, H. A., Greer, M. L., Carey, C. C., & Weathers, K. C. (2015). Cyanobacteria as biological drivers of lake nitrogen and phosphorus cycling. *Ecosphere*, *6*(1), art1. https://doi.org/10.1890/ES14-00174.1

Crowe, J.-A. (1972a). Pollution monitoring, Lake Winnipeg south basin 1967. *Manitoba Department of Mines, Natural Resources and Environment Manuscript Report No. 71-11*, 70.

Crowe, J.-A. (1972b). The south basin of Lake Winnipeg, 1970. *Manitoba Department of Mines, Resources and Environmental Management Manuscript Report No. 71-13*, 31.

Currie, R. S., Williamson, D. A., & Brigham, M. E. (1998). A Preliminary Assessment of Environmental Impacts Associated with the 1997 Red River Flood, with focus on Water Quality. *International Red River Basin Task Force*, 1–47.

de Maagd, P. G.-J., Hendriks, A. J., Seinen, W., & Sijm, D. T. H. M. (1999). pH-Dependent hydrophobicity of the cyanobacteria toxin microcystin-LR. *Water Research (Oxford)*, *33*(3), 677–680.

Derksen, A. J., & Hangasjarvi, E. I. (1979). A Survey of Net Plankton in the North Basin of Lake Winnipeg, July 1974. *Manitoba Department of Mines, Natural Resources and Environment Manuscript Report No. 79-46*, 50.

Dodds, W. (2002). *Freshwater Ecology: Concepts and Environmental Applications*. Academic Press. https://doi.org/10.2307/1468442

Dolman, A. M., Rücker, J., Pick, F. R., Fastner, J., Rohrlack, T., Mischke, U., & Wiedner, C. (2012). Cyanobacteria and Cyanotoxins: The Influence of Nitrogen versus Phosphorus. *PLoS ONE*, *7*(6), 1–14. https://doi.org/10.1371/journal.pone.0038757

Dzialowski, A. R., Smith, V. H., Wang, S. H., Martin, M. C., & DeNoyelles, F. (2011). Effects of non-algal turbidity on cyanobacterial biomass in seven turbid Kansas reservoirs. *Lake and Reservoir Management*, *27*(1), 6–14. https://doi.org/10.1080/07438141.2011.551027

Edwards, C., Graham, D., Fowler, N., & Lawton, L. A. (2008). Biodegradation of microcystins and nodularin in freshwaters. *Chemosphere*, *73*(8), 1315–1321. https://doi.org/10.1016/j.chemosphere.2008.07.015

Ehmann, K., Kelleher, C., & Condon, L. E. (2019). Monitoring turbidity from above: Deploying small unoccupied aerial vehicles to image in-stream turbidity. *Hydrological Processes*, *33*(6), 1013–1021. https://doi.org/10.1002/hyp.13372

Environment and Climate Change Canada, & Manitoba Agriculture and Resource Development. (2020). *State of Lake Winnipeg, 2nd Edition*. https://www.gov.mb.ca/sd/pubs/water/lakes-beaches-rivers/state_lake_wpg_report_tech.pdf

Environment Canada, & Manitoba Water Stewardship. (2011). *State of Lake Winnipeg : 1999 to 2007*. https://www.gov.mb.ca/sd/pubs/water/lakes-beaches-rivers/state_of_lake_winnipeg_rpt_technical_high_resolution.pdf

Evangelista, V., Barsanti, L., Frassanito, A. M., Passarelli, V., & Gualtieri, P. (2008). Algal Toxins: Nature, Occurrence, Effect and Detection. In V. Evangelista, L. Barsanti, A. M. Frassanito, V. Passarelli, & P. Gualtieri (Eds.), *NATO Science for Peace and Security Series*. Springer.

Eyster, H. C. (1952). Necessity of Boron for *Nostoc muscorum*. *Nature*, *170*(4331), 755.

Eyster, H. C. (1958). The Micro-Element Nutrition of *Nostoc Muscorum*. *The Ohio Journal of Science*, *58*(1), 25–33. http://hdl.handle.net/1811/4502

Fan, J., Ho, L., Hobson, P., & Brookes, J. (2013). Evaluating the effectiveness of copper sulphate, chlorine, potassium permanganate, hydrogen peroxide and ozone on cyanobacterial cell integrity. *Water Research*, *47*(14), 5153–5164. https://doi.org/10.1016/j.watres.2013.05.057

Filstrup, C. T., Wagner, T., Soranno, P. A., Stanley, E. H., Stow, C. A., Webster, K. E., & Downing, J. A. (2014). Regional variability among nonlinear chlorophyll-phosphorus relationships in lakes. *Limnology and Oceanography*, *59*(5), 1691–1703. https://doi.org/10.2307/26955897

Fox, J., Bouchet-Valat, M., Andronic, L., Ash, M., Boye, T., Calza, S., Chang, A., Gegzna, V., Grosjean, P., Heiberger, R., Pour, K. K., Kerns, G. J., Lancelot, R.,

Lesnoff, M., Ligges, U., Messad, S., Maechler, M., Muenchen, R., Murdoch, D., … Wright, K. (2020). *Rcmdr: R Commander*. R Package Version 2.7-1. https://socialsciences.mcmaster.ca/jfox/Misc/Rcmdr/

Francy, D. S., Brady, A. M. G., Ecker, C. D., Graham, J. L., Stelzer, E. A., Struffolino, P., Dwyer, D. F., & Loftin, K. A. (2016). Estimating microcystin levels at recreational sites in western Lake Erie and Ohio. *Harmful Algae*, *58*, 23–34. https://doi.org/10.1016/j.hal.2016.07.003

Fristachi, A., Sinclair, J. L., Hall, S., Hambrook Berkman, J. A., Boyer, G., Burkholder, J., Bruns, J., Carmichael, W., DuFour, A., Frazier, W., Morton, S. L., O'Brien, E., & Walker, S. (2008). Occurrence of Cyanobacterial Harmful Algal Blooms Workgroup Report. In H. K. Hudnell (Ed.), *Cyanobacterial Harmful Algal Blooms: State of the Science and Research Needs* (p. 912). Springer.

Galloway, J. N., & Cowling, E. B. (2002). Reactive Nitrogen and The World: 200 Years of Change. *Royal Swedish Academy of Sciences*, *31*(2), 64–71.

Garcia-Gonzalez, M., Mateo, P., & Bonilla, I. (1991). Boron Requirement for Envelope Structure and Function in *Anabaena* PCC 7119. *Journal of Experimental Botany*, *42*(240), 925–929. https://about.jstor.org/terms

Goldman, J. C., Azov, Y., Riley, C. B., & Dennett, M. R. (1982). The Effect of pH in Intensive Microalgal Cultures. I. Biomass Regulation. *Journal of Experimental Marine Biology and Ecology*, *57*(1), 1–13. https://doi.org/10.1016/0022-0981(82)90140-X

Goldman, J. C., Riley, C. B., & Dennett, M. R. (1982). The Effect of pH in Intensive Microalgal Cultures. II. Species Competition. *Journal of Experimental Marine Biology and Ecology*, *57*, 15–24.

Gopalakrishnakone, P., Tubaro, A., Kim, E., Kem, W. R., & Haddad Jr., V. (2016). *Marine and Freshwater Toxins* (P. Gopalakrishnakone, V. Haddad Jr., A. Tubaro, E. Kim, & W. R. Kem (eds.)). Springer Netherlands. https://doi.org/10.1007/978-94-007-6419-4

Government of Manitoba. (2019). *Lake Winnipeg: Nutrients and Loads*. https://www.gov.mb.ca/sd/pubs/water/lakes-beaches-rivers/lake_winnipeg_nutrients_status_report.pdf

Graham, J. L., Jones, J. R., Jones, S. B., Downing, J. A., & Clevenger, T. E. (2004). Environmental factors influencing microcystin distribution and concentration in the Midwestern United States. *Water Research*, *38*(20), 4395–4404. https://doi.org/10.1016/j.watres.2004.08.004

Graham, J. L., Loftin, K. A., Meyer, M. T., & Ziegler, A. C. (2010). Co-occurrence of Toxins and Taste-and-Odor Compounds in Cyanobacterial Blooms from the Midwestern United States. *Environmental Science & Technology*, *44*(19), 7361–7368. https://doi.org/10.1021/es1008938

Graham, J. L., Loftin, K. A., Ziegler, A. C., & Meyer, M. T. (2008a). Guidelines for design and sampling for cyanobacterial toxin and taste-and-odor studies in lakes and reservoirs. In *United States Geological Survey*. http://purl.access.gpo.gov/GPO/LPS97055

Graham, J. L., Loftin, K. A., Ziegler, A. C., & Meyer, M. T. (2008b). National Field Manual for the Collection of Water-Quality Data - Cyanobacteria in Lakes and Reservoirs : Toxin and Taste-and- Odor Sampling Guidelines. In *United States Geological Survey*. https://water.usgs.gov/owq/FieldManual/Chapter7/7.5.html

Greenfield, D. I., Duquette, A., Goodson, A., Keppler, C. J., Williams, S. H., Brock, L. M., Stackley, K. D., White, D., & Wilde, S. B. (2014). The Effects of Three Chemical Algaecides on Cell Numbers and Toxin Content of the Cyanobacteria Microcystis aeruginosa and Anabaenopsis sp. *Environmental Management*, *54*(5), 1110–1120. https://doi.org/10.1007/s00267-014-0339-2

Gupta, R., & Gupta, P. K. (2012). The impact of artificial circulation on phytoplankton community in a freshwater eutrophic lake. *Journal of Ecophysiology and Occupational Health*, *12*(3–4), 1–20.

Hansen, P. J. (2002). Effect of high pH on the growth and survival of marine phytoplankton: implications for species succession. *Aquatic Microbial Ecology*, *28*, 279–288.

Hanson, M. J., & Stefan, H. G. (1984). Side Effects of 58 Years of Copper Sulfate Treatment of the Fairmont Lakes, Minnesota. *JAWRA Journal of the American Water Resources Association*, *20*(6), 889–900. https://doi.org/10.1111/j.1752-1688.1984.tb04797.x

Hastie, T., Tibshirani, R., Leisch, F., Hornik, K., Ripley, B. D., & Narasimhan, B. (2020). *mda: Mixture and Flexible Discriminant Analysis* (0.5-2). https://cran.r-project.org/web/packages/mda/mda.pdf

Helbling, E. W., Banaszak, A. T., & Villafañe, V. E. (2015). Global change feed-back inhibits cyanobacterial photosynthesis. *Scientific Reports*, *5*(9103), 1–6. https://doi.org/10.1038/srep14514

Heng, L., Jun, N., Wen-jie, H., & Guibai, L. (2009). Algae removal by ultrasonic irradiation-coagulation. *Desalination*, *239*(1–3), 191–197. https://doi.org/10.1016/j.desal.2007.12.035

Hou, D., He, J., Lü, C., Sun, Y., Zhang, F., & Otgonbayar, K. (2013). Effects of environmental factors on nutrients release at sediment-water interface and assessment of trophic status for a typical shallow lake, northwest china. *The Scientific World Journal*, *2013*, 716342–16. https://doi.org/10.1155/2013/716342

Huisman, J., Codd, G. A., Paerl, H. W., Ibelings, B. W., Verspagen, J. M. H., & Visser, P. M. (2018). Cyanobacterial blooms. *Nature Reviews Microbiology*, *16*(August), 471–483. https://doi.org/10.1038/s41579-018-0040-1

Huyshe, G. L. (1871). *The Red River Expedition*. MacMillan and Co. https://hdl.handle.net/2027/uc2.ark:/13960/t9571kq40

Iredale, R. S., McDonald, A. T., & Adams, D. G. (2012). A series of experiments aimed at clarifying the mode of action of barley straw in cyanobacterial growth control. *Water Research*, *46*(18), 6095–6103. https://doi.org/10.1016/j.watres.2012.08.040

Jackson, D. F. (1964). *Algae and man : based on lectures presented at the NATO Advanced Study Institute, July 22-August 11, 1962, Louisville, Kentucky*. NATO Advanced Study Institute. Scientific Affairs Division. https://doi.org/10.1007/978-1-4684-1719-7

Jakubowska, N., & Szeląg-Wasielewska, E. (2015). Toxic Picoplanktonic Cyanobacteria—Review. *Marine Drugs*, *13*, 1497–1518. https://doi.org/10.3390/md13031497

Jones, G., Gurney, S., & Rocan, D. (1998). Blue-Green Algae and Microcystin-LR in surface water supplies of southestern Manitoba. *Manitoba Environment Report No. 98-06*, 90.

Kassambara, A. (2018). *Cross-Validation Essentials in R*. http://www.sthda.com/english/articles/38-regression-model-validation/157-cross-validation-essentials-in-r/

Kaya, K., & Watanabe, M. M. (1990). Microcystin composition of an axenic clonal strain of Microcystis viridis and *Microcystis viridis*-containing waterblooms in Japanese freshwaters. *Journal of Applied Phycology*, *2*(2), 173–178. https://doi.org/10.1007/BF00023379

Kling, H. J. (1998). A summary of past and recent plankton of Lake Winnipeg, Canada using algal fossil remains. *Journal of Paleolimnology*, *19*(3), 297–307. https://doi.org/10.1023/A:1007990217568

Kling, H. J., Watson, S. B., McCullough, G. K., & Stainton, M. P. (2011). Bloom development and phytoplankton succession in Lake Winnipeg: a comparison of historical records with recent data. *Aquatic Ecosystem Health & Management*, *14*(2), 219–224. https://doi.org/10.1080/14634988.2011.577722

Knappe, R., Detlef, R. U., Belk, C., Briley, D. S., Grandy, S. R., Rastogi, N., & Rike, A. H. (2004). *Algae detection and removal strategies for drinking water treatment plants. AWWA* (R. Knappe, R. U. Detlef, C. Belk, D. S. Briley, S. R. Grandy, N. Rastogi, & A. H. Rike (eds.)). American Water Works Association.

Kotak, B. G. (2009). Occurrence of the Cyanobacterial Toxin, Microcystin, in Lake Winnipeg in 2007. *Water Stewardship Fund Project 26037 Report*, 24.

Kotak, B. G., Lam, A. K.-Y., Prepas, E. E., & Hrudey, S. E. (2000). Role of chemical and physical variables in regulating microcystin-LR concentration in phytoplankton of eutrophic lakes. *Canadian Journal of Fisheries and Aquatic Sciences*, *57*(8), 1584–

1593. https://doi.org/10.1139/f00-091

Kotak, B. G., Lam, A. K.-Y., Prepas, E. E., Kenefick, S. L., & Hrudey, S. E. (1995). Variability of the hepatotoxin microcystin-LR in hypereutrophic drinking water lakes. *Journal of Phycology*, *31*(2), 248–263. https://doi.org/10.1111/j.0022-3646.1995.00248.x

Kotak, B. G., & Zurawell, R. W. (2007). Cyanobacterial toxins in Canadian freshwaters: A review. *Lake and Reservoir Management*, *23*(2), 109–122. https://doi.org/10.1080/07438140709353915

Kotak, B. G., Zurawell, R. W., Prepas, E. E., & Holmes, C. F. B. (1996). Microcystin-LR concentration in aquatic food web compartments from lakes of varying trophic status. *Canadian Journal of Fisheries and Aquatic Sciences*, *53*(9), 1974–1985. https://doi.org/10.1139/cjfas-53-9-1974

Kuhn, M., Wind, J., Weston, S., Williams, A., Keefer, C., Engelhardt, A., Cooper, T., Mayer, Z., Kenkel, B., R Core Team, Lescarbeau, R., Ziem, A., Scrucca, L., Tang, Y., Candan, C., & Hunt, T. (2022). *caret: Classification and Regression Training* (6.0-91). https://cran.r-project.org/web/packages/caret/caret.pdf

Lake Winnipeg Research Consortium. (2005). *Lake Winnipeg Research Consortium Inc. - About The Namao*. https://www.lakewinnipegresearch.org/motor-vessel-namao/

Lake Winnipeg Research Consortium. (2008). *The Lake Winnipeg Research Consortium Inc .* (Issue June). https://www.lakewinnipegresearch.org/wp-content/uploads/2018/08/2008-LWRC-Report_Final-1.pdf

Lake Winnipeg Stewardship Board. (2006). *Reducing Nutrient Loading to Lake Winnipeg and its Watershed: Our Collective Responsibility and Commitment to Action*. https://mspace.lib.umanitoba.ca/xmlui/bitstream/handle/1993/33947/2006_Lake_Winnipeg_Stewardship_Board_Reducing_Nutrient_Loading_Watershed.pdf?sequence=1&isAllowed=y

Lee, R. E. (2008). *Phycology* (4th Editio). Cambridge University Press. http://www.dbbe.fcen.uba.ar/contenido/objetos/PhycologyLee_1395342784413494.pdf

Lee, S. J., Jang, M. H., Kim, H. S., Yoon, B. D., & Oh, H. M. (2000). Variation of microcystin content of *Microcystis aeruginosa* relative to medium N:P ratio and growth stage. *Journal of Applied Microbiology*, *89*(2), 323–329. https://doi.org/10.1046/j.1365-2672.2000.01112.x

Lesht, B. M., Barbiero, R. P., & Warren, G. J. (2013). A band-ratio algorithm for retrieving open-lake chlorophyll values from satellite observations of the Great Lakes. *Journal of Great Lakes Research*, *39*(1), 138–152. https://doi.org/10.1016/j.jglr.2012.12.007

Lin, T.-F., Chang, D.-W., Lien, S.-K., Tseng, Y.-S., Chiu, Y.-T., & Wang, Y.-S. (2009). Effect of chlorination on the cell integrity of two noxious cyanobacteria and their releases of odorants. *Journal of Water Supply: Research and Technology - AQUA*, *58*(8), 539–551. https://doi.org/10.2166/aqua.2009.117

Liu, X., Lu, X., & Chen, Y. (2011). The effects of temperature and nutrient ratios on *Microcystis* blooms in Lake Taihu, China: An 11-year investigation. *Harmful Algae*, *10*(3), 337–343. https://doi.org/10.1016/j.hal.2010.12.002

Long, B. M., Jones, G. J., & Orr, P. T. (2001). Cellular Microcystin Content in N-Limited *Microcystis aeruginosa* Can Be Predicted from Growth Rate. *Applied and Environmental Microbiology*, *67*(1), 278–283. https://doi.org/10.1128/AEM.67.1.278-283.2001

Lukač, M., & Aegerter, R. (1993). Influence of trace metals on growth and toxin production of *Microcystis aeruginosa*. *Toxicon*, *31*(3), 293–305. https://doi.org/10.1016/0041-0101(93)90147-B

Manitoba, H., & Manitoba, G. of. (2008). *Manitoba/Manitoba Hydro Coordianted Aquatic Monitoring Program*. http://www.nscons.ca/projects/camp.html

Manitoba Water Stewardship. (2011). *Manitoba Clean Beaches Program*. https://gov.mb.ca/sd/water/lakes-beaches-rivers/manitoba-beaches.html

Mariani, M. A., Padedda, B. M., Kaštovský, J., Buscarinu, P., Sechi, N., Virdis, T., & Lugliè, A. (2015). Effects of trophic status on microcystin production and the dominance of cyanobacteria in the phytoplankton assemblage of Mediterranean reservoirs. *Scientific Reports*, *5*(1), 17964–17964. https://doi.org/10.1038/srep17964

Matthijs, H. C. P., Visser, P. M., Reeze, B., Meeuse, J., Slot, P. C., Wijn, G., Talens, R., & Huisman, J. (2012). Selective suppression of harmful cyanobacteria in an entire lake with hydrogen peroxide. *Water Research*, *46*(5), 1460–1472. https://doi.org/10.1016/j.watres.2011.11.016

Mazerolle, M. J. (2020). *AICcmodavg: Model selection and multimodel inference based on (Q)AIC(c).* (2.3-1). https://cran.r-project.org/web/packages/AICcmodavg/index.html

McCullough, G. K. (2015). Analysis of Inter-laboratory Effects on Phosphorus Concentrations Reported for Lakes and Rivers in Manitoba. *Prepared for the Manitoba Department of Conservation*, 49.

McCullough, G. K., Page, S. J., Hesslein, R. H., Stainton, M. P., Kling, H. J., Salki, A. G., & Barber, D. G. (2012). Hydrological forcing of a recent trophic surge in Lake Winnipeg. *Journal of Great Lakes Research*, *38*(SUPPL. 3), 95–105. https://doi.org/10.1016/j.jglr.2011.12.012

Mohamed, Z. A. (2001). Alum and lime-alum removal of toxic and nontoxic

phytoplankton from the Nile river water: Laboratory study. *Water Resources Management*, *15*(4), 213–221. https://doi.org/10.1023/A:1013373420314

Neilan, B. A., Pearson, L. A., Muenchhoff, J., Moffitt, M. C., & Dittmann, E. (2013). Environmental conditions that influence toxin biosynthesis in cyanobacteria. *Environmental Microbiology*, *15*(5), 1239–1253. https://doi.org/10.1111/j.1462-2920.2012.02729.x

Orihel, D. M., Bird, D. F., Brylinsky, M., Chen, H., Donald, D. B., Huang, D. Y., Giani, A., Kinniburgh, D., Kling, H., Kotak, B. G., Leavitt, P. R., Nielsen, C. C., Reedyk, S., Rooney, R. C., Watson, S. B., Zurawell, R. W., & Vinebrooke, R. D. (2012). High microcystin concentrations occur only at low nitrogen-to-phosphorus ratios in nutrient-rich Canadian lakes. *Canadian Journal of Fisheries and Aquatic Sciences*, *69*(9), 1457–1462. https://doi.org/10.1139/f2012-088

Paerl, H. W. (2008). *Cyanobacterial Harmful Algal Blooms: State of the Science and Research Needs* (H. K. Hudnell (ed.); Vol. 619). Springer.

Paerl, H. W., & Otten, T. G. (2013). Harmful Cyanobacterial Blooms: Causes, Consequences, and Controls. *Microbial Ecology*, *65*(4), 995–1010. https://doi.org/10.1007/s00248-012-0159-y

Pip, E., & Bowman, L. (2014). Microcystin and Algal Chlorophyll in Relation to Nearshore Nutrient Concentrations in Lake Winnipeg, Canada. *Environment and Pollution*, *3*(2), 36–47. https://doi.org/10.5539/ep.v3n2p36

Polyak, Y., Zaytseva, T., & Medvedeva, N. (2013). Response of toxic cyanobacterium *Microcystis aeruginosa* to environmental pollution. *Water, Air, and Soil Pollution*, *224*(4), 1–13. https://doi.org/10.1007/s11270-013-1494-4

R Core Team. (2021). *R: A Language and Environment for Statistical Computing*. https://www.r-project.org/

Rajabi, H., Filizadeh, Y., Soltani, M., & Fotokian, M. H. (2010). The use of Barley Straw for Controlling of Cyanobacteria under Field Application. *Journal of Fisheries and Aquatic Science*, *5*(5), 394–401. https://doi.org/10.3923/jfas.2016.12.27

Redondo-Nieto, M., Maunoury, N., Mergaert, P., Kondorosi, E., Bonilla, I., & Bolaños, L. (2012). Boron and calcium induce major changes in gene expression during legume nodule organogenesis. Does boron have a role in signalling? *The New Phytologist*, *195*(1), 14–19. https://doi.org/10.2307/newphytologist.195.1.14

Ripley, B. D., & Vanables, W. N. (2002). *Modern Applied Statistics with S* (4th ed.). Springer.

Rose, V., Bollens, S. M., & Rollwagen-Bollens, G. (2017). Interactive effects of phosphorus and zooplankton grazing on cyanobacterial blooms in a shallow temperate lake. *Hydrobiologia*, *788*(1), 345–359. https://doi.org/10.1007/s10750-016-3011-4

Ruiz, M., Galanti, L., Ruibal, A. L., Rodriguez, M. I., Wunderlin, D. A., & Amé, M. V. (2013). First report of microcystins and anatoxin-a co-occurrence in San Roque reservoir (Córdoba, Argentina). *Water, Air, and Soil Pollution*, *224*(6). https://doi.org/10.1007/s11270-013-1593-2

Rybicki, R. W. (1966). Limnological Survey of the North Basin of Lake Winnipeg 1963 and 1964. *Manitoba Department of Mines, Natural Resources and Environment Manuscript Report 66-11*, 74.

Sakai, H., Hao, A., Iseri, Y., Wang, S., Kuba, T., Zhang, Z., & Katayama, H. (2013). Occurrence and distribution of microcystins in Lake Taihu, China. *The Scientific World Journal*, *2013*. https://doi.org/10.1155/2013/838176

Salvador, D., Churro, C., & Valério, E. (2016). Evaluating the influence of light intensity in mcyA gene expression and microcystin production in toxic strains of *Planktothrix agardhii* and *Microcystis aeruginosa*. *Journal of Microbiological Methods*, *123*, 4–12. https://doi.org/10.1016/j.mimet.2016.02.002

Sarkar, D. (2008). *Lattice: Multivariate Data Visualization with R*. Springer. https://cran.r-project.org/web/packages/lattice/lattice.pdf

Schindler, D. W., Hecky, R. E., Findlay, D. L., Stainton, M. P., Parker, B. R., Paterson, M. J., Beaty, K. G., Lyng, M., & Kasian, S. E. M. (2008). Eutrophication of lakes cannot be controlled by reducing nitrogen input: Results of a 37-year whole-ecosystem experiment. *Proceedings of the National Academy of Sciences*, *105*(32), 11254–11258. https://doi.org/10.1073/pnas.0805108105

Schindler, D. W., Hecky, R. E., & McCullough, G. K. (2012). The rapid eutrophication of Lake Winnipeg: Greening under global change. *Journal of Great Lakes Research*, *38*(SUPPL. 3), 6–13. https://doi.org/10.1016/j.jglr.2012.04.003

Scott, J. T., McCarthy, M. J., Otten, T. G., Steffen, M. M., Baker, B. C., Grantz, E. M., Wilhelm, S. W., & Paerl, H. W. (2013). Comment: An alternative interpretation of the relationship between TN:TP and microcystins in Canadian lakes. *Canadian Journal of Fisheries and Aquatic Sciences*, *70*, 1265–1268. https://doi.org/10.1139/cjfas-2012-0490

Sivonen, K. (1990). Effects of Light, Temperature, Nitrate, Orthophosphate, and Bacteria on Growth of and Hepatotoxin Production by *Oscillatoria agardhii* Strains. *Applied and Environmental Microbiology*, *56*(9), 2658–2666.

Smyth, G., Hu, Y., Dunn, P., Phipson, B., & Chen, Y. (2021). *statmod: Statistical Modeling*. https://cran.r-project.org/web/packages/statmod/index.html

Song, L.-Y., & Wang, Y.-Q. (2015). Investigation of microbial community structure of a shallow lake after one season copper sulfate algaecide treatment. *Microbiological Research*, *170*, 105–113. https://doi.org/10.1016/j.micres.2014.08.008

Song, L., Sano, T., Li, R., Watanabe, M. M., Liu, Y., & Kaya, K. (1998). Microcystin

production of *Microcystis viridis* (cyanobacteria) under different culture conditions. *Phycological Research*, *46*(s2), 19–23. https://doi.org/10.1111/j.1440-1835.1998.tb00266.x

Srivastava, A., Ko, S. R., Ahn, C. Y., Oh, H. M., Ravi, A. K., & Asthana, R. K. (2016). Microcystin Biosynthesis and mcyA Expression in Geographically Distinct *Microcystis* Strains under Different Nitrogen, Phosphorus, and Boron Regimes. *BioMed Research International*, *2016*, 5985987–13. https://doi.org/10.1155/2016/5985987

Statology. (2022, March). *How to Calculate R-Squared for glm in R*. https://www.statology.org/glm-r-squared/

Stumpf, R. P., Johnson, L. T., Wynne, T. T., & Baker, D. B. (2016). Forecasting annual cyanobacterial bloom biomass to inform management decisions in Lake Erie. *Journal of Great Lakes Research*, *42*(6), 1174–1183. https://doi.org/10.1016/j.jglr.2016.08.006

Taranu, Z. E., Pick, F. R., Creed, I. F., Zastepa, A., & Watson, S. B. (2019). Meteorological and Nutrient Conditions Influence Microcystin Congeners in Freshwaters. *Toxins*, *11*(11), 1–21.

Tharwat, A., Gaber, T., Ibrahim, A., & Hassanien, A. E. (2017). Linear discriminant analysis: A detailed tutorial. *AI Communications*, *30*(2), 169–190. https://doi.org/10.3233/AIC-170729

Tonk, L., Visser, P. M., Christiansen, G., Dittmann, E., Snelder, E. O. F. . M., Wiedner, C., Mur, L. R., & Huisman, J. (2005). The Microcystin Composition of the Cyanobacterium *Planktothrix agardhii* Changes toward a More Toxic Variant with Increasing Light Intensity. *Appl. Environ. Microbiol.*, *71*(9), 5177–5181. https://doi.org/10.1128/AEM.71.9.5177

UCLA: Statistical Consulting Group. (2011, October). *FAQ: What are pseudo R-squareds?* https://stats.oarc.ucla.edu/other/mult-pkg/faq/general/faq-what-are-pseudo-r-squareds/

van der Westhuizen, A. J., & Eloff, J. N. (1985). Effect of temperature and light on the toxicity and growth of the blue-green alga *Microcystis aeruginosa* (UV-006). *Planta*, *163*(1), 55–59. https://doi.org/10.1007/BF00395897

Van Hullebusch, E., Deluchat, V., Chazal, P. M., & Baudu, M. (2002). Environmental impact of two successive chemical treatments in a small shallow eutrophied lake: Part II. Case of copper sulfate. *Environmental Pollution*, *120*(3), 627–634. https://doi.org/10.1016/S0269-7491(02)00191-4

Vézie, C., Rapala, J., Vaitomaa, J., Seitsonen, J., & Sivonen, K. (2002). Effect of nitrogen and phosphorus on growth of toxic and nontoxic *Microcystis* strains and on intracellular microcystin concentrations. *Microbial Ecology*, *43*(4), 443–454. https://doi.org/10.1007/s00248-001-0041-9

Visser, P. M., Ibelings, B. W., Van Der Veer, B., Koedood, J., & Mur, L. R. (1996). Artificial mixing prevents nuisance blooms of the cyanobacterium *Microcystis* in Lake Nieuwe Meer, the Netherlands. *Freshwater Biology*, *36*(2), 435–450. https://doi.org/10.1046/j.1365-2427.1996.00093.x

Walls, J. T., Wyatt, K. H., Doll, J. C., Rubenstein, E. M., & Rober, A. R. (2018). Hot and toxic: Temperature regulates microcystin release from cyanobacteria. *Science of the Total Environment*, *610–611*, 786–795. https://doi.org/10.1016/j.scitotenv.2017.08.149

Wang, L., Qiao, J., Hu, Y., Wang, L., Zhang, L., Zhou, Q., & Gao, N. (2013). Pre-oxidation with KMnO4 changes extra-cellular organic matter's secretion characteristics to improve algal removal by coagulation with a low dosage of polyaluminium chloride. *Journal of Environmental Sciences*, *25*(3), 452–459. https://doi.org/10.1016/S1001-0742(12)60087-4

Weirich, C. A., Robertson, D. M., & Miller, T. R. (2019). Physical, biogeochemical, and meteorological factors responsible for interannual changes in cyanobacterial community composition and biovolume over two decades in a eutrophic lake. *Hydrobiologia*, *828*(1), 165–182. https://doi.org/10.1007/s10750-018-3810-x

West, M., & Louda, J. W. (2011). Effect of External pH on Cyanobacterial Pigment. *Florida Scientist*, *74*(3), 181–186. https://about.jstor.org/terms

Whitman, R. L., & Nevers, M. B. (2003). Foreshore sand as a source of *Escherichia coli* in nearshore water of a Lake Michigan Beach. *Applied and Environmental Microbiology*, *69*(9), 5555–5562. https://doi.org/10.1128/AEM.69.9.5555-5562.2003

Wickham, H., & Girlich, M. (2022). *tidyr: Tidy Messy Data* (1.3.1). https://cran.r-project.org/web/packages/tidyr/index.html

Wu, S. K., Xie, P., Liang, G. D., Wang, S. B., & Liang, X. M. (2006). Relationships between microcystins and environmental parameters in 30 subtropical shallow lakes along the Yangtze River, China. *Freshwater Biology*, *51*(12), 2309–2319. https://doi.org/10.1111/j.1365-2427.2006.01652.x

Wu, X., Joyce, E. M., & Mason, T. J. (2011). The effects of ultrasound on cyanobacteria. *Harmful Algae*, *10*(6), 738–743. https://doi.org/10.1016/j.hal.2011.06.005

Xie, L., Rediske, R. R., Gillett, N. D., O'Keefe, J. P., Scull, B., & Xue, Q. (2016). The impact of environmental parameters on microcystin production in dialysis bag experiments. *Scientific Reports*, *6*, 1–10. https://doi.org/10.1038/srep38722

Xie, L., Xie, P., Li, S., Tang, H., & Liu, H. (2003). The low TN:TP ratio, a cause or a result of *Microcystis* blooms? *Water Research*, *37*(9), 2073–2080. https://doi.org/10.1016/S0043-1354(02)00532-8

Ye, J., Janardan, R., Park, C., & Park, H. (2004). A new optimization criterion for generalized discriminant analysis on undersampled problems. *IEEE Transactions*

on Pattern Analysis and Machine Intelligence, *26*(8), 982–994.

Zamyadi, A., Ho, L., Newcombe, G., Bustamante, H., & Prévost, M. (2012). Fate of toxic cyanobacterial cells and disinfection by-products formation after chlorination. *Water Research*, *46*(5), 1524–1535. https://doi.org/10.1016/j.watres.2011.06.029

Zeileis, A., Kleiber, C., & Jackman, S. (2008). Regression Models for Count Data in R. *Journal of Statistical Software*, *27*(8). http://cran.r-project.org/package=pscl.

Zhang, G., Zhang, P., Wang, B., & Liu, H. (2006). Ultrasonic frequency effects on the removal of *Microcystis aeruginosa*. *Ultrasonics Sonochemistry*, *13*(5), 446–450. https://doi.org/10.1016/j.ultsonch.2005.09.012

Zuur, A. F., Ieno, E. N., & Elphick, C. S. (2010). A protocol for data exploration to avoid common statistical problems. *Methods in Ecology and Evolution*, *1*(1), 3–14. https://doi.org/10.1111/j.2041-210x.2009.00001.x

6.0 APPENDICES

Appendix 1. Table of vessels and workboats used for each spring, summer and fall research surveys on Lake Winnipeg from 1999 to 2017 (*The CCGS *Namao* did not run a science research survey due to drydock; used alternative vessel and workboat; **The MV *Namao* did not run a science research survey due to drydock; used alternative workboat).

Years	Spring	Summer	Fall
1999	-	CCGS *Namao*	-
2000	-	-	-
2001	-	-	-
2002	CCGS *Namao*	CCGS *Namao*	CCGS *Namao*
2003	CCGS *Namao*	CCGS *Namao*	CCGS *Namao*
2004	CCGS *Namao*	CCGS *Namao*	CCGS *Namao*
2005	CCGS *Namao*	CCGS *Namao*	* MV *Siggy Oliver* and 20-24ft Zag Fab
2006	MV *Namao*	MV *Namao*	MV *Namao*
2007	MV *Namao*	MV *Namao*	MV *Namao*
2008	MV *Namao*	MV *Namao*	MV *Namao*
2009	MV *Namao*	MV *Namao*	MV *Namao*
2010	MV *Namao*	MV *Namao*	MV *Namao*
2011	MV *Namao*	MV *Namao*	MV *Namao*
2012	MV *Namao*	MV *Namao*	MV *Namao*
2013	MV *Namao*	MV *Namao*	MV *Namao*
2014	** LWRC Workboat-21ft Zag	MV *Namao*	MV *Namao*
2015	MV *Namao*	MV *Namao*	MV *Namao*
2016	MV *Namao*	MV *Namao*	MV *Namao*
2017	MV *Namao*	MV *Namao*	MV *Namao*

Appendix 2. Table of all the W, Auxiliary, Near Shore, CAMP, Clean Beaches Program and Non-Routine Stations on Lake Winnipeg from 1999 to 2017. W=W Station; AUX=Auxiliary Station; NS=Near Shore Station; CAMP=CAMP Station; CBP=Clean Beaches Program Station; N-R=Non-Routine Station.

Routine Stations	Station Number	Latitude	Longitude	Basin	Station	Currently Monitored
W1	MB05SHS014	53.37633	-98.39033	North	W	Yes
W2	MB05SHS004	53.26403	-99.02443	North	W	Yes
W3	MB05RFS002	53.17067	-97.83750	North	W	Yes
W4	MB05SGS004	52.86567	-98.25075	North	W	Yes
W5	MB05RES005	52.79443	-97.56135	North	W	Yes
W6	MB05SFS002	52.64300	-97.73475	North	W	Yes
W7	MB05RDS007	52.43467	-97.33733	North	W	Yes
W8	MB05RBS003	51.76318	-96.83937	Narrows	W	Yes
W9	MB05RAS078	51.02190	-96.58333	South	W	Yes
W10	MB05SCS005	50.84633	-96.76917	South	W	Yes
W11	MB05SAS004	50.76083	-96.45348	South	W	Yes
W12	MB05SBS126	50.51692	-96.83340	South	W	Yes
W13	MB05SCS145	51.44167	-96.63333	Narrows	W	Yes
W14	MB05RDS011	52.25000	-97.18750	Narrows	W	Yes
2	MB05SBS316	50.43333	-96.83333	South	AUX	No
4	MB05SBS314	50.46667	-96.80833	South	AUX	No
6	MB05SAS083	50.75833	-96.59167	South	AUX	No
8	MB05RAS139	50.74583	-96.47500	South	AUX	No

11	MB05SCS144	50.95833	-96.68333	South	AUX	No
15	MB05RBS008	51.73333	-96.83333	Narrows	AUX	No
17	MB05RES009	52.80833	-97.64167	North	AUX	No
18	MB05RES010	52.67083	-97.50000	North	AUX	No
20	MB05RFS008	53.17500	-97.59170	North	AUX	No
25	MB05SGS014	53.20833	-98.90833	North	AUX	No
28	MB05SHS020	53.22083	-99.25000	North	AUX	No
41	MB05SGS009	52.82917	-98.45417	North	AUX	No
48	MB05SFS007	52.64583	-97.84167	North	AUX	No
53	MB05RDS008	52.12083	-97.12917	Narrows	AUX	No
55	MB05RDS010	51.86250	-96.93750	Narrows	AUX	No
56	MB05RBS009	51.60833	-96.71667	Narrows	AUX	No
57	MB05SCS143	50.86667	-96.80833	South	AUX	No
59	MB05SAS081	50.69167	-96.74167	South	AUX	No
60	MB05SBS310	50.57917	-96.78333	South	AUX	No
61	MB05SBS312	50.52500	-96.80417	South	AUX	No
62	MB05SBS313	50.50833	-96.94167	South	AUX	No
69	MB05SDS041	52.00833	-97.17917	Narrows	AUX	No
10A	MB05RAS135	51.00000	-96.55000	South	AUX	No
10S	MB05RAS141	50.92083	-96.56667	South	AUX	No
12B	MB05SCS146	51.13398	-96.62208	South	AUX	No
20S	MB05RFS007	53.22500	-97.93333	North	AUX	No
23B	MB05SHS023	53.66250	-98.27083	North	AUX	No
23ES	MB05SGS010	53.32500	-98.24167	North	AUX	No

26S	MB05SHS021	53.41250	-98.76667	North	AUX	No
27S	MB05SHS016	53.40915	-99.07339	North	AUX	No
35S	MB05SHS022	53.50417	-98.57500	North	AUX	No
36S	MB05SAS094	50.73560	-96.92933	South	AUX	No
37S	MB05SBS322	50.79202	-96.76232	South	AUX	No
38S	MB05SCS166	51.02160	-96.56559	South	AUX	No
3C	MB05SAS092	50.46194	-96.62030	South	AUX	No
42S	MB05SGS012	52.82500	-98.06667	North	AUX	No
44S	MB05SCS147	51.21645	-96.72578	South	AUX	No
47S	MB05RAS138	51.22917	-96.34167	South	AUX	No
49S	MB05RAS153	51.25374	-96.52536	South	AUX	No
50S	MB05RES011	52.48333	-97.49267	North	AUX	No
58S	MB05RAS075	50.63610	-96.31722	South	AUX	No
62B	MB05SBS318	50.63333	-96.95000	South	AUX	No
1	MB05SBS315	50.38750	-96.81667	South	AUX	Yes
5	MB05SAS082	50.67917	-96.63750	South	AUX	Yes
7	MB05SAS084	50.65000	-96.37917	South	AUX	Yes
9	MB05RAS140	50.87917	-96.39583	South	AUX	Yes
19	MB05RES008	52.92083	-97.67083	North	AUX	Yes
21	MB05RFS006	53.43750	-97.85833	North	AUX	Yes
31	MB05SHS017	53.61250	-98.95000	North	AUX	Yes
33	MB05SHS019	53.84583	-98.49167	North	AUX	Yes
39	MB05SGS011	53.04167	-98.19167	North	AUX	Yes
45	MB05SFS006	52.63750	-98.32500	North	AUX	Yes

54	MB05RDS009	52.00000	-97.04167	Narrows	AUX	Yes
64	MB05SES003	52.24167	-97.62917	North	AUX	Yes
68	MB05SDS040	52.10417	-97.41667	Narrows	AUX	Yes
13B	MB05RAS137	51.33750	-96.57917	Narrows	AUX	Yes
22	MB05SHS024	53.62917	-97.97083	North	AUX/CAMP	Yes
23S	MB05SGS013	53.20500	-98.61667	North	AUX	Yes
34S	MB05SHS018	53.66250	-98.48333	North	AUX	Yes
3B	MB05SBS317	50.44290	-96.70935	South	AUX	Yes
43S	MB05SGS037	52.83444	-98.18889	North	AUX	Yes
46S	MB05RAS154	51.14226	-96.42292	South	AUX	Yes
57B	MB05SCS157	50.99451	-96.89214	South	AUX	Yes
60B	MB05SBS311	50.63333	-96.95000	South	AUX	Yes
60C	MB05SBS319	50.51250	-96.89167	South	AUX	Yes
65S	MB05SES012	52.16722	-97.85363	North	AUX	Yes
Near Shore 1-East Side, North	MB05RES017	52.88666	-97.39568	North	NS	Yes
Near Shore 2-West Side, North	MB05SGS038	52.64051	-98.70877	North	NS	Yes
Near Shore 3-Gimli	MB05SBS346	50.63838	-96.98022	South	NS	Yes
Near Shore 4-South Shore	MB05SBS347	50.40960	-96.90378	South	NS	Yes
Near Shore 5-Hillside	MB05SAS114	50.67383	-96.58758	South	NS	Yes
Near Shore 6-Hecla	MB05SCS170	51.12430	-96.66217	South	NS	Yes
Near Shore 7-Manigotagan	MB05RAS162	51.17355	-96.37740	South	NS	Yes
Near Shore 8-Pine Dock	MB05SDS048	51.60152	-96.72433	Narrows	NS	Yes
Near Shore 9-Bloodvein	MB05RBS014	51.86028	-96.80778	Narrows	NS	Yes
Near Shore 10-George Island	MB05RES018	52.81755	-97.62797	North	NS	Yes

Near Shore 11-North Shore	MB05SHS051	53.85128	-98.50123	North	NS	Yes
Near Shore 12-Grand Rapids	MB05SHS052	53.21157	-99.26718	North	NS	Yes
Near Shore 13-McBeth Point	MB05SES013	52.13212	-97.54732	Narrows	NS	No
Nelson River @ Warren	MB05UBS010	53.70000	-97.86667	North	CAMP	Yes
Two-Mile Channel Inlet	MB05UBS020	53.75002	-98.07871	North	CAMP	Yes
Two-Mile Channel Outlet	MB05UBS021	53.76670	-98.04280	North	CAMP	Yes
Big Mossy Point	MB05SHS053	53.69819	-98.20044	North	CAMP	Yes
Albert Beach	MB05SAS087	50.68305	-96.51289	South	CBP	Yes
East Grand Beach	MB05SAS015	50.56830	-96.60583	South	CBP	Yes
Hillside Beach	MB05SAS088	50.67269	-96.55955	South	CBP	Yes
Lester Beach	MB05SAS014	50.58133	-96.58391	South	CBP	Yes
Patricia Beach	MB05SAS017	50.42339	-96.61678	South	CBP	Yes
Sunset Beach	MB05SAS093	50.51800	-96.60515	South	CBP	Yes
Victoria Beach - Clubhouse	MB05SAS012	50.69863	-96.56149	South	CBP	Yes
Victoria Beach - Red Cross	MB05SAS013	50.69675	-96.56113	South	CBP	Yes
West Grand Beach	MB05SAS016	50.56060	-96.62556	South	CBP	Yes
Black's Point Beach	MB05SCS159	51.23740	-96.74770	South	CBP	Yes
Gimli Beach	MB05SBS012	50.63530	-96.98333	South	CBP	Yes
Grindstone Beach	MB05SCS151	51.26797	-96.68515	South	CBP	Yes
Gull Harbour Beach	MB05SCS149	51.19140	-96.62190	South	CBP	Yes
Hnausa Beach	MB05SCS150	50.89906	-96.99192	South	CBP	Yes
Matlock Beach	MB05SBS025	50.43042	-96.94858	South	CBP	No
Milne Beach	MB05SBS348	50.44221	-96.95478	South	CBP	Yes
Sandy Bar Beach	MB05SCS148	50.98660	-96.93046	South	CBP	Yes

Sandy Hook Beach	MB05SBS023	50.54022	-96.98335	South	CBP	Yes
Spruce Sands Beach	MB05SBS320	50.78691	-96.98025	South	CBP	Yes
Winnipeg Beach Beach	MB05SBS024	50.49708	-96.96378	South	CBP	Yes
Bloom 1 2008	MB05SHS111	50.67770	-96.91172	South	N-R	No
Bloom 2 2008	MB05SHS111	50.80255	-96.80023	South	N-R	No
Bloom 1 2009	MB05SHS111	No		North	N-R	No
Bloom 2 2009	MB05SHS111	No		North	N-R	No
Bloom 3 2009	MB05SHS111	53.23545	-97.65612	North	N-R	No
Bloom 4 2009	MB05SHS111	53.23045	-98.59723	North	N-R	No
Bloom 1 2010	MB05SHS111	No		South	N-R	No
Bloom 1 2012	MB05SHS111	No		North	N-R	No
Bloom 2 2012	MB05SHS111	No		North	N-R	No
Bloom 3 2012	MB05SHS111	No		North	N-R	No
Bloom 1 2015	MB05SHS111	52.81870	-97.58678	North	N-R	No
Bloom 2 2015	MB05SHS111	53.67630	-98.46467	North	N-R	No
Bloom 1 2016	MB05SHS111	52.38727	-97.25952	North	N-R	No
Bloom 2 2016	MB05SHS111	52.84182	-97.56715	North	N-R	No
Bloom 3 2016	MB05SHS111	52.89875	-97.57653	North	N-R	No
Bloom 4 2016	MB05SHS111	52.11245	-98.31718	North	N-R	No
Bloom 5 2016	MB05SHS111	52.82857	-98.26163	North	N-R	No
Bloom 6 2016	MB05SHS111	52.59192	-97.71632	North	N-R	No
Bloom 7 2016	MB05SHS111	52.44715	-97.37095	North	N-R	No
Bloom 8 2016	MB05SHS111	53.48317	-98.38890	North	N-R	No
Bloom 9 2016	MB05SHS111	50.51800	-96.85095	South	N-R	No

Bloom 1 2017	MB05SHS111	50.56303	-96.87960	South	N-R	No

Appendix 3. Table of all samples taken at all 14 W stations in the spring, summer and fall Lake Winnipeg science cruises from 1999 to 2017. Sp=Spring, Su=Summer, Fa=Fall; Y=Yes, N=No.

	W1			W2			W3			W4			W5			W6			W7		
Years	**Sp**	**Su**	**Fa**	**Sp**	**Su**	**Fa**	**Sp**	**Su**	**Fa**	**Sp**	**Su**	**Fa**	**Sp**	**Su**	**Fa**	**Sp**	**Su**	**Fa**	**Sp**	**Su**	**Fa**
1999	N	N	N	N	Y	N	N	N	N	N	N	N	N	N	N	N	N	N	N	N	N
2000	N	Y	Y	N	Y	Y	Y	Y	N	Y	Y	N	Y	Y	N	Y	Y	Y	Y	Y	Y
2001	Y	Y	Y	N	Y	Y	Y	N	Y	Y	N	Y	Y	N	Y	Y	N	Y	Y	N	Y
2002	Y	Y	Y	Y	Y	Y	N	Y	N	N	Y	Y	N	Y	N	N	Y	N	N	Y	N
2003	Y	Y	Y	Y	Y	Y	Y	N	N	Y	Y	N	Y	N	N	Y	N	N	N	N	N
2004	Y	Y	Y	Y	Y	Y	Y	N	Y	Y	N	N	Y	Y	Y	Y	Y	Y	Y	Y	Y
2005	Y	N	Y	N	N	Y	N	Y	N	N	Y	Y	N	Y	Y	N	Y	N	N	Y	N
2006	Y	Y	Y	Y	Y	Y	Y	Y	Y	Y	Y	Y	Y	Y	N	Y	Y	Y	Y	Y	Y
2007	Y	Y	Y	Y	Y	Y	Y	Y	Y	Y	Y	Y	Y	Y	Y	Y	Y	Y	Y	Y	Y
2008	Y	Y	Y	Y	Y	Y	Y	Y	Y	Y	Y	Y	Y	Y	Y	Y	Y	Y	Y	Y	Y
2009	Y	Y	Y	Y	Y	Y	Y	Y	Y	Y	Y	Y	Y	Y	Y	Y	Y	Y	Y	Y	Y
2010	Y	Y	Y	Y	Y	Y	Y	Y	Y	Y	Y	Y	Y	Y	Y	Y	Y	Y	Y	Y	Y
2011	Y	Y	Y	Y	Y	Y	Y	Y	Y	Y	Y	Y	Y	Y	Y	Y	Y	Y	Y	Y	Y
2012	Y	Y	Y	Y	Y	Y	Y	Y	Y	Y	Y	Y	Y	Y	Y	Y	Y	Y	Y	Y	Y
2013	Y	Y	Y	Y	Y	Y	Y	Y	Y	Y	Y	Y	Y	Y	Y	Y	Y	Y	Y	Y	Y
2014	N	Y	Y	N	Y	Y	N	Y	Y	N	Y	Y	N	Y	Y	N	Y	Y	N	Y	Y
2015	Y	Y	Y	Y	Y	Y	Y	Y	Y	Y	Y	Y	Y	Y	Y	Y	Y	Y	Y	Y	Y
2016	Y	Y	Y	Y	Y	Y	Y	Y	Y	Y	Y	Y	Y	Y	Y	Y	Y	Y	Y	Y	Y
2017	Y	Y	Y	Y	Y	Y	Y	Y	Y	Y	Y	Y	Y	Y	Y	Y	Y	Y	Y	Y	Y

	W8			W9			W10			W11			W12			W13			W14		
Years	**Sp**	**Su**	**Fa**	**Sp**	**Su**	**Fa**	**Sp**	**Su**	**Fa**	**Sp**	**Su**	**Fa**	**Sp**	**Su**	**Fa**	**Sp**	**Su**	**Fa**	**Sp**	**Su**	**Fa**

1999	N	N	N	N	N	N	N	N	N	N	N	N	N	N	N	N	N	N	N	N	N
2000	N	Y	Y	Y	Y	Y	N	Y	Y	N	Y	Y	Y	Y	Y	N	N	N	N	N	N
2001	Y	N	Y	Y	Y	N	N	Y	N	N	Y	Y	N	N	N	N	N	N	N	N	N
2002	N	Y	N	Y	Y	N	Y	Y	Y	N	N	N	N	N	N	N	N	Y	N	N	N
2003	Y	Y	Y	Y	Y	Y	N	Y	Y	Y	Y	N	N	Y	N	N	N	N	N	N	N
2004	N	Y	N	Y	N	Y	Y	N	Y	N	Y	N	N	N	Y	N	N	N	N	N	N
2005	Y	Y	Y	N	Y	Y	N	Y	Y	Y	N	N	N	N	Y	N	N	N	N	N	N
2006	Y	Y	Y	Y	Y	Y	Y	Y	Y	Y	Y	Y	Y	Y	Y	Y	Y	N	Y	Y	N
2007	Y	Y	N	Y	Y	Y	Y	Y	Y	Y	Y	N	Y	Y	Y	Y	Y	Y	Y	Y	Y
2008	Y	Y	Y	Y	Y	Y	Y	Y	Y	Y	Y	Y	Y	Y	Y	Y	Y	Y	Y	Y	Y
2009	Y	Y	Y	Y	Y	Y	Y	N	Y	Y	Y	Y	Y	Y	Y	Y	Y	Y	Y	Y	Y
2010	Y	Y	Y	Y	Y	Y	Y	Y	Y	Y	Y	Y	Y	Y	Y	Y	Y	Y	Y	Y	Y
2011	Y	Y	Y	Y	Y	Y	Y	Y	Y	Y	Y	Y	Y	Y	Y	Y	Y	Y	Y	Y	Y
2012	Y	Y	Y	Y	Y	Y	Y	Y	Y	Y	Y	Y	Y	Y	Y	Y	Y	Y	Y	Y	Y
2013	Y	Y	Y	Y	Y	Y	Y	Y	Y	Y	Y	Y	Y	Y	Y	Y	Y	Y	Y	Y	Y
2014	Y	Y	Y	Y	Y	Y	Y	Y	Y	Y	Y	Y	Y	Y	Y	Y	Y	Y	N	Y	Y
2015	Y	Y	Y	Y	Y	Y	Y	Y	Y	Y	Y	Y	Y	Y	Y	Y	Y	Y	Y	Y	Y
2016	Y	Y	Y	Y	Y	Y	Y	Y	Y	Y	Y	Y	Y	Y	Y	Y	Y	Y	Y	Y	Y
2017	Y	Y	Y	Y	Y	Y	Y	Y	Y	Y	Y	Y	Y	Y	Y	Y	Y	Y	Y	Y	Y

Appendix 4. Table of the chemical, nutrient, metal and biological parameters taken at each station on Lake Winnipeg from April 2001 to March 2009. Cantest Laboratories (formerly Maxxam Analytics, now Bureau Veritas) analyzed any chemical, nutrient and metal parameters and ALS analyzed any biological parameters.

Lab Analysis	**W Stations**	**Auxiliary Stations**
Chemical, Nutrient, Metal and Biological Parameters		
Alkalinity - CO_3	x	
Alkalinity - HCO_3	x	
Alkalinity - OH	x	
Biochemical Oxygen Demand	x	x
Chlorophyll *a*	x	x
Conductivity	x	x
Dissolved Aluminum	x	
Dissolved Chloride	x	
Dissolved Oxygen	x	
Hardness - $CaCO_3$	x	
Nitrogen Dissolved NO_3 & NO_2	x	x
pH	x	x
Pheophytin *a*	x	x
Phytoplankton Biomass and Composition	x	
Reactive Silica	x	
Sulphate Dissolved	x	
Total Acid Hydrolyzable Phosphorus	x	x
Total Acid Reactive Phosphorus	x	x
Total Alkalinity - $CaCO_3$	x	
Total Aluminum	x	
Total Ammonia - NH_3	x	x
Total Antimony	x	
Total Arsenic	x	
Total Barium	x	
Total Beryllium	x	
Total Bismuth	x	
Total Boron	x	
Total Cadmium	x	

Total Calcium	x	
Total Carbon	x	x
Total Cesium	x	
Total Chromium	x	
Total Cobalt	x	
Total Copper	x	
Total Dissolved Phosphorus	x	x
Total Dissolved Solids	x	
Total Inorganic Carbon	x	x
Total Iron	x	
Total Kjeldahl Nitrogen	x	x
Total Lead	x	
Total Lithium	x	
Total Magnesium	x	
Total Manganese	x	
Total Microcystin	x	
Total Molybdenum	x	
Total Nickel	x	
Total Organic Carbon	x	x
Total Particulate Phosphorus	x	x
Total Phosphorus	x	x
Total Potassium	x	
Total Rubidium	x	
Total Selenium	x	
Total Silicon	x	
Total Silver	x	
Total Sodium	x	
Total Strontium	x	
Total Suspended Solids	x	x
Total Tellurium	x	
Total Thallium	x	
Total Thorium	x	
Total Tin	x	
Total Titanium	x	
Total Uranium	x	
Total Vanadium	x	
Total Zinc	x	
Total Zirconium	x	

True Colour	x	
Turbidity	x	
Field Measurements		
Air Temperature	x	x
Secchi Disk Depth	x	x
Water Depth	x	x
Water Temperature	x	x
Wind Direction	x	x
Wind Speed	x	x
Total Parameters	**71**	**22**

Appendix 5. Table of the chemical, nutrient, metal and biological parameters taken at each station on Lake Winnipeg from April 2009 to September 2017 and analyzed by ALS Laboratories (*Taken only if algal bloom was present).

Lab Analysis	W Stations	Auxiliary Stations	Nearshore Stations	CAMP Stations	Non-Routine Stations
Chemical, Nutrient, Metal and Biological Parameters					
Alkalinity - CO_3	x			x	
Alkalinity - HCO_3	x			x	
Alkalinity - OH	x			x	
Biochemical Oxygen Demand	x	x	x		x
Chloride	x			x	
Chlorophyll *a*	x	x	x		x
Conductivity	x	x	x	x	x
Dissolved Aluminum	x				
Dissolved Inorganic				x	
Dissolved Organic				x	
Dissolved Oxygen	x				
Fluoride				x	
Hardness - $CaCO_3$	x			x	
Nitrate - NO_3-N				x	
Nitrite - NO_2-N				x	
Nitrogen Dissolved NO_3 & NO_2	x	x	x	x	x
ODB/ODA (Chlorophyll *a* / Pheophytin *a* Ratio)	x	x	x		x
pH	x	x	x	x	x
Pheophytin *a*	x	x	x		x
Phytoplankton Biomass and Composition	x	x*	x*	x*	x*
Reactive Silica	x				
Sulphate	x			x	
Total Acid Hydrolyzable Phosphorus	x	x	x		x
Total Acid Reactive Phosphorus	x	x	x		x

Total Alkalinity - CaCO3	x			x	
Total Aluminum	x			x	
Total Ammonia - NH3	x	x	x	x	x
Total Antimony	x			x	
Total Arsenic	x			x	
Total Barium	x			x	
Total Beryllium	x			x	
Total Bismuth	x			x	
Total Boron	x			x	
Total Cadmium	x			x	
Total Calcium	x		x	x	
Total Carbon	x	x	x	x	x
Total Cesium	x			x	
Total Chromium	x			x	
Total Cobalt	x			x	
Total Copper	x			x	
Total Dissolved Carbon				x	
Total Dissolved	x	x	x	x	x
Total Dissolved Solids	x			x	
Total Hexavalent	x				
Total Inorganic Carbon	x	x	x	x	x
Total Inorganic	x	x	x		x
Total Iron	x			x	
Total Kjeldahl Nitrogen	x	x	x	x	x
Total Lead	x			x	
Total Lithium	x			x	
Total Magnesium	x			x	
Total Manganese	x			x	
Total Mercury				x	
Total Microcystin	x	x*	x*	x*	x*
Total Molybdenum	x			x	
Total Nickel	x			x	
Total Nitrogen	x	x	x		x
Total Organic Carbon				x	
Total Particulate	x			x	
Total Phosphorus	x	x	x	x	x
Total Potassium	x			x	
Total Rubidium	x			x	

Total Selenium	x			x	
Total Silicon	x			x	
Total Silver	x			x	
Total Sodium	x			x	
Total Strontium	x			x	
Total Suspended Solids	x	x	x	x	x
Total Tellurium	x			x	
Total Thallium	x			x	
Total Thorium	x			x	
Total Tin	x			x	
Total Titanium	x			x	
Total Tungsten	x			x	
Total Uranium	x			x	
Total Vanadium	x			x	
Total Zinc	x			x	
Total Zirconium	x			x	
True Colour	x			x	
Turbidity	x			x	x
Field Measurements					
Air Temperature	x	x	x	x	x
Secchi Disk Depth	x	x	x	x	
Water Depth	x	x	x	x	x
Water Temperature	x	x	x	x	x
Wind Direction	x	x	x	x	x
Wind Speed	x	x	x	x	x
Total Parameters	**78**	**20**	**21**	**66**	**20**

Appendix 6. List of ALS and Cantest parameter methods, date ranges, if parameter is still analyzed presently, units, detection limit (DL), method source/ description or comment.

VMV Code	Variable Code	Variable Name	Start Date (MDY)	End Date (MDY)	Units	Method DL	National Method Code	Method Source/Description or Comment
-	-	ALGAE-*ANABAENA* BIOMASS	1999-08-10	2017-10-05	mg/m^3	1	-	APHA 10200 C & F
-	-	ALGAE-*APHANIZOMENON* BIOMASS	1999-08-10	2017-10-05	mg/m^3	1	-	APHA 10200 C & F
-	-	ALGAE-*APHANOCAPSA* BIOMASS	1999-08-18	2017-09-27	mg/m^3	1	-	APHA 10200 C & F
-	-	ALGAE-*APHANOTHECE* BIOMASS	2003-09-23	2017-10-03	mg/m^3	1	-	APHA 10200 C & F
-	-	ALGAE-BACILLARIOPHYCEAE BIOMASS	1999-08-10	2017-10-05	mg/m^3	1	-	APHA 10200 C & F
-	-	ALGAE-CHLOROPHYCEAE BIOMASS	1999-08-10	2017-10-04	mg/m^3	1	-	APHA 10200 C & F
-	-	ALGAE-*CHROOCOCCUS* BIOMASS	1999-10-18	2016-09-18	mg/m^3	1	-	APHA 10200 C & F
-	-	ALGAE-CHRYSOPHYCEAE BIOMASS	1999-08-10	2017-10-05	mg/m^3	1	-	APHA 10200 C & F
-	-	ALGAE-*COELOSPHARIUM* BIOMASS	2005-10-18	2008-09-27	mg/m^3	1	-	APHA 10200 C & F

-	-	ALGAE-CRYPTOPHYCEAE BIOMASS	1999-08-10	2017-10-05	mg/m^3	1	-	APHA 10200 C & F
-	-	ALGAE-CYANOBACTERIA SPECIES RICHNESS	1999-08-10	2017-10-05	SUM	-	-	Sum; Total number of species from Cyanophyceae
-	-	ALGAE-CYANOPHYCEAE BIOMASS	1999-08-10	2017-10-05	mg/m^3	1	-	APHA 10200 C & F
-	-	ALGAE-DINOPHYCEAE BIOMASS	1999-08-13	2017-09-27	mg/m^3	1	-	APHA 10200 C & F
-	-	ALGAE-EUGLENOPHYCEAE BIOMASS	1999-08-18	2017-09-25	mg/m^3	1	-	APHA 10200 C & F
-	-	ALGAE-*GOMPHOSPHAERIA* BIOMASS	1999-08-10	2017-09-22	mg/m^3	1	-	APHA 10200 C & F
-	-	ALGAE-*LIMNOTHRIX* BIOMASS	2008-07-28	2017-07-30	mg/m^3	1	-	APHA 10200 C & F
-	-	ALGAE-*LYNGBYA* BIOMASS	1999-08-10	2013-09-25	mg/m^3	1	-	APHA 10200 C & F
-	-	ALGAE-*MERISMOPEDIA* BIOMASS	2001-07-10	2017-10-03	mg/m^3	1	-	APHA 10200 C & F
-	-	ALGAE-*MICROCYSTIS* BIOMASS	1999-08-23	2017-10-05	mg/m^3	1	-	APHA 10200 C & F
-	-	ALGAE-*OSCILLATORIA* BIOMASS	2004-09-15	2017-09-23	mg/m^3	1	-	APHA 10200 C & F
-	-	ALGAE-PHYTOPLANKTON BIOMASS	1999-08-10	2017-10-05	mg/m^3	1	-	APHA 10200 C & F

-	-	ALGAE-PHYTOPLANKTON SPECIES RICHNESS	1999-08-10	2017-10-05	SUM	-	-	Sum; Total number of species from Bacillariophyceae, Chlorophyceae, Chrysophyceae, Cryptophyceae, Cyanophyceae, Dinophyceae, Euglenophyceae
-	-	ALGAE-*PLANKTOLYNGBYA* BIOMASS	2008-06-04	2017-10-05	mg/m^3	1	-	APHA 10200 C & F
-	-	ALGAE-*PLANKTOTHRIX* BIOMASS	2009-09-26	2011-06-17	mg/m^3	1	-	APHA 10200 C & F
-	-	ALGAE-*PSEUDOANABAENA* BIOMASS	1999-08-13	2017-10-04	mg/m^3	1	-	APHA 10200 C & F
-	-	ALGAE-*SNOWELLA* BIOMASS	1999-08-10	1999-08-20	mg/m^3	1	-	APHA 10200 C & F
-	-	ALGAE-UNIDENTIFIED FILAMENTOUS BIOMASS	2006-09-19	2017-07-24	mg/m^3	1	-	APHA 10200 C & F
99957	364	ALKALINITY, TOTAL - $CACO_3$	2001-04-17	2005-06-27	mg/L	0.5	2122	Potentiometric titration with sulfuric acid standardized using sodium carbonate
99965	364	ALKALINITY, TOTAL - $CACO_3$	2002-05-16	2009-06-11	mg/L	1	2119	BCELM and SMEWW
104218	364	ALKALINITY, TOTAL - $CACO_3$	1999-08-10	2001-03-06	mg/L	30	3128	APHA 2320B

104222	364	ALKALINITY, TOTAL - $CACO_3$	2009-05-29	2017-10-04	mg/L	1	3128	APHA 2320B
99958	3534	ALKALINITY, TOTAL - CO_3	2001-04-17	2005-06-27	mg/L	0.5	2122	Potentiometric titration with sulfuric acid standardized using sodium carbonate
99966	3534	ALKALINITY, TOTAL - CO_3	2002-05-16	2009-06-11	mg/L	0.5	2119	BCELM and SMEWW
104224	3534	ALKALINITY, TOTAL - CO_3	2009-05-29	2017-10-04	mg/L	0.6	3128	APHA 2320B
104230	3534	ALKALINITY, TOTAL - CO_3	1999-08-10	2001-03-06	mg/L	20	3128	Calculated from APHA 2320B
99960	3533	ALKALINITY, TOTAL - HCO_3	2001-04-17	2005-06-27	mg/L	0.5	2122	Potentiometric titration with sulfuric acid standardized using sodium carbonate
99968	3533	ALKALINITY, TOTAL - HCO_3	2002-05-16	2009-06-11	mg/L	0.5	2119	BCELM and SMEWW
104229	3533	ALKALINITY, TOTAL - HCO_3	1999-08-10	2001-03-06	mg/L	40	3128	APHA 2320B
104232	3533	ALKALINITY, TOTAL - HCO_3	2009-05-29	2017-10-04	mg/L	2	3128	Calculated from APHA 2320B
99959	3535	ALKALINITY, TOTAL - OH	2001-04-17	2005-06-27	mg/L	0.5	2122	Potentiometric titration with sulfuric acid standardized using sodium carbonate
99967	3535	ALKALINITY, TOTAL - OH	2002-05-16	2009-06-11	mg/L	0.5	2119	BCELM and SMEWW
104231	3535	ALKALINITY, TOTAL - OH	1999-08-10	2001-03-06	mg/L	10	3128	APHA 2320B

104233	3535	ALKALINITY, TOTAL - OH	2009-05-29	2017-10-04	mg/L	0.4	3128	Calculated from APHA 2320B
99591	370	ALUMINUM, DISSOLVED	2001-04-17	2009-06-11	mg/L	0.001	2123	Mass spectrometer
104552	370	ALUMINUM, DISSOLVED	1999-08-10	2001-03-06	mg/L	0.01	3158	EPA 200.8 REV 5.4 MAY 1994-DU
107244	370	ALUMINUM, DISSOLVED	2009-05-29	2017-10-04	mg/L	0.002	3158	EPA 200.8 REV 5.4 MAY 1994-DU
4761	373	ALUMINUM, TOTAL	2017-07-24	2017-10-04	mg/L	0.003	480	EPA 200.2/6020A (modified)
99623	373	ALUMINUM, TOTAL	2007-09-12	2007-09-12	mg/L	0.02	2126	ICPOES
99651	373	ALUMINUM, TOTAL	2001-04-17	2009-06-11	mg/L	0.001	2125	ICP/MS
104550	373	ALUMINUM, TOTAL	1999-08-10	2001-03-06	mg/L	0.02	3158	EPA 200.8 REV 5.4 MAY 1994-TU
106560	373	ALUMINUM, TOTAL	2009-05-29	2017-06-15	mg/L	0.005	3158	APHA 3030E/EPA 6020 A-TL
4762	766	ANTIMONY, TOTAL	2017-07-24	2017-10-04	mg/L	0.0001	480	EPA 200.2/6020A (modified)
99652	766	ANTIMONY, TOTAL	2001-04-17	2009-06-11	mg/L	0.0002	2125	ICP/MS
104555	766	ANTIMONY, TOTAL	1999-08-10	2017-06-15	mg/L	0.001	3158	APHA 3030E/EPA 6020A-TL
4763	379	ARSENIC, TOTAL	2017-07-24	2017-10-04	mg/L	0.0001	480	EPA 200.2/6020A (modified)
99653	379	ARSENIC, TOTAL	2001-04-17	2009-06-11	mg/L	0.0002	2125	ICP/MS
104554	379	ARSENIC, TOTAL	1999-08-10	2017-06-15	mg/L	0.0005	3158	APHA 3030E/EPA 6020A-TL
80060	2710	BACTERIA, *ESCHERICHIA COLI*	2015-02-25	2017-10-04	MPN/ 100 mL	1	1842	APHA 9223B QT97

104002	2710	BACTERIA, *ESCHERICHIA COLI*	1999-08-10	2014-09-28	CFU/ 100 mL	1	3100	APHA 9222B and HACH 10029; Mcoli Blue
104008	2710	BACTERIA, *ESCHERICHIA COLI*	2014-06-17	2017-09-23	MPN/ 100 mL	3	3104	APHA 9223B QT51
104779	2710	BACTERIA, *ESCHERICHIA COLI*	1999-08-10	1999-08-25	MPN/G	3	3101	Multiple tube procedure-Most probable number
104780	2710	BACTERIA, *ESCHERICHIA COLI*	2000-08-18	2003-09-23	MPN/G	3	3101	Multiple tube procedure-Most probable number
106176	2710	BACTERIA, *ESCHERICHIA COLI*	2004-09-15	2013-10-03	CFU/ 100 mL	10	3100	APHA 9222B and HACH 10029; Mcoli Blue
107983	3059	BACTERIA, *ESCHERICHIA COLI*	2010-06-04	2011-10-03	CFU/ 100 mL	10	3009	Hach 10029/SM-9222B; Mcoli Blue
104000	433	BACTERIA, TOTAL COLIFORMS	1999-08-10	2003-02-05	CFU/ 100 mL	1	3100	APHA 9222B and HACH 10029
104003	433	BACTERIA, TOTAL COLIFORMS	1999-08-10	1999-08-25	MPN/ 100 mL	3	3101	Multiple tube procedure-Most probable number
104007	434	BACTERIA, TOTAL COLIFORMS	2014-06-17	2017-09-23	MPN/ 100 mL	3	3104	APHA 9223B QT51
104777	433	BACTERIA, TOTAL COLIFORMS	2000-08-18	2000-08-22	MPN/G	3	3101	Multiple tube procedure-Most probable number
4764	388	BARIUM, TOTAL	2017-07-24	2017-10-04	mg/L	0.00005	480	EPA 200.2/6020A (modified)
99654	388	BARIUM, TOTAL	2001-04-17	2009-06-11	mg/L	0.0002	2125	ICP/MS
104558	388	BARIUM, TOTAL	1999-08-10	2017-06-15	mg/L	0.0003	3158	APHA 3030E/EPA 6020A-TL

4765	393	BERYLLIUM, TOTAL	2017-07-24	2017-10-04	mg/L	0.0001	480	EPA 200.2/6020A (modified)
99655	393	BERYLLIUM, TOTAL	2001-04-17	2009-06-11	mg/L	0.0002	2125	ICP/MS
104559	393	BERYLLIUM, TOTAL	1999-08-10	2017-06-15	mg/L	0.001	3158	APHA 3030E/EPA 6020A-TL
4766	1049	BISMUTH, TOTAL	2017-07-24	2017-10-04	mg/L	0.00005	480	EPA 200.2/6020A (modified)
99656	1049	BISMUTH, TOTAL	2001-04-17	2009-06-11	mg/L	0.0002	2125	ICP/MS
104564	1049	BISMUTH, TOTAL	1999-08-10	2017-06-15	mg/L	0.0001	3158	APHA 3030E/EPA 6020A-TL
4767	401	BORON, TOTAL	2017-07-24	2017-10-04	mg/L	0.01	480	EPA 200.2/6020A (modified)
99629	401	BORON, TOTAL	2002-05-16	2009-06-11	mg/L	0.01	2126	ICPOES
99657	401	BORON, TOTAL	2001-04-17	2003-07-02	mg/L	0.01	2125	ICP/MS
104562	401	BORON, TOTAL	1999-08-10	2017-06-15	mg/L	0.01	3158	APHA 3030E/EPA 6020A-TL
4768	412	CADMIUM, TOTAL	2017-07-24	2017-10-04	mg/L	0.000005	480	EPA 200.2/6020A (modified)
99658	412	CADMIUM, TOTAL	2001-04-17	2009-06-11	mg/L	0.00004	2125	ICP/MS
104566	412	CADMIUM, TOTAL	1999-08-10	2017-06-15	mg/L	0.0002	3158	APHA 3030E/EPA 6020A-TL
107245	412	CADMIUM, TOTAL	2009-05-29	2011-08-09	mg/L	0.00001	3158	US EPA 200.8-TL
4769	408	CALCIUM, TOTAL	2017-07-24	2017-10-04	mg/L	0.05	480	EPA 200.2/6020A (modified)
99631	408	CALCIUM, TOTAL	2002-05-16	2009-06-11	mg/L	0.01	2126	ICPOES

99659	408	CALCIUM, TOTAL	2001-04-17	2003-07-02	mg/L	0.01	2125	ICP/MS
104569	408	CALCIUM, TOTAL	1999-08-10	2017-06-15	mg/L	0.1	3158	APHA 3030E/EPA 6020A-TL
104304	475	CARBON, DISSOLVED INORGANIC	2016-09-21	2017-07-29	mg/L	1	3142	APHA 5310 B-WP
104313	479	CARBON, DISSOLVED ORGANIC	2013-09-28	2014-09-24	mg/L	1	3142	APHA 5310 B-WP
1616	492	CARBON, TOTAL	2015-07-20	2015-08-06	mg/L	1	602	Calculated; Sum of total organic and total inorganic carbon (TC=TIC+TOC)
99753	492	CARBON, TOTAL	2001-04-17	2009-06-11	mg/L	1	2106	BCELM and SMEWW
104306	492	CARBON, TOTAL	1999-08-18	2017-10-05	mg/L	1	3142	APHA 5210B
104303	481	CARBON, TOTAL DISSOLVED	2016-09-21	2017-09-23	mg/L	1	481	APHA 5310 B-WP
99754	485	CARBON, TOTAL INORGANIC	2001-04-17	2009-06-11	mg/L	1	2106	BCELM and SMEWW
104307	485	CARBON, TOTAL INORGANIC	1999-08-18	2017-10-05	mg/L	1	3142	APHA 5210B
1615	487	CARBON, TOTAL ORGANIC	2015-07-20	2015-09-30	mg/L	0.5	3301	APHA 5210B
6001	487	CARBON, TOTAL ORGANIC	2011-07-14	2014-08-03	mg/L	0.5	95	APHA 5210B
99755	487	CARBON, TOTAL ORGANIC	2001-04-17	2009-06-11	mg/L	1	2106	5310A,B Standard Methods (21 edition); Method X314 in BC Laboratory Manual (2005)

104308	488	CARBON, TOTAL ORGANIC	1999-08-18	2015-07-16	mg/L	1	3142	APHA 5210B
4770	1003	CESIUM, TOTAL	2017-07-24	2017-10-04	mg/L	0.00001	480	EPA 200.2/6020A (modified)
99670	1003	CESIUM, TOTAL	2001-04-17	2009-06-11	mg/L	0.0001	2125	ICP/MS
104577	1003	CESIUM, TOTAL	1999-08-10	2017-06-15	mg/L	0.0001	3158	APHA 3030E/EPA 6020A-TL
99494	426	CHLORIDE, DISSOLVED	2006-08-02	2006-08-02	mg/L	0.1	2027	ICP/MS
5666	422	CHLORIDE, TOTAL	2010-10-08	2017-10-05	mg/L	0.1	663	EPA 300.1 IC (modified)
97700	414	CHLOROPHYLL *A*	2003-06-02	2009-06-11	µg/L	0.5	1906	SMEWW
99288	414	CHLOROPHYLL *A*	2001-04-17	2003-03-13	µg/L	0.1	1999	Flourometer
104273	418	CHLOROPHYLL *A*	1999-08-10	2001-03-06	µg/L	1	3138	Spectrophotometric
107230	414	CHLOROPHYLL *A*	2009-05-29	2017-10-05	µg/L	0.6	3455	APHA 10200H
107272	4199	CHLOROPHYLL, ODB/ODA (CHLOROPHYLL-*A* / PHEOPHYTIN-*A* RATIO)	2009-05-29	2017-10-05	NO UNITS	-	3455	APHA 10200H
97701	1109	CHLOROPHYLL, PHEOPHYTIN *A*	2003-06-02	2009-06-11	µg/L	0.5	1906	SMEWW
107231	1109	CHLOROPHYLL, PHEOPHYTIN *A*	2009-05-29	2017-10-05	µg/L	1	3455	APHA 10200H
99422	459	CHROMIUM, DISSOLVED HEXAVALENT	2001-04-17	2009-03-28	mg/L	0.02	2016	EPA 7196A

104328	459	CHROMIUM, DISSOLVED HEXAVALENT	2000-03-13	2010-09-14	mg/L	0.01	1127	EPA 7199
104329	459	CHROMIUM, DISSOLVED HEXAVALENT	1999-08-10	1999-08-25	mg/L	0.02	1127	EPA 7199
4771	463	CHROMIUM, TOTAL	2017-07-24	2017-10-04	mg/L	0.0001	480	EPA 200.2/6020A (modified)
99671	463	CHROMIUM, TOTAL	2001-04-17	2009-06-11	mg/L	0.0002	2125	ICP/MS
104571	463	CHROMIUM, TOTAL	1999-08-10	2017-06-15	mg/L	0.002	3158	APHA 3030E/EPA 6020A-TL
5703	458	CHROMIUM, TOTAL HEXAVALENT	2010-09-15	2015-03-30	mg/L	0.01	667	EPA 7199
5704	458	CHROMIUM, TOTAL HEXAVALENT	2015-03-31	2017-10-05	mg/L	0.001	667	EPA 7199
4772	456	COBALT, TOTAL	2017-07-24	2017-10-04	mg/L	0.0001	480	EPA 200.2/6020A (modified)
99672	456	COBALT, TOTAL	2001-04-17	2009-06-11	mg/L	0.0002	2125	ICP/MS
104573	456	COBALT, TOTAL	1999-08-10	2017-06-15	mg/L	0.0002	3158	APHA 3030E/EPA 6020A-TL
2021	443	COLOUR, TRUE	2009-05-29	2010-10-02	rel units	-	24	Visual comparison between aliquot and standard colour solutions
99436	443	COLOUR, TRUE	1999-08-10	2009-06-11	CU	5	2023	BCELM and SMEWW
107999	443	COLOUR, TRUE	2010-10-08	2017-10-04	CU	5	3535	APHA 2120C
99961	1038	CONDUCTIVITY	2001-04-17	2002-03-05	µS/cm	1	2122	Potentiometric titration with sulfuric acid standardized

								using sodium carbonate
99964	1038	CONDUCTIVITY	2002-05-16	2009-06-11	µS/cm	1	2120	BCELM and SMEWW
104228	1038	CONDUCTIVITY	2009-05-29	2017-10-05	µS/cm	0.4	3128	APHA 2510B
104234	1038	CONDUCTIVITY	1999-08-10	2001-03-06	µS/cm	100	3128	APHA 2320B
4773	470	COPPER, TOTAL	2017-07-24	2017-10-04	mg/L	0.0005	480	EPA 200.2/6020A (modified)
99673	470	COPPER, TOTAL	2001-04-17	2009-06-11	mg/L	0.0002	2125	ICP/MS
104575	470	COPPER, TOTAL	1999-08-10	2017-06-15	mg/L	0.001	3158	APHA 3030E/EPA 6020A-TL
104755	3551	DEPTH, SECCHI DISC	1999-08-24	2017-10-05	m	0.01	3192	Secchi disc
104748	497	DEPTH, SURFACE SAMPLE	1999-08-10	2017-10-05	m	0.01	3185	Standard Namao Protocol-See Methods section
2	-	DEPTH, TOTAL STATION	2005-08-05	2017-10-05	m	-	-	Standard Namao Protocol-Taken from MV *Namao* depth sensor
99297	542	HARDNESS, TOTAL - $CACO_3$	2001-04-17	2003-07-02	mg/L	1	2125	ICP/MS
99298	542	HARDNESS, TOTAL - $CACO_3$	2002-05-16	2009-06-11	mg/L	1	2126	ICPOES
104316	542	HARDNESS, TOTAL - $CACO_3$	1999-08-10	2001-03-06	mg/L	0.07	3143	Calculated; Hardness=Ca*2.497 + Mg*4.117
107249	542	HARDNESS, TOTAL - $CACO_3$	2009-05-29	2017-10-04	mg/L	0.3	3143	APHA 2340B

4774	519	IRON, TOTAL	2017-07-24	2017-10-04	mg/L	0.01	480	EPA 200.2/6020A (modified)
99674	519	IRON, TOTAL	2001-04-17	2009-06-11	mg/L	0.01	2125	ICP/MS
104580	519	IRON, TOTAL	1999-08-10	2017-06-15	mg/L	0.01	3158	APHA 3030E/EPA 6020A-TL
107246	519	IRON, TOTAL	2009-05-29	2011-08-09	mg/L	0.02	3158	EPA 200.8 REV 5.4 MAY 1994-TU
4775	683	LEAD, TOTAL	2017-07-24	2017-10-04	mg/L	0.00005	480	EPA 200.2/6020A (modified)
99675	683	LEAD, TOTAL	2001-04-17	2009-06-11	mg/L	0.0002	2125	ICP/MS
104582	683	LEAD, TOTAL	1999-08-10	2017-06-15	mg/L	0.0005	3158	APHA 3030E/EPA 6020A-TL
4776	576	LITHIUM, TOTAL	2017-07-24	2017-10-04	mg/L	0.001	480	EPA 200.2/6020A (modified)
99676	576	LITHIUM, TOTAL	2001-04-17	2009-06-11	mg/L	0.0002	2125	ICP/MS
104585	576	LITHIUM, TOTAL	1999-08-10	2017-06-15	mg/L	0.001	3158	APHA 3030E/EPA 6020A-TL
107810	576	LITHIUM, TOTAL	2009-06-03	2015-02-26	mg/L	0.0002	3158	APHA 3030E/EPA 6020 A-TL
107812	576	LITHIUM, TOTAL	2009-05-29	2011-08-09	mg/L	0.002	3158	US EPA 200.8-TL
4777	585	MAGNESIUM, TOTAL	2017-07-24	2017-10-04	mg/L	0.005	480	EPA 200.2/6020A (modified)
99637	2690	MAGNESIUM, TOTAL	2002-05-16	2009-06-11	mg/L	0.01	2126	ICPOES
99677	2690	MAGNESIUM, TOTAL	2001-04-17	2003-07-02	mg/L	0.01	2125	ICP/MS
104588	2690	MAGNESIUM, TOTAL	1999-08-10	2017-06-15	mg/L	0.01	3158	APHA 3030E/EPA 6020A-TL

4778	591	MANGANESE, TOTAL	2017-07-24	2017-10-04	mg/L	0.0001	480	EPA 200.2/6020A (modified)
99678	591	MANGANESE, TOTAL	2001-04-17	2009-06-11	mg/L	0.0002	2125	ICP/MS
104591	591	MANGANESE, TOTAL	1999-08-10	2017-06-15	mg/L	0.0002	3158	APHA 3030E/EPA 6020A-TL
5894	549	MERCURY, TOTAL	2016-10-14	2017-10-05	µg/L	0.005	549	EPA 245.7 V2.0 CVAF
5895	549	MERCURY, TOTAL	2012-04-25	2016-10-13	mg/L	0.00002	549	EPA 245.7 V2.0 CVAF
106167	1218	MICROCYSTIN, TOTAL	2004-06-06	2017-10-05	µg/L	0.2	3338	ENVIROLOGIX QUANTIPLATE KIT CAT. EP022 ; Extraction of microcystin-freeze thaw
5444	4023	MICROCYSTIN, TOTAL	2013-09-28	2017-09-23	µg/L	0.2	3035	ENVIROLOGIX QUANTIPLATE KIT CAT. EP022 ; Extraction of microcystin-sonication
4779	595	MOLYBDENUM, TOTAL	2017-07-24	2017-10-04	mg/L	0.00005	480	EPA 200.2/6020A (modified)
99679	595	MOLYBDENUM, TOTAL	2001-04-17	2009-06-11	mg/L	0.0002	2125	ICP/MS
104594	595	MOLYBDENUM, TOTAL	1999-08-10	2017-06-15	mg/L	0.0001	3158	APHA 3030E/EPA 6020A-TL
4780	610	NICKEL, TOTAL	2017-07-24	2017-10-04	mg/L	0.0005	480	EPA 200.2/6020A (modified)
99680	610	NICKEL, TOTAL	2001-04-17	2009-06-11	mg/L	0.0002	2125	ICP/MS

104596	610	NICKEL, TOTAL	1999-08-10	2017-06-15	mg/L	0.002	3158	APHA 3030E/EPA 6020A-TL
7111	628	NITROGEN, DISSOLVED - NO_3 & NO_2	2010-02-22	2010-10-02	mg/L	0.002	245	APHA 4500 NO3E
99490	628	NITROGEN, DISSOLVED - NO_3 & NO_2	2001-04-17	2009-06-11	mg/L	0.01	2026	BCELM and SMEWW
103392	616	NITROGEN, DISSOLVED - NO_3 & NO_2	2010-08-07	2017-10-04	mg/L	0.005	2962	APHA 4500; 2005/Lachat; 1997, 1999; NO_2 and NO_3 by Ion Chromatography; (NO_3+NO_2-N)=(NO_3-N) + (NO_2-N)
104294	628	NITROGEN, DISSOLVED - NO_3 & NO_2	1999-08-10	2017-10-05	mg/L	0.01	3141	APHA 4500; 2005/Lachat; 1997, 1999; FIA or SFA
99426	604	NITROGEN, DISSOLVED AMMONIA	2004-08-13	2008-10-01	mg/L	0.01	2020	ICP/MS
107991	9138	NITROGEN, NITRATE - NO_3-N	2011-06-06	2011-07-05	mg/L	0.005	3390	EPA 300.1 (modified)
5663	9138	NITROGEN, NITRATE - NO_3-N	2011-07-06	2017-09-23	mg/L	0.005	661	EPA 300.1 (modified)
5669	9138	NITROGEN, NITRITE - NO_2-N	2011-07-06	2017-09-23	mg/L	0.001	665	EPA 300.1 (modified)
7602	636	NITROGEN, TOTAL	2014-09-26	2017-10-05	mg/L	0.2	301	Calculated; TKN + Nitrate/Nitrite
102626	603	NITROGEN, TOTAL AMMONIA - NH_3	2010-02-22	2017-10-05	mg/L	0.01	2894	APHA 4500 NH3F
107447	603	NITROGEN, TOTAL AMMONIA - NH_3	2010-05-27	2010-10-02	mg/L	0.005	2894	APHA 4500 NH3F

4106	626	NITROGEN, TOTAL KJELDAHL	2016-07-19	2017-10-05	mg/L	0.2	3213	APHA 4500 NorgD (modified)
7021	626	NITROGEN, TOTAL KJELDAHL	2015-09-23	2015-09-29	mg/L	0.05	235	APHA 4500-NORG (TKN)
99545	626	NITROGEN, TOTAL KJELDAHL	2001-04-17	2009-06-11	mg/L	0.2	2108	4500-N Standard Methods (21 edition); Method X325 in BC Laboratory Manual (2005)
104265	626	NITROGEN, TOTAL KJELDAHL	1999-08-10	2016-06-16	mg/L	0.2	3136	Quickchem method 10-107-06-02-E Lachat; FIA
8202	647	OXYGEN, BIOLOGICAL DEMAND	2001-01-30	2017-10-05	mg/L	1	325	APHA 5210B
99758	647	OXYGEN, BIOLOGICAL DEMAND	2001-04-17	2009-06-11	mg/L	1	2107	BCELM and SMEWW
8101	659	OXYGEN, DISSOLVED	2009-05-29	2017-10-04	mg/L	0.1	324	APHA 4500-O-C
99439	659	OXYGEN, DISSOLVED	1999-08-10	2009-06-11	mg/L	0.1	2025	BCELM and SMEWW
99962	687	PH	2001-04-17	2002-03-06	pH units	0.01	2122	Potentiometric titration with sulfuric acid standardized using sodium carbonate
99963	687	PH	2001-07-10	2009-06-11	pH units	0.01	2121	BCELM and SMEWW
104226	687	PH	1999-08-10	2017-10-05	pH units	0.01	3128	APHA 4500H
99556	2568	PHOSPHORUS, ACID HYDROLYZABLE	2001-04-17	2009-06-11	mg/L	0.001	2171	BCELM and SMEWW

104775	3561	PHOSPHORUS, ACID HYDROLYZABLE	2001-01-30	2001-03-06	mg/L	0.001	3200	APHA 4500-P CALC-AHP; Combined SFA and FIA
104783	2568	PHOSPHORUS, ACID HYDROLYZABLE	2001-02-08	2014-04-08	mg/L	0.001	3200	APHA 4500-P CALC-AHP; Combined SFA and FIA; Low Range
108471	3565	PHOSPHORUS, ACID HYDROLYZABLE	2011-03-14	2014-04-08	mg/L	0.01	3133	APHA 4500-P CALC-AHP; Combined SFA and FIA; High Range
50458	2568	PHOSPHORUS, ACID HYDROLYZABLE	2014-04-09	2017-10-05	mg/L	0.014	788	APHA 4500-P CALC-AHP; Calculated-Difference between TIP and TRP; High Range
50452	2568	PHOSPHORUS, ACID HYDROLYZABLE	2014-04-09	2017-10-05	mg/L	0.0042	781	APHA 4500-P CALC-AHPL; Calculated-Difference between TIP and TRP; Low Range
99551	716	PHOSPHORUS, DISSOLVED ORTHO	2001-08-23	2001-11-05	mg/L	0.001	2171	BCELM and SMEWW
99552	725	PHOSPHORUS, PARTICULATE	2001-04-17	2009-06-11	mg/L	0.001	2171	BCELM and SMEWW
104246	725	PHOSPHORUS, PARTICULATE	2011-03-14	2014-04-08	mg/L	0.01	3133	APHA 4500 P Calc Part; Calculated-Difference between TP and TDP; High Range

104253	725	PHOSPHORUS, PARTICULATE	1999-08-10	2014-04-08	mg/L	0.001	3133	APHA 4500 P Calc Part; Calculated-Difference between TP and TDP; Low Range
50460	4539	PHOSPHORUS, PARTICULATE	2014-04-09	2017-10-05	mg/L	0.014	790	APHA 4500 P Calc Part; Calculated-Difference between TP and TDP; High Range
50454	4539	PHOSPHORUS, PARTICULATE	2014-04-09	2017-10-05	mg/L	0.0028	783	APHA 4500 P Calc Part; Calculated-Difference between TP and TDP; Low Range
4781	730	PHOSPHORUS, TOTAL	2017-07-29	2017-09-23	mg/L	0.05	480	EPA 200.2/6020A (modified)
99548	730	PHOSPHORUS, TOTAL	2001-04-17	2009-06-11	mg/L	0.001	2171	BCELM and SMEWW
104248	730	PHOSPHORUS, TOTAL	2011-03-14	2014-04-08	mg/L	0.01	3133	APHA 4500 P PHOSPHORUS; Combined SFA and FIA; High Range
104252	730	PHOSPHORUS, TOTAL	1999-08-10	2014-04-08	mg/L	0.001	3133	APHA 4500 P PHOSPHORUS-L; Combined SFA and FIA; Low Range
50459	730	PHOSPHORUS, TOTAL	2014-04-09	2017-10-05	mg/L	0.01	789	APHA 4500 P PHOSPHORUS, B.5, H; FIA; High Range
50455	730	PHOSPHORUS, TOTAL	2014-04-09	2017-10-05	mg/L	0.001	784	APHA 4500 P PHOSPHORUS-L,

								B.5, E; Discrete Analyer; Low Range
99549	731	PHOSPHORUS, TOTAL DISSOLVED	2001-04-17	2009-06-11	mg/L	0.001	2171	BCELM and SMEWW
104245	731	PHOSPHORUS, TOTAL DISSOLVED	2011-03-14	2014-04-08	mg/L	0.01	3133	APHA 4500 P PHOSPHORUS; Combined SFA and FIA; High Range
104254	731	PHOSPHORUS, TOTAL DISSOLVED	1999-08-10	2014-04-08	mg/L	0.001	3133	APHA 4500 P PHOSPHORUS-L; Combined SFA and FIA; Low Range
50461	731	PHOSPHORUS, TOTAL DISSOLVED	2014-04-09	2017-10-05	mg/L	0.01	791	APHA 4500 P PHOSPHORUS, B.1, B.5, H; FIA; High Range
50453	731	PHOSPHORUS, TOTAL DISSOLVED	2014-04-09	2017-10-05	mg/L	0.001	782	APHA 4500 P PHOSPHORUS-L, B.1, B.5, E; Discrete Analyzer; Low Range
107808	719	PHOSPHORUS, TOTAL INORGANIC	2009-05-29	2014-04-08	mg/L	0.001	3133	APHA 4500 P PHOSPHORUS; Combined SFA and FIA; High Range
108469	719	PHOSPHORUS, TOTAL INORGANIC	2011-03-14	2014-04-08	mg/L	0.01	3133	APHA 4500 P PHOSPHORUS-L; Combined SFA and FIA; Low Range
50462	719	PHOSPHORUS, TOTAL INORGANIC	2014-04-09	2017-10-05	mg/L	0.01	792	APHA 4500 P PHOSPHORUS, B.2, H; FIA; High Range

50456	719	PHOSPHORUS, TOTAL INORGANIC	2014-04-09	2017-10-05	mg/L	0.001	785	APHA 4500 P PHOSPHORUS-L, B.2, E; Discrete Analyzer; Low Range
99554	723	PHOSPHORUS, TOTAL ORGANIC	2001-05-31	2001-05-31	mg/L	0.001	2171	BCELM and SMEWW
104776	723	PHOSPHORUS, TOTAL ORGANIC	2001-01-30	2001-03-06	mg/L	0.001	3200	APHA 4500-P CALC-AHP; Combined SFA and FIA
99550	2570	PHOSPHORUS, TOTAL REACTIVE	2001-04-17	2009-06-11	mg/L	0.001	2171	BCELM and SMEWW
104247	716	PHOSPHORUS, TOTAL REACTIVE	2009-05-29	2014-04-08	mg/L	0.001	3133	APHA 4500 P PHOSPHORUS; Combined SFA and FIA; High Range
108470	2569	PHOSPHORUS, TOTAL REACTIVE	2011-03-14	2014-04-08	mg/L	0.01	3133	APHA 4500 P PHOSPHORUS-L; Combined SFA and FIA; Low Range
50463	2569	PHOSPHORUS, TOTAL REACTIVE	2014-04-09	2017-10-05	mg/L	0.01	793	APHA 4500 P PHOSPHORUS, H; FIA; High Range
50457	2569	PHOSPHORUS, TOTAL REACTIVE	2014-04-09	2017-10-05	mg/L	0.001	787	APHA 4500 P PHOSPHORUS-L, E; Discrete Analyzer; Low Range
4782	567	POTASSIUM, TOTAL	2017-07-24	2017-10-04	mg/L	0.05	480	EPA 200.2/6020A (modified)
99682	567	POTASSIUM, TOTAL	2001-04-17	2009-06-11	mg/L	0.002	2125	ICP/MS

104601	567	POTASSIUM, TOTAL	1999-08-10	2017-06-15	mg/L	0.05	3158	APHA 3030E/EPA 6020A-TL
4783	1008	RUBIDIUM, TOTAL	2017-07-24	2017-10-04	mg/L	0.0002	480	EPA 200.2/6020A (modified)
99683	1008	RUBIDIUM, TOTAL	2001-04-17	2009-06-11	mg/L	0.0002	2125	ICP/MS
104603	1008	RUBIDIUM, TOTAL	1999-08-10	2017-06-15	mg/L	0.0002	3158	APHA 3030E/EPA 6020A-TL
104747	3453	SAMPLING SEQUENCE	2014-09-17	2017-08-30	NO UNITS	-	3197	Sequence in nearshore transect of 3 spots where sampled
4784	782	SELENIUM, TOTAL	2017-07-24	2017-10-04	mg/L	0.00005	480	EPA 200.2/6020A (modified)
99684	782	SELENIUM, TOTAL	2001-04-17	2009-06-11	mg/L	0.0004	2125	ICP/MS
104606	782	SELENIUM, TOTAL	1999-08-10	2017-06-15	mg/L	0.002	3158	APHA 3030E/EPA 6020A-TL
104260	3541	SILICA, DISSOLVED REACTIVE	1999-08-10	2010-08-13	mg/L	0.1	3134	Technicon 105-71W; APHA 450 E D
99216	2728	SILICON, TOTAL	2002-06-12	2009-06-11	mg/L	0.0001	2126	ICPOES
99229	2728	SILICON, TOTAL	2001-04-17	2009-06-11	mg/L	0.01	2125	ICP/MS
107814	2728	SILICON, TOTAL	2010-02-24	2017-06-15	mg/L	0.3	3158	APHA 3030E/EPA 6020 A-TL
4786	350	SILVER, TOTAL	2017-07-24	2017-10-04	mg/L	0.00001	480	EPA 200.2/6020A (modified)
99685	350	SILVER, TOTAL	2001-04-17	2009-06-11	mg/L	0.00002	2125	ICP/MS
104607	350	SILVER, TOTAL	1999-08-10	2017-06-15	mg/L	0.0004	3158	APHA 3030E/EPA 6020A-TL

107248	350	SILVER, TOTAL	2009-05-29	2011-08-09	mg/L	0.0001	3158	APHA 3030E/EPA 6020 A-TL
99643	2691	SODIUM, TOTAL	2002-05-16	2009-06-11	mg/L	0.00002	2126	ICPOES
99686	2691	SODIUM, TOTAL	2001-04-17	2003-07-02	mg/L	0.01	2125	ICP/MS
104611	2691	SODIUM, TOTAL	1999-08-10	2017-06-15	mg/L	0.02	3158	APHA 3030E/EPA 6020A-TL
99558	836	SOLIDS, TOTAL DISSOLVED	2001-04-17	2009-06-11	mg/L @180C	5	2139	Method 2540 C; SMEWW
104212	836	SOLIDS, TOTAL DISSOLVED	2001-06-01	2017-10-04	mg/L @180C	5	3126	APHA 2540 SOLIDS C,E
104213	836	SOLIDS, TOTAL DISSOLVED	1999-08-10	2001-03-06	mg/L @105C	5	3126	2540C Standard Methods (21 edition)
99435	1032	SOLIDS, TOTAL SUSPENDED	2001-04-17	2009-06-11	mg/L	1	2022	2540D Standard Methods (21 edition); Method X332 in BC Laboratory Manual (2005)
104214	1032	SOLIDS, TOTAL SUSPENDED	1999-08-10	2017-10-05	mg/L	5	3126	APHA 2540 D (modified)
4788	823	STRONTIUM, TOTAL	2017-07-24	2017-10-04	mg/L	0.0002	480	EPA 200.2/6020A (modified)
99644	823	STRONTIUM, TOTAL	2002-05-16	2009-06-11	mg/L	0.0001	2126	ICPOES
99687	823	STRONTIUM, TOTAL	2001-04-17	2003-07-02	mg/L	0.0002	2125	ICP/MS
104613	823	STRONTIUM, TOTAL	1999-08-10	2017-06-15	mg/L	0.0001	3158	APHA 3030E/EPA 6020A-TL
99492	814	SULPHATE, DISSOLVED	2006-08-02	2006-08-02	mg/L	0.5	2027	ICP/MS

5668	813	SULPHATE, TOTAL	2010-02-16	2017-10-05	mg/L	0.3	663	EPA 300.1 (modified)
4789	2737	TELLURIUM, TOTAL	2017-07-24	2017-10-04	mg/L	0.0002	480	EPA 200.2/6020A (modified)
99689	2737	TELLURIUM, TOTAL	2001-04-17	2009-06-11	mg/L	0.0002	2125	ICP/MS
104619	2737	TELLURIUM, TOTAL	1999-08-10	2017-06-15	mg/L	0.001	3158	APHA 3030E/EPA 6020A-TL
1	-	TEMPERATURE, AIR	2007-05-30	2017-10-05	Deg C	-	-	Standard Namao Protocol-Taken from MV *Namao* weather station
80209	3461	TEMPERATURE, WATER	2001-04-17	2017-10-05	Deg C	0.5	1828	Standard Namao Protocol-Taken from MV *Namao* or workboat depth sensor
4790	861	THALLIUM, TOTAL	2017-07-24	2017-10-04	mg/L	0.00001	480	EPA 200.2/6020A (modified)
99690	861	THALLIUM, TOTAL	2001-04-17	2009-06-11	mg/L	0.00002	2125	ICP/MS
104615	861	THALLIUM, TOTAL	1999-08-10	2017-06-15	mg/L	0.0001	3158	APHA 3030E/EPA 6020A-TL
4791	854	THORIUM, TOTAL	2017-07-24	2017-10-04	mg/L	0.0001	480	EPA 200.2/6020A (modified)
99228	854	THORIUM, TOTAL	2001-04-17	2009-06-11	mg/L	0.0001	2125	ICP/MS
107816	854	THORIUM, TOTAL	2009-05-29	2017-06-15	mg/L	0.001	3158	APHA 3030E/EPA 6020 A-TL
4792	812	TIN, TOTAL	2017-07-24	2017-10-04	mg/L	0.0001	480	EPA 200.2/6020A (modified)
99688	812	TIN, TOTAL	2001-04-17	2009-06-11	mg/L	0.0002	2125	ICP/MS

104616	812	TIN, TOTAL	1999-08-10	2017-06-15	mg/L	0.0005	3158	APHA 3030E/EPA 6020A-TL
4793	858	TITANIUM, TOTAL	2017-07-24	2017-10-04	mg/L	0.0003	480	EPA 200.2/6020A (modified)
99691	858	TITANIUM, TOTAL	2001-04-17	2009-06-11	mg/L	0.0002	2125	ICP/MS
104621	858	TITANIUM, TOTAL	1999-08-10	2017-06-15	mg/L	0.0005	3158	APHA 3030E/EPA 6020A-TL
4794	1013	TUNGSTEN, TOTAL	2017-07-24	2017-09-23	mg/L	0.0001	480	EPA 200.2/6020A (modified)
104627	1013	TUNGSTEN, TOTAL	1999-08-10	2016-09-21	mg/L	0.0002	3158	APHA 3030E/EPA 6020A-TL
99425	864	TURBIDITY	2001-04-17	2009-06-11	Ntu	0.1	2019	BCELM and SMEWW
101168	864	TURBIDITY	1999-08-10	2017-10-05	Ntu	0.01	2752	APHA 2130B (modified)
99692	2725	URANIUM, TOTAL	2001-04-17	2009-06-11	mg/L	1E-07	2125	ICP/MS
104623	2725	URANIUM, TOTAL	1999-08-10	2017-06-15	mg/L	0.0001	3158	APHA 3030E/EPA 6020A-TL
4796	878	VANADIUM, TOTAL	2017-07-24	2017-10-04	mg/L	0.0005	480	EPA 200.2/6020A (modified)
99693	878	VANADIUM, TOTAL	2001-04-17	2009-06-11	mg/L	0.0002	2125	ICP/MS
104624	878	VANADIUM, TOTAL	1999-08-10	2017-06-15	mg/L	0.001	3158	APHA 3030E/EPA 6020A-TL
3	-	WIND DIRECTION	2007-09-14	2017-10-04	Degree	-	-	Standard Namao Protocol-Taken from MV *Namao* weather station
4	-	WIND SPEED	2007-09-14	2017-10-04	Knots	-	-	Standard Namao Protocol-Taken from

								MV *Namao* weather station
4797	890	ZINC, TOTAL	2017-07-24	2017-10-04	mg/L	0.003	480	EPA 200.2/6020A (modified)
99694	890	ZINC, TOTAL	2001-04-17	2009-06-11	mg/L	0.001	2125	ICP/MS
104629	890	ZINC, TOTAL	1999-08-10	2017-06-15	mg/L	0.02	3158	APHA 3030E/EPA 6020A-TL
4798	1015	ZIRCONIUM, TOTAL	2017-07-24	2017-10-04	mg/L	0.00006	480	EPA 200.2/6020A (modified)
99695	1015	ZIRCONIUM, TOTAL	2001-04-17	2009-06-11	mg/L	0.002	2125	ICP/MS
104631	1015	ZIRCONIUM, TOTAL	1999-08-10	2017-06-15	mg/L	0.0002	3158	APHA 3030E/EPA 6020A-TL

Appendix 7. R code for data exploration.

Data exploration was done using raw and log transformed euphotic and surface datasets using the eight-step protocol written by (Zuur et al., 2010).

Appendix 8. Multi-panel Scatterplots of microcystin detected data.

```
#Euphotic dataset
setwd("D:/Desiree/USB - April 13 2020/Step 6 with only micro hits/Step 6")
Euphotic1 <- read.table("D:/Desiree/USB - April 13 2020/Step 6 with only micro
hits/Step 6/EUPH.csv", header=TRUE, sep=",", na.strings=c("", "NA"), dec=".",
strip.white=TRUE)

Euphotic1 <- read.table(file = "EUPH.csv", header = TRUE, sep=",", na.strings=c("",
"NA"), dec=".", strip.white=TRUE)
source(file = "HighstatLib.R")
MyNames <- c("TOTAL BORON", "PHEOPHYTIN A", "pH", "CRYPTOPHYCEAE
BIOMASS", "MICROCYSTIN")
pairs(Euphotic1[,c(29, 39, 67, 7, 56)], lower.panel = panel.cor, cex.labels=1.3,
labels=MyNames,
panel = function(x, y, ...) {
        tmp <- lm(y ~ x, na.action = na.omit)
          abline(tmp)
        points(x, y) })

Euphotic1 <- read.table(file = "EUPH.csv", header = TRUE, sep=",", na.strings=c("",
"NA"), dec=".", strip.white=TRUE)
source(file = "HighstatLib.R")
MyNames <- c("SURFACE SAMPLE DEPTH", "TOTAL SAMPLE DEPTH",
"HARDNESS", "TOTAL LITHIUM", "MICROCYSTIN")
pairs(Euphotic1[,c(48, 49, 50, 53, 56)], lower.panel = panel.cor, cex.labels=1.3,
labels=MyNames,
panel = function(x, y, ...) {
        tmp <- lm(y ~ x, na.action = na.omit)
          abline(tmp)
        points(x, y) })

Euphotic1 <- read.table(file = "EUPH.csv", header = TRUE, sep=",", na.strings=c("",
"NA"), dec=".", strip.white=TRUE)
source(file = "HighstatLib.R")
MyNames <- c("TOTAM MAGNESIUM", "N:P RATIO", "TOTAL DISSOLVED SOLIDS",
"AIR TEMPERATURE", "MICROCYSTIN")
pairs(Euphotic1[,c(54, 58, 81, 86, 56)], lower.panel = panel.cor, cex.labels=1.3,
labels=MyNames,
panel = function(x, y, ...) {
        tmp <- lm(y ~ x, na.action = na.omit)
          abline(tmp)
        points(x, y) })

Euphotic1 <- read.table(file = "EUPH.csv", header = TRUE, sep=",", na.strings=c("",
"NA"), dec=".", strip.white=TRUE)
source(file = "HighstatLib.R")
```

```
MyNames <- c("TOTAL THALLIUM", "TOTAL URANIUM", "DINOPHYCEAE
BIOMASS", "MICROCYSTIN")
pairs(Euphotic1[,c(88, 94, 10, 56)], lower.panel = panel.cor, cex.labels=1.3,
labels=MyNames,
panel = function(x, y, ...) {
        tmp <- lm(y ~ x, na.action = na.omit)
          abline(tmp)
        points(x, y) })

Euphotic1 <- read.table(file = "EUPH.csv", header = TRUE, sep=",", na.strings=c("
"NA"), dec=".", strip.white=TRUE)
source(file = "HighstatLib.R")
MyNames <- c("ALKALINITY CO3", "TOTAL CALCIUM", "CONDUCTIVITY",
"DISSOLVED OXYGEN", "MICROCYSTIN")
pairs(Euphotic1[,c(18, 31, 45, 66, 56)], lower.panel = panel.cor, cex.labels=1.3,
labels=MyNames,
panel = function(x, y, ...) {
        tmp <- lm(y ~ x, na.action = na.omit)
          abline(tmp)
        points(x, y) })

Euphotic1 <- read.table(file = "EUPH.csv", header = TRUE, sep=",", na.strings=c("
"NA"), dec=".", strip.white=TRUE)
source(file = "HighstatLib.R")
MyNames <- c("TOTAL POTASSIUM", "TOTAL SODIUM", "TOTAL SULPHATE",
"MICROCYSTIN")
pairs(Euphotic1[,c(74, 80, 84, 56)], lower.panel = panel.cor, cex.labels=1.3,
labels=MyNames ,
panel = function(x, y, ...) {
        tmp <- lm(y ~ x, na.action = na.omit)
          abline(tmp)
        points(x, y) })
Euphotic1 <- read.table(file = "EUPH.csv", header = TRUE, sep=",", na.strings=c("
"NA"), dec=".", strip.white=TRUE)
source(file = "HighstatLib.R")
MyNames <- c("TOTAL ANTIMONY", "TOTAL CADMIUM", "ACID-HYDROLYZABLE
PHOSPHORUS", "MICROCYSTIN")
pairs(Euphotic1[,c(23, 30, 68, 56)], lower.panel = panel.cor, cex.labels=1.3,
labels=MyNames,
panel = function(x, y, ...) {
        tmp <- lm(y ~ x, na.action = na.omit)
          abline(tmp)
        points(x, y) })

Euphotic1 <- read.table(file = "EUPH.csv", header = TRUE, sep=",", na.strings=c("
"NA"), dec=".", strip.white=TRUE)
```

```
source(file = "HighstatLib.R")
MyNames <- c("TOTAL PHOSPHORUS", "TOTAL DISSOLVED PHOSPHORUS",
"TOTAL REACTIVE PHOSPHORUS", "TOTAL ZIRCONIUM", "MICROCYSTIN")
pairs(Euphotic1[,c(70, 71, 73, 90, 56)], lower.panel = panel.cor, cex.labels=1.3,
labels=MyNames,
panel = function(x, y, ...) {
        tmp <- lm(y ~ x, na.action = na.omit)
          abline(tmp)
        points(x, y) })

Euphotic1 <- read.table(file = "EUPH.csv", header = TRUE, sep=",", na.strings=c("
"NA"), dec=".", strip.white=TRUE)
source(file = "HighstatLib.R")
MyNames <- c("TOTAL MANGANESE", "DISSOLVED NO3 + NO2", "WIND SPEED",
"MICROCYSTIN")
pairs(Euphotic1[,c(55, 60, 97, 56)], lower.panel = panel.cor, cex.labels=1.3,
labels=MyNames,
panel = function(x, y, ...) {
        tmp <- lm(y ~ x, na.action = na.omit)
          abline(tmp)
        points(x, y) })

Euphotic1 <- read.table(file = "EUPH.csv", header = TRUE, sep=",", na.strings=c("
"NA"), dec=".", strip.white=TRUE)
source(file = "HighstatLib.R")
MyNames <- c("ANABAENA BIOMASS", "BIOCHEMICAL OXYGEN DEMAND", "N:P
RATIO", "WIND SPEED", "MICROCYSTIN")
pairs(Euphotic1[,c(1, 65, 58, 97, 56)], lower.panel = panel.cor, cex.labels=1.3,
labels=MyNames,
panel = function(x, y, ...) {
        tmp <- lm(y ~ x, na.action = na.omit)
          abline(tmp)
        points(x, y) })

Euphotic1 <- read.table(file = "EUPH.csv", header = TRUE, sep=",", na.strings=c("
"NA"), dec=".", strip.white=TRUE)
source(file = "HighstatLib.R")
MyNames <- c("TOTAL KJELDAHL NITROGEN", "TOTAL CARBON", "TOTAL
NITROGEN", "DISSOLVED NO3 + NO2", "MICROCYSTIN")
pairs(Euphotic1[,c(64, 32, 62, 60, 56)], lower.panel = panel.cor, cex.labels=1.3,
labels=MyNames,
panel = function(x, y, ...) {
        tmp <- lm(y ~ x, na.action = na.omit)
          abline(tmp)
        points(x, y) })
```

```
-----------------------------------------
#Surface dataset
setwd("D:/Desiree/USB - April 13 2020/Step 6 with only micro hits/Step 6")
Surface1 <- read.table("D:/Desiree/USB - April 13 2020/Step 6 with only micro hits/Step
6/Step6Surface.csv", header=TRUE, sep=",", na.strings=c('', "NA"), dec=".",
strip.white=TRUE)

Surface1 <- read.table(file = "SUR.csv", header = TRUE, sep=",", na.strings=c('', "NA"),
dec=".", strip.white=TRUE)
source(file = "HighstatLib.R")
MyNames <- c("ANABAENA BIOMASS", "TOTAL KELDAHL NITROGEN",
"BIOCHEMICAL OXYGEN DEMAND", "TOTAL SUSPENDED SOLIDS",
"MICROCYSTIN")
pairs(Surface1[,c(1, 28, 29, 37, 22)], lower.panel = panel.cor, cex.labels=1.3,
labels=MyNames,
panel = function(x, y, ...) {
        tmp <- lm(y ~ x, na.action = na.omit)
          abline(tmp)
        points(x, y) })

Surface1 <- read.table(file = "SUR.csv", header = TRUE, sep=",", na.strings=c('', "NA"),
dec=".", strip.white=TRUE)
source(file = "HighstatLib.R")
MyNames <- c("CYANOPHYCEAE BIOMASS", "PHYTOPLANKTON BIOMASS",
"CHLOROPHYLL A", "TOTAL NITROGEN", "MICROCYSTIN")
pairs(Surface1[,c(8, 9, 16, 26, 22)], lower.panel = panel.cor, cex.labels=1.3,
labels=MyNames,
panel = function(x, y, ...) {
        tmp <- lm(y ~ x, na.action = na.omit)
          abline(tmp)
        points(x, y) })

Surface1 <- read.table(file = "SUR.csv", header = TRUE, sep=",", na.strings=c('', "NA"),
dec=".", strip.white=TRUE)
source(file = "HighstatLib.R")
MyNames <- c("CRYPTOPHYCEAE BIOMASS", "SECCHI DISC DEPTH", "WIND
SPEED", "MICROCYSTIN")
pairs(Surface1[,c(6, 19, 41, 22)], lower.panel = panel.cor, cex.labels=1.3,
labels=MyNames,
panel = function(x, y, ...) {
        tmp <- lm(y ~ x, na.action = na.omit)
          abline(tmp)
        points(x, y) })

Surface1 <- read.table(file = "SUR.csv", header = TRUE, sep=",", na.strings=c('', "NA"),
dec=".", strip.white=TRUE)
```

```
source(file = "HighstatLib.R")
MyNames <- c("PHEOPHYTIN A", "TOTAL CARBON", "DISSOLVED NO3 + NO2",
"N:P RATIO", "MICROCYSTIN")
pairs(Surface1[,c(18, 13, 24, 23, 22)], lower.panel = panel.cor, cex.labels=1.3,
labels=MyNames,
panel = function(x, y, ...) {
        tmp <- lm(y ~ x, na.action = na.omit)
          abline(tmp)
        points(x, y) })

-------------------------------------------------
#All euphotic and surface data together in one file
setwd("D:/Desiree/USB - April 13 2020/Step 6 with only micro hits/Step 6")
All1 <- read.table("D:/Desiree/USB - April 13 2020/Step 6 with only micro hits/Step
6/Step6All.csv", header=TRUE, sep=",", na.strings=c(", "NA"), dec=".",
strip.white=TRUE)

All1 <- read.table(file = "Step6All.csv", header = TRUE, sep=",", na.strings=c(", "NA"),
dec=".", strip.white=TRUE)
source(file = "HighstatLib.R")
MyNames <- c("PHEOPHYTIN A", "ANABAENA BIOMASS", "N:P RATIO", "TOTAL
KJELDAHL NITROGEN", "MICROCYSTIN")
pairs(All1[,c(45, 7, 64, 70, 62)], lower.panel = panel.cor, cex.labels=1.3,
labels=MyNames,
panel = function(x, y, ...) {
        tmp <- lm(y ~ x, na.action = na.omit)
          abline(tmp)
        points(x, y) })

All1 <- read.table(file = "Step6All.csv", header = TRUE, sep=",", na.strings=c(", "NA"),
dec=".", strip.white=TRUE)
source(file = "HighstatLib.R")
MyNames <- c("DISSOLVED NO3+NO2", "WIND SPEED", "TOTAL CARBON", "pH",
"TOTAL NITROGEN", "MICROCYSTIN")
pairs(All1[,c(266, 103, 38, 73, 68, 62)], lower.panel = panel.cor, cex.labels=1.3,
labels=MyNames,
panel = function(x, y, ...) {
        tmp <- lm(y ~ x, na.action = na.omit)
          abline(tmp)
        points(x, y) })
```

Appendix 9. Linear Discriminant Analysis.

```
#Euphotic dataset
setwd("D:/Desiree/USB - April 13 2020/Discriminant Analysis/LDA")

EUPH <- read.table("D:/Desiree/USB - April 13 2020/Discriminant
Analysis/LDA/EUPH1.csv", header=TRUE, sep=",", na.strings=c(", "NA"), dec=".",
strip.white=TRUE)

library(tidyverse)
library(mda)
library(klaR)
library(MASS)
library(caret)
library(lattice)

set.seed(13)
sample_n(EUPH, 10)
training_sample <- sample(c(TRUE, FALSE), nrow(EUPH), replace = T, prob =
c(0.3,0.7))
train <- EUPH[training_sample, ]
test <- EUPH[!training_sample, ]
lda.EUPH <- lda(GROUP ~ ANABAENA + BORON +
CYANOBACTERIASPECIESRICHNESS + DO + PSEUDOANABAENA + TP +
WINDSPEED, data = train)
lda.EUPH
plot(lda.EUPH) #grouped plot in folder

E1 <- predict(lda.EUPH, test)
ldahist(data = E1$x[,1], g = test$GROUP) #histogram LD1
ldahist(data = E1$x[,2], g = test$GROUP) #histogram LD2

E2 <- predict(lda.EUPH, train)$class
tab1 <- table(Predicted = E2, Actual = train$GROUP)
tab1
sum(diag(tab1))/sum(tab1)

E3 <- predict(lda.EUPH, test)$class
tab1 <- table(Predicted = E3, Actual = test$GROUP)
tab1
sum(diag(tab1))/sum(tab1)

-----------------------------------------
#Surface dataset
setwd("D:/Desiree/USB - April 13 2020/Discriminant Analysis/LDA")
```

```
SUR <- read.table("D:/Desiree/USB - April 13 2020/Discriminant
Analysis/LDA/SUR1.csv", header=TRUE, sep=",", na.strings=c('', "NA"), dec=".",
strip.white=TRUE)

library(tidyverse)
library(mda)
library(klaR)
library(MASS)
library(caret)
library(lattice)

set.seed(13)
sample_n(SUR, 10)
training_sample <- sample(c(TRUE, FALSE), nrow(SUR), replace = T, prob =
c(0.3,0.7))
train <- SUR[training_sample, ]
test <- SUR[!training_sample, ]
lda.SUR <- lda(GROUP ~ NPRATIO + PH + TP + WINDSPEED, data = train)
lda.SUR
plot(lda.SUR) #grouped plot in folder

E1 <- predict(lda.SUR, test)
ldahist(data = E1$x[,1], g = test$GROUP) #histogram LD1
ldahist(data = E1$x[,2], g = test$GROUP) #histogram LD2

E2 <- predict(lda.SUR, train)$class
tab1 <- table(Predicted = E2, Actual = train$GROUP)
tab1
sum(diag(tab1))/sum(tab1)

E3 <- predict(lda.SUR, test)$class
tab1 <- table(Predicted = E3, Actual = test$GROUP)
tab1
sum(diag(tab1))/sum(tab1)
```

Appendix 10. Linear Model – AIC Model Selection and Hurdle Model

```
###Euphotic dataset Gaussian identity link
library(AICcmodavg)
library(statmod)

setwd("D:/Desiree/USB - April 13 2020/GLM/Mar 22-detects only")

EUPHGLMP <- read.table("D:/Desiree/USB - April 13 2020/GLM/Mar 22-detects
only/EuphoticGLMPos.csv", header=TRUE, sep=",", na.strings=c('', "NA"), dec=".",
strip.white=TRUE)

#Microcystin logged
EUPHGLMP$logMICROCYSTIN <- with(EUPHGLMP, log10(MICROCYSTIN))

#Models
#Anabaena ('Anabaena')                  β0 + β1X1
#Anabaena + Wind Speed                  β0 + β1X1 + β7X7
#Anabaena + Boron                       β0 + β1X1 + β2X2
#Anabaena + TP                          β0 + β1X1 + β6X6
#Wind Speed                             β0 + β7X7
#TP + Wind Speed                        β0 + β6X6 + β7X7
#Boron + Wind Speed                     β0 + β2X2 + β7X7
#Total Boron ('Boron')                  β0 + β2X2
#Boron + TP                             β0 + β2X2 + β6X6
#Total Phosphorus ('TP')                β0 + β6X6
#Intercept only                         β0

#Models to input into AIC
model1 <- lm(logMICROCYSTIN ~ ANABAENA, data = EUPHGLMP)
model2 <- lm(logMICROCYSTIN ~ BORON, data = EUPHGLMP)
model3 <- lm(logMICROCYSTIN ~ TP, data = EUPHGLMP)
model4 <- lm(logMICROCYSTIN ~ WINDSPEED, data = EUPHGLMP)
model5 <- lm(logMICROCYSTIN ~ ANABAENA + BORON, data = EUPHGLMP)
model6 <- lm(logMICROCYSTIN ~ ANABAENA + TP, data = EUPHGLMP)
model7 <- lm(logMICROCYSTIN ~ ANABAENA + WINDSPEED, data = EUPHGLMP)
model8 <- lm(logMICROCYSTIN ~ BORON + TP, data = EUPHGLMP)
model9 <- lm(logMICROCYSTIN ~ BORON + WINDSPEED, data = EUPHGLMP)
model10 <- lm(logMICROCYSTIN ~ TP + WINDSPEED, data = EUPHGLMP)
model11 <- lm(logMICROCYSTIN ~ 1, data = EUPHGLMP)

models <- list(model1, model2, model3, model4, model5, model6, model7, model8,
model9, model10, model11)
mod.names <- c('ANABAENA', 'BORON', 'TP', 'WINDSPEED', 'ANABAENA+BORON',
'ANABAENA+TP', 'ANABAENA+WINDSPEED', 'BORON+TP', 'BORON+WINDPSEED',
'TP+WINDPSEED', 'INTERCEPT')
aictab(cand.set = models, modnames = mod.names)
```

```
##QQ plot for BORON + WINDSPEED (AICc weight of 0.84 in AIC spreadsheet)
EUPH.gausBORW <- glm(logMICROCYSTIN ~ BORON + WINDSPEED, family =
gaussian(link = "identity"), data = EUPHGLMP)
summary(EUPH.gausBORW)

#McFadden's pseudo R-squared
library(DescTools)
PseudoR2(EUPH.gausBORW)

#k-fold cross validation Gaussian euphotic dataset
set.seed(123)
train.control <- trainControl(method = "cv", number = 6)
model <- train(logMICROCYSTIN ~ BORON + WINDSPEED, data = EUPHGLMP,
method = "lm", na.action=na.omit, trControl = train.control)
print(model)

plot(x=predict(model), y=EUPHGLMP$logMICROCYSTIN,
    xlab='Predicted Values',
    ylab='Actual Values',
    main='Predicted vs. Actual Values')
abline(a=0, b=1)

-------------------------------------
###Euphotic dataset binomial
setwd("D:/Desiree/USB - April 13 2020/GLM/Mar 22-detects only")

EUPHGLMP1 <- read.table("D:/Desiree/USB - April 13 2020/GLM/Mar 22-detects
only/EuphoticGLMPos1.csv", header=TRUE, sep=",", na.strings=c("", "NA"), dec=".",
strip.white=TRUE)

#MICROCYSTIN_bin -> presence=1; absence=0
#Models
#Anabaena ('Anabaena')          β0 + β1X1
#Anabaena + Wind Speed          β0 + β1X1 + β7X7
#Anabaena + Boron               β0 + β1X1 + β2X2
#Anabaena + TP                  β0 + β1X1 + β6X6
#Wind Speed                     β0 + β7X7
#TP + Wind Speed                β0 + β6X6 + β7X7
#Boron + Wind Speed             β0 + β2X2 + β7X7
#Total Boron ('Boron')          β0 + β2X2
#Boron + TP                     β0 + β2X2 + β6X6
#Total Phosphorus ('TP')        β0 + β6X6
#Intercept only                 β0

#Models to input into AIC
```

```
model1 <- glm(MICROCYSTIN_bin ~ ANABAENA, family = binomial, data =
EUPHGLMP1)
model2 <- glm(MICROCYSTIN_bin ~ BORON, family = binomial, data = EUPHGLMP1)
model3 <- glm(MICROCYSTIN_bin ~ TP, family = binomial, data = EUPHGLMP1)
model4 <- glm(MICROCYSTIN_bin ~ WINDSPEED, family = binomial, data =
EUPHGLMP1)
model5 <- glm(MICROCYSTIN_bin ~ ANABAENA + BORON, family = binomial, data =
EUPHGLMP1)
model6 <- glm(MICROCYSTIN_bin ~ ANABAENA + TP, family = binomial, data =
EUPHGLMP1)
model7 <- glm(MICROCYSTIN_bin ~ ANABAENA + WINDSPEED, family = binomial,
data = EUPHGLMP1)
model8 <- glm(MICROCYSTIN_bin ~ BORON + TP, family = binomial, data =
EUPHGLMP1)
model9 <- glm(MICROCYSTIN_bin ~ BORON + WINDSPEED, family = binomial, data =
EUPHGLMP1)
model10 <- glm(MICROCYSTIN_bin ~ TP + WINDSPEED, family = binomial, data =
EUPHGLMP1)
model11 <- glm(MICROCYSTIN_bin ~ 1, family = binomial, data = EUPHGLMP1)

models <- list(model1, model2, model3, model4, model5, model6, model7, model8,
model9, model10, model11)
mod.names <- c('ANABAENA', 'BORON', 'TP', 'WINDSPEED', 'ANABAENA+BORON',
'ANABAENA+TP', 'ANABAENA+WINDSPEED', 'BORON+TP', 'BORON+WINDPSEED',
'TP+WINDPSEED', 'INTERCEPT')
aictab(cand.set = models, modnames = mod.names)

##QQ plot for ANABAENA + WINDSPEED (AICc weight of 1 in AIC spreadsheet)
EUPH.binAW <- glm(MICROCYSTIN_bin ~ ANABAENA + WINDSPEED, family =
binomial, data = EUPHGLMP1)
summary(EUPH.binAW)

#McFadden's pseudo R-squared
library(DescTools)
PseudoR2(EUPH.binAW)

#k-fold cross validation binomial euphotic dataset
set.seed(123)
train.control <- trainControl(method = "cv", number = 6)
model <- train(MICROCYSTIN_bin ~ ANABAENA + WINDSPEED, data =
EUPHGLMP1, method = "glm", family=binomial, na.action=na.omit, trControl =
train.control)
print(model)
-----------------------------------------------------
###Surface dataset Gaussian identity link
library(AICcmodavg)
```

```
library(statmod)

setwd("D:/Desiree/USB - April 13 2020/GLM/Mar 22-detects only")

SURGLMP <- read.table("D:/Desiree/USB - April 13 2020/GLM/Mar 22-detects
only/SurfaceGLMPos.csv", header=TRUE, sep=",", na.strings=c('', "NA"), dec=".",
strip.white=TRUE)

#Microcystin logged
SURGLMP$logMICROCYSTIN <- with(SURGLMP, log10(MICROCYSTIN))

#Models
#N:P ratio + Wind Speed                  β0 + β1X1 + β4X4
#N:P ratio ('N:P ratio')                 β0 + β1X1
#Wind Speed ('Wind Speed')               β0 + β4X4
#N:P ratio + TP                          β0 + β1X1 + β3X3
#Total Phosphorus ('TP')                 β0 + β3X3
#TP + Wind Speed                         β0 + β3X3 + β4X4
#Intercept only                          β0

#Models to input into AIC
model1 <- lm(logMICROCYSTIN ~ NPRATIO, data = SURGLMP)
model2 <- lm(logMICROCYSTIN ~ TP, data = SURGLMP)
model3 <- lm(logMICROCYSTIN ~ WINDSPEED, data = SURGLMP)
model4 <- lm(logMICROCYSTIN ~ NPRATIO + TP, data = SURGLMP)
model5 <- lm(logMICROCYSTIN ~ NPRATIO + WINDSPEED, data = SURGLMP)
model6 <- lm(logMICROCYSTIN ~ TP + WINDSPEED, data = SURGLMP)
model7 <- lm(logMICROCYSTIN ~ 1, data = SURGLMP)

models <- list(model1, model2, model3, model4, model5, model6, model7)
mod.names <- c('NPRATIO', 'TP', 'WINDSPEED', 'NPRATIO+TP',
'NPRATIO+WINDSPEED', 'TP+WINDPSEED', 'INTERCEPT')
aictab(cand.set = models, modnames = mod.names)

##QQ plot for NPRATIO + WINDSPEED (AICc weight of 0.97 in AIC spreadsheet)
library(statmod)
SUR.gausNPRW <- glm(logMICROCYSTIN ~ NPRATIO + WINDSPEED, family =
gaussian(link = "identity"), data = SURGLMP)
summary(SUR.gausNPRW)

#McFadden's pseudo R-squared
library(DescTools)
PseudoR2(SUR.gausNPRW)

#k-fold cross validation Gaussian surface dataset
set.seed(123)
```

```
train.control <- trainControl(method = "cv", number = 6)
model <- train(logMICROCYSTIN ~ NPRATIO + WINDSPEED, data = SURGLMP,
method = "lm", na.action=na.omit, trControl = train.control)
print(model)

plot(x=predict(model), y=SURGLMP$logMICROCYSTIN,
    xlab='Predicted Values',
    ylab='Actual Values',
    main='Predicted vs. Actual Values')
abline(a=0, b=1)

-----------------------------------------------
#Surface dataset binomial
setwd("D:/Desiree/USB - April 13 2020/GLM/Mar 22-detects only")

SURGLMP1 <- read.table("D:/Desiree/USB - April 13 2020/GLM/Mar 22-detects
only/SurfaceGLMPos1.csv", header=TRUE, sep=",", na.strings=c('', "NA"), dec=".",
strip.white=TRUE)

#MICROCYSTIN_bin -> presence=1; absence=0
#Models to input into AIC
model1 <- glm(MICROCYSTIN_bin ~ NPRATIO, family = binomial, data = SURGLMP1)
model2 <- glm(MICROCYSTIN_bin ~ TP, family = binomial, data = SURGLMP1)
model3 <- glm(MICROCYSTIN_bin ~ WINDSPEED, family = binomial, data =
SURGLMP1)
model4 <- glm(MICROCYSTIN_bin ~ NPRATIO + TP, family = binomial, data =
SURGLMP1)
model5 <- glm(MICROCYSTIN_bin ~ NPRATIO + WINDSPEED, family = binomial, data
= SURGLMP1)
model6 <- glm(MICROCYSTIN_bin ~ TP + WINDSPEED, family = binomial, data =
SURGLMP1)
model7 <- glm(MICROCYSTIN_bin ~ 1, family = binomial, data = SURGLMP1)

models <- list(model1, model2, model3, model4, model5, model6, model7)
mod.names <- c('NPRATIO', 'TP', 'WINDSPEED', 'NPRATIO+TP',
'NPRATIO+WINDSPEED', 'TP+WINDPSEED', 'INTERCEPT')
aictab(cand.set = models, modnames = mod.names)

#McFadden's pseudo R-squared
library(DescTools)
PseudoR2(SUR.binNPRW)

#k-fold cross validation binomial surface dataset
set.seed(123)
train.control <- trainControl(method = "repeatedcv", number = 10, repeats = 3)
```

```
model <- train(MICROCYSTIN_bin ~ NPRATIO + WINDSPEED, data = SURGLMP1,
method = "glm", family=binomial, na.action=na.omit, trControl = train.control)
print(model)
```

Appendix 11. Ways to reduce the impacts of cyanobacteria algal blooms. This section was written in fulfillment of the requirements of the University of Manitoba course BIOL 7600.

Over the past few decades, freshwater cyanobacteria blooms have been increasing in the offshore and nearshore areas. The increase of cyanobacteria blooms can be harmful to human health due to the toxins they can release. There have been several methods that have been used to control cyanobacterial blooms. In this section methods such as ultrasonic radiation, darkening of water, artificial circulation, copper sulfate, chlorine, potassium permanganate, hydrogen peroxide, barley straw and lime will be looked at in this section.

There have been multiple studies suggesting that ultrasonic radiation can control algal blooms in eutrophic lakes as well as it can also lyse cells therefore possibly releasing algal toxins into the water. Ultrasound uses cavitation (the collapse of bubbles within a liquid, rarefaction and compression) to concentrate diffuse sound energy (Ahn et al., 2003). Ultrasonic radiation can breakdown the gas vesicles, inhibit photosynthesis and cell division, produce free radicals and enhance coagulation (Ahn et al., 2003; Zhang et al., 2006; Heng et al., 2009). A study using raw water in the Luan River in China indicates that ultrasonic frequency of 40 kHz, 60 W power supply and irradiation duration of 15 seconds are key in cyanobacteria removal and coagulation (Heng et al., 2009). Looking at cultures of *Microcystis aeruginosa*, high frequencies (580 kHz) with medium amount of power (0.0041 W/cm) leads to inactivation and the cells not rupturing (Wu et al., 2011). Cultured *Microcystis aeruginosa* cells exposed to a frequency rate of 80 kHz, 32 W for 5 minutes showed no change in microcystin concentrations however,

an increase from 0.87 to 3.1 µg/L were observed at 80 kHz, 80 W for 5 minutes (Zhang et al., 2006). In the same *Microcystis aeruginosa* culture study showed that at higher ultrasound frequencies (1320 kHz), there was 90% cell removal in just 20 minutes (Zhang et al., 2006). A field study done in Jeonmin-dong, Daejeon, Korea showed that total N (1.25 mg/L to 0.75 mg/L in 9 days) was lower in the sonication enclosure and a decrease in total P was minimal (around 150 µg/L to 75 µg/L in 9 days) (Ahn et al., 2003). This field study also showed that chlorophyll *a* concentrations decreased from 111.3 to 32.5 µg/L after 3 days (Ahn et al., 2003). The percentage of cyanophytes was only 13% in the enclosure whereas they inhabited 47% of the control enclosure implying ultra sonication inhibited cyanobacteria and not other algal species (Ahn et al., 2003). An ultrasonic processor cost roughly $8,050 CAD and can process samples up to 19 L. The area an ultrasonic processor can treat is based on the (Ahn et al., 2003) study for the area of a cylinder (1.88 m^2) where Lake Winnipeg's area is 23,750 km^2=2.375x10^{10} m^2, I calculated that we would need 4.465x10^{10} ultrasonic processors and it would cost $3.58x$10^{14}$. Studies using ultrasonic radiation to rid cyanobacteria have shown to work quickly with higher frequency and ultrasound power also treating Lake Winnipeg with ultrasonic radiation would be very costly.

Darkening of the water column can be used to control or reduce cyanobacteria growth by limiting the amount of light used for photosynthesis. Cyanobacteria spp. showed to be more sensitive than natural phytoplankton communities with the fluctuating solar radiation and darkening of the water column (r^2=0.7) (Helbling et al., 2015). A study on Ward Lake in showed that average chlorophyll *a* concentrations decreased from 86.9 in 2010 to 34.9 mg/m in 2012 as well zooplankton decreased from

0.9 in 2010 to 0.5 g/m^2 in 2012 (Batt et al., 2015). Products such as Aquashade ($208 CAD for 4 Gallon that can treat 4 acres of surface water) used on Lake Winnipeg (23,750km^2=5,868,753 acres) would cost $305 million dollars for one use. Evidence suggests that darkening the water column does in fact show a decrease in cyanobacteria growth and applying Aquashade to Lake Winnipeg would be expensive.

Artificial circulation can be used in a waterbody to increase mixing throughout the water column to prevent thermal stratification and to prevent cyanobacteria from getting light therefore minimizing algal growth. Artificial circulation can be done by means of air bubbles, jets or pumps and should be designed to have mixing velocities > 1m/h and mix around 80% of the volume of water (Knappe et al., 2004; Chen & Yeh, 2005). A study done on Lake Nieuwe Meer in the Netherlands, showed the application of a vertical mixing device showed chlorophyll *a* concentrations to decrease from 28.1 µg/L in 1990 to 6.2 µg/L in 1994 (Visser et al., 1996). In the same study on Lake Nieuwe Meer, *Microcystis* abundance decreased from $47.2x10^{10}$ m^2 in 1990 to $2.1x10^{10}$ m^2 in 1994, *Anabaena* decreased as well from $1.8x10^{10}$ m^2 in 1990 to $0.5x10^{10}$ m^2 in 1994 and *Aphanizomenon* increased from $0.1x10^{10}$ m^2 in 1990 to $9.8x10^{10}$ m^2 in 1994 (Visser et al., 1996). A study on Nainital Lake in India over 7 months of aeration showed that mean cyanobacteria compromised about 9% of the total phytoplankton population pre-aeration or $10.6x10^5$ cells/L and decreased to 0% or $0.17x10^5$ cells/L ($p<0.05$) during the 7 months of aeration (Gupta & Gupta, 2012). In Manitoba, at Fort Whyte Alive in Winnipeg Lake Devonian and Lake Cargill, the Boyne River in Carmen and Stephenfield Lake are aerated. Aerators used on Lake Winnipeg (23,750 km^2=5,868,753 acres) where a bottom aerator costing $4,200 for 8 to 45 ft deep ponds and covers 4 acres

would cost $6,160,000,000 billion dollars for one use. Artificial circulation has been shown to decrease the abundance of phytoplankton and chlorophyll *a* concentrations as well as applying artificial circulation to Lake Winnipeg would be very expensive.

Copper sulfate is a common algicide that is easy to apply, economical and effective to get rid of cyanobacteria blooms. Cyanobacteria have been found to be very sensitive to high copper concentrations therefore with added copper sulfate, cyanobacteria biomass will decrease. Copper toxicity is associated with thylakoid disruption, electron transport inhibition in photosystem II and substituting magnesium in chlorophyll *a* (Greenfield et al., 2014). A one-time addition of copper sulfate does not rid cyanobacteria permanently from a waterbody, but multiple applications are to be applied to keep algal populations under control over the summer months (Song & Wang, 2015). These multiple additions of copper sulfate can cause changes in the abiotic and biotic ecosystem structure such as shifting algal species distribution and P recycling (Hanson & Stefan, 1984; Song & Wang, 2015). There was an increase in lysed cells with increased concentrations of copper sulfate (Greenfield et al., 2014). With copper sulfate concentrations of 1.5, 1 and 0.5 mg/L added to *Microcystis aeruginosa* cultures had 95, 70 and 13% of cyanobacterial cell membranes lost integrity after one day of treatment (Fan et al., 2013). A study on a 0.053 km^2 pond on Kiawah Island in South Carolina showed the copper sulfate-based algicides (Captain* and K-Tea™) at the manufacture's recommended dose (Captain*=0.4 mg/L, K-Tea™=0.5 mg/L and Pak™ 27=6.5 lbs acre/ft) and twice the manufacture's recommended dose reduced *Anabaenopsis* sp. and *Microcystis aeruginosa* cells in control treatments within 7 days more effectively than the sodium percarbonate-based compound (Pak™ 27) (Greenfield et al., 2014). In

the same study, initial microcystin concentrations of 11-30ppb showed that when copper sulfate applied to a cyanobacteria bloom can cause cells to lyse and release microcystin toxins into the water column where levels were generally 2-10 times higher than the initial levels (Van Hullebusch et al., 2002); Greenfield et al., 2014. Chlorophyll *a* declined in a study on Courtille Lake in France 2 days after 0.25 mg/L of copper sulfate was added to the treatment and *Microcystis* spp. had completely disappeared (Van Hullebusch et al., 2002). As well as the accumulation of cooper can occur in the sediments and coper toxicity can occur in zooplankton and fish (Knappe et al., 2004; Chen & Yeh, 2005). Copper sulfate used on Lake Winnipeg (23,750 km^2=5,868,753 acres) where it would cost $265 CAD for 50 lbs that covers 4 acres would cost $388 million dollars for one use. Studies have shown that copper sulfate additions to a waterbody will decline cyanobacteria and chlorophyll *a* concentrations but when algal cells are lysed by copper sulfate, it has been shown to increase microcystin concentrations as well copper sulfate additions to Lake Winnipeg are very expensive.

Chlorine pre-oxidation can cause a loss of membrane integrity and induce the lysis of cells and the release of toxins. In drinking water treatment plants, chlorination has been applied as a disinfectant. With chlorine additions of 3, 4 and 5 mg/L added to *Microcystis aeruginosa* cultures, 97, 95 and 88% of membrane integrity was lost after one minute of exposure (Fan et al., 2013). Cultures and natural blooms of *Anabaena circinalis, Aphanizomenon issatsckenk* and *Cylindrospermopsis raciborskii* from Prospect Reservoir in New South Wales, Australia showed that with the chlorine addition of <8 mg/L, the number of active cells present decreased to 1% (Zamyadi et al., 2012). In the same study, *Microcystis aeruginosa* culture and natural blooms, the

addition of 31 mg/L of chlorine was needed to damage >99% of the living algal cells (Zamyadi et al., 2012). *Microcystis aeruginosa* cultures with a cell concentration of $1.3x10^5$ cells/mL showed that within 1 minute of adding 6 mg/L of chlorine, 60% of algal cells were ruptured, 80% ruptured within 5 minutes and 100% ruptured within 30 minutes (Lin et al., 2009). In *Anabaena circinalis* cultures with a cell concentration of 6.0x105 cells/mL and 2 mg/L of chlorine added, within 1 minute around 90% of the algal cells ruptured (Lin et al., 2009). Chlorine studies showed that cyanobacteria abundance decreased rapidly with the addition of chlorine.

Potassium permanganate is used as a disinfectant and algicide as well as a pre-oxidizer to enhance coagulation in algal cells. In *Microcystin aeruginosa* cultures, membrane integrity was not affected by potassium permanganate concentrations of 1 and 3 mg/L (Fan et al., 2013). In the same study, when *Microcystis aeruginosa* cultures were exposed to 5 mg/L, intact cells were decreased to 74% after 6 hours of exposure (Fan et al., 2013). In *Microcystin aeruginosa* cultures, polyaluminum chloride at 30 mg/L concentrations was used as a coagulant in addition to 2 mg/L of potassium permanganate which showed at day 21 in the stationary growth phase, 100% removal of algal cells and chlorophyll *a* (Wang et al., 2013). With 3 hours of exposure to a 3 mg/L dose of potassium permanganate, around 80% of algal cells were removed for *Anabaena flos-aquae, Microcystis aeruginosa* and *Synura petersenii* (Knappe et al., 2004; Chen & Yeh, 2005). Potassium permanganate doses of 3 and 5 mg/L showed a decline in cyanobacteria concentrations.

Hydrogen peroxide is an oxidant that occurs naturally in surface water as a by-product from biological respiration, photosynthesis and other metabolic processes.

Hydrogen peroxide can inhibit photosynthetic activity and electron transport therefore inactivation photosystem II (Fan et al., 2013; Greenfield et al., 2014). Cell membrane integrity was maintained 86, 46 and 51% after one day of hydrogen peroxide doses of 10.2, 51 and 102 mg/L (Fan et al., 2013). After two days of the initial 10.2, 51 and 102 mg/L doses, intact cells of *Microcystis aeruginosa* cultures decreased to 16, 31 and 7% (Fan et al., 2013). A lab study at the Water Corporation's Burekup wastewater treatment plant in Perth, Western in Australia showed that cyanobacteria decreased at concentrations of $3.2x10^{-5}$ gH_2O_2/µg chl-*a* (Barrington & Ghadouani, 2008). In a field study at the Burekup wastewater treatment plant in Perth, Western in Australia showed a 57% reduction in cyanobacterial as well as total cyanobacteria was reduced by 70% occurred with a dose of $1.3x10^{-4}$ gH_2O_2/µg chl-*a* (Barrington et al., 2011). A study on Lake Koetshuis in the Netherlands showed that within 10 days after about 2 mg/L of hydrogen peroxide was added, the abundance of cyanobacteria decreased from $600x10^3$ cells/mL to $10x10^3$ cells/mL as well the cyanobacterial abundance stayed low for about 7 weeks (Matthijs et al., 2012). In the same study, it was shown that in lake enclosure experiments that more than 2.5 mg/L of hydrogen peroxide can harm the herbivores zooplankton present in the lake (Matthijs et al., 2012). Lab and field studies show that the addition of hydrogen peroxide has decreased cyanobacteria abundance.

Decomposing barley straw can be used to rid cyanobacteria blooms can produce chemical substances such as free radicals or oxidized phenolics that can inhibit growth. Nine 300 m^2 ponds in Guilan Province, Iran showed that *Anabaena* (9.43x103 mL to 5.74x103 mL), *Aphanizomenon* (4.41x103 mL to 0.87x103 mL) and *Microcystis* (11.76 x103 mL to 0.84x103 mL) biomass decreased from April to August with 40 g m^{-1} barley

straw (Rajabi et al., 2010). The same study also showed that *Anabaena* (7.69x103 mL to 1.50x103 mL^{-1}), *Aphanizomenon* (4.53x103 mL to 0.45x103 mL) and *Microcystis* (8.76 x103 mL to 0.57x103 mL) biomass decreased from April to August with 80 g/m barley straw (Rajabi et al., 2010). Growth inhibition in *Microcystis* cultures occurred at a temperature of 20 and 27°C with fresh finely chopped straw at concentrations of 5 g (dry weight)/L (Iredale et al., 2012). If barley straw pellets were used on Lake Winnipeg (23,750 km^2=5,868,753 acres) where a pond size of 2 acres would need 240 lbs ($1,020) of pellets for one application would cost $3 billion dollars. Field and lab studies showed that adding barley straw decreased the *Anabaena*, *Aphanizomenon* and *Microcystis* biomass as well as if barley straw was added to Lake Winnipeg it would be very expensive.

The addition of lime can remove P and coagulate cells without releasing toxins to the water. Lime has been found to decrease the zooplankton abundance as well as increase pH levels above 10 in lakes (Mohamed, 2001). With the addition of lime-alum to samples from the Nile River at Sohag city, Upper Egypt, chlorophyll *a* content did not change after week 1 to week 4 (0.5 µg/mL) of the experiment but lime-alum precipitated phosphate decreased from around 0.3 to 0.2 µg/mL (Mohamed, 2001). Results from initial treatments of lime with dosages of 75 mg/L to the open water was shown to reduce P concentrations from 207 to 94 µg/L in Valencia lake, from 260 to 86 µg/L in Andorra lake and from 264 to 56 µg/L in Beaumaris lake (Babin et al., 1992). With the same study in Andorra lake, a maximum chlorophyll *a* concentration of 100 µg/L was recorded on July 22 and decreased to 4.5 µg/L two weeks later reflecting an algal bloom collapse (Babin et al., 1992). Studies have shown that the addition of lime can reduce

phosphate and P concentrations as well chlorophyll *a* concentrations were either reduced or stayed the same.